LIBRARY
Michigan State
University

PLACE IN RETURN BOX to remove this checkout from your record.
TO AVOID FINES return on or before date due.

DATE DUE	DATE DUE	DATE DUE

MSU Is An Affirmative Action/Equal Opportunity Institution
c:\circ\datedue.pm3-p.1

RESPONSE OF ANAEROBIC SYSTEMS TO LONG-TERM PERIODIC SUBSTRATE PERTURBATIONS

By

Jian Xing

A DISSERTATION

Submitted to
Michigan State University
in partial fulfillment of the requirements
for the degree of

DOCTOR OF PHILOSOPHY

Department of Civil and Environmental Engineering

1996

ABSTRACT

RESPONSE OF ANAEROBIC SYSTEMS TO LONG-TERM PERIODIC SUBSTRATE PERTURBATIONS

By

Jian Xing

Three 1.5 L working volume anaerobic chemostats ("daughter" reactors), fed with glucose as sole carbon and energy source, were used to investigate the response of anaerobic systems to long-term periodic substrate perturbations.

The daughter reactors were originally operated under constant fed conditions (inlet glucose concentration of 8 g/L and hydraulic retention time of 10 days). After reaching steady-state, the daughter reactors were subjected to periodic applied organic loading patterns in which the influent glucose concentrations were periodically changed in amplitude from 16 g/L to 0 g/L (mineral media only) with time on total cycle times of 2, 6 and 10 days. The average organic loading rates for all systems equal to the steady-state organic loading rate of 0.8 g glucose/L-d. A 10 day hydraulic retention time was maintained for all systems.

The anaerobic microbial communities were sensitive to the periodic substrate perturbations. Rapid accumulation of glucose fermentation intermediates occurred immediately after the initiation of the substrate perturbations. The response of the reactor microbial communities to the substrate perturbations can be broken down into four distinct stages: (1) rapid VFA and COD accumulation; (2) establishment of a transient "pseudo steady-state" at reduced COD removal efficiency; (3) rapid VFA degradation; and (4) re-establishment of steady-state with high COD removal efficiency.

The anaerobic systems were able to adapt to the periodic substrate perturbations through changes in microbial communities. This was verified by comparison of DNA extracts and FAME profiles from the steady-state control reactor and the daughter reactors, changes in substrate degradation rates, and microscopic examinations.

The perturbation interval appeared to significantly affected the structure and function of the perturbed anaerobic communities. Stable microbial communities was only be re-established in two of three systems.

The periodic substrate addition mode appears to provide a strong selection force on the populations of the anaerobic chemostat communities. The operational and kinetic performance of the re-established daughter reactors, especially the system operated with 1/1 day substrate perturbation, was superior to the performance of the stable control reactor. This suggests a more robust microbial community structure can be selected and established using this type of substrate perturbation resulting in enhanced treatment efficiency and operational stability.

Copyright by
JIAN XING
1996

Dedicated to my father Jinzhong Xing, my mother Jia He,

and my wife Yi Yu, my daughter Fei and Jing

whom I love.

ACKNOWLEDGMENT

I would like to express gratitude to my major professor and research advisor, Dr. Robert F. Hickey, for his instruction, guidance and encouragement during my Ph. D study. Special thanks are extended to my other research advisor, Dr. Craig S. Criddle for his instruction, guidance and encouragement through out this research work.

I wish to express my sincere thanks to Dr. James Tiedje and Dr. Thomas C. Voice for their advice, assistance and valuable comments on this research. Thanks are extended to Dr. Bruce Dale for his time and effort spent on reviewing this dissertation, and for his valuable comments and suggestions.

Special thanks are extended to Dr. Poul Loconto, Dr. Wei-min Wu, Dr. Jizhong Zhou, Dr. Dave Odelson, Y. L. Pan, Hung Nguyen, Daniel Wigner, Helen L. Garshow and Mathuram Stanley for their invaluable help and assistance during this work.

I also thank my fellow students for their friendship, support and stimulating discussions during my years at Michigan State University.

This study was funded by a grant from the National Science Foundation Center for Microbial Ecology at Michigan State University under Microbial Ecology Grant NSF BIR 9120006.

TABLE OF CONTENTS

LIST OF TABLES xi

LIST OF FIGURES xiv

KEY TO ABBREVIATIONS xix

CHAPTER 1
INTRODUCTION 1

CHAPTER 2
BACKGROUND 3
2.1 Anaerobic degradation process 3
2.2 Methanogenesis 5
2.3 Acetogenesis 8
2.4 Anaerobic fermentation of glucose 11
2.5 Ecological point of view of anaerobic degradation 18

CHAPTER 3
CULTIVATION OF ANAEROBIC CULTURE IN LAB-SCALE ANAEROBIC REACTOR FED WITH GLUCOSE AS SOLE CARBON AND ENERGY SOURCE 20
3.1 Introduction 20
3.2 Materials and Methods 21
3.2.1 Laboratory-scale anaerobic reactor 21
3.2.2 Substrate 23
3.2.3 Nutrients 23
3.2.4 Analytical methods 25
3.2.5 MPN enumeration method 25
3.2.6 Inoculum material 26
3.3 Results 27
3.3.1 Mixing characteristics of the mother reactor 27
3.3.2 Reactor start-up 27
3.3.3 Reactor operational performance under steady-state conditions 33
3.3.4 Biomass characteristics 36
3.3.5 Mass balance calculation for the baseline steady-state operation 39
3.3.6 MPN enumeration results 40
3.3.7 Microscopic examination 41
3.4 Discussion 42
3.5 Summary 43

CHAPTER 4
RESPONSE OF ANAEROBIC COMMUNITY TO A LONG-TERM ONE DAY FEAST-ONE DAY FAMINE PERIODIC SUBSTRATE PERTURBATION... 44
4.1 Introduction... 44
4.2 Materials and methods... 46
4.2.1 Anaerobic reactor... 46
4.2.2 Substrate and nutrients... 48
4.2.3 Analytical methods... 50
4.2.4 Measurement of maximum substrateconversion rate.. 50
4.2.5 Measurement of decay coefficients of biomass and substrate utilization capacities... 52
4.2.6 Reactor inoculation... 53
4.2.7 Experimental procedure... 53
4.3 Results... 56
4.3.1 Effects of the periodic substrate perturbation... 56
4.3.2 Gas production during perturbation period... 64
4.3.3 Maximum substrate conversion rate... 67
4.3.4 Decay characteristics... 68
4.3.5 Protein measurement results... 75
4.3.6 Enumeration results... 79
4.3.7 Microscopic observation... 84
4.4 Discussion... 86
4.5 Summary... 92

CHAPTER 5
RESPONSE OF ANAEROBIC COMMUNITY TO A LONG-TERM THREE DAY FEAST-THREE DAY FAMINE PERIODIC SUBSTRATE PERTURBATION... 93
5.1 Introduction... 93
5.2 Materials and methods... 94
5.2.1 Anaerobic reactor... 94
5.2.2 Substrate and nutrients... 94
5.2.3 Analytical methods... 96
5.2.4 Free energy calculations... 96
5.2.5 Reactor inoculation... 97
5.2.6 Experimental procedure... 98
5.3 Results... 100
5.3.1 Effects of periodic substrate perturbation... 100
5.3.2 Changes in gas production rate during substrate perturbation period... 109
5.3.3 Changes in un-dissociated VFA concentrations during the perturbation period... 112
5.3.4 Free energy calculations for anaerobic oxidation of glucose metabolic intermediates... 116
5.3.5 Electron equivalents mass balance... 121
5.3.6 Microscopic observations... 124
5.4 Discussion... 126
5.5 Summary... 132

CHAPTER 6
RESPONSE OF ANAEROBIC COMMUNITY TO A LONG-TERM FIVE DAY FEAST-FIVE DAY FAMINE PERIODIC SUBSTRATE PERTURBATION 133
6.1 Introduction 133
6.2 Materials and methods 134
6.2.1 Anaerobic reactor 134
6.2.2 Substrate and nutrients 134
6.2.3 Analytical methods 134
6.2.4 Reactor inoculation 136
6.2.5 Experimental design 136
6.3 Results 138
6.3.1 Effects of the periodic substrate perturbation 138
6.3.2 Observation of protozoa density change 150
6.3.3 Microscopic observations 154
6.3.4 Results of genetic analysis 156
6.4 Discussion 158
6.5 Summary 162

CHAPTER 7
OPERATIONAL CHARACTERISTICS OF THE RE-ESTABLISHED MICROBIAL POPULATIONS UNDER STEADY-STATE AND SHOCK LOADING CONDITIONS 163
7.1 Introduction 163
7.2 Materials and methods 164
7.2.1 Anaerobic reactors 164
7.2.2 Substrate and nutrient solutions 164
7.2.3 Analytical methods 164
7.2.4 Experimental procedures 165
7.3 Results 167
7.3.1 Operational performance of the daughter reactors 167
7.3.2 Response of anaerobic populations to glucose and temperature shocks 177
7.4 Discussion 186
7.5 Summary 188

CHAPTER 8
CHARACTERIZATION OF MICROBIAL COMMUNITY STRUCTURE CHANGE IN RESPONSE TO LONG-TERM PERIODIC SUBSTRATE FEED BY FATTY ACID METHYLESTERS (FAME) ANALYSIS 189
8.1 Introduction 189
8.2 Materials and methods 191
8.2.1 Anaerobic reactors 191
8.2.2 Sample collection and storage 191
8.2.3 FAME extraction 191
8.2.4 FAME analysis 191
8.2.5 Numerical analysis methods 192
8.2.6 Experimental design 193
8.2.7 Nonmenclature for fatty acids configuration 193
8.3 Results 194
8.3.1 Determination of minimum sample size for FAME analysis 194
8.3.2 Characterization of microbial community structure in anaerobic reactor populations by FAME analysis 196

8.3.3 Feasibility of monitoring microbial community structure changes by FAME analysis 202
8.3.4 Effects of starvation on FAME profiles 218
8.3.5 Effects of shock loading on FAME profiles 222
8.3.6 FAME analysis results for mother and 1/1 day daughter reactor MPN samples 226
8.4 Discussion 230
8.5 Summary 235

CHAPTER 9
CONCLUSIONS AND ENGINEERING SIGNIFICANCE 236

CHAPTER 10
SUGGESTIONS FOR FUTURE RESEARCH 240

APPENDIX
A. General analytical methods 241
B. MPN enumeration method 244
C. Epifluorescence microscopy direct counting methods 248
D. Protein measurement procedure 252
E. Effects of pH and VFA concentrations on hydrogen-utilizing methanogens maximum hydrogen utilization capacity 254
F. Development of free energy equation 258
G. FAME extraction procedure 260
H. Nomenclature of cell membrane fatty acids 262

LIST OF REFERENCES 267

LIST OF TABLES

TABLE

2-1.	Reactions involved in conversion of glucose to methane.....	13
2-2.	Metabolic pathways of glucose fermentation under low and high hydrogen partial pressures.....	17
3-1.	Nutrient supply for the glucose feed anaerobic reactor (mg/10 g Glucose).....	24
3-2.	Mineral solution for the glucose feed anaerobic reactor (mg/10 g Glucose).....	24
3-3.	Characteristics of the inoculum taken from Jackson Wastewater Treatment Plant.....	26
3-4.	Batch operation results of the mother reactor.....	29
3-5.	Operation parameters used in the mother reactor step-up loading increase period.....	32
3-6.	Operational characteristics of the mother reactor under steady-state conditions.....	35
3-7.	Volumetric and specific loading rates and gas production rates during the steady-state operation.....	36
3-8.	Characteristics of the anaerobic biomass in the mother reactor during the steady-state operation.....	37
3-9.	COD/VSS ratio measured during the experimental period.....	38
3-10.	Percentage contents of carbon, nitrogen and hydrogen in volatile fraction of biological sludge observed in various different studies...	39
3-11.	COD mass balance calculation results for the baseline data acquisition period of the mother reactor.....	40
3-12.	MPN values of anaerobic microorganisms in the mother reactor evaluated using 5 tube dilution.....	41
4-1.	Concentration of the nutrients in the combined influent fed to the anaerobic reactor.....	49

4-2. Substrate concentrations applied to the mother and the daughter reactors during the maximum substrate conversion rate measurements..... 52

4-3. Summary of reactor operational results during the different stages of the perturbation period..... 63

4-4. Specific maximum substrate utilization rates observed for the mother and the re-established daughter reactor..... 67

4-5. Decay parameters of the mother and the daughter reactor cultures.. 68

4-6. Decay rates of the glucose degrader and hydrogen-utilizing methanogens in the mother and the daughter reactor cultures..... 74

4-7. Summary of protein and VSS measurement results..... 79

4-8. DTAF direct counting results for the mother and the daughter reactor cultures..... 80

4-9. Acridine orange direct counting results for the mother and the daughter reactor cultures..... 81

4-10. Summary of acridine orange and DTAF direct counting results for the mother and the 1/1 day daughter reactor cultures..... 82

4-11. MPN values of anaerobic microorganisms in the re-established daughter reactor culture..... 83

5-1. Free energy associated with the anaerobic oxidation of glucose fermentation intermediates..... 97

5-2. Summary of reactor operational results during the different stages of the perturbation experiment..... 110

5-3. Summary of non-ionized Ac and non-ionized VFA concentrations (as acetic acid) observed during the 3/3 day and 1/1 day substrate perturbations..... 114

5-4. Free energy values (KJ/mol) observed for the anaerobic oxidation of glucose metabolic intermediates during substrate perturbation.... 119

5-5. Electron equivalents (eq) of the anaerobic reactor substrate, intermediates and biomass..... 122

5-6. Electron equivalents distribution (mmol) in anaerobic reactor effluent during the three day on/ three day off long-term periodic substrate perturbation..... 122

6-1. Apparent propionate degradation rate changes during the first four substrate perturbation cycles (40 days)..... 141

6-2. Summary of reactor operational performance during the baseline steady-state and new established steady-state 146

6-3. COD and VFA accumulation rate in the beginning of the substrate perturbation 158

7-1. Experimental conditions used in the glucose and temperature shocks 166

7-2. Summary of operational performance of the mother and the daughter reactors 173

7-3. Specific maximum substrate utilization rates measured for the mother and the daughter reactor cultures 173

7-4. Baseline operation results for reactor 1/1 and m-1 177

7-5. Peak levels of glucose fermentation intermediates and other operational parameters in reactor 1/1 and m-1 during glucose shock loading tests 183

8-1. Sample volumes and equivalent biomass (as VSS) of the mother reactor culture used for minimum sampling size determination 195

8-2. Effect of sample volume on FAME analysis results 195

8-3. FAME profiles for the mother and the daughter reactor microbial populations 197

8-4. Abundance (%) of the saturated, branched, unsaturated and cyclopropyl fatty acids in the different reactor populations 198

8-5. Similarity matrix (So, %) calculated based on FAME data listed in Table 8-3 198

E-1. VFA concentrations examined in the H_2-CO_2 degradation experiment 249

LIST OF FIGURES

FIGURE

2-1.	Substrate flow for anaerobic digestion of complex organic materials...	4
2-2.	Graphical representation of hydrogen-dependent thermodynamic favorability of acetogenic oxidations and inorganic respirations associated with the anaerobic degradation of waste organics.....	10
2-3.	General outline of possible biochemical conversion occurring on anaerobic degradation of glucose.....	12
2-4.	Population dynamic control model for anaerobic acidogenesis in anaerobic digestion.....	14
2-5.	Acidogenic phase of glucose fermentation under low and high hydrogen partial pressures to form acetic acid, propionic acid, H_2 gas and CO_2.....	16
3-1.	Schematic diagram of laboratory-scale anaerobic reactor.....	22
3-2.	Tracer test results of the mother reactor.....	28
3-3.	Batch operation results for COD reduction and gas production.....	30
3-4.	Batch operation results for biomass production and pH change.....	31
3-5.	Reactor performance during stepwise loading increase period.....	34
4-1.	Experimental set up.....	47
4-2.	Substrate feeding pattern used for perturbation experiment.....	55
4-3.	VFA concentration changes during the perturbation period.....	57
4-4.	COD variation during the perturbation period.....	58
4-5.	pH change during the perturbation period.....	60
4-6.	Average gas production in the two-day cycle during the perturbation period.....	62
4-7.	Daily gas production during the substrate perturbation period.....	65

4-8. Deterioration of gas production on days when glucose was not supplied during stage 1 66

4-9. Biomass decay of the mother and the daughter reactor cultures under starvation condition 69

4-10. Estimation of biomass decay parameters for the mother and the daughter reactor cultures 70

4-11. Estimation of decay parameters for hydrogen-utilization activity in the mother and the daughter reactor cultures 72

4-12. Estimation of decay parameters for glucose degradation activity in the mother and the daughter reactor cultures 73

4-13. Protein and biomass concentration changes in the mother and the daughter reactor cultures 76

4-14. Protein and biomass concentration changes in the daughter reactor during two complete perturbation cycles 77

4-15. Protein/VSS ratio changes in the mother and the daughter reactor cultures 78

4-16. Microscopic observation of the mother (a) and daughter (b) reactor cultures 85

5-1. Schematic of the experimental set up 95

5-2. Substrate feeding pattern used for perturbation experiment 99

5-3. VFA concentration changes during the perturbation period 101

5-4. COD variation during the perturbation period 102

5-5. Hydrogen and ethanol concentration changes during the first stage of the perturbation period 104

5-6. pH change during the perturbation period 106

5-7. Gas production during the perturbation period 107

5-8. Daily gas production during the perturbation period 111

5-9. Summary of non-ionized volatile fatty acids, pH and anaerobic reactor performance 113

5-10. Changes in non-ionized VFA concentrations during the 1/1 day and 3/3 day substrate perturbation tests 115

5-11. Free energy available for the anaerobic oxidation of hydrogen and carbon dioxide, and acetate during the substrate perturbation period 117

5-12. Free energy available for the anaerobic oxidation of butyrate and propionate during the substrate perturbation period..... 118

5-13. Free energy available for the anaerobic oxidation of ethanol during the substrate perturbation period..... 120

5-14. Electron mass balance during the perturbation period..... 123

5-15. Microscopic observation of the mother (a) and the daughter (b, c) reactor cultures..... 125

6-1. Schematic of the experimental set up..... 135

6-2. Substrate feeding pattern for the 5/5 perturbation experiment..... 137

6-3. COD and VFA concentration changes during the first stage of the 5/5 perturbation experiment..... 139

6-4. Hydrogen concentration changes during the first stage of the 5/5 perturbation period..... 142

6-5. pH and non-ionized VFA concentration changes during the first stage of the perturbation period..... 144

6-6. Free energy available for the anaerobic oxidation of propionate and butyrate during the substrate perturbation period..... 145

6-7. COD and VFA concentration changes during the entire substrate perturbation period..... 147

6-8. Biomass concentration change during the substrate perturbation period..... 149

6-9. Microscopic observation of the protozoa in the 5/5 reactor culture... 151

6-10. Protozoa density changes during observation period..... 152

6-11. Changes in protozoa density and total biomass concentration under starvation condition..... 153

6-12. Microscopic observations of the mother (a), the 5/5 (b), 1/1 (c) and 3/3 (d) daughter reactor cultures..... 155

6-13. DNA analysis results for the mother and the daughter reactor cultures. 157

7-1. Recovery processes of the 1/1, 3/3 and 5/5 day daughter reactor populations..... 168

7-2. COD concentration changes in the re-established daughter reactors. 169

7-3. VSS concentration changes in the re-established daughter reactors..... 170

7-4. Hydrogen concentration pressure changes in the re-established daughter reactors 171

7-5. Gas production changes in the re-established daughter reactors 172

7-6. Effect of perturbation interval on maximum glucose and propionate utilization rates 175

7-7. Effect of perturbation interval on maximum acetate, butyrate and hydrogen utilization rates 176

7-8. Changes in (a) COD and (b) glucose concentrations during the glucose shock loading experiment 178

7-9. Changes in concentrations of glucose fermentation inter mediates for the a) m-1 and b) 1/1 reactors during the glucose chock loading experiment 180

7-10. Changes in a) hydrogen and b) biomass concentrations during the glucose shock loading experiment 181

7-11. Changes in pH observed during the glucose shock loading experiment 182

7-12. Changes in (a) temperature and (b) COD concentrations during the temperature shock experiments 184

8-1. Principal component analysis of the FAME profiles presented in Table 8-3 200

8-2. Clustering of the anaerobic reactor populations using the 1-Pearson correlation coefficient, median linkage method with FAME profiles presented in Table 8-3 201

8-3. Changes in major cell membrane fatty acids abundance during perturbation period in 3/3 day reactor populations 203

8-4. Changes in grouped cell membrane fatty acids abundance during perturbation period in 3/3 day reactor populations 205

8-5. Changes in similarity coefficient So during perturbation period in 3/3 day reactor populations 206

8-6. Principal-component analyses of the FAME profiles obtained from 3/3 day reactor populations 208

8-7. Clustering of the anaerobic reactor populations using the 1-Pearson correlation coefficient, single linkage method with FAME profiles obtained from 3/3 day reactor populations 209

8-8. Correlation between the reactor effluent COD and the similarity coefficient So, the abundance of the saturated fatty acids and the branched fatty acids 210

8-9. Changes in major cell membrane fatty acids abundance during the 5/5 day substrate perturbation period 212

8-10. Changes in grouped cell membrane fatty acids abundance during the 5/5 day substrate perturbation period 213

8-11. Changes in similarity coefficient So during the 5/5 day substrate perturbation period 215

8-12. Principal-component analysis of FAME profiles obtained from 5/5 day substrate perturbation experiment 216

8-13. Clustering of the FAME profiles obtained from 5/5 day experiment using the 1-Pearson correlation coefficient, single linkage method .. 217

8-14. Changes in grouped fatty acids abundance during the starvation period 219

8-15. Changes in similarity coefficient So during the starvation period for the mother and the 1/1 day daughter reactor cultures 220

8-16. Principal component analysis results for the FAME profiles obtained during the starvation test 221

8-17. Changes in major cell membrane fatty acids abundance during shock loading experiment 223

8-18. Changes in grouped cell membrane fatty acids abundance during the glucose shock loading test 224

8-19. Similarity coefficient changes during the glucose shock loading test 225

8-20. FAME profiles obtained from mother and 1/1 daughter reactor glucose MPN enrichment cultures 227

8-21. DNA analysis results for mother and 1/1 daughter reactor glucose MPN enrichment cultures 228

E-1. pH effect on hydrogen conversion rates 256

E-2. VFA effect on hydrogen conversion rates at pH 7.4. (a) acetate; (b) propionate; (c) butyrate 257

KEY TO ABBREVIATIONS

ADP	Adenosine diphosphate
ATP	Adenosine triphosphate
BOD	Biological oxygen demand
COD	Chemical oxygen demand
DNA	Deoxyribonucleic acid
DO	Dissolved oxygen
FAME	Fatty acid methyl esters
FID	Flame ionization detector
GC	Gas chromatography
HRT	Hydraulic retention time
MPN	Most probable number
NAD^+	Oxidized form of nicotinamide adenine dinucleotide
NADH	Reduced form of nicotinamide adenine dinucleotide
OD	Optical density
SS	Suspended solids
STP	Standard pressure and temperature
TCD	Thermal conductivity detector
VFA	Volatile fatty acid
VSS	Volatile suspended solids

Chapter 1

INTRODUCTION

Anaerobic processes have received increased application in recent years, both for the treatment of industrial wastewaters and for the conversion of biomass to methane. Despite the many advantages possessed by the anaerobic processes (McCarty, 1982), due to the inherent slow growth rate of the methanogenic and acetogenic bacteria and the complex interactions between different groups of bacteria, anaerobic systems can be sensitive to environmental changes. In engineered systems, such as anaerobic digesters, a sudden increase in the organic or hydraulic applied loading rate can result in serious operational problems including reactor failure. Long recovery periods are often required.

Many studies have examined the response of anaerobic systems to environmental perturbations, especially changes in organic loading rate (Cohen et al., 1981; Mosey et al., 1989; Hickey and Switzenbaum, 1991b, 1991c; Gupta, 1994). These studies are of three different types: (1) pulse feed experiments in which a substrate pulse is injected suddenly into an anaerobic reactor; (2) step feed experiments in which the reactor organic or hydraulic loading rate is suddenly increased to a higher level for a period of time then returned to the steady-state conditions; and (3) periodic feed experiments in which the influent substrate concentration is periodically changed.

Essentially all of the perturbation experiments described to date were performed over a relatively short time period (from a few days to a few weeks). Little is known about the effects of long-term, continuous periodic substrate perturbations on anaerobic community structure and function. This is despite the fact that long-term periodic substrate loadings are common in nature and in engineered systems.

This project was designed to investigate the response of anaerobic chemostats to long-term, continuous periodic substrate perturbations. The major objectives were to (1) demonstrate the influence of long-term, periodic substrate perturbations on anaerobic system operational, kinetic, thermodynamic and metabolic performance and (2) investigate whether long-term adaptive changes in microbial community might occur in such systems.

Chapter 2

BACKGROUND

2-1. Anaerobic degradation process

Anaerobic degradation of complex organic materials can be considered as a step-wise processes which proceeds as both successive stages and parallel reactions (McCarty, 1964; Kaspar and Wuhrmann, 1978; Zehnder, 1978; Gujer and Zehnder, 1983; Pavlostathis, 1991). The whole sequence of anaerobic degradation of organic materials can be regarded as a microbial energy web with a product produced by one bacterium being used by another. The conversion of complex organic materials to methane takes place in four stages and involves at least three groups of microorganisms (Figure 2-1). First, complex polymeric materials such as polysaccharides, proteins, and lipids are hydrolyzed into small, soluble products (amino acids, sugars and long-chain fatty acids) which can be assimilated by the bacterial cells. Second, the assimilated compounds are fermented or anaerobically oxidized to short-chain fatty acids plus hydrogen gas and carbon dioxide. In the third step, the short-chain fatty acids, mainly butyrate and propionate, are converted to acetate, hydrogen gas and carbon dioxide. Finally, methanogenisis occurs from carbon dioxide reduction by hydrogen and from decarboxylation of acetate.

The three major groups of bacteria which mediate the anaerobic degradation of organic materials are as follows: 1. Acidogenic bacteria, which include hydrolytic and fermentative bacteria (Ia and Ib); 2. acetogenic bacteria (II); 3. methanogenic bacteria, which include acetophilic and hydrogenophilic methanogens (IIIa and IIIb). In addition to the three major groups of bacteria mentioned above, several other groups of organisms

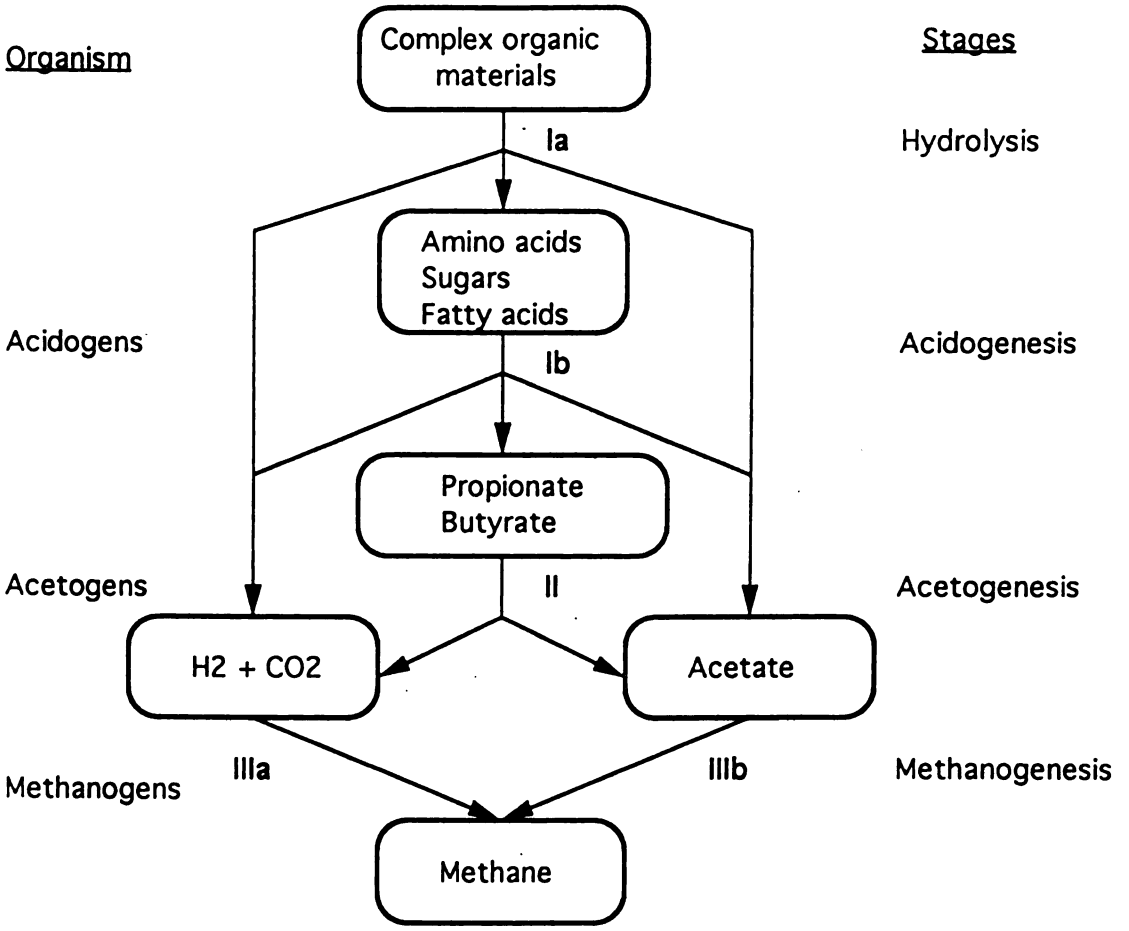

Fig 2-1. Substrate flow for anaerobic digestion of complex organic materials (adapted from Palns Sam-Soon, (1987) and Zinder (1984))

also involved in anaerobic degradation including sulfate reducing bacteria (Zeikus, 1979; Zehnder et al., 1981), homoacetogens (Zeikus, 1979; Widdel, 1988) and protozoa (Williams and Harfoot, 1976; Fenchel, 1987). Due to the limited amount of available energy and the normal environmental conditions, these organisms usually only contribute a small portion of the COD removal from anaerobic systems. Although the anaerobic microorganisms and the reactions that they mediate can be theoretically separated into several groups/stages, overall methanogenesis is strongly dependent on close interaction between the bacterial groups in each stage.

2-2. Methanogenesis

Methanogenic bacteria, which mediate the terminal step in anaerobic degradation, play the most important role in anaerobic degradation. Methanogenic bacteria are a morphologically diverse group of bacteria unified by their ability to produce methane. They possess some unique features, which distinguish them as a special group of bacteria, including the absence of peptidoglycan in the cell wall; the presence of mainly ether-linked isoprenoids rather than ester-linked phospholipids in the membranes; and the presence of unusual coenzymes such as coenzyme M, factor F_{420}, Factor F_{430}, methanopterin, and methanofuran (Jain et al. 1991). Methanogens utilize a very limited number of simple carbon compounds as carbon and energy sources for methanogenesis, i.e. acetate, H_2 plus CO_2, formate, methanol and CO.

Acetate-utilizing methanogens normally control the pH value of the fermentation by removal of acetate and formation of carbon dioxide. They are responsible for the majority of COD removal and organic compound stabilization. McCarty (1964) reported that for waste solids digestion about 70% of the COD was converted into methane via acetate decarboxylation. Based on theoretical calculations, Mosey (1981) estimated that 67% of CH_4 produced from glucose was generated by acetate decarboxylation. These organisms are quite sensitive to pH changes and grow well only within a narrow pH range of ca. 6.5 to 7.4 (McCarty, 1964; van den Berg et al., 1976; Yong and Okos, 1987). It has been

found that at a pH value about 7, the methanogens can tolerate an acetate concentration as high as ca. 6,000-7,000 mg/L without loss their normal acetate metabolic capacity. Yang and Okos (1987) published a study on pure culture of methanogens utilizing acetate at pH 7 and 35 °C, in which the optimum acetate concentrations for the methanogenic bacteria *Methanosarsina barkeri* and *Methanosarsina mazei* were 7,000 and 6,800 mg/L, respectively. Van den Berg et al. (1976) reported similar results for an acetate enrichment culture growth at pH 7 and 35 °C. In this study it was observed that acetate conversion rates were not significantly affected by acetate concentration up to 6,000 mg/L, but when the reactor pH dropped to below 6.5, methanogenic activity decreased rapidly. In a pilot study, Duarte and Anderson (1982) found that a pH level of 6.4 was critical for a continuously fed acetate catabolizing digester (35 °C, 4.5 day HRT). When reactor pH was decreased from 6.5 to 6.3, methane production decreased by 65%, even though the digester had previously operated successfully at the same acetate concentration (ca. 2500 mg/l). This inhibition of acetate metabolism was mainly attributed to the increased unionized acetic acid concentration at the lower pH (Andreson et al, 1982; Attal et al., 1988).

The acetate-utilizing methanogens function at relatively high saturation levels (the ratio of steady-state substrate utilization rate V_0 to the maximum substrate utilization rate V_{max}) compared to other anaerobic bacteria. When digesting sludge from a full-scale municipal digester (33 °C, 40 day HRT) was tested for its acetate degradation rate by spiking acetate in a lab-scale digester, the rate increased from 18.3 mg acetate/L-h at steady-state to 27.8 mg acetate/L-h at enzyme saturation conditions (Kaspar and Wuhrmann, 1978). The estimated half-saturation constant varied from 14 mg/L to 31 mg/L acetate. These results indicate, that in the full-scale digester, the acetate-degrading system was saturating ca. 50%. A similar result, ca. 45% saturation level, was reported by Valcke and Verstraete (1983) in their study of sludge fermentation. The relatively high saturation level indicates that the acetate-utilizing methanogens have limited additional capacity to handle sudden increase in substrate loading rate.

The free energy available for growth of acetate-utilizing methanogenes is relatively low. Mosey (1981) estimated that only ca. 0.5 moles of ATP can be obtained for acetate-utilizing methanogens to break down one mole acetate. The acetate-utilizing methanogens are among the slowest growing bacteria in the anaerobic microbial community with an experimentally observed growth yield of 0.01 to 0.05 g/g-acetate, and the kinetics of their growth often dominates the overall rate of anaerobic reactions (Harper and Pohland, 1985; Lin et a., 1986). Due to the inherent characteristics mentioned above, the acetate-utilizing methanogenes are sensitive to environmental changes, and long periods are likely to be required for this group of bacteria to adjust to new environmental conditions.

The hydrogen-utilizing methanogens contribute to ca. 20% to 30% of methane production depending on original substrate composition (Pavlostathis and Giraldo-Gomez, 1991). In spite of the quantitative methane production, interspecies hydrogen transfer and utilization is far more important function of these methanogens since it regulates the rate of H_2-producing reactions by controlling the partial pressure of hydrogen. In anaerobic systems no other compounds can so quickly change system thermodynamic conditions like molecular hydrogen (or formate). Under inhibitory or surge loading conditions, the hydrogen partial pressure can increase by several orders of magnitude within a few hours (Harper and Pohland, 1985; Smith, 1987; Mosey and Fernandez, 1989; Bae and McCarty, 1993). This can seriously inhibit or stop acetogenic reactions, and significantly change fermentation intermediate distribution in anaerobic digesters. In well-operating systems, the hydrogen partial pressure is maintained within a relatively low range of ca. 30 to 200 ppm (gas phase) by hydrogen-utilizing methanogens, which is necessary for many anaerobic reactions to occur (Mosey, 1983; Lovely, 1985; Cord-Ruwisch, 1988; Zinder 1990; Bea and McCarty, 1993).

The hydrogen-utilizing methanogens are relatively fast growing species, with estimated doubling time of 4 to 12 hours (Gujer and Zehnder, 1983; Archer and Powell 1985; Mosey and Fernandes, 1989; Pavlostathis et al., 1990). They have been found to be

resistant to elevated concentrations of VFA. Hobson and Shaw (1978) reported that at a pH of 7.1, an acetate or butyrate concentration up to 10,000 mg/L (as acetic acid) did not inhibit *M. formicicum*, the principal hydrogen-utilizing bacterium in a piggery-waste digester. Experimental results also indicate that the H_2-utilizing methanogens are also quite resistant to changes in pH values. A optimum pH range of 5.4 to 7.2 was reported for hydrogen-utilizing methanogens in digester sludge by Attal et al. (1988). Kasper and Wuhrmann (1978) reported that under steady state condition the saturation level of the hydrogen-utilizing methanogens in a mature digester was only about 1%. Similar results have also been reported by Shea et al. (1968). There is, therefore, a vast extra utilization capacity available for increased H_2 oxidation during surge loading conditions. These characteristics endow the hydrogen-utilizing methanogens with the ability to quickly and effectively respond to changes in environmental conditions. Prolonged hydrogen accumulation is rarely observed under organic-hydraulic perturbation experiments (Smith and McCarty, 1989; Mosey and Fernandes, 1989; Hickey and Switzenbaum, 1991c).

2-3. Acetogenesis

The anaerobic oxidation of short chain fatty acids and ethanol is an important stage in anaerobic degradation, because no methanogens have been found to acquire the ability to directly utilize these fermentation intermediates (Zeikus, 1977). Nineteen species of sytrophic acetogens have been identified so far, including five species capable of converting butyrate and the others capable of converting propionate and higher VFAs (Li et al., 1994). Enrichment culture studies indicate that acetogens growth relatively slowly even under optimum conditions, with estimated minimum doubling time of 1.5-5.0 days (Lawrence and McCarty, 1969; Gujer and Zehnder, 1983; Heyes and Hall, 1983; Lin et al., 1986).

The reactions mediated by acetogens are thermodynamically unfavorable under standard conditions. In order for these reactions to proceed, it is necessary for the reaction products (acetate and H_2) to be present at sufficient low concentrations to yield a negative

value for the actual available free energy change ($\Delta G^{o'}$) under physiological concentrations (Thauer et al., 1977). Thermodynamically related product inhibitions have been illustrated by experimental observations (Heyes and Hall, 1981; Kaspar and Wuhrmann, 1989; Hickey and Switzenbaum, 1991c; Smith and McCarty, 1989). Ahring and Westerman (1987) reported that a hydrogen partial pressure in the gas phase up to 2×10^{-2} atm could completely block butyrate degradation. Dwyer et al. (1988) found that removal of acetate from the butyrate rich media increased the butyrate degradation rate. Mosey (1981) reported a reactor failure which was directly related to thermodynamic inhibition of hydrogen to propionate degradation. As shown in Figure 2-2, thermodynamic calculations associated with acetogenic and methanogenic reactions indicate that in order for anaerobic degradation to proceed for all the important anaerobic fermentation intermediates the hydrogen partial pressure in the digester headspase (assuming equilibrium with the liquid phase) must be maintained in a narrow range of ca. 10^{-4} to 10^{-6} atm. Actually, in well operated anaerobic systems the hydrogen partial pressure has been found to be within a range of ca. 4×10^{-5} to 2×10^{-4} atm (Kaspar and Wuhrmann, 1978; Heyes and Hall, 1983; Mosey, 1983b; Smith, 1987). This is sufficient low so that butyrate and propionate oxidation is energetically favored.

The number of acetogens existing in an anaerobic process has been reported dependent upon the feeding schedule of a given reactor and its associated stability history (Harper and Pohland, 1985). Following a shock loading or other process upset, the proportion of acetogens will increase to accommodate accumulated short chain fatty acids. In contrast, under steady-state conditions, the number of electrons channeled through propionic and butyric acids can be greatly decreased (Palns, 1987; Mosey 1981), and the number of acetogens will decrease accordingly. Considering the inherent slow growth rate of acetogenic bacteria, this dynamic situation is essential for understanding the effects of environmental perturbations on the overall stability and efficiency of anaerobic systems, especially during transient accumulation and recovery stages (Fongastitkul et al. 1994).

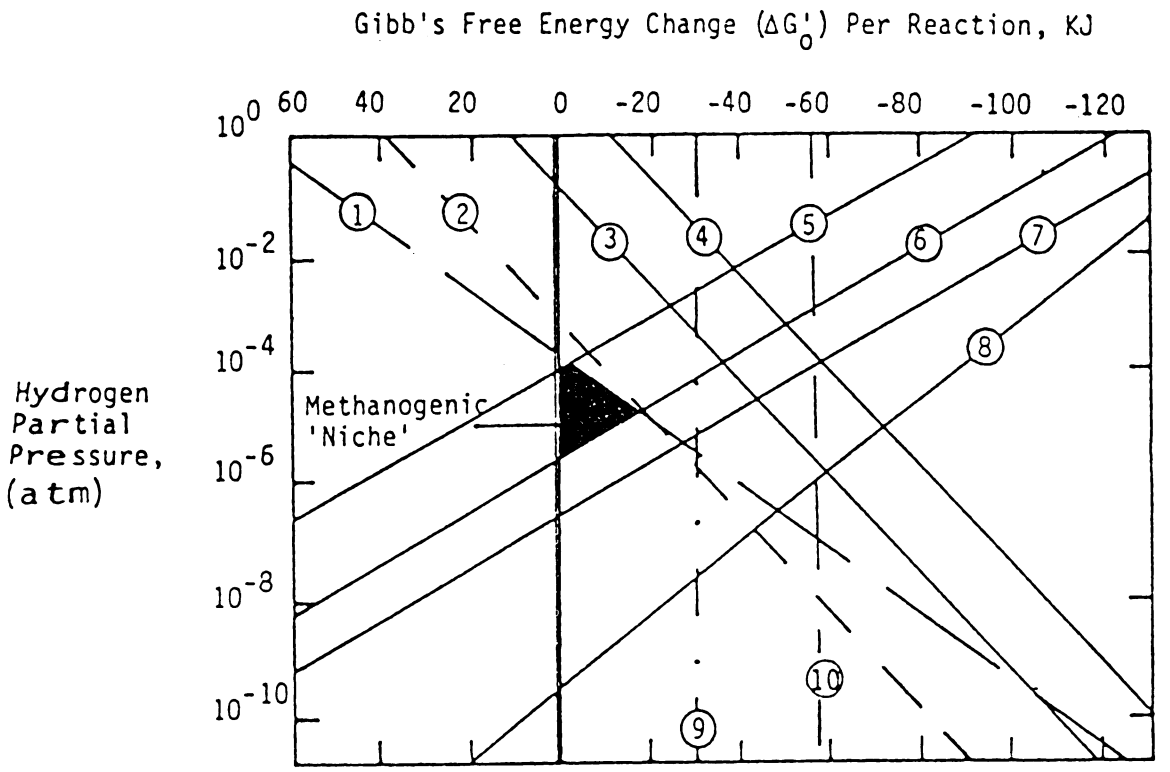

Fig 2-2. Graphical representation of hydrogen-dependent thermodynamic favorability of acetogenic oxidations and inorganic respirations associated with the anaerobic degradation of waste organics. (1) Propionic acid oxidation to acetic acid. (2) Butyric acid oxidation to acetic acid. (3) Ethanol to acetic acid. (4) Lactic acid to acetic acid. (5) Acetogenic respiration of bicarbonate (CO_2). (6) Methanogenic respiration of bicarbonate (CO_2). (7) Respiration of sulfate to sulfide. (8) Respiration of sulfite to sulfude. (9) Methanogenic cleavage of acetic acid. (10) Sulfate reducing bacteria mediated cleavage of acetic acid. Acetic acid, 25 mM; propionic, butyric, lactic acids, and ethanol, 10 mM; bicarbonate, 20 mM, methane, 0.7 atm. After Harper and Pohland (1985).

With further research and exploration, it can be regarded as one of the key considerations to stabilizing and improving anaerobic treatment.

2-4. Anaerobic fermentation of glucose

In this study a simple carbohydrate, glucose, was used as the sole energy and carbon source. Studies on methane fermentation of glucose using ^{14}C tracers have shown that glucose fermentation primarily involves the Embden-Meyethof-Parnas pathway (Jeris and McCarty, 1962). After glycolysis, pyruvate is formed which can be fermented by a number of pathways (Kisaalita et al., 1989; Linden, 1989). The most important metabolic routes of anaerobic decomposition of glucose can be assembled in a general outline, showing the three degradative stages (Figure 2-3). The major intermediates produced from glucose fermentation are acetate, butyrate, propionate, ethanol and gaseous products of H_2 (and CO_2). These fermentation intermediates are eventually converted to methane and carbon dioxide via subsequent acetogenic and methanogenic stages. The most important reactions, which may occur during glucose anaerobic degradation, are depicted in Table 2-1 (Thauer et al., 1977).

For acidogenic bacteria, the reaction which converts glucose into acetate, is preferred one. It provides the acid-forming bacteria with the largest energy yield for growth and provides methanogens with their prime substrates. In spite of this, significant changes in distribution of glucose fermentation intermediates are often observed, especially under stressed conditions (Zoetemeyer et al., 1982a, 1982b; Cohen et al., 1983; Harper and Pohland, 1986; Bae and McCarty, 1993). In a chemostat glucose acidogenesis experiment, Cohen et al. (1983) recognized the existence of two glucose fermentation routes which occurred complementary to each other. The so called "butyric acid type" fermentation is characterized by production of acetate, butyrate, carbon dioxide and hydrogen as the main fermentation products; while the "propionic acid type" fermentation is characterized by the formation of acetate, propionate, and carbon dioxide, with much lower hydrogen

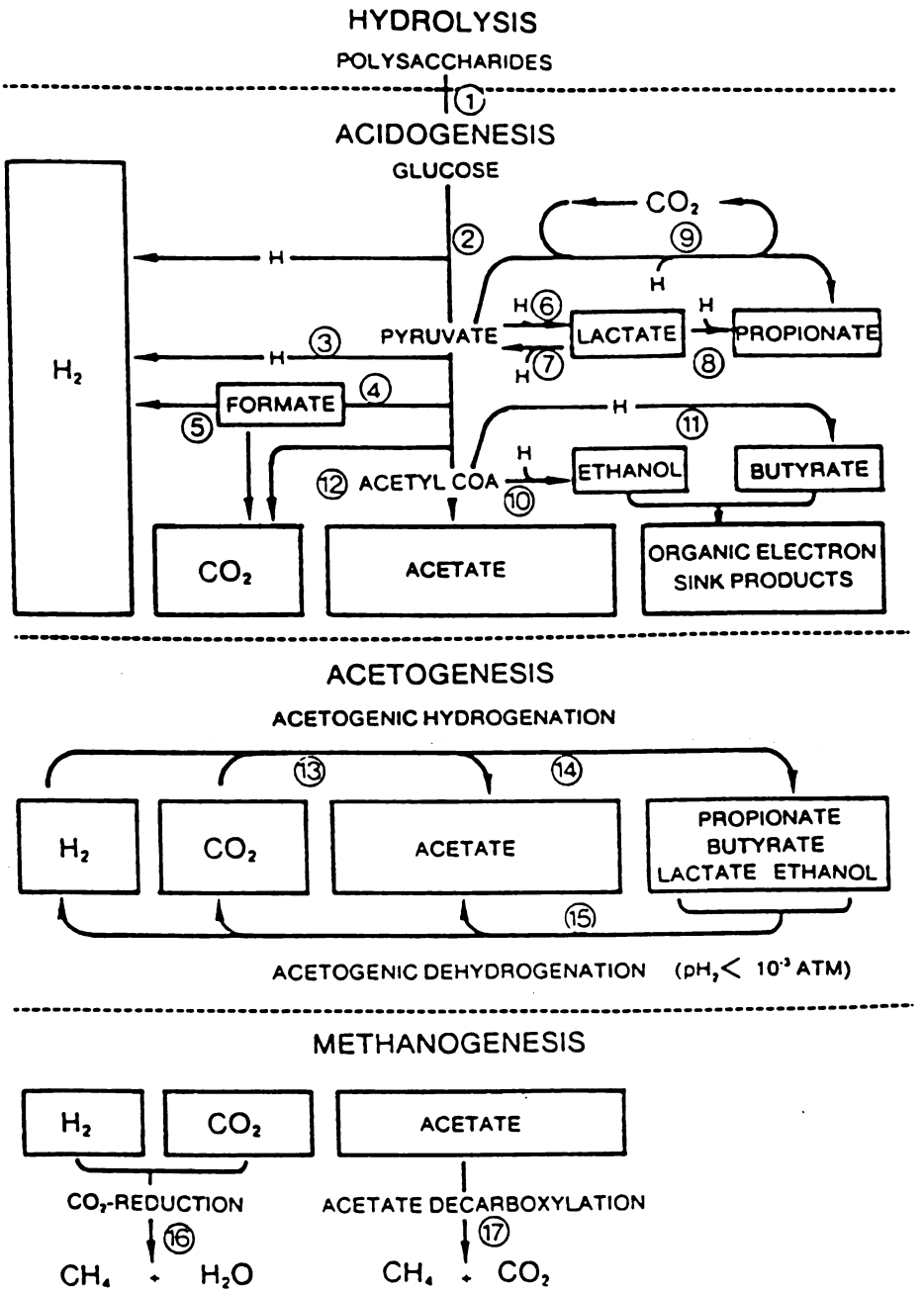

Figure 2-3. General outline of possible biochemical conversion occurring on anaerobic degradation of glucose. After T. Cohen (1982).

Table 2-1. Reactions involved in conversion of glucose to methane

	$\Delta G^{o'}$ (KJ)
1. Acidogenic reactions	
(1) $C_6H_{12}O_6 + 4H_2O = 2CH_3COO^- + 4H^+ + 2HCO_3^- + 4H_2$	-206.0
(2) $C_6H_{12}O_6 + 2H_2O = CH_3CH_2CH_2COO^- + 3H^+ + 2H_2 + 2HCO_3^-$	-255.0
(3) $C_6H_{12}O_6 = 4/3CH_3CH_2COO^- + 2/3CH_3COO^- + 8/3H^+ + 2/3HCO_3^-$	-220.0
(4) $C_6H_{12}O_6 + 2H_2O = 2CH_3CH_2OH + 2H^+ + 2HCO_3^-$	-226.0
2. Acetogenic reactions	
(5) $CH_3CH_2OH + H_2O = CH_3COO^- + H^+ + 2H_2$	9.6
(6) $CH_3CH_2COO^- + 2H_2O = CH_3COO^- + 3H_2 + CO_2$	76.1
(7) $CH_3CH_2CH_2COO^- + 2H_2O = 2CH_3COO^- + 2H_2 + H^+$	48.1
3. Methanogenic reactions	
(9) $CH_3COO^- + H^+ = CH_4 + CO_2$	- 35.8
(8) $4H_2 + CO_2 = CH_4 + 2H_2O$	-130.7

concentrations. The two different types of glucose fermentation were assumed to be carried out by different fermentation species.

Based on observation of VFA accumulation patterns during overload and recovery periods, McCarty and Mosey (1991) proposed a population dynamics model for anaerobic acidogenesis of carbohydrates. In this model the anaerobic fermentation of carbohydrates is proposed as competition between "propionic" and "butyric" bacteria (Figure 2-4). According to this model, under normal operating conditions (low concentration of hydrogen and modest organic loading rate) butyrate forming bacteria will directly produce acetate plus CO_2 and H_2, so that the maximum free energy can be

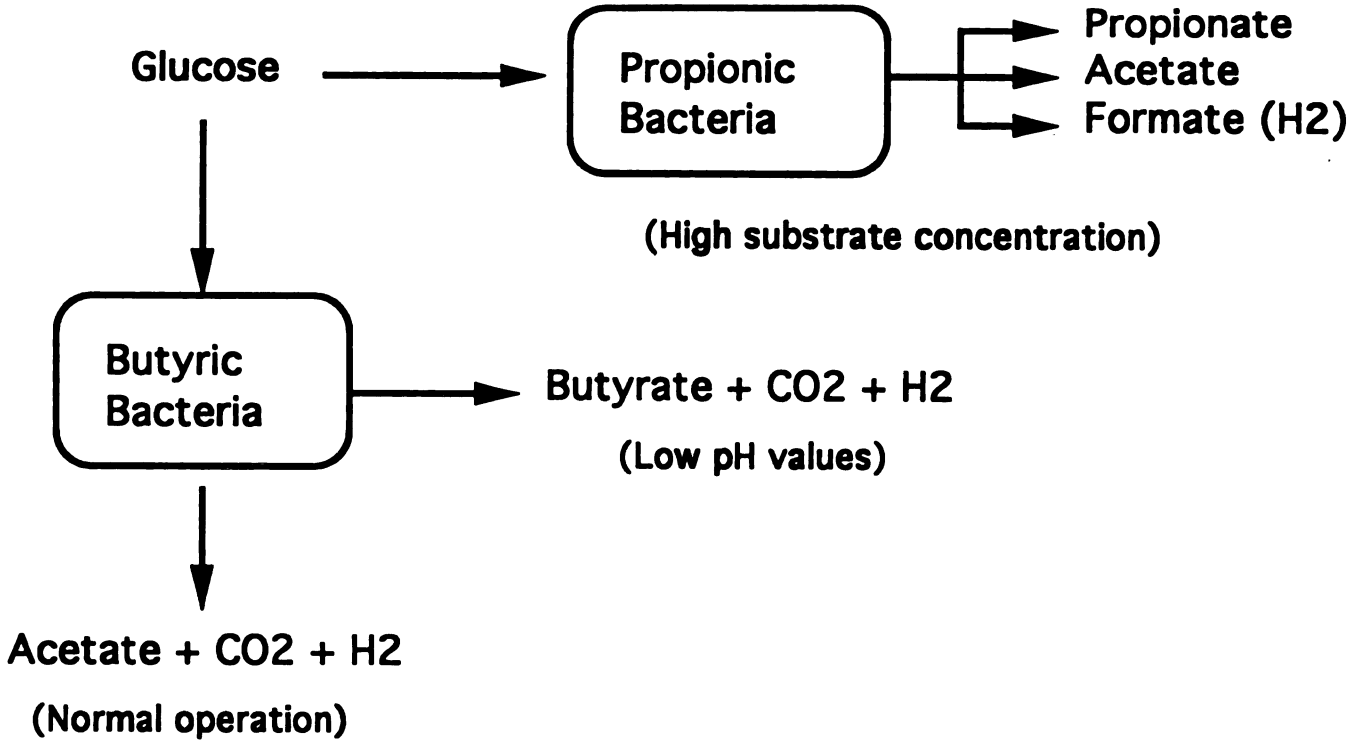

Figure 2-4. Population dynamic control model for anaerobic acidogenesis in anaerobic digestion. After McCarty and Mosey (1991).

obtained. At low pH, the butyric forming bacteria will produce butyrate plus CO_2 and H_2 to reduce the production of protons. As proposed by this model, the propionic bacteria become predominant only under surge loading conditions (high substrate concentration). The main fermentation products would be propionate, acetate and formate. Although this model generally agreed with experimental observations, as the authors noted, this model, which was deduced from digester operational performance, remains to be rigorously tested.

Based on thermodynamic calculations, Duarte and Anderson (1982) proposed that under normal conditions (pH 7 and temperature of 35 °C), the butyrate type fermentation is thermodynamically more favorable than the propionate type fermentation. Palns Sam-soon et al. (1987) proposed two alternative glucose acidogenesis metabolic pathways based on biochemical and thermodynamic considerations (Figure 2-5). According to Palns Sam-soon, depending on digester hydrogen partial pressure the acidogenesis of glucose could go through either of the two alternative metabolic pathways as shown in Table 2-2. Pathway I is the favorable metabolic pathway employed by acidogens. Four moles of ATP can be generated from one mole glucose metabolized. However, this pathway is available for acidogens only under low hydrogen partial pressure ($< 10^{-4}$ atm.). Under conditions of stress, a shift in the metabolic pathway to pathway II could occur, resulting in a shift towards more propionate production.

A model using a regulator function based on concentrations of hydrogen gas in digester headspace was developed by Mosey (1983) to simulate accumulation and decay of the major volatile fatty acids during hydraulic overload and recovery in a glucose fed digester. In this model, the hydrogen partial pressure is assumed to be directly linked to the NADH regeneration and, therefore, regulates the acidogenic reactions at several points in the glycolytic pathway. By providing a framework to thermodynamically relate hydrogen accumulation to the rate of acidogenic and acetogenic reactions, this model is a good start in helping to uncover how these systems operate. But as mentioned by the

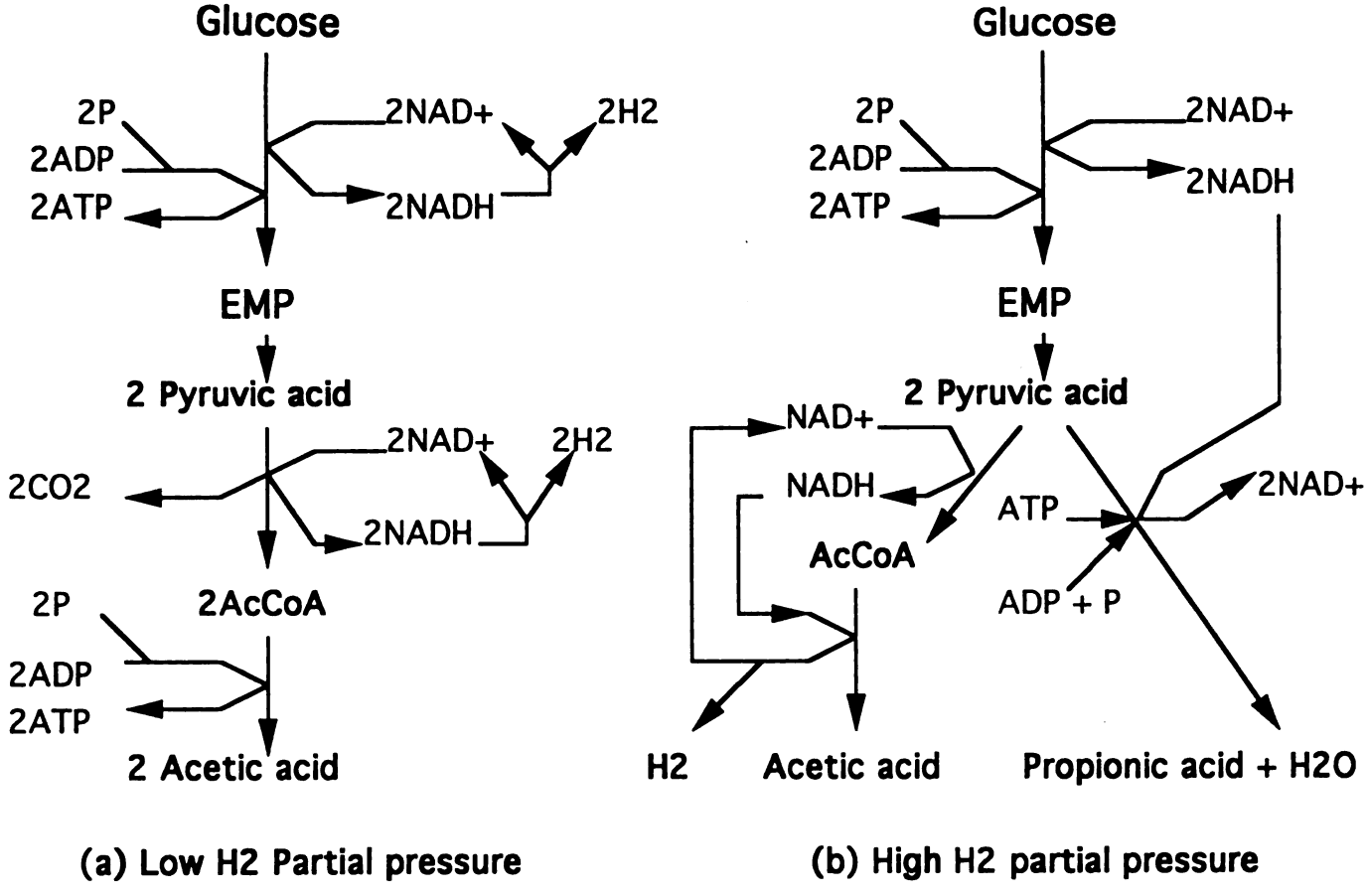

Figure 2-5. Acidogenic phase of glucose fermentation under low and high hydrogen partial pressures to form acetic acid, propionic acid, H_2 gas and CO_2. After Palns Sam-soon et al. (1987). Abbreviations: EMP: Embden-Meyerhof pathway; AcCoA: Acetyl coenzyme A; P: inorganic phosphate.

Table 2-2. Metabolic pathways of glucose fermentation under low and high hydrogen partial pressures, after Palns Sam-soon et al. (1987)

Pathway I (Low hydrogen partial pressure):

$C_6H_{12}O_6 + 2NAD^+ + 2ADP + 2P = 2CH_3COCOOH + 2NADH + 2ATP$ (1)

$2NADH = 2NAD^+ + 2H_2$ (2)

$2CH_3COCOOH + 2NAD^+ = 2CH_3CoA + 2CO_2 + 2NADH$ (3)

$2CH_3CoA + 2ADP + 2P = 2CH_3COOH + 2ATP$ (4)

Overall:

$C_6H_{12}O_6 + 2H_2O + 2NAD^+ + 4ADP + 4P = 2CH_3COOH + 2CO_2 + 4H_2 + 4ATP$

Pathway II (High hydrogen partial pressure):

$C_6H_{12}O_6 + 2NAD^+ + 2ADP + P = 2CH_3COCOOH + 2NADH + 2ATP$ (1)

$CH_3COCOOH + 2NADH + ADP + P = CH_3CH_2COOH + 2NAD^+ + ATP + H_2O$ (2)

$CH_3COCOOH + NAD^+ = CH_3CoA + CO_2 + HADH$ (3)

$CH_3CoA + NADH = CH_3COOH + H_2 + NAD^+$ (4)

Overall:

$C_6H_{12}O_6 + 3ADP + 3P = CH_3CH_2COOH + CH_3COOH + CO_2 + H_2 + 3ATP$

---

author and other researchers, this theoretical model, which only considers the effect of hydrogen partial pressure on glucose metabolic processes, has limited use in modeling behavior of acidogenesis (McCarty and Mosey, 1991) and probably acetogenesis (Hickey and Switzenbaum, 1991c).

Due to the complexity of the glucose fermentation routes, the interactions, and the microorganisms involved, no single theory or model proposed to date can be used to correctly predict the response of anaerobic populations to sudden loading rate changes. For example, the effect that accumulation of acetate may have on the fermentation route has not been clearly delineated. More experiments are, therefore, necessary to acquire a

better understanding of the mechanisms of glucose (and other sugars and starches) fermentation.

2.5. Ecological point of view of anaerobic degradation

The anaerobic bacteria form a special "energy web" which is different from the classical food chains, (1) the grazing food chain and (2) the later developed detritus food chain. As generally defined by Ehrlich (1985), the food chain formed by anaerobic microorganisms, may be described as a "dissimilatory food chain" with the "stepwise decomposition of complex organic molecules to simpler organic molecules by different organisms at successive trophic levels". The microorgamisms in this food chain can be characterized as more diverse redox cycles, specialized extracellular enzymes and uptake systems, and unique types of interspecific cooperation. This food chain may be named as "solutivory" food chain as proposed by Tiedje et al. (1995), because the majority of the carbon and energy sources transferred in this food chain is in soluble phase; or it may be named as "waste web" as proposed by Dolfing and Prins (1996), because in this web waste products rather than the organisms of one trophic level serve as the substrate for the organisms on the next trophic level. Perhaps the most appropriate name is the anaerobic "energy web".

The major difference between this energy web and the conventional food chains is that the different trophic levels in anaerobic systems work in concert for the benefit of each other rather than in competitive or predatory fashion as is typical of food chains. Therefore the relationships of the different trophic groups in this food chain can be described as synergism or mutualism (Atlas and Bartha, 1987). For example, acetogenesis and methanogenesis are two of the major trophic levels in this dissimilatory energy web. The acetogenic bacteria provide the methanogenic bacteria their prime substrates, while the methanogenic bacteria maintain the hydrogen partial pressure within the narrow range suitable for acetogenic metabolism to effectively proceed (McCarty, 1983). In anaerobic systems the mutualistic relationships between acetogens and methanogens are so strong

that the acetogens can not be cultured without H_2-utilizing methonogens or some other methods to keep the H_2 partial pressure low (McInerney et al., 1979; Thiele and Zeikus, 1988). In this unique energy web, competition occurs within each trophic group (or guild) rather than between guilds.

The other major characteristics of the dissimilatory energy web is the weak balance between different trophic groups. Variations in chemical, physical or biological conditions can cause adaptive changes in the associated microbiological populations. This may include changes in bacterial metabolism at the enzymatic level, or growth or decay of certain physiologically active parts of the population. An illustrative example of the complexity of adaptive alterations, after changes in substrate composition, was presented by Hattingh et al. (1967). Under stressed conditions, the failure of one trophic group may cause collapse of the whole anaerobic community. Considering this, exploring the response of different anaerobic trophic groups to environmental perturbations is an interesting topic in microbial ecology. The results of such study could provide insight into the relationships between diversity and stability of microbial communities, an old puzzle in microbial ecology.

Chapter 3

CULTIVATION OF ANAEROBIC CULTURE IN LAB-SCALE ANAEROBIC REACTOR FED WITH GLUCOSE AS SOLE ENERGY AND CARBON SOURCE

3.1 INTRODUCTION

Start-up of anaerobic reactors is a critical step towards successful application of anaerobic treatment systems. Although hundreds of anaerobic systems have been set up and put into operation, due to the complexity of the wastes involved and the variety of anaerobic systems that exist, start-up is largely based on laboratory- or pilot-scale assessment of the particular waste to be treated. Variables such as design loading rate (g COD/L-d), expected conversion (percentage COD removal), nutrient requirement, nature of target organic waste and inoculation source, have significant effects on anaerobic system start-up and steady-state operation (Lettinga et al. 1983; Hickey et al, 1991a; Alphenaar et al, 1993). Consequently , it is difficult to generalize start-up procedures with respect to the practical design of an anaerobic digester for a particular waste under particular environmental conditions.

This chapter details experimental results obtained from a 15 L working volume anaerobic chemostat (the "mother" reactor) operated at a hydraulic retention time (HRT) of 10 days (dilution rate of 0.1 d^{-1}), organic loading rate of 0.85 g COD/L-d and temperature of 35 ^{o}C. Glucose was fed as the sole carbon and energy source. The mother reactor was inoculated with digester sludge taken from Jackson, MI, wastewater treatment plant. During the start-up period, a stepwise loading increase method was employed, in which the substrate concentration and flow rate were gradually increased in several steps until the designed steady-state operation conditions of 10 day HRT and 0.85 g COD/L-d organic

loading rate were achieved. The steady-state operational performance data of the mother reactor were collected and compared with other lab and industrial reactors.

The continuously operated mother reactor served as inoculum source for the daughter reactors in the following long-term periodic substrate perturbation experiments. The mother reactor also served as a stable control by which to compare changes in activity levels and in microbial community with daughter reactors.

3.2 MATERIALS AND METHODS

3.2.1 Laboratory-scale anaerobic reactor

A schematic diagram of the continuous feed anaerobic system is presented in Figure 3-1. A polycarbonate culture vessel (Nalge Company, Rochester, NY), approximately 25 cm in diameter and 35 cm in height, having a liquid working volume of 15 liters and a headspace of ca. 5 liters, was used as the anaerobic reactor. Mixing energy was supplied by a magnetic stir bar inside the reactor. The stir bar was driven by a Corning Model PC-520 magnetic stir plate (Corning Inc., Corning, New York) at a speed of 400 rpm.

Continuous feed was introduced into the reactors from feed reservoir by a Watson-Marlow Model 502E peristaltic pump (Watson Marlow Inc. Wilmington, MA) at a constant flow rate of 1.5 liters per day. The mineral nutrient free, sodium bicarbonate buffered glucose solution was stored in a feed reservoir. The mineral nutrient solution was directly injected into the reactor using a 60 ml plastic B-D syringe (Becton Dickinson & CO., Rutherford, NJ) mounted on a Harvard Model 22 syringe infusion pump (Harvard Apparatus, South Natick, MA). Nutrients were supplied separately to minimize growth in the glucose feed reservoir.

Effluent exited the reactor through an inverted U-shaped, air tight, water seal effluent tube to prevent the reactor contents from being exposed to oxygen. Liquid samples were taken from a sampling port which was located at the mid-point of the reactor liquid phase. An airtight gas bag was connected to the reactor headspace to balance the gas pressure when a large amount of liquid sample was removed from the reactor.

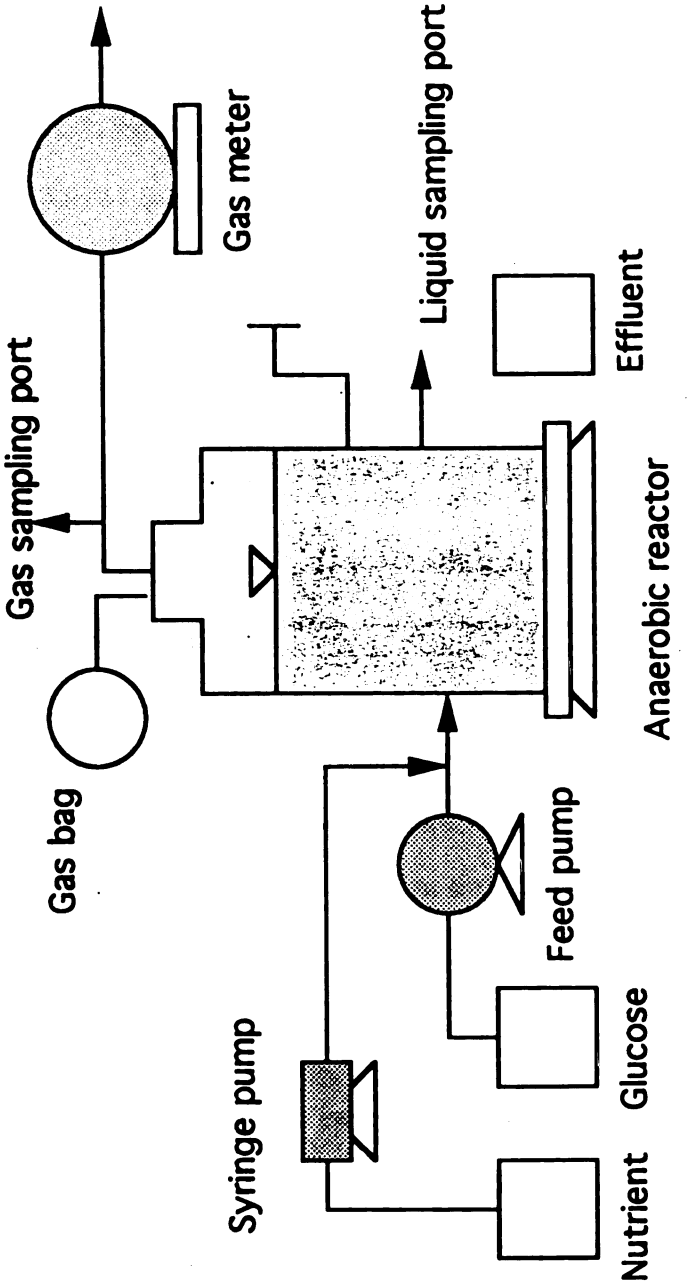

Figure 3-1. Schematic diagram of laboratory-scale anaerobic reactor

Biogas collected from the top space of the anaerobic reactor was measured using a Precision Scientific, Wet Test gas meter (Precision Scientific Co., Chicago, IL) and discharged. A glass sampling box with septum was connected to the reactor gas outlet for gas sampling.

This constant loading reactor (the "mother" reactor) served as inoculum source for the small-scale daughter reactors used for the substrate perturbation experiments. The "mother" reactor also served as a stable control by which to compare changes in activity levels and microbial community structure in the daughter reactors. The entire system was installed in a constant temperature room (35 ± 0.5 °C) located in the Environmental Engineering Teaching Lab, Michigan State University.

3.2.2 Substrate

Glucose was supplied as the sole carbon and energy source. Analytical reagent grade granular glucose (Mallinckrodt Specific Chemical Co., Paris, KE) was used to prepare the 8 g/L glucose solution. Sodium bicarbonate was added to the feed to provide buffer for pH control. A buffer solution, prepared with reagent grade powder sodium bicarbonate (J, T. Baker Inc., Philipsburg, NJ), was mixed with the above glucose solutions to obtain 7 g/L N_aHCO_3. Both the glucose solution and the sodium bicarbonate buffer solution were prepared with deionized water.

3.2.3 Nutrients

Mineral nutrients for this experiments were selected based on the compounds and their concentrations used by several researchers (Zoetemeyer et al. 1988, Zehnder et al. 1987, and Cohn et al. 1982). The nutrients supplied for 10 g glucose is shown in Tables 3-1 and 3-2. Stock solutions were prepared by dissolving the proper mass of each chemical in 1 liter volumetric slask with D. I. water such that 1 ml of stock solution is equivalent to 1 gram glucose in the feed. In order to dissolve the salts in the stock nutrient solution, the pH was reduced by the addition of 30 ml concentrated HCl per 1.0 liter

Table 3-1. Nutrient supply for the glucose feed anaerobic reactor (mg/10 g Glucose)

Element	Conc.(mg)	Salts (mg)	Formula	Stock Conc.(g/L)
N	350	1340	NH_4Cl	134
P	78	340	KH_2PO_4	34

Table 3-2. Mineral solution for the glucose feed anaerobic reactor (mg/10 g Glucose)

Ion	Conc.(mg)	Salts (mg)	Formula	Stock Conc.(g/L)
K^+	97.8	340	KH_2PO_4	34.0
SO_4^{2-}	38.4	70	Na_2SO_4	7.0
Mg^{2+}	7.35	64	$MgCl_2.4H_2O$	6.4
Ca^{2+}	0.2	0.72	$CaCl_2.2H_2O$	0.07
Fe^{3+}	1.39	6.9	$FeSO_4.7H_2$	0.692
Zn^{2+}	0.41	0.8	$ZnCl_2$	0.08
Cu^{2+}	0.08	0.22	$CuCl_2.2H_2O$	0.042
Co^{2+}	0.15	0.61	$CoCl_2.6H_2O$	0.061
BO_3^{3-}	0.08	0.084	H_3BO_3	0.008
MoO_4^{2-}	0.003	0.0041	$Na_2MoO_4.H_2O$	0.0023
Mn^{2+}	0.71	2.18	$MnSO_4.H_2O$	0.218
Ni^{2+}	0.20	0.81	$NiCl_2.6H_2O$	0.032

of s

sol

the

wa

12.

C

gas p

Co. (

M

mix

12.5

M

prob

load

expec

does

utiliz

nature

Sam

Archi

Archi

Archi

Archi

Mecha

Mech

Mech

of stock nutrient solution. The stock nutrient solution was stored at 4 °C. This stock solution was diluted to prepare the nutrient feed solution for the anaerobic reactor. Both the stock nutrient solution and the feed nutrient solution were prepared with deionized water.

3.2.4 Analytical methods

General analytical methods used in this chapter are described in Appendix A. Total gas production was measured with a Precision Wet Test gas meter (Precision Scientific Co., Chicago, IL).

Microscopic observations were performed using an Olympus BH-2 phase contrast microscope (Scientific Supply Company, Schiller Park, IL 60176).

3.2.5. MPN enumeration method

Microbial populations for anaerobic reactor sludge were enumerated using the most probable number (MPN) technique in sealed pressure tubes. All the tubes contained the basal medium (9 ml) buffered with 20 mM phosphate and 20 mM bicarbonate, respectively, substrate and 1.0 mM sodium sulfide as a reductant. The headspace of the tubes was pressurized to 20 psig using a N_2-CO_2 (95:5) gas mixture except tubes for H_2-utilizing methanogens, which were pressurized with a 20 psig H_2-CO_2 (80:20) gas mixture.

Samples were withdrawn from the anaerobic reactor and injected into prepared anaerobic tubes using a 22-gauge needle and glass syringe. These anaerobic samples were then diluted serially from 10^{-1} to 10^{-11} using 5 tubes for each dilution. The pressure tubes were incubated at 35 °C for 60 days. Preparation and sterilization of medium and dilution of samples were performed under an oxygen-free nitrogen atmosphere.

Methane production (> 0.5 mM CH_4) was checked by gas chromatography to establish whether or not the tubes were positive for methanogens and acetogens. Hydrolytic and fermentative bacterial populations were enumerated in the tubes containing

th

T

an

in

co

MF

3.2

Jac

inc

Tabl
Jack

Para

Colo
pH
SS
VSS
VSS/
C %
H %
N %

the basal medium with 2 g/L of glucose. The tubes were incubated at 37 °C for two weeks. Tubes were scored as positive on the basis of increase in optical density (> 0.2) at 650 nm and production of volatile fatty acids (> 5 mM total VFA), when compared with non-inoculated control tubes.

The MPN values and 95% confidence limits were calculated by using a MPN index computation table in Standard Methods (APHA, 1989). A more detailed description of MPN enumeration is provided in Appendix B.

3.2.6 Inoculum material

The inoculum for the mother reactor was anaerobic digester sludge taken from the Jackson Wastewater Treatment Plant (Jackson, Michigan). The characteristics of the inoculum are shown in table 3-3.

Table 3-3. Characteristics of the inoculum taken from Jackson Wastewater Treatment Plant

Parameter	Value
Color	black
pH	7.4
SS (g/L)	17.3
VSS (g/L)	9.8
VSS/SS (%)	56.6
C (% of ash free dry weight)	51.5
H (% of ash free dry weight)	8.2
N (% of ash free dry weight)	5.9

3.3 RESULTS

3.3.1 Mixing characteristics of the mother reactor

The mother reactor was designed to operate as a completely-mixed stirred tank reactor (CSTR) without recycle. In order to illustrate the mixing characteristics of the reactor, a methyl blue dye tracer test was performed. In this test 1.5 ml concentrated methyl blue dye was injected into the reactor as an impulse and samples were then continuously collected from reactor effluent port at a pre determined time schedule. The collected samples were immediately transferred into 1.5 ml Standard polystyrene curettes (Life Science Products, Inc., Denver, Colorado) and the adsorption of the samples was obtained using a Perkin Elmer Lambda 6 UV/VIS spectrophotometer (Perkin-Elmer Co., Norwalk, CT) at a wavelength of 425 nm against D. I. water. The dye concentrations were obtained from a dye adsorption-concentration calibration curve prepared prior to the experiment. The effect of methyl blue dye adsorbed to the inner wall of the reactor was negligible.

The data obtained from the tracer test along with the theoretical curve of an ideal CSTR (Levenspiel, 1972) is shown in Figure 3-2. The good fit of the experimental data with theoretical suggests that the mixing behavior of the mother reactor is close to an ideal CSTR.

3.3.2 Reactor start-up

The digester sludge added to the "mother" reactor was first passed through a 2 mm screen to remove coarse debris, and then diluted with tap water to obtain a VSS concentration of 1 g/L. The reactor liquid phase was continuously purged with nitrogen gas during inoculation to prevent the anaerobic microorganisms from being exposed to oxygen.

After inoculation, a fast start-up operation was unsuccessfully attempted. During this unsuccessful start-up operation, the reactor was operated at an inlet glucose concentration of 8 g/L and hydraulic retention time of 15 days. Failure was caused by a rapid glucose to

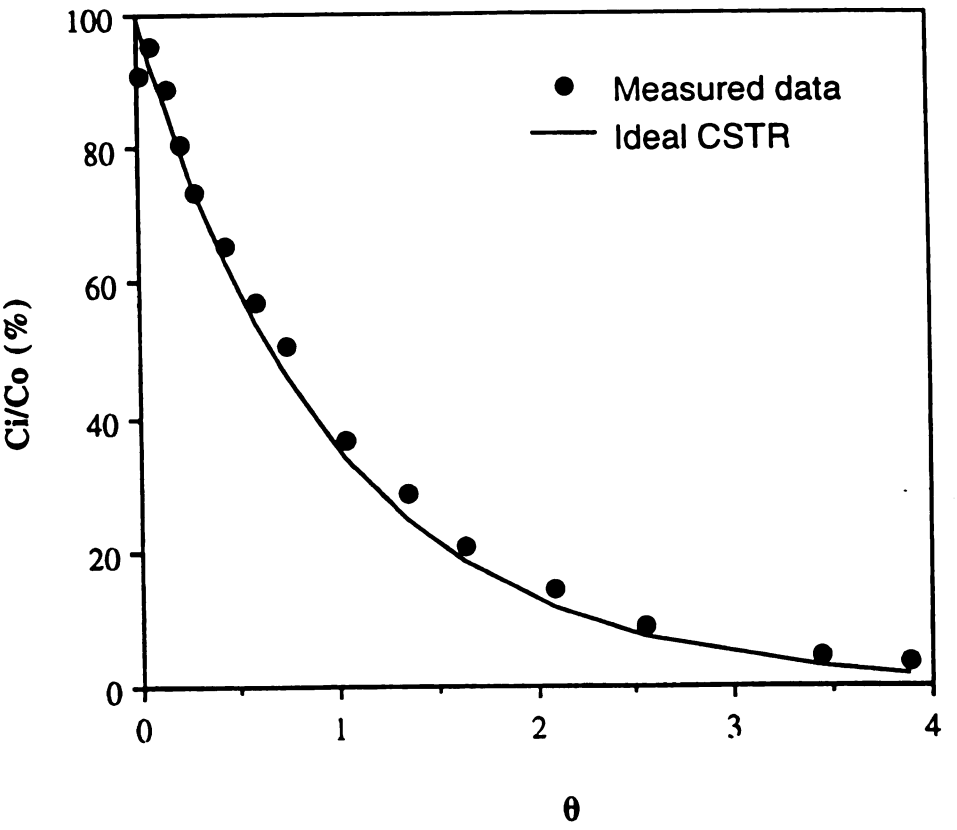

Figure 3-2. Results obtained from the mother reactor tracer test

methane and carbon dioxide. The average daily COD reduction rates observed after the three consecutive batch feeding operations indicated increasing methanogenic activity. During batch operation the reactor pH ranged from 6.9 to 7.2. accumulation of VFA accompanied by a sharp decrease in reactor pH and gas production. Under this condition the reactor soon became a so called "stuck" reactor (McCarty, 1982) with poor COD removal efficiency (< 20%). Attempts to effect a quick recovery of the reactor failed.

Subsequently a combined batch and stepwise increase in the organic loading rate was employed for start-up. It took ca. 150 days to complete the start-up process in this reactor including ca. 45 days of batch operation. Initially, 5 grams glucose was added into the reactor re-inoculated with active anaerobic microorganisms. When continuous gas production and COD reduction were observed, three batch feeding operations were subsequently performed. In the first run, 20 grams glucose was injected into the reactor. For the following two operations 35 grams of glucose was injected into the reactor. Proper amounts of buffer and nutrient solutions were also added

Variations of COD, gas production, VSS and pH in the reactor during batch operation are illustrated in Figure 3-3 and 3-4, respectively. The experimental data obtained from batch operations are presented in Table 3-4. Close to stoichiometric amounts of gas

Table 3-4. Batch operation results of the mother reactor

Parameters	Run 1	Run 2	Run 3
Amount of glucose addition (g)	20	35	35
Operation time (days)	15	16	13
Initial COD (mg/L)	1490	2470	2640
Final COD (mg/L)	160	220	310
Total gas production (L)[1]	14.2	25.9	25.3
Final VSS (mg/L)	880	890	910
Final pH	7.12	7.04	7.10
COD reduction rate (mg/L-d)	90	140	180

1: Gas production under standard condition (0 °C and 1 atm)

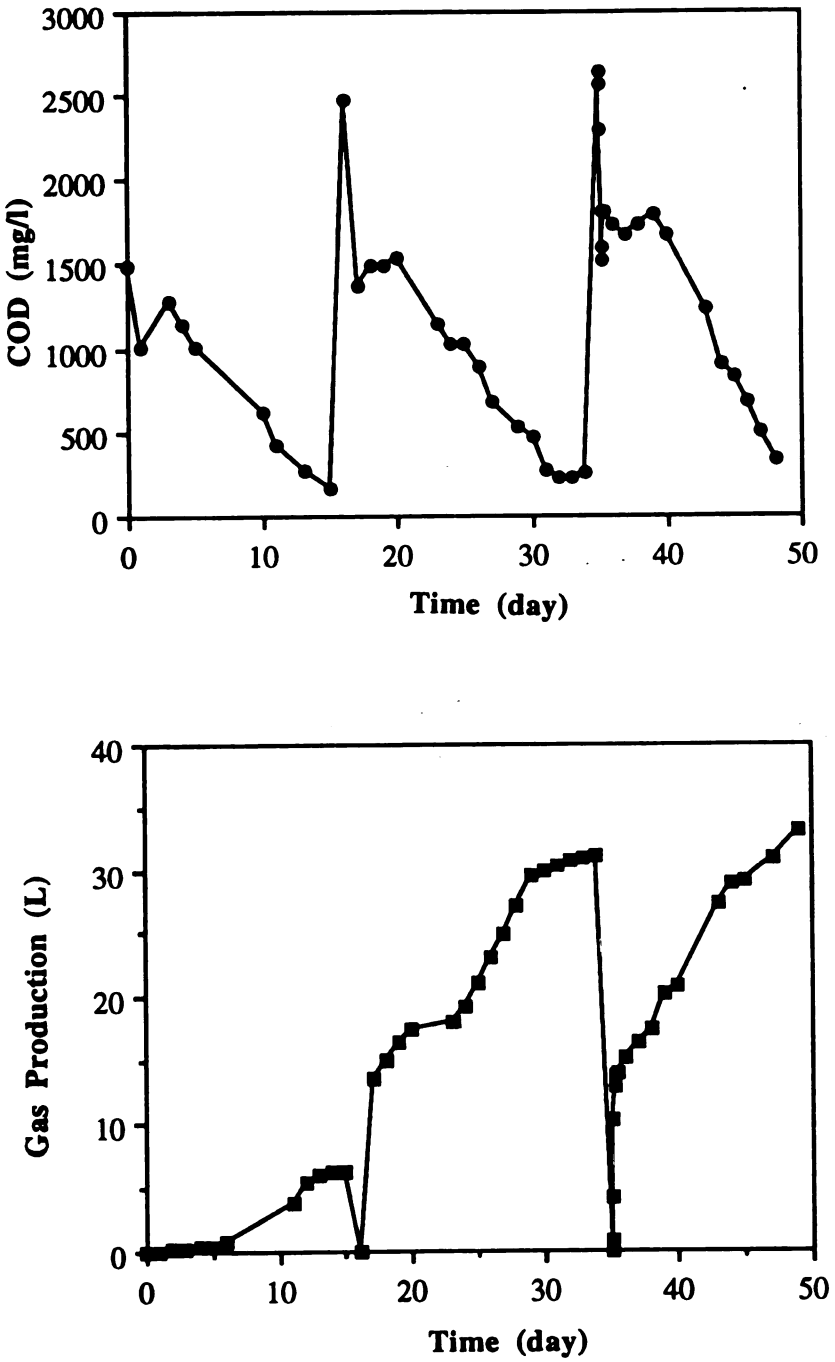

Figure 3-3. Batch operation results for COD reduction and gas production

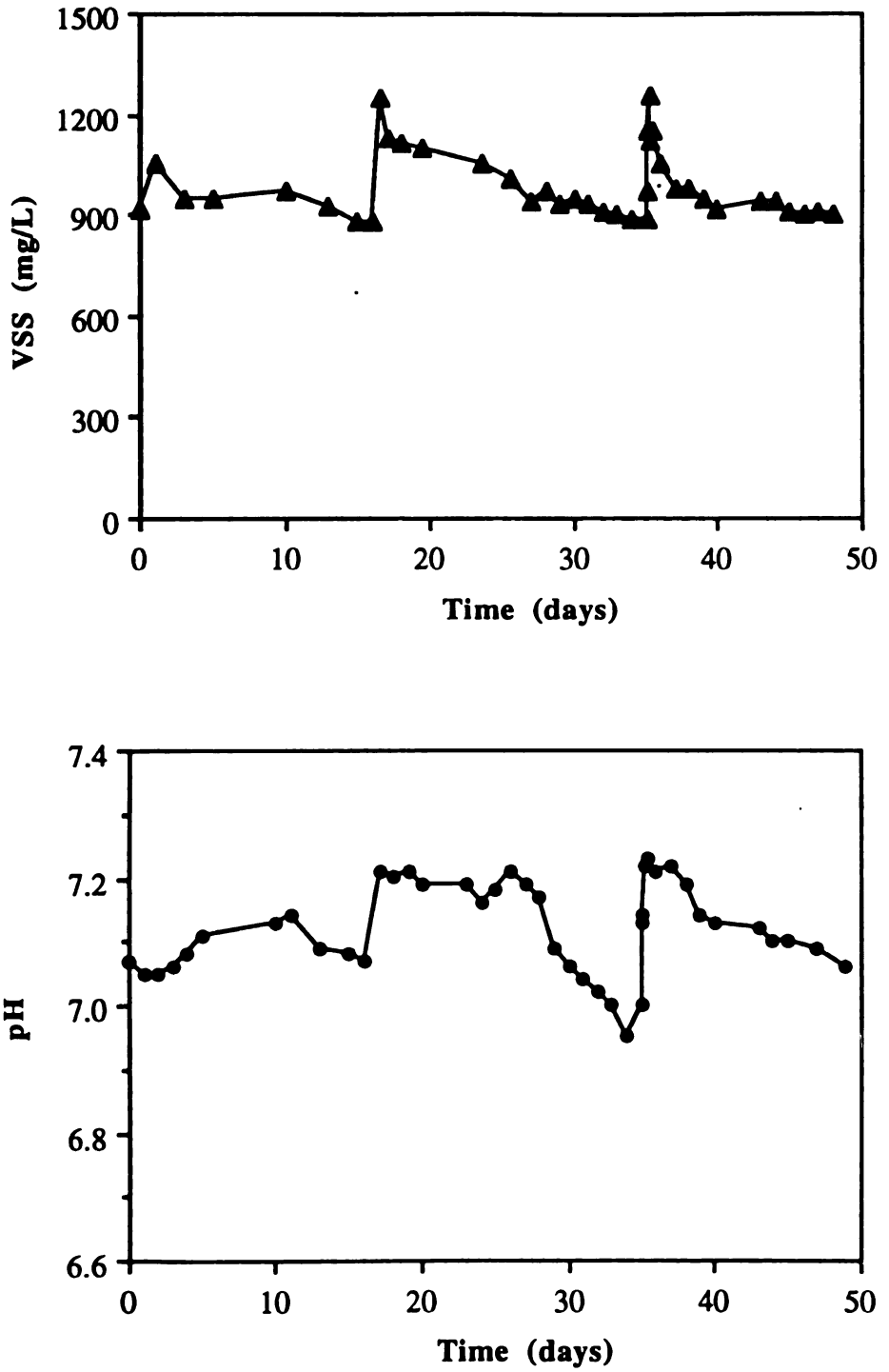

Figure 3-4. Batch operation results for biomass production and pH change

production were observed during batch operation. This indicates complete conversion of glucose to methane and carbon dioxide. The average daily COD reduction rates observed after the three consecutive batch feeding operations indicated increasing methanogenic activity. During batch operation the reactor pH ranged from 6.9 to 7.2.

Following the third batch feed, the reactor was switched to continuous feed mode. An initial inlet glucose concentration of 4 g/L and hydraulic retention time of 20 days was used. Under this condition the reactor had a volumetric COD loading rate of 0.21 g/L-d, which was close to the average daily COD utilization rate of 0.18 g/L-d obtained in the last run of the batch operation. After that, an increase in either the glucose feed concentration or reactor flow rate (Table 3-5) was employed when the system appeared able to accommodate increased loading rates. About 110 days were required to reach the desired operating conditions of 8 g/L glucose feed and 10 day HRT. By the end of the start-up period, a new community had been established in the reactor. Theoretically less than 0.1% of the original inoculum remained after over 7 HRTs. After that, analyses of the contents reflected only biological activity resulting from utilization of the glucose fed to the reactor.

Table 3-5. Operation parameters used in the mother reactor step-up loading increase period

No.	HRT (days)	Glucose feed (g/L)	Loading rate (COD g/L-d)
1	20	4	0.21
2	20	6	0.32
3	15	6	0.42
4	15	8	0.56
5	10	8	0.85

Operational data including influent and effluent COD concentrations, COD removal efficiency and volumetric COD loading rate, are illustrated in Figure 3-5. The pH in the reactor was maintained between 6.8 to 7.1, with the alkalinity ranging from 2,300 to 4,400 mg/L (as $CaCO_3$). During the stepwise loading increase period, no glucose was detected in the reactor liquid phase (< 0.5 mg/L).

3.3.3 Reactor operational performance under steady-state conditions

After start-up, the reactor was continuously operated at an inlet glucose concentration of 8 g/L, temperature of 35 °C and hydraulic retention time of 10 days. Once steady-state conditions were established in the reactor, as indicated by consistent effluent COD and VSS concentrations and gas production, the steady-state baseline operation parameters of the mother reactor were intensively collected and analyzed over a period of ca. 50 days. The information collected during this period included influent and effluent COD, pH, SS and VSS, gas production and gas composition, and VFA concentrations. No significant variations were noted for any of the parameters measured during the baseline information collection period. The baseline experimental data are summarized in Table 3-6. The calculated volumetric and specific loading rates and gas production rates are presented in Table 3-7. The yield of bacteria was 0.156 (g VSS formed/ g COD consumed) or 0.165 (g VSS formed/g glucose consumed). Glucose was not detected in the effluent (< 0.5 mg/l) throughout the experimental period.

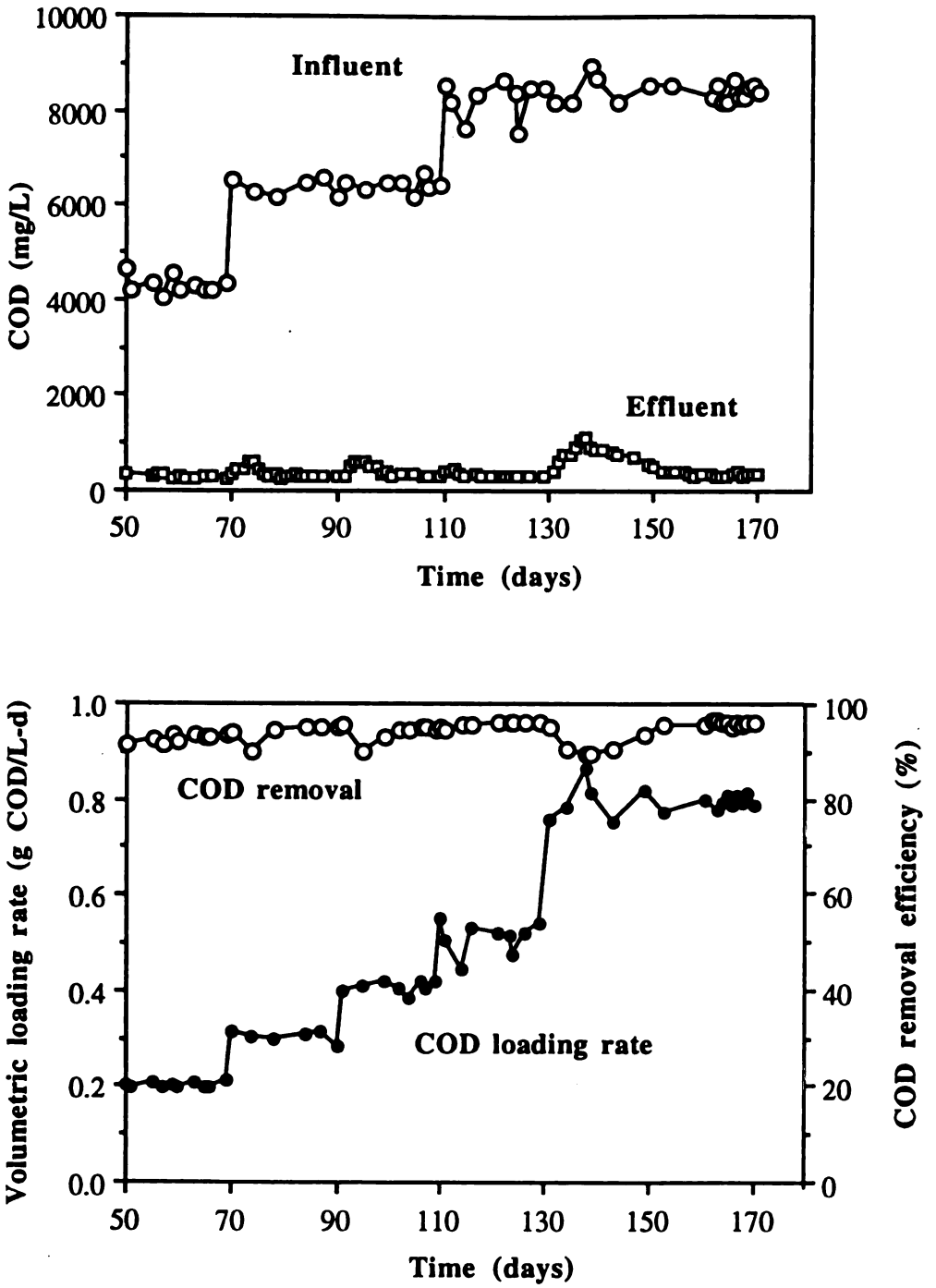

Figure 3-5. Reactor performance during stepwise loading increase period

Table 3-6. Operational characteristics of the mother reactor under steady-state conditions

Parameter	Value	No of observations
COD_{in} (mg/L)	8400 ±250[1]	30
COD_e (mg/L)	320 ±40	30
COD removal (%)	96.2	
pH	7.03 ±0.05	45
SS (g/L)	1.34 ±0.11	33
VSS (g/L)	1.26 ±0.11	33
VSS/SS (%)	94.0	
Gas production (ml/L-d)	430[2] ±60	45
CH_4 (%)	51 ±2	15
H_2 (ppm)	37 ±7.8	15
Alkalinity (mg/L as $CaCO_3$)	3800 ±80	30
Acetate (mg/L)	120 ±50	20
Propionate (mg/L)	12 ±5	20
Butyrate (mg/L)	4 ±3	20

1. Standard deviation
2. Value presented at 273 K, 1 atm.

Table 3-7. Volumetric and specific organic loading rates and gas production rates during steady-state operation

Parameter	Value
Volumetric Loading rate (g COD/L-d)	0.85
Specific Loading rate (g COD/g VSS-d)	0.68
Volumetric gas production (ml/L-d)	438
Specific gas production (ml/g VSS-d)	348
Volumetric methane production (ml/L-d)	223
Specific methane production (ml/g VSS-d)	178
Gas production (ml/g-COD)	522
Gas production (ml/g-glucose)	554
Methane production (ml/g-COD)	265
Methane production (ml/g-glucose)	282

3.3.4 Biomass characteristics

Results of eight independent elemental analysis of the biological solids in the mother reactor are presented in Table 3-8. Based on the average content of the elemental carbon, hydrogen, nitrogen and oxygen in the ash-free volatile fraction of the anaerobic sludge, an empirical chemical formula of the anaerobic biomass in the mother reactor was:

$$CH_{1.7}O_{0.4}N_{0.2} \qquad (3\text{-}1)$$

Based on this empirical formula, the oxidation reaction of the biomass in the mother reactor can be written as:

$$CH_{1.7}O_{0.4}N_{0.2} + 1.075\ O_2 = CO_2 + 0.2\ NH_3 + 0.55\ H_2O \qquad (3\text{-}2)$$

$$22.9 \quad + \quad 34.4 \quad = \quad 44 \quad + \quad 3.4 \quad + \quad 9.9$$

Based on equation (3-2), to completely oxidize one mole biomass, which has a theoretical molecular weight of 22.9 g, 1.075 moles of oxygen is required, which gives a COD/VSS ratio of 1.5 (g/g). This theoretically calculated COD/VSS ratio was confirmed by experimentally measured COD/VSS ratio. As shown in Table 3-9, an averaged

COD/VSS ratio of 1.515 ± 0.177 (g/g) was obtained from 18 groups of independently measured data.

The empirical formula of anaerobic solids found in this study compared closely with empirical formulations of anaerobic and aerobic biological solids reported in the literature. The elemental content of carbon, nitrogen and hydrogen in the ash-free (volatile) fraction of various anaerobic and aerobic biomass reported in the literature are compared to those obtained in this study in Table 3-10.

Table 3-8. Characteristics of the anaerobic biomass in the mother reactor during steady-state operation

	Elemental content in ash-free dry weight (%)				
	Carbon	Hydrogen	Nitrogen	Oxygen[1]	Ash (%)
1	52.29	7.83	9.59	30.29	5.1
2	51.55	7.80	9.34	31.31	7.7
3	53.40	7.44	10.30	28.86	6.6
4	51.85	7.44	10.20	30.51	5.4
5	53.69	7.70	10.60	28.01	6.2
6	54.56	7.67	10.92	26.85	5.5
7	54.41	7.68	10.53	27.38	8.1
8	54.02	7.69	10.45	27.84	5.4
Ave.	53.22	7.66	10.24	28.88	6.3
Std[2]	1.10	0.14	0.49	1.53	1.1

1. Estimated
2. Standard deviation

Table 3-9. COD/VSS ratio measured for the mother reactor

No	COD_T	COD_e	COD_{VSS}	VSS	COD/VSS
1	1854	439	1415	840	1.685
2	1756	366	1390	880	1.580
3	1805	341	1464	980	1.493
4	1902	341	1561	840	1.858
5	1805	292	1513	1000	1.513
6	1902	341	1561	900	1.734
7	1854	293	1561	1100	1.419
8	2000	293	1707	1060	1.610
9	1658	546	1112	940	1.183
10	1756	530	1226	1020	1.202
11	2000	585	1415	987	1.433
12	2000	415	1585	920	1.722
13	1902	488	1414	1020	1.386
14	1951	463	1488	1080	1.378
15	2000	536	1464	910	1.609
16	2000	463	1564	1100	1.422
17	1951	536	1415	920	1.538
Ave.	1888	428	1462	970	1.516
Std.	±101	±97	±135	±83	±0.176

Table 3-10. Percentage contents of carbon, nitrogen and hydrogen in volatile fraction of biological sludges observed in various different studies

C Content in VSS (%)	N	H	Formulae	Substrate	Reference
51.2	11.7	8.2	$CH_{1.9}O_{0.4}N_{0.2}$	glucose	1
50.4	12.8	7.3	$CH_{1.7}O_{0.4}N_{0.2}$	glycerol	2
47.4	10.7	7.1	$CH_{1.8}O_{0.6}N_{0.2}$	glucose	3
48.6	10.8	7.0	$CH_{1.7}O_{0.5}N_{0.2}$	Starch	3
45.2	11.1	6.4	$CH_{1.7}O_{0.6}N_{0.2}$	Glycine	3
45.4	10.6	7.6	$CH_{2.0}O_{0.6}N_{0.2}$	Acetate	3
53.2	10.2	7.7	$CH_{1.7}O_{0.4}N_{0.2}$	Glucose	This study

1: Cohen (1982)
2: Herbert (1975)
3: Speece (1964)

3.3.5 Mass balance calculation for the baseline steady-state period

Removal efficiency and loading rates shown in Figure 3-5 and Table 3-6 were based upon the COD concentration in the feed and on the average COD of the solids-free effluent. As a check on the reliability of the data, a mass balance was made based on the COD input to the system and the COD output from the system. The feed glucose was the only source of COD input, while the effluent and methane were the two sources of COD output. By determining the effluent COD which included the solids-free dissolved COD and the COD equivalents of effluent solids and methane, a COD balance was made for the entire baseline operation period and is recorded in Table 3-11. Based on this calculation, an overall COD recovery of ca. 102% was achieved.

The mass balance calculation results show that of the total COD removed from the glucose fed mother reactor, ca. 77 percent was converted to methane and 23 percent was converted to biomass. This result was in good agreement with theoretically predicted

Table 3-11. COD mass balance calculation results for the baseline data acquisition period of the mother reactor

Total COD input[1]	12.570 g/d
Effluent soluble COD	0.479 g/d
COD equivalent of biomass[2]	2.835 g/d
COD equivalent of methane	9.557 g/d
Total COD output	12.871 g/d
COD recovery (%)	102

1: Calculated based on measured average influent COD concentration.
2: Calculated based on the theoretical COD/VSS ratio of 1.5/1 obtained in this study.

glucose conversion ratio of 75/25 (methane/biomass based on COD) in anaerobic methane fermentation (Mosey, 1981).

3.3.6 MPN enumeration results

When the anaerobic reactor reached its steady-state condition at a HRT of 10 days and a glucose feed concentration of 8 g/L, most probable number (MPN) enumeration was performed to determine some measure of the microbial community structure. The results of MPN enumeration for different microbial trophic groups in the glucose fed anaerobic reactor culture are presented in Table 3-12.

Based on the MPN values, the major microorganisms in the glucose fed anaerobic reactor were fermentative bacteria. Fermentative bacteria contributed ca. 69% of the total culturable microbial populations present. H_2- and acetate-utilizing methanogens contributed about 10% of the population. Sytrophic acetogens contributed ca. 21% of population measured via the MPN test. Based on the MPN results, the number of total anaerobic bacteria was estimated to be ca. 1.3×10^{11} cells/g VSS.

Table 3-12. MPN values of anaerobic microorganisms in the mother reactor evaluated using 5 tube dilution ($x10^8$/ml)

		95% confidence limits ($x10^8$/ml)	
Substrate	MPN ($x10^8$/ml)	lower	upper
Glucose	1.10	0.40	3.00
Acetate	0.13	0.05	0.39
Butyrate	0.17	0.07	0.48
Propionate	0.17	0.07	0.48
Hydrogen	0.028	0.012	0.07

3.3.7 Microscopic examination

The digester sludge used for inoculation was black in color with large amount of microbial flocks and organic and inorganic particles. A vast number of different mophotypes were present. Biomass in the steady-state mother reactor was white in color and consisted of well-separated dispersed cells. Differences in the microbial composition of these cultures were easily observed using phase contrast microscopy. The predominant morphologies in the steady-state mother reactor culture were long filamentous rods and short rods.

3.4 DISCUSSIONS

It has been noted that in complex microbial habitats, such as anaerobic reactors, the composition of the microbial community depends on the type and amounts of substrates supplied (Toerien, 1966; Hattingh, 1967). When the composition of the substrate supplied is changed, a change in the composition of the microbial population will occur (Chynoweth and Mah, 1977). Due to the significant differences in growth rates of the various anaerobic microorganisms, adaptation will not be rapid. In the present study, the failure of a "fast start-up" attempt indicates that the inoculated community, which was acclimated to convert biomass to methane, did not quickly adapt to the new substrate. A significant imbalance among the different trophic groups occurred.

In view of this, a combined batch and stepwise increased loading strategy was employed. As proposed by Barford (1989), this start-up method is essentially an empirical "trial and error" procedure. This start-up strategy performed more smoothly and effectively. The start-up procedure of the mother reactor was completed within ca. 150 days, including ca. 50 days of batch operation. This start-up time is reasonable compared with similar anaerobic reactor start-up operations (Bae and McCarty, 1993). It has been reported that, depending on inoculation materials and target compounds, two to six months can be required for start-up of anaerobic reactors (Barford, 1989; Hickey et al, 1991a). If the inocula for reactor start-up is not adapted to the target compounds, as in the present study, longer times can be expected (Hattingh, 1967).

Under steady-state conditions, a specific loading rate of 0.67 g COD/g VSS-d and a COD removal efficiency of 96% was achieved in the mother reactor. These values are relatively high when compared with values obtained from other lab-scale anaerobic reactors operated under similar conditions (Speece and McCarty, 1964; Cohen et al., 1980). The operational performance data obtained from the mother reactor during the intensive data collection period are therefore, valid reference points for comparison to the following periodic substrate perturbations.

3.6. SUMMARY

The combined batch-stepwise start-up procedure employed in this study is a workable approach to start-up glucose-fed anaerobic reactors. By this method a stable microbial community was established within ca. 150 days.

Under steady-state conditions (temperature of 35 °C, HRT of 10 days and organic loading rate of 0.85 g COD/L-d) the following operational performance data were obtained in the mother reactor: COD removal of 96%, Gas Production of 430 ml/L-d, VSS of 1.26 g/L and methane content of 50% in the biogas. An empirical biomass elemental formula of $CH_{1.7}O_{0.4}N_{0.2}$ was obtained from this study.

Compared with other lab-scale anaerobic reactors, the mother reactor was operated under optimum conditions with relatively high specific loading rate and COD removal efficiency. Reactor performance data obtained in this study are used as references for the following long-term periodic substrate perturbation studies.

Chapter 4

RESPONSE OF ANAEROBIC COMMUNITY TO A LONG-TERM ONE DAY FEAST-ONE DAY FAMINE PERIODIC SUBSTRATE PERTURBATION

4.1 INTRODUCTION

Methane fermentation results in the conversion of organic materials to methane and carbon dioxide in the absence of molecular oxygen. Conversion of carbohydrates, fats and proteins to methane requires the combined activity of fermentative, acetogenic, and methanogenic bacteria (Novaes, 1986; Pavlostathis, 1991). Due to the inherent slow growth rate of methanogenic and acetogenic bacteria, anaerobic systems can be sensitive to environmental changes (Lawrence, 1967). In engineered systems, such as anaerobic digesters, a sudden increase in the organic or hydraulic applied loading rate can result in serious operational problems including reactor failure-long recovery periods are often required (McCarty, 1964; McCarty and Mosey, 1991; Fongastitkul et al, 1994). As a result, anaerobic systems, and particularly suspended growth systems, are sometimes characterized as difficult to operate (Ross and Smollen, 1981).

Many studies have examined the response of anaerobic systems to environmental perturbations, especially changes in organic loading (Cohen et al, 1981; Pavlostathis and Giraldo-Gomez, 1981; Hickey and Switzenbaum, 1991b, 1991c; Gupta et al, 1994; Fox and Suidan, 1996). These studies are of three different types: (1) pulse feed experiments in which a substrate pulse is injected suddenly into an anaerobic reactor; (2) step feed experiments in which the reactor organic or hydraulic loading rate is suddenly increased to a higher level for a period of time then returned to the steady-state condition; and (3) periodic feed experiments in which the influent substrate concentration is periodically

changed. Fongastitkul et al. (1994) conducted a combined hydraulic-organic overloading test in a two phase UASB reactor to investigate system feasibility, maximum loading capacity and system failure and recovery. Using a lab scale anaerobic reactor Hickey and Switzenbaum (1991c) examined the acetate accumulation and its subsequent effect on the build-up of other volatile fatty acids during step feed organic and hydraulic perturbation experiments. Following a series of pulse feed perturbations, Smith and McCarty (1988) studied energetic and reaction-rate interactions between hydrogenic and hydrogentrophic bacteria. The response of anaerobic populations to a periodically fed skimmed-milk solution was studied by Mosey and Fenader (1981) using a lab-scale digester. These perturbation experiments have provided useful information on the response of anaerobic populations to sudden environmental changes, the upset and recovery patterns, and kinetic and thermodynamic changes.

Essentially all of the perturbation experiments described to date were performed over a relatively short time period (from a few days to a few weeks). Little is known about the effects of long-term, continuous periodic substrate perturbations on anaerobic community structure and function. This is despite the fact that long-term periodic substrate loadings are common in nature and in engineered systems. Examples include aquifer environments subject to tidal influence, the rumen, high rate anaerobic processes treating effluents from food processing, agriculture, and other industries.

In order to determine whether long-term adaptive changes might occur in anaerobic systems, a long term (> 200 days) periodic substrate perturbation was applied to an anaerobic chemostat. In this experiment, identical steady-state communities were established in a "mother" and a "daughter" reactor. After reaching steady-state, the daughter reactor was subjected to a periodic organic loading pattern in which the influent glucose concentration was alternately varied from 16 g/L to 0 g/L on a two day cycle. The average organic loading rate for the perturbation cycle was equal to the steady-state glucose loading rate and the dilution rate was maintained unchanged during the perturbation period. The response of the daughter reactor microbial community to the

periodic substrate perturbation, in terms of operational performance, substrate kinetics, genetic and overall microbial composition changes, were investigated following the initiation of the substrate perturbation.

4.2 MATERIALS AND METHODS

4.2.1 Anaerobic reactor

A schematic representation of the experimental apparatus used for the perturbation experiment is shown in Figure 4-1. The cylindrical all glass reactor (Constructed by the Glass Shop, Chemistry Department, Michigan State University), was approximately 15 cm in diameter and 12 cm in height. The reactor had a working volume of 1.5 liters and a headspace of 0.5 liters. Three, 2-cm diameter threaded all glass outlets and two 0.5-cm diameter glass outlets located in top of the reactor were used to connect with liquid and gas sampling valves and gas production meter. The substrate and nutrient solutions were injected into the reactor through a rubber septum.

A bell shaped, internal mixing chamber was installed to enhance mixing and to improve liquid and gas phase mass transfer. Liquid continuously entered the internal mixing chamber through four 0.5 cm diameter holes evenly located near the reactor liquid surface and was "pumped" out of the mixing chamber through four 0.5 cm diameter holes located near the bottom of the chamber. A spinning stir bar, located inside the mixing chamber, acted as an impeller and created a high speed down-flow liquid stream that continuously entrained gas from the reactor headspace mixing it with liquid inside the chamber. The magnetic stir bar was driven by a Corning Model PC-310 magnetic stir plate (Corning Inc., Corning, New York) at a speed of 500 run per minute.

Continuous feed was introduced into the reactor with a timer controlled pump system. Two Watson-Marlow Model 101U/R pumps (Watson-Marlow, Inc., Wilmington, MA) were used to alternately supply glucose plus mineral media and mineral media alone (no glucose) at a flow rate 150 ml/d to the daughter reactor. Power to the Watson-Marlow 101

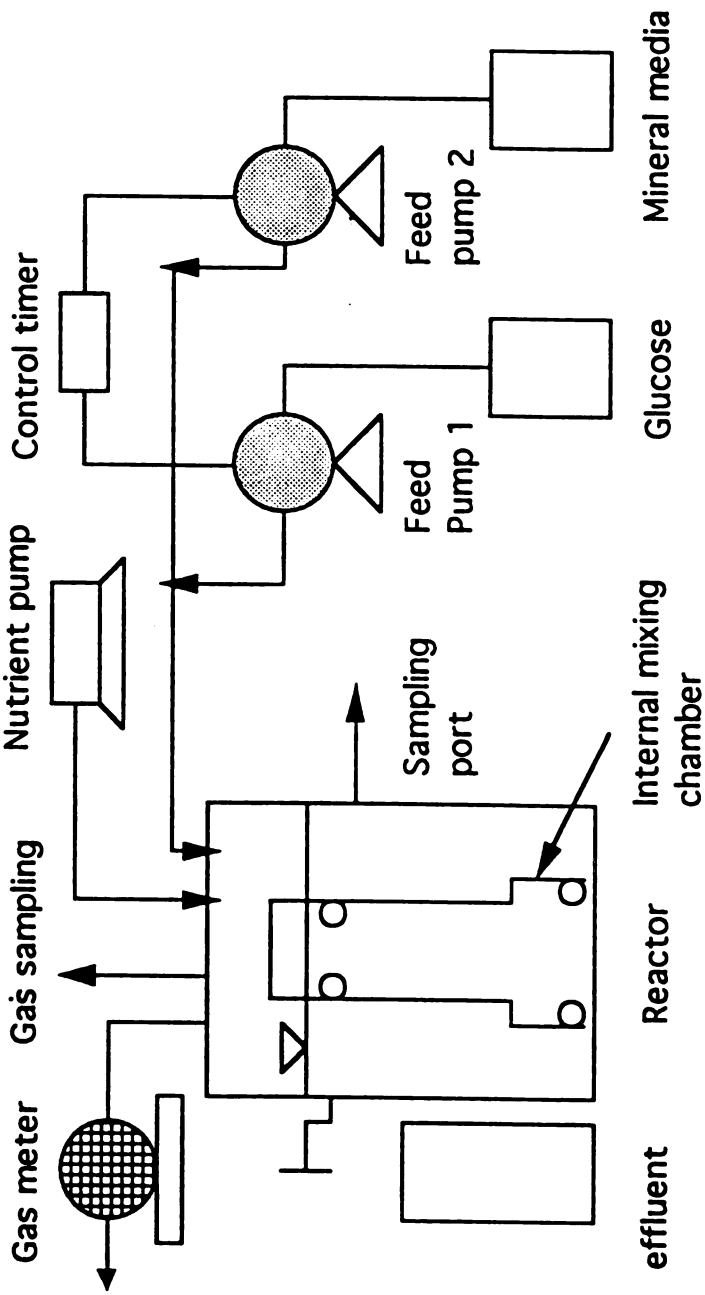

Figure 4-1 Experimental set up

U/R pumps was channeled through a electronic ChronTrol XT timer (ChronTrol Co., San Diego, CA). This programmable timer was used to control on/off operation of the two feed pumps to obtain the desired substrate feed schedule. The nutrient solution was directly injected into the reactor from a 60 ml plastic B-D syringes (Becton Dickinson & CO., Rutherford, NJ) mounted on a Harvard Model 22 syringe infusion pump (Harvard Apparatus, South Natick, Mass.). Nutrients were supplied separately to minimize growth in the glucose feed reservoirs.

Effluent exited the reactor through an inverted U-shaped air-tight water seal effluent tube to prevent the reactor content from being exposed to oxygen. Liquid samples were taken from the reactor liquid sampling port at approximately the mid-point of the reactor liquid phase. Samples were centrifuged using a Hermle compact centrifuge (Model Z203, National Labnet Co., Woodbridge, HJ) at 3,500 g for 10 minutes, and either analyzed immediately or frozen at -30 °C and stored for analysis. Gas production was quantified using a digital liquid displacement based gas meter and discharged. Gas samples were drawn from the gas sampling port located at the top of the anaerobic reactor.

The entire apparatus was located in a constant temperature room (Nor-Lake Scientific, Hudson, WI) set at a temperature of 35 ± 0.5 °C.

4.2.2 Substrate and nutrients

Glucose was supplied as the sole carbon and energy source. Analytical reagent grade granular glucose (Mallinckrodt Specific Chemical Co., Paris, KE) was used to prepare the 8 g/L and 16 g/L glucose solutions. Sodium bicarbonate was added to the feed to provide buffer for pH control. A buffer solution, prepared with reagent grade powder sodium bicarbonate (J, T. Baker Inc., Philipsburg, NJ), was mixed with the above glucose solutions to obtain 7 g/L and 14 g/L N_aHCO_3 respectively. Both the glucose solution and the sodium bicarbonate buffer solution were prepared with deionized water.

The mineral nutrient solution was selected based on the compounds and their concentrations used by several researchers (Cohn et al. 1982; Zoetemeyer et al. 1982a;

Zehnder et al. 1987). The concentration of the various components in the substrate feed solution is presented in Table 4-1. In order to dissolve the salts in the stock nutrient solution, the pH was reduced by the addition of 30 ml concentrated HCl per 1 liter of stock nutrient solution. The prepared stock nutrient solution was stored at 4 °C. This stock solution was diluted to prepare the nutrient feed solution for the anaerobic reactors.

TABLE 4-1. Concentration of the nutrients in the combined influent fed to the anaerobic reactor

Chemicals	Concentration (mg/l)
NH_4Cl	1070
KH_2PO_4	275
NaCl	120
$MgCl_2 \cdot 6H_2O$	49
Na_2SO_4	43
$FeSO_4 \cdot 7H_2O$	5.53
$MnCl_2 \cdot 4H_2O$	2.02
$CaCl_2 \cdot 2H_2O$	0.59
$ZnCl_2$	0.67
$NiCl_2 \cdot 6H_2O$	0.65
$Cu\ Cl_2 \cdot 2H_2O$	0.16
$CoCl_2 \cdot 6H_2O$	0.48
H_3BO_3	0.063
$Na_2MoO_4 \cdot 2H_2O$	0.0045

4.2.3 Analytical methods

Reactor performance was monitored daily for effluent pH, total gas production and gas composition. Analyses for COD, VFAs and VSS were performed on a daily to weekly basis, depending on reactor performance. Analytical methods used for determination of COD, pH, VSS, VFA, gas composition are described in Appendix I.

Epifluorescence microscopy direct count methods, which were used for estimating living cells in the anaerobic reactor cultures, are described in Appendix C.

Protein was determined using a commercial Coomassie protein assay reagent (No. 23200, Pierce, Rockford, IL 61105). The sampling and analysis procedures for protein measurement are described in Appendix D.

Microscopic observations were performed using an Olympus BH-2 phase-contract microscope (Scientific Supply Company, Schiller Park, IL 60176).

4.2.4 Measurement of maximum substrate conversion rate

When the perturbed daughter reactor again reached steady-state, the maximum substrate conversion rates by cultures in the mother and the daughter reactors were measured based on substrate consumption. Maximum substrate conversion rates (V_{max}) were estimated from the glucose and glucose metabolic intermediates degradation curves following pulse substrate injection.

Assuming the substrate degradation can be described by Michaelis-Menten kinetics, the rate of substrate utilization becomes:

$$-dS/dt = V'_{max}\, S/(S + K_S) \qquad (4\text{-}1)$$

Where:

V'_{max} = maximum volumetric rate of substrate conversion, mg/l-d

S = concentration of growth-limiting substrate, mg/l

K_S = substrate saturation constant, mg/l

After addition of high substrate concentration, S > Ks, the substrate utilization equation can be written as:

$$-ds/dt \approx V'_{max} \qquad (4\text{-}2)$$

Therefore as indicated by equation (4-2), at high substrate concentrations, substrate conversion rate is independent of substrate concentration, following zero-order kinetics. That is true if there is no substrate inhibition and the increase of biomass due to growth is small compared with the total biomass concentration. V'_{max} can be estimated by using the integrated form of equation (4-2):

$$S = S_o - V'_{max}\, t \qquad (4\text{-}3)$$

Where:

S = substrate concentration at time t, mg/l

S_o = original substrate concentration, mg/l

t = reaction time, day

Specific maximum conversion rates were then determined by:

$$V_{max} = V'_{max}/X \qquad (4\text{-}4)$$

Where:

X = reactor biomass concentration, mg/l

In this experiment, the maximum substrate conversion rates for different substrates, except hydrogen, were determined directly in the mother and the daughter reactors by pulse injecting concentrated stock solutions of different substrates to obtain an elevated substrate concentration in the systems. Maximum hydrogen conversion rates were measured indirectly in pH controlled batch experiments with 158 ml serum bottles. The substrate concentrations used for the maximum substrate conversion rate measurements are listed in Table 4-2.

Table 4-2. Substrate concentrations applied to the mother and the daughter reactors during the maximum substrate conversion rate measurements

Substrate	Concentration (mg/L)
Glucose	200
Butyrate	300
Propionate	300
Acetate	600
Hydrogen	20 (psig)

4.2.5 Measurement of decay coefficients of biomass and substrate utilization capacities

Under starvation conditions the change in biomass concentration is proportional to the existing biomass concentration (McCarty, 1966):

$$dX/dt = - K_d X \qquad (4\text{-}5)$$

Where:

X = biomass concentration, g/l

K_d = decay coefficient, day^{-1}

K_d can be estimated using the integrated form of equation (4-5):

$$\ln X = \ln X_o - K_d t \qquad (4\text{-}6)$$

Where:

X = biomass concentration at time t, g/l

X_o = original biomass concentration, g/l

t = decay time, day

Biomass decay coefficients were measured in batch experiments using 158 ml serum bottles using cultures taken from the anaerobic reactors.

For mixed cultures, like anaerobic sludge, it is difficult to directly measure the actual decay rate of the individual trophic groups of bacteria. Assuming the maximum substrate conversion rates possessed by the anaerobic cultures are proportional to the active population for that substrate, the decrease in the maximum substrate conversion rates under starvation conditions will directly reflect the decay rate of the associated trophic group. To use this concept, the decay coefficients of the different trophic groups can also be estimated by using equation (4-6). In this case the only difference is that the terms of X and X_o in equation (4-6) are replaced by V_{max} and $V_{max,\,o}$ respectively (Wu et al., 1995).

4.2.6 Reactor inoculation

The inoculum (1,500 ml) for the daughter reactor was obtained from a 15 L laboratory-scale mother reactor operated under steady state conditions with a 10 day HRT and a constant 8 g/L glucose feed, as described in Chapter 3. The mother reactor was operated under steady-state conditions for more than two hundred days before the daughter reactor was started. The mother reactor also served as a stable control and as reference for changes in activity levels and community structure in the daughter reactor.

The inoculated "daughter" reactor was initially operated under the same conditions as the mother reactor (10 day HRT with continuous input of 8 g/l glucose) for 50 days. Once steady-state was reached and sufficient "base-line" information obtained, a square wave perturbation in feed concentration was applied to the daughter reactor.

4.2.7 Experimental procedure

In this study, a long term periodic substrate perturbation was applied to the anaerobic "daughter" reactor. The response of the system to the perturbation was investigated. During the perturbation, the reactor influent glucose concentration was alternately changed in amplitude from 16 g/L to 0 g/L (mineral media only) on a 2 day square wave cycle (see

Figure 4-2), i.e. the reactor was fed 16 g/l glucose solution for one day followed by glucose-free mineral media at the same flow rate on the next day. A 10 day hydraulic retention time (dilution rate of 0.1 d^{-1}) was maintained throughout the experiment. The perturbation loading pattern was chosen so that the average influent glucose concentration during the perturbation period was equal to the steady-state concentration of 8 g/L applied to the control mother reactor.

The daughter reactor was continuously operated for a period of 250 days including ca. 50 days under steady-state baseline conditions and ca. 200 days under perturbation conditions.

Copyright © 2024 Elsevier Ltd. All rights reserved.

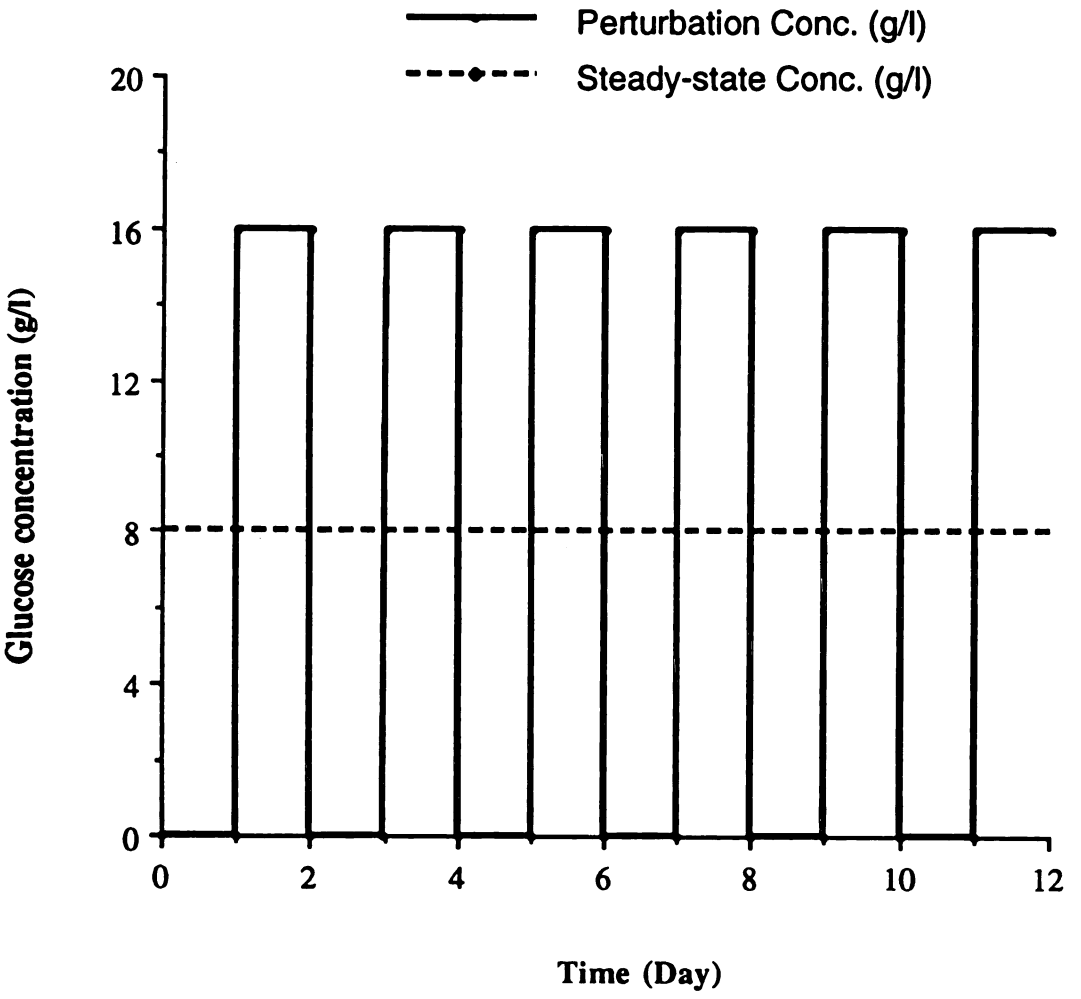

Figure 4-2. Substrate feeding pattern used for perturbation experiment

4.3 RESULTS

4.3.1 Effects of the periodic substrate perturbation

Based on the experimental results, the response of the daughter reactor community to the periodic substrate perturbation can be broken down into four distinct stages: (1) rapid VFA and COD accumulation; (2) establishment of a metastable steady-state at reduced COD removal efficiency; (3) rapid VFA degradation; and (4) re-establishment of steady-state with high COD removal efficiency. Stage 1 can be further divided into two sub-stages: (1a) rapid acetate and propionate accumulation, and (1b) rapid butyrate accumulation while acetate and propionate levels stabilized. Each of the above stages is discussed in greater detail in the following sections.

Stage 1a (day 0 to day 20)

As shown in Figure 4-3, the steady-state microbial community was highly sensitive to the variation in organic feed concentration. A rapid accumulation of VFAs occurred nearly immediately after the start of the substrate perturbation. The acetate-utilizing methanogens were immediately impacted by the substrate perturbation as evidenced by a sharp increase in the effluent acetate concentration and a drop in methane production. Effluent acetate concentration increased almost linearly from 120 mg/l to ca. 2,200 mg/l, accumulating at a rate of 105 mg/l-d. Effluent COD concentration continuously increased from 370 mg/L to ca. 3,800 mg/L, accumulating at a rate of 170 mg/l-d (Figure 4-4). Thus, acetate contributed ca. 65% of the total increase in COD observed during this period. Subsequently, acetate concentration stabilized.

A linear accumulation of propionate was also observed during the initial 20 days of the substrate perturbation. Effluent propionate concentration increased from less than 40 mg/l to a peak concentration of ca. 700 mg/l at an average daily accumulating rate of ca. 33 mg/l-d. Thus propionate contributed about 30% of the total accumulated COD. Propionate formation from glucose can be written as (Thauer et al., 1977):

$$C_6H_{12}O_6 = 4/3CH_3CH_2COO^- + 2/3CH_3COO^- + 2/3HCO_3^- + 8/3H^+ \quad (4\text{-}7)$$

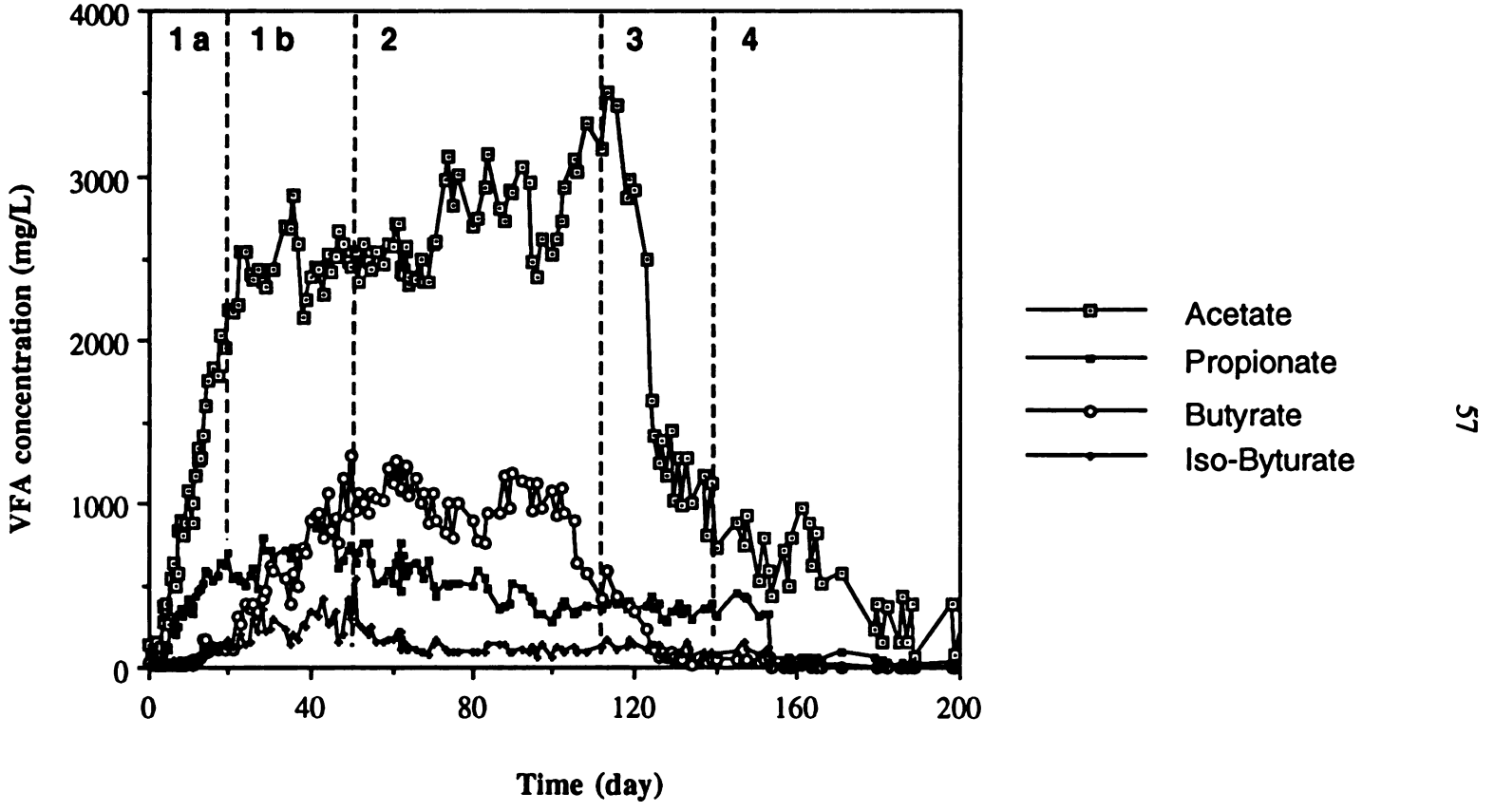

Figure 4-3. Concentration changes in VFA's during the perturbation period

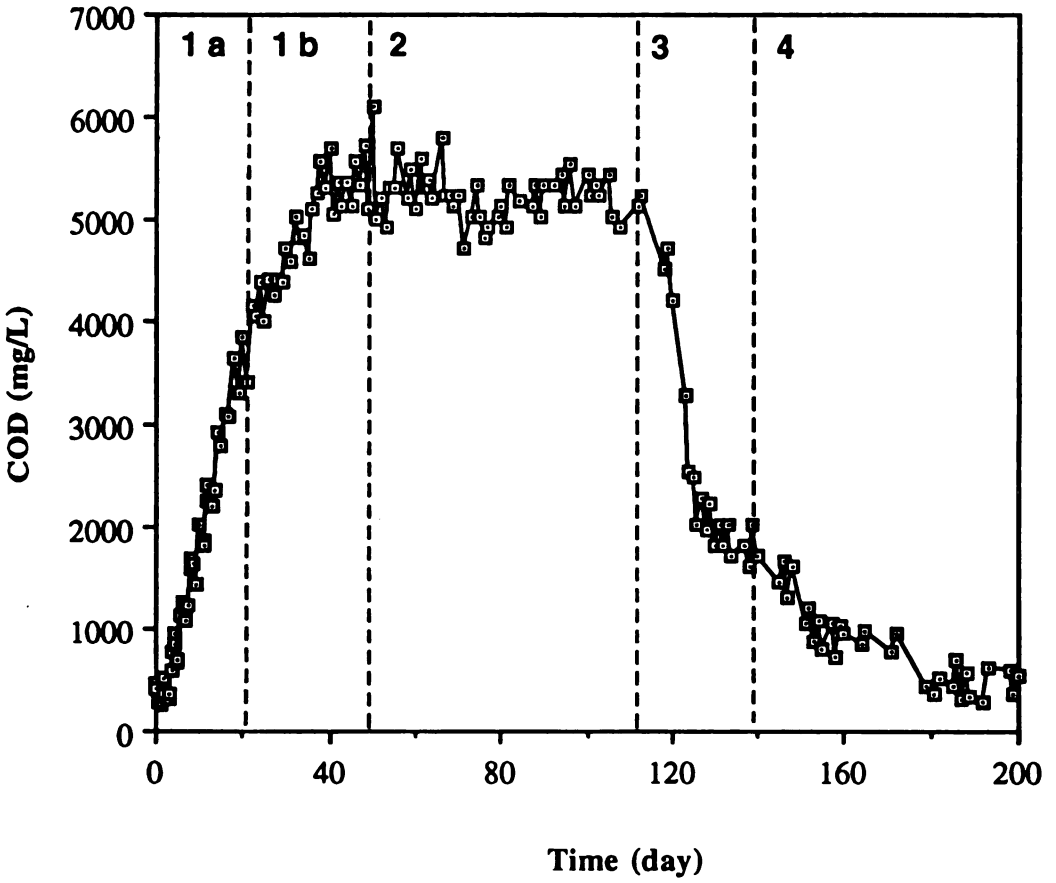

Figure 4-4. COD variation during the perturbation period

Based on this, the substrate flowing through the propionate fermentation route contributed as much as 37% of the total accumulated COD during this period.

During the glucose feeding period, no glucose (< 0.5 mg/l) was detected in the reactor liquid phase. No other glucose metabolism intermediates, such as ethanol and other long chain fatty acids, accumulated during this period. As shown in Figure 4-5, the pH decreased from a steady-state value of 7.0 to ca. 6.4 during the first 20 days. Subsequently, reactor pH stabilized at ca. 6.4.

Stage 1b (day 21 to day 50)

Effluent butyrate and iso-butyrate concentrations remained low during the first 20 days of the perturbation. Over the following 30 days, effluent butyrate concentration increased rapidly. Butyrate and iso-butyrate concentrations reached levels of ca. 1,200 mg/l and 200 mg/l, respectively. Effluent COD concentration concurrently increased to a average level of ca. 5,500 mg/l (Figure 4-4). Accumulated butyrate and iso-butyrate accounted for as much as 45% of the total accumulated COD during this period. Accumulation of butyrate and iso-butyrate did not significantly affect pH.

Stage 2 (day 51 to day 110)

When the effluent COD concentration reached an average value of ca. 5,200 mg/l, a metastable "steady-state" period was established. Effluent COD fluctuated around this new "steady-state" for about 60 days. COD removal efficiency averaged about 40 % as compared to ca. 95% during the baseline period. Average daily gas production rate decreased to 45% of the baseline value, and CH_4 content in the reactor headspace was 30% compared to 50% prior to the perturbation. During this period, methane fermentation essentially shifted to a rumen type system, with extremely low acetate-utilizing methanogenic activity, (Hungate, 1975).

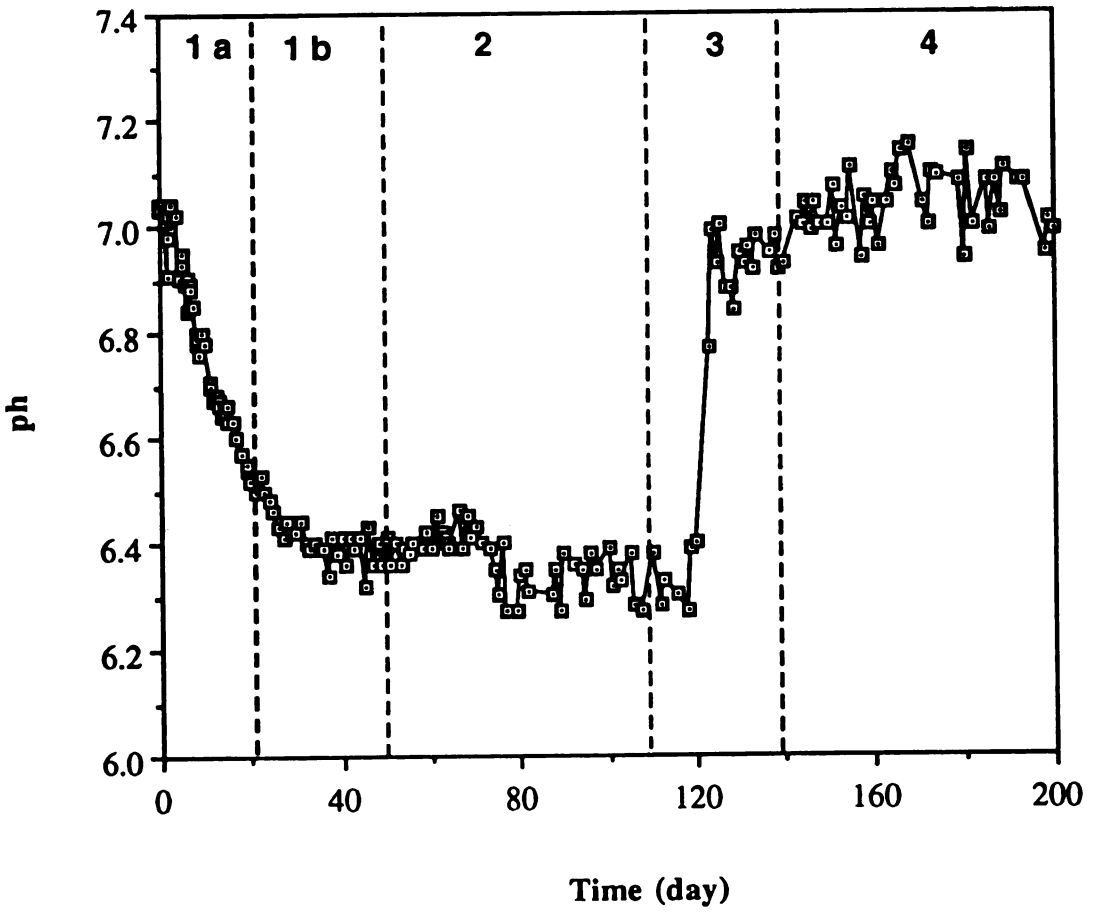

Figure 4-5. pH change during the perturbation period

Although effluent COD remained relatively stable during the metastable steady-state, a large change in the relative composition of the VFAs was observed. Propionate and iso-butyrate concentrations decreased steadily from their peak levels of ca. 700 mg/L and 250 mg/L to ca. 400 mg/L and 100 mg/L respectively. Simultaneously, acetate and butyrate concentrations varied in a cyclic pattern: when butyrate levels increased, acetate levels decreased and vice-versa. Anaerobic oxidation of butyrate produces two moles of acetate per mole of butyrate. Thus, the decrease in butyrate concentration corresponded to an increase in acetate concentration. Starting on day 60, butyrate concentration and acetate concentration increased concurrently. When the acetate concentration increased above 3,000 mg/L, butyrate degradation slowed down. A new cycle of butyrate accumulation was then observed. On day 100, when the reactor acetate concentration decreased to 2,500 mg/L, more rapid butyrate degradation was again observed. This resulted in a concurrent increase in acetate concentration to a peak level of 3,500 mg/l in the end of this stage. At that time acceleration in the rate of acetate degradation broke the repeating pattern of acetate and butyrate oscillation and triggered to a recovery of the whole system.

Stage 3 (day 110 to day 140)

A rapid decrease in acetate concentration began on day 110. During the ensuing 20 days, acetate concentration decreased from 3,500 mg/l to ca. 1,000 mg/l, and effluent pH value simultaneously increased from 6.3-6.4 to about 7.0. Thereafter, the acetate concentration continuously decreased, but at a slower rate, to ca. 800 mg/l. Meanwhile the butyrate and iso-butyrate concentrations quickly decreased to pre-perturbation levels (less than 100 mg/l). At this point, propionate concentration began a steady decrease to the original steady-state concentration. The gas production rate also reflected the drastic change in VFA metabolism. A peak gas production rate of ca. 610 ml/l-d corresponded to the sharp decrease in acetate concentration (Figure 4-6).

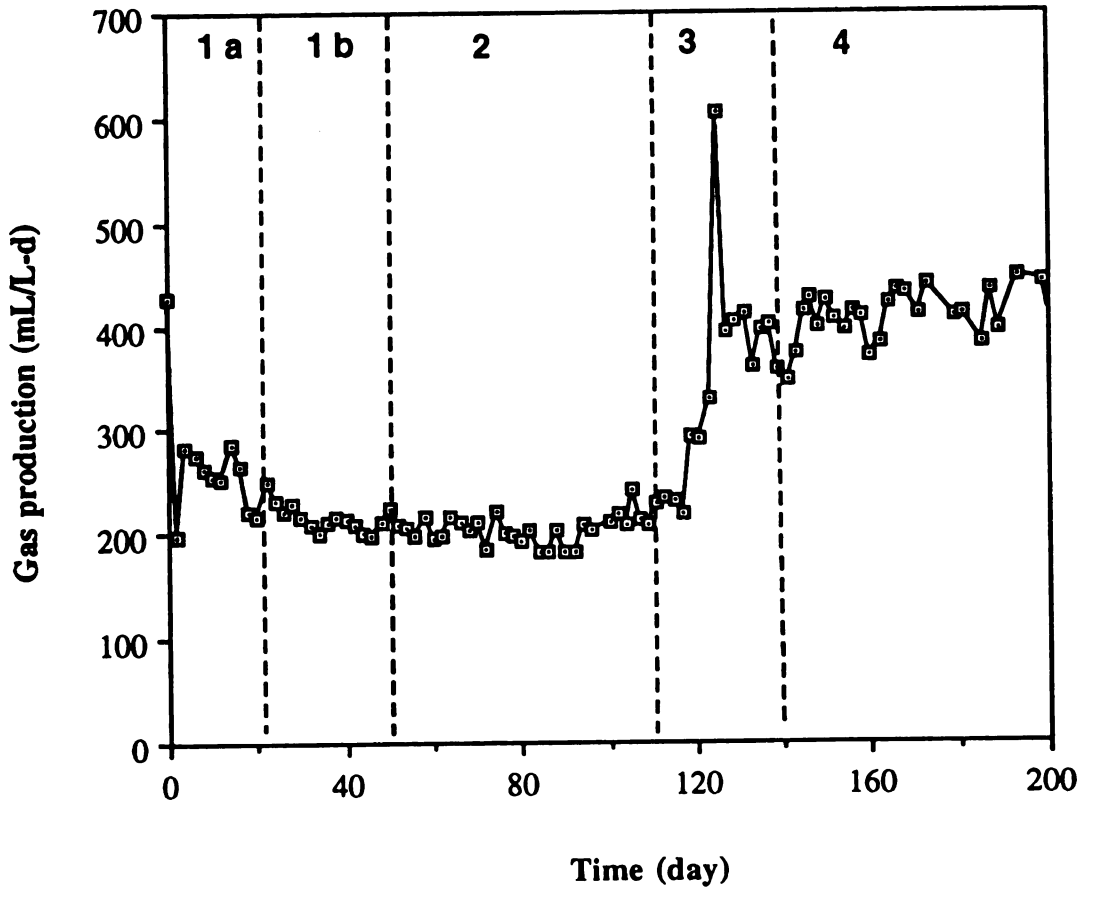

Figure 4-6. Average gas production in the two-day cycle during the perturbation period

Stage 4 (day 140 to day 200)

Except for acetate, all VFAs stabilized at new steady-state levels within ca. 40 days subsequent to the start of rapid acetate degradation. After 80 days, a new steady-state was re-established in the anaerobic reactor. At that time, the average COD effluent concentration, pH and biogas production rate were similar to those observed before the substrate perturbation. A comparison of reactor performance during the original steady-state condition, the metastable steady-state condition, and the new steady-state condition established during the substrate perturbation, is shown in Table 4-3. The data clearly demonstrates that the anaerobic microbial community was able to adapt to the long term perturbation of periodic influent substrate concentration.

TABLE 4-3. Summary of reactor operational results during the different stages of the perturbation period

	Baseline Steady-state	metastable steady-state[1]	New steady-state[1]
CODin (mg/l)	8500	8500	8500
CODe (mg/l)	420 ± 50[2]	5200 ± 250	430 ± 140
VSS (mg/l)	1160 ± 160	730 ± 80	1300 ± 170
Gas (ml/l-d)	400 ± 60	210 ± 10	410 ± 230
CH_4 (%)	50 ± 2	30 ± 2	50 ± 2
pH	7.02 ± 0.04	6.37 ± 0.05	7.02 ± 0.06
Acetate (mg/l)	170 ± 30	2660 ± 220	210 ± 100
Propionate (mg/l)	20 ± 15	540 ± 140	30 ± 16
Butyrate (mg/l)	20 ± 7	1010 ± 130	7 ± 2

1: Average value for two day cycle,
2: Standard deviation.

4.3.2 Gas production during substrate perturbation period

Gas production also reflected the impact of the periodic substrate feeding pattern on the microbial community. During the stage 1 the average daily gas production (average value for the 2-day cycle) concurrently decreased from about 430 ml/L-d to 210 ml/L-d (Figure 4-6). Most of the gas was produced on days when glucose was provided (410 to 440 ml/l-d).

Gas production on days when glucose was not provided (famine days) was a useful indicator of acetate-catabolizing methanogenic activity. Gas production on the famine days decreased steadily from ca. 100 ml/d to less than 5 ml/d (detection limit of the gas meter) within ca. 25 days (Figure 4-7a), deteriorating at an average rate of ca. 4% daily. The decline in the gas production curve is fairly close what would be anticipated due to hydraulic washout (Fig 4-8). The actual gas production observed is somewhat above the "washout" line suggesting limited growth of acetate-utilizing methanogens.

Gas production on famine days was below the gas meter detection limit (< 5 ml/d) for about 30 days. Subsequently, after day 55, limited gas production (ca. 10 to 20 ml/l-d) was again observed on famine days (Figure 4-7b). By day 110, gas production on famine days had increased to near pre-perturbation levels. Subsequently, a sudden increase in gas production rate was observed on days when glucose was not provided. On day 125, a peak gas production of ca. 425 ml/l-d on the famine day was observed (Figure 4-7c). This increase coincided with a sharp drop in acetate concentration in the reactor. Gas production on famine days stabilized at a level of ca. 150 ml/l-d thereafter.

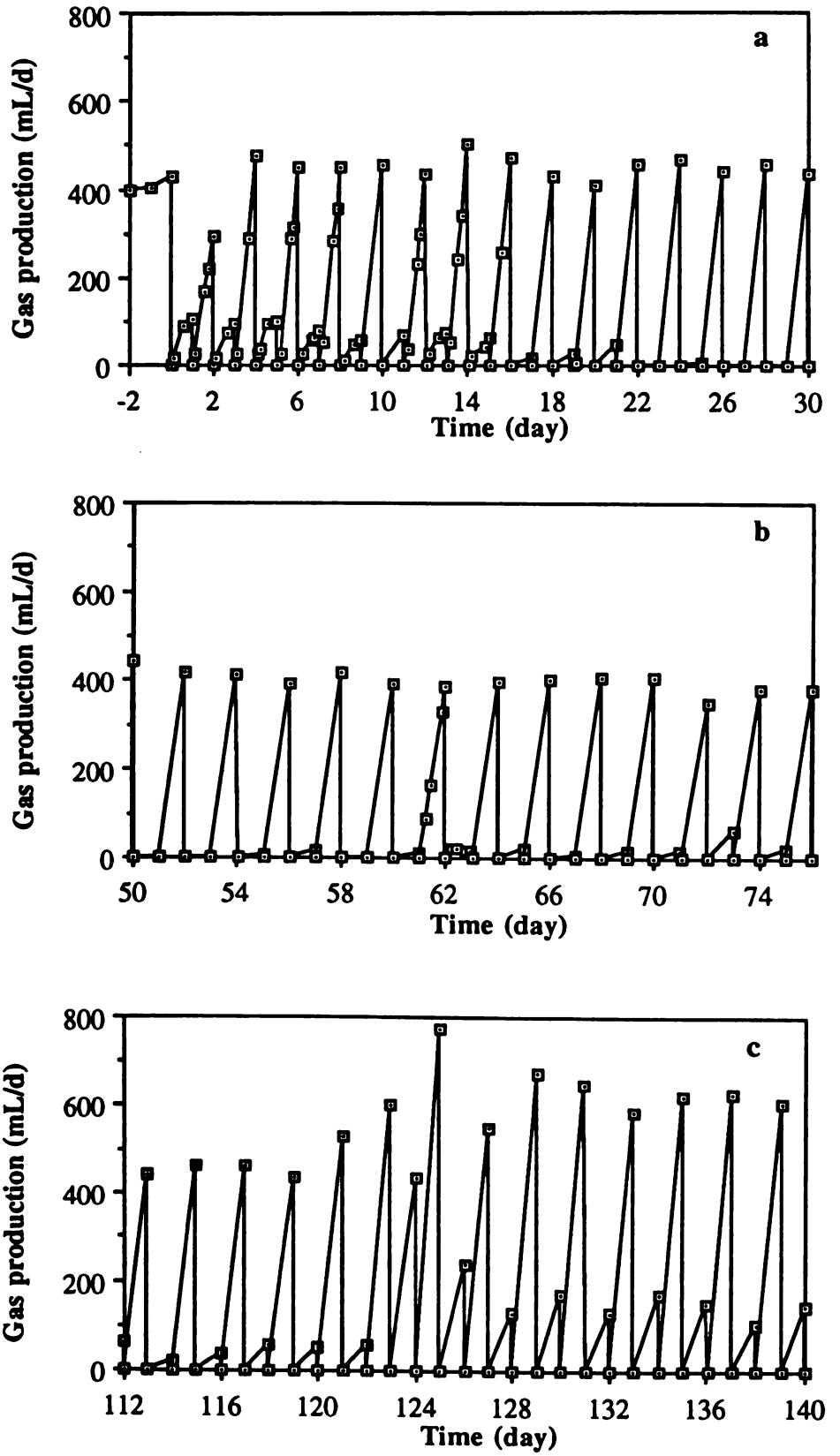

Figure 4-7. Daily gas production during the substrate perturbation period

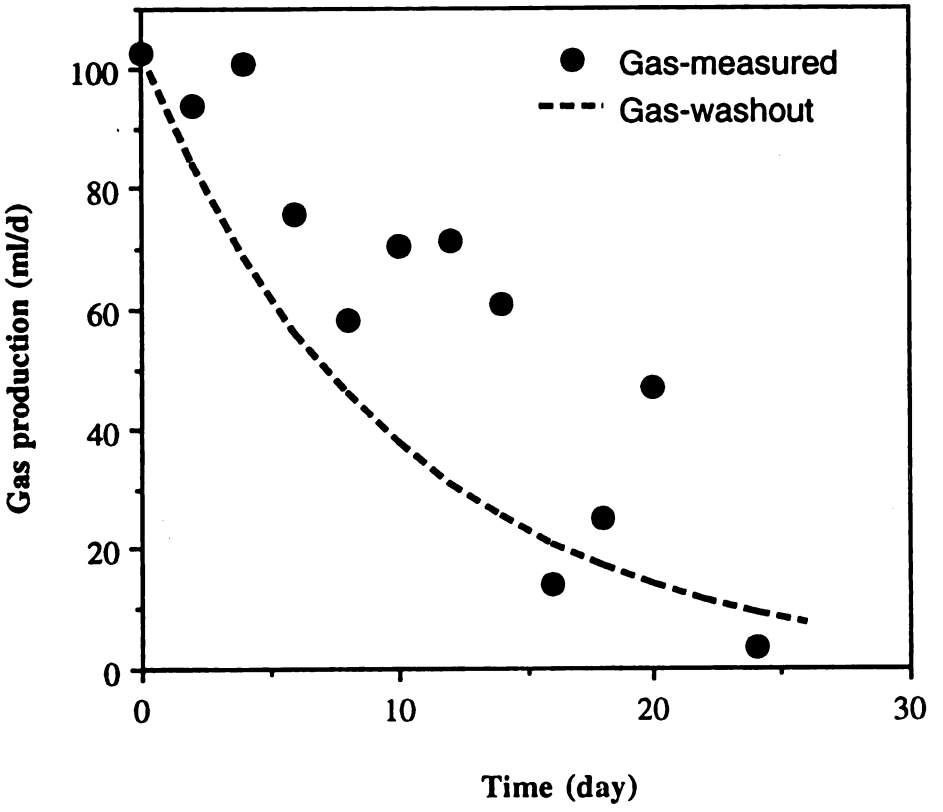

Figure 4-8. Deterioration of gas production on days when glucose was not supplied during stage 1

4.3.3 Maximum substrate conversion rate

Once the perturbed chemostat was judged to have achieved a new steady-state, measurement of maximum specific substrate conversion rate for cultures in the mother and the daughter reactors was performed to document changes in community structure and kinetic capacity. These results, summarized in Table 4-4, were average values of three independent measurements for each substrate.

Population differences were indicated by the observed specific maximum substrate conversion rates (V_{max}) of the two cultures. Experimental data show that these two cultures essentially possessed the same glucose conversion rate. Compared with the control mother reactor, the culture established in the new steady-state daughter reactor, possessed higher substrate utilization capacities for all measured intermediate products from glucose. This was especially true for propionate and hydrogen degrading populations. The conversion rates for hydrogen and propionate were 1.9- and 12.7- times higher in the daughter reactor culture compared to the mother reactor culture.

TABLE 4-4. Specific maximum substrate utilization rates observed for the mother and the re-established daughter reactors

		Mother reactor (M)	Daughter reactor (D)	D/M
$V_{glucose}$	(mg/g vss. d)	3790 ± 177[1]	4140 ± 180	1.1
$V_{acetate}$	(mg/g vss. d)	780 ± 73	1050 ± 78	1.3
$V_{Propionate}$	(mg/g vss. d)	4.8 ± 0.97	61 ± 9.9	12.7
$V_{Butyrate}$	(mg/g vss. d)	250 ± 28	350 ± 40	1.4
V_{H2}	(mmole/g vss . d)	81 ± 14	155 ± 16	1.9

1: Standard deviation

4.3.4 Decay characteristics

When the daughter reactor performance stabilized from the impact of the substrate perturbations, the decay characteristics for the mother and the daughter reactor cultures were examined using batch experiments under starvation conditions.

a. Biomass decay

Cultures taken from the mother and the daughter reactors were incubated in 158 ml serum bottles at 35 °C under starvation conditions. Biomass concentration changes were monitored for a period of ca. 40 days. Three independent decay tests were performed for the mother and the daughter reactor cultures.

Typical biomass decay curves of the mother and the daughter reactor cultures are presented in Figure 4-9. Biomass decay under starvation conditions can be divided into two stages based on the observed decay rates. In the first stage the biomass concentration decreased rapidly; while in the second stage the biomass concentration decreased at a much slower rate (Figure 4-10). This was true for both the daughter and the mother reactor cultures. The decay rates observed during the first stage were 7 to 9 times higher than the decay rates observed during the second stage. The biomass decay parameters of the mother and the daughter reactor cultures are summarized in Table 4-5, in which K_{d1} and K_{d2} represent the decay parameters obtained from the first and the second stage, respectively.

Table 4-5. Decay parameters of the mother and the daughter reactor cultures

Parameter	Mother reactor	Daughter reactor
K_{d1} (day $^{-1}$)	0.128 ±0.028	0.182 ±0.020
K_{d2} (day $^{-1}$)	0.017 ±0.010	0.020 ±0.004

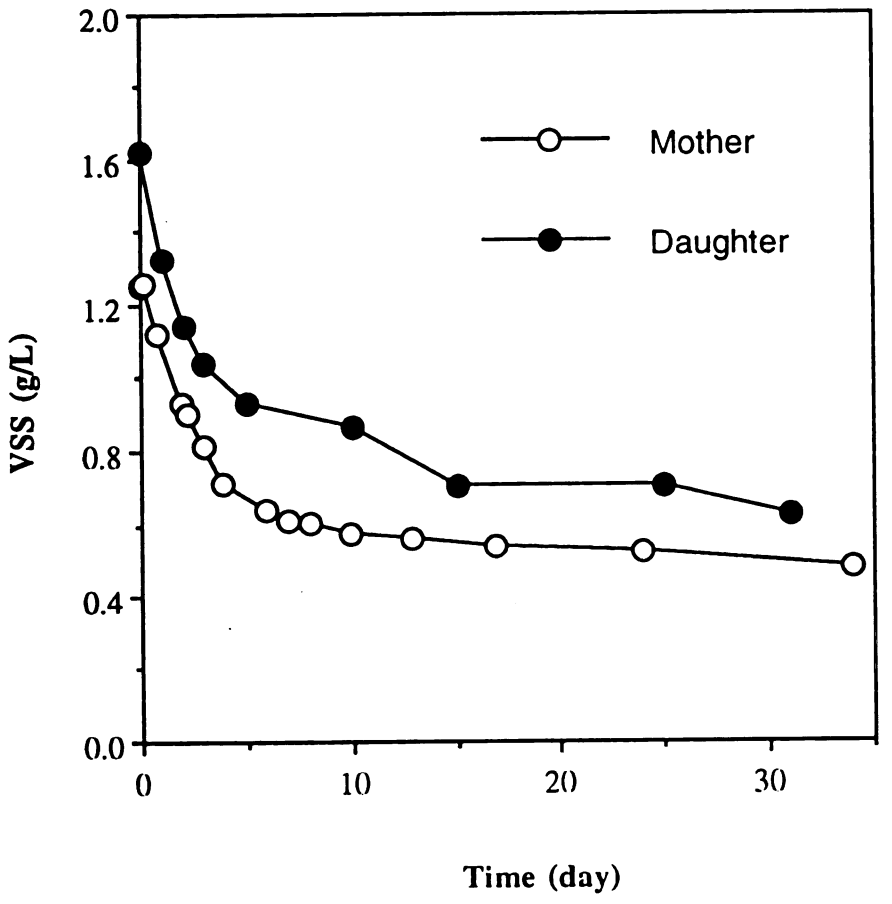

Figure 4-9. Biomass decay of the mother and the daughter reactor cultures under starvation condition.

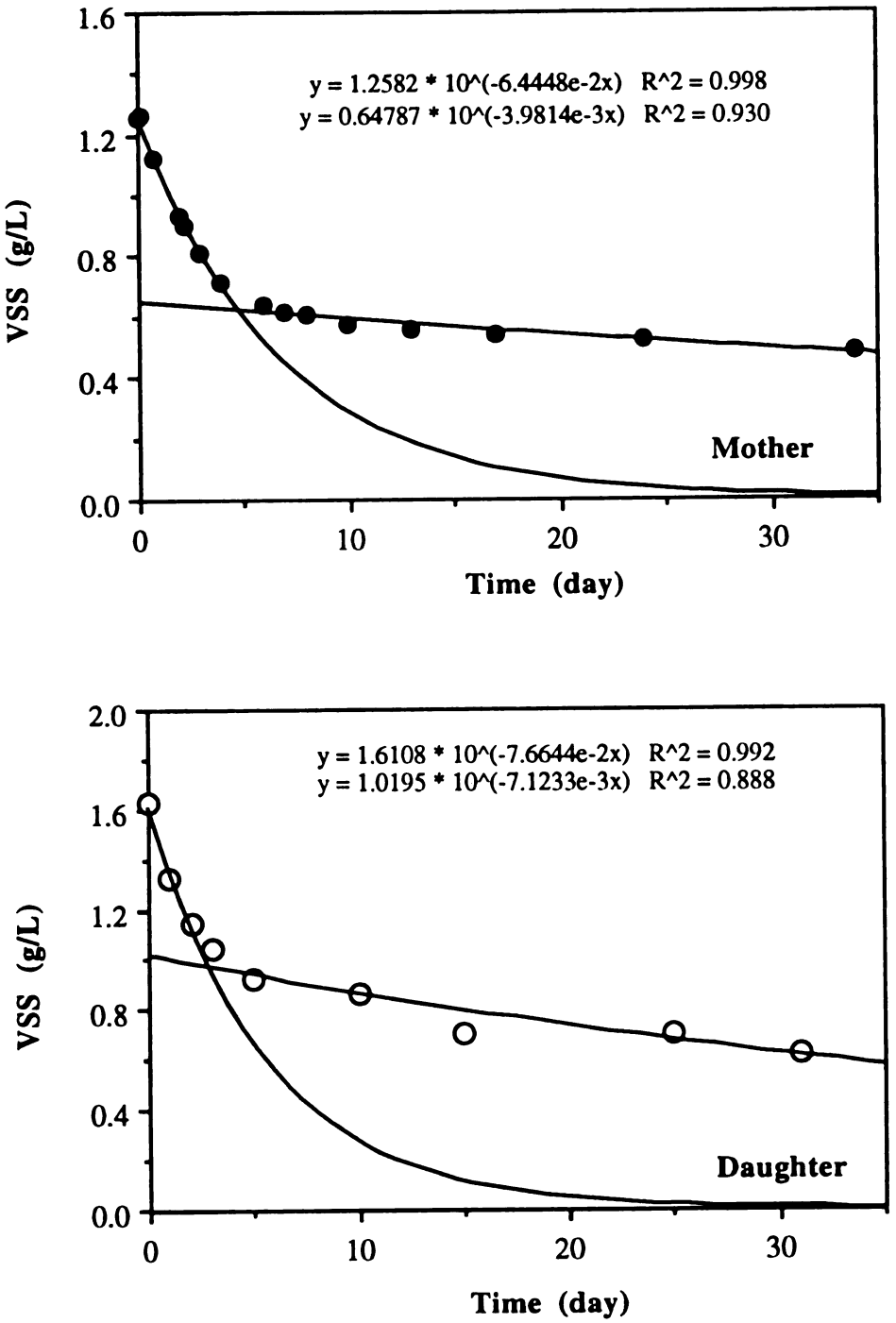

Figure 4-10. Estimation of biomass decay parameters for the mother and the daughter reactor cultures.

As presented in Table 4-5, the daughter reactor culture had significantly higher first stage decay rates. The second stage decay rate of the daughter reactor culture was essentially the same as the decay rate observed in the mother reactor culture. The biomass decay rates observed in the second stage (K_{d2}) are very close to the literature reported values of 0.020 to 0.025 d^{-1} for glucose fed anaerobic sludge (Stewart, 1958; Agardy et al., 1963).

b. Decay characteristics of hydrogen-utilizing methanogens and acidogens during a starvation period

Cultures taken from the mother and the daughter reactors were transferred into 158 ml anaerobic serum bottles and incubated at 35 °C without feed. Maximum substrate utilization rates were measured at different incubation times using concentrated substrates (glucose or H_2-CO_2 gas) over a period of ca. 70 days.

The decay rates of the hydrogen-utilizing methanogens in the mother and the daughter reactor cultures are presented in Figure 4-11. From this figure it can be seen that the decay curves of the hydrogen-utilizing methanogens could be divided into two stages. During the first stage, the maximum hydrogen utilization capacity decreased rapidly, while in the second stage a much slower decay rate was observed. The decay rates observed in the daughter reactor culture, both in the first and the second stages, were significantly lower than the values observed in the mother reactor culture.

The decay progress of the acidogens in the mother and the daughter reactor cultures is shown in Figure 4-12. From this figure it can be seen that the decay process of the acidogens in the mother and the daughter reactor cultures also can be divided into two stages: in the first stage the maximum glucose degradation capacity decreased rapidly with decay rates of 0.24 d^{-1} and 0.17 d^{-1} for the mother and the daughter reactor cultures, respectively; during the second stage the decay rate was relatively slow with calculated rates of 0.019 d^{-1} and 0.023 d^{-1} for the mother and the daughter reactor cultures, respectively.

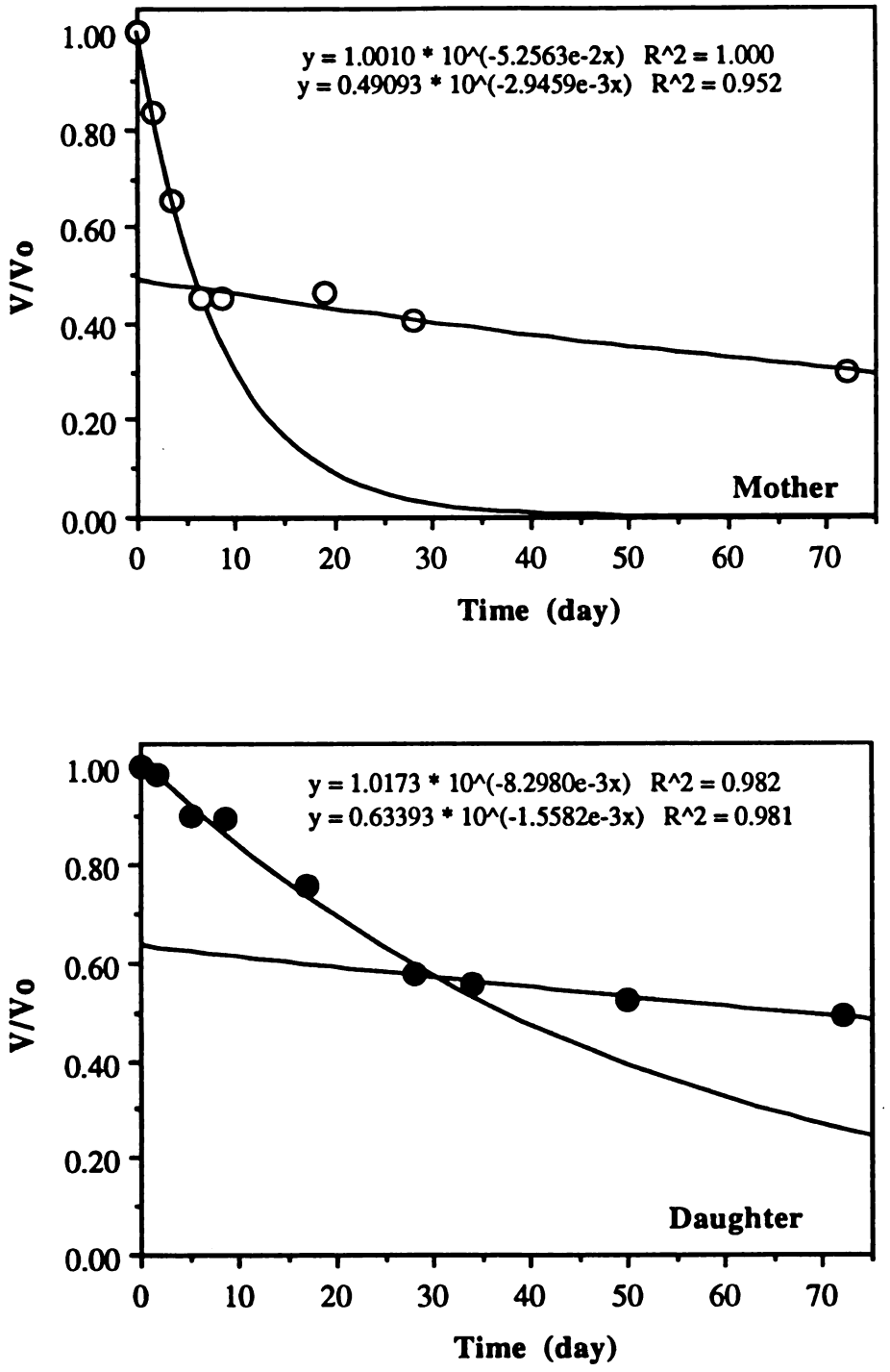

Figure 4-11. Estimation of decay parameters for hydrogen-utilization activity in the mother and the daughter reactor cultures.

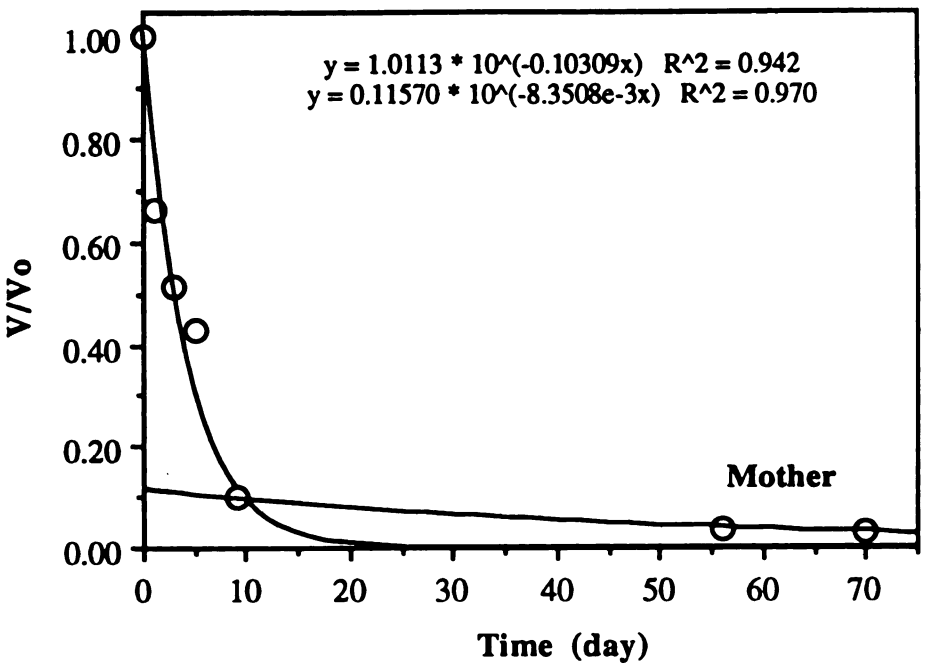

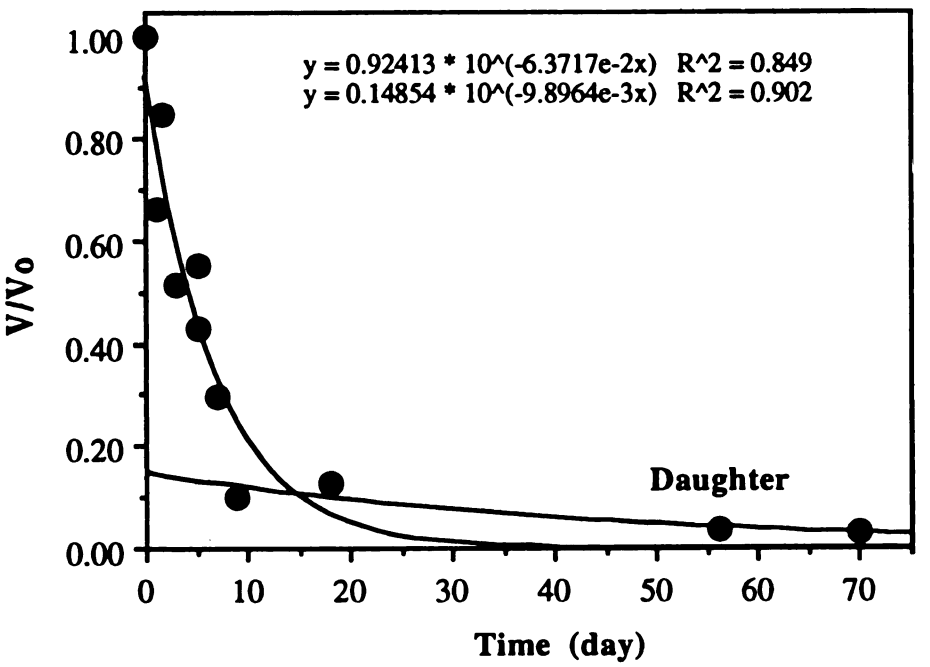

Figure 4-12. Estimation of decay parameters for glucose degradation activity in the mother and the daughter reactor cultures.

Table 4-6. Decay rates of the glucose degrader and hydrogen-utilizing methanogens in the mother and the daughter reactor cultures

	Mother reactor	Daughter reactor
Glucose		
K_{d1} (d^{-1})	0.240	0.170
K_{d2} (d^{-1})	0.019	0.023
Hydrogen		
K_{d1} (d^{-1})	0.120	0.019
K_{d2} (d^{-1})	0.007	0.004

The decay rates, estimated based on the reduction of the maximum substrate utilization rates, of the acidogens and hydrogen-utilizing methanogens in the mother and the daughter reactor cultures are summarized in Table 4-6.

4.3.5 Protein measurement results.

Changes in protein concentrations were investigated when the daughter reactor again established steady-state. Samples were collected on a daily basis for two weeks from the mother and the daughter reactors. More intensive sample collection (every 4 to 6 hours) was employed for the daughter reactor culture over two complete perturbation cycles (4 days). During this period, changes in VSS and COD were also monitored.

Cyclic changes in protein and VSS concentrations were observed in the periodically fed daughter reactor (Figure 4-13). Although both protein and VSS concentrations responded positively to the periodic substrate feed, much larger fluctuations in VSS concentrations were observed (Figure 4-14). This indicates that the change in protein concentration was not proportional to changes in VSS concentration. A large variation in the ratio of protein/VSS occurred during the substrate perturbation period (Figure 4-15a). The daily change in the ratio of protein/VSS varied inversely with reactor VSS changes (Figure 4-15b). The highest ratio of protein/VSS (and lowest VSS) was always observed at the end of the no-substrate period, while the lowest ratio of protein/VSS (and the highest VSS) was observed at the end of the substrate feed period.

The protein and VSS measurement results of the mother reactor culture are presented in Figures 4-13 and 4-15, respectively. Based on the experimental data, the average protein concentration of the mother reactor culture was 462 mg/L, while the average VSS concentration was 1,183 mg/L. This gives an average protein/VSS ratio of 0.391 in the mother reactor culture.

The protein and VSS measurement results obtained during this experiment are summarized in Table 4-7. The average protein/VSS ratio measured in the mother reactor culture was higher than the average value measured in the daughter reactor culture. That was mainly due to the high VSS concentration observed in the daughter reactor culture, because the average protein concentration was essentially the same in the mother and in

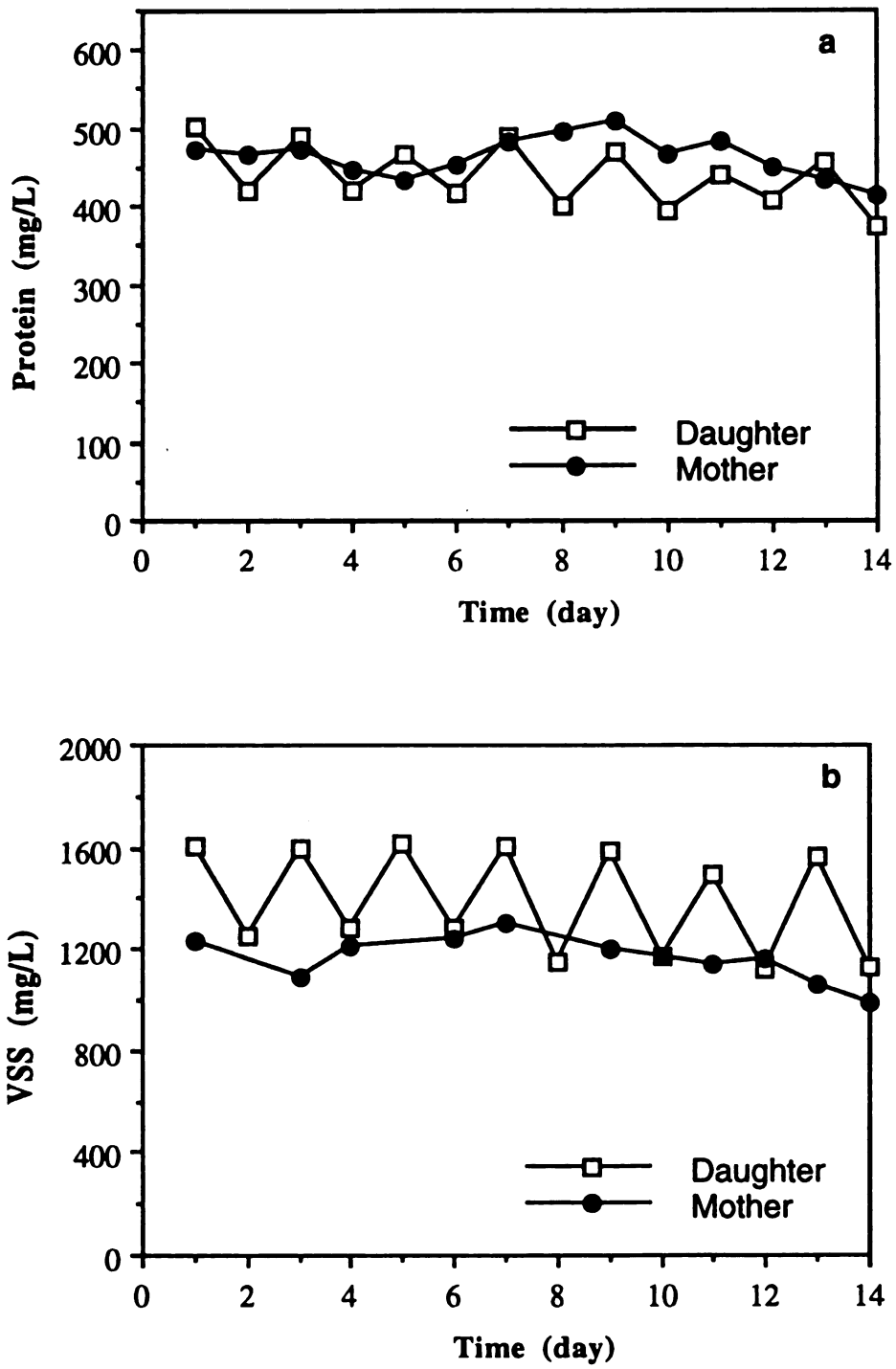

Figure 4-13. Protein and biomass concentration changes in the mother and the daughter reactor cultures.

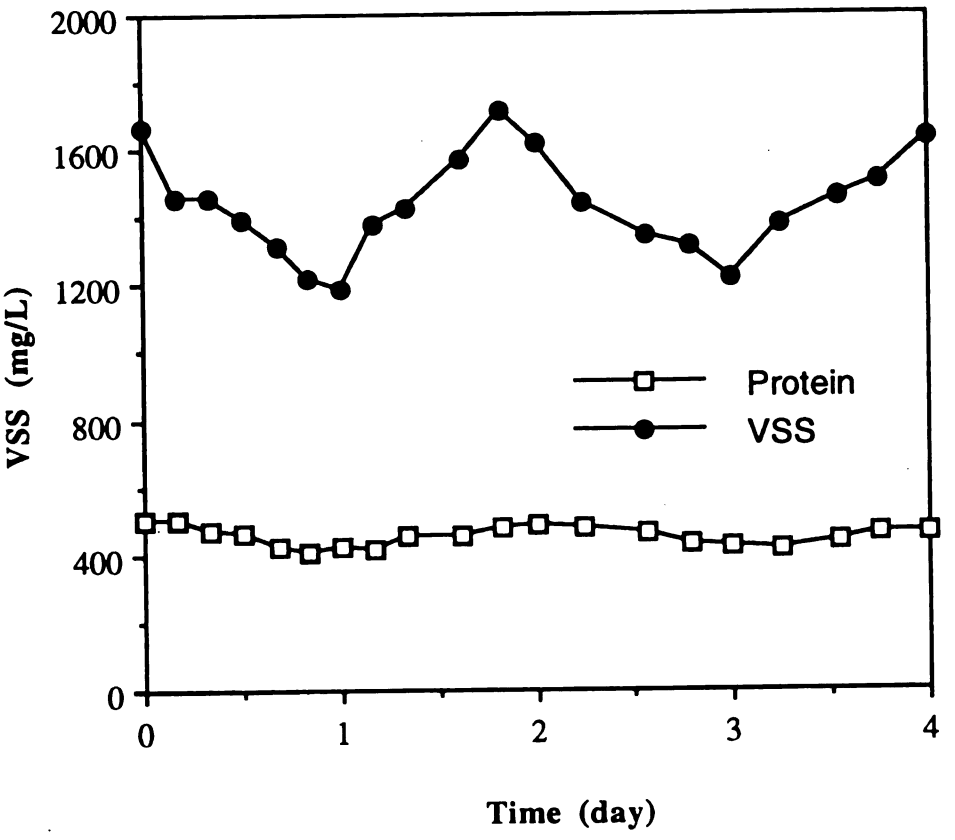

Figure 4-14. Protein and biomass concentration changes in the daughter reactor during two complete perturbation cycles.

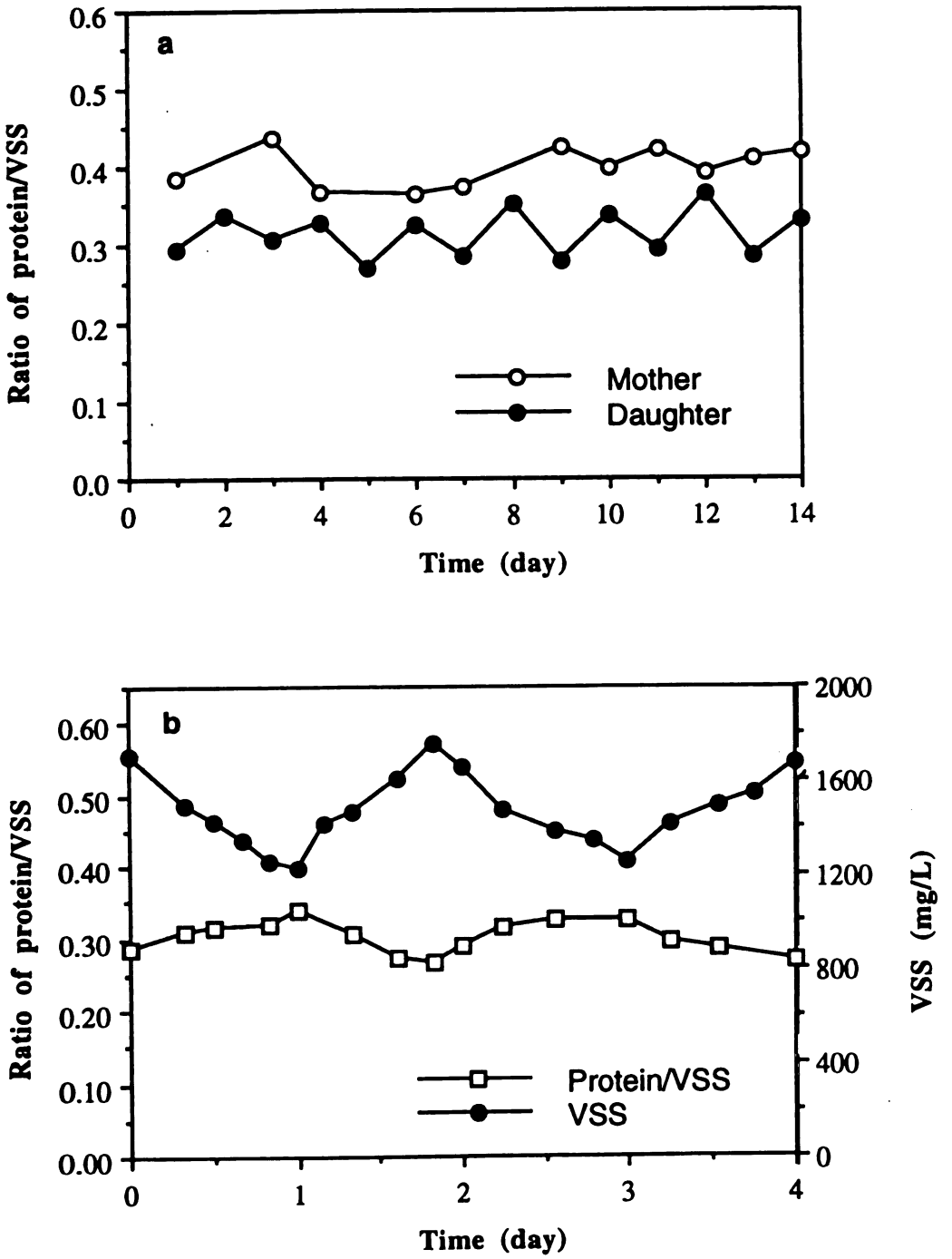

Figure 4-15. Protein/VSS ratio changes (a) in the mother and the daughter reactor cultures during the experimental period, and (b) in the daughter reactor during two complete perturbation cycles.

Table 4-7. Summary of protein and VSS measurement results

	Protein (g/L)	VSS (mg/L)	P/VSS	COD (mg/L)
Mother	462±26	1183± 87	0.391±0.024	369±23
Daughter Ave.	439±39	1357±158	0.324±0.027	340±88
Daughter (16g/L)[1]	43±20	1523± 79	0.311±0.012	416±32
Daughter (0g/L)[2]	45±16	1191± 64	0.339±0.013	264±49

1: Data obtained in the end of 16g/L glucose feed period.
2: Data obtained in the end of 0 g/L glucose feed period.

the daughter reactor cultures. The values of the protein content in total biomass obtained in this experiment are in good agreement with values reported in the literature. Hattingh et al. (1967) reported that a protein/VSS ratio of 0.362 was obtained for anaerobic sludge at the end of the sludge adaptation period.

4.3.6 Enumeration results

Epifluorescence microscopy direct counting methods were employed to estimate total living cells in the daughter reactor and the mother reactor cultures, while the MPN enumeration method was used to estimate the distribution of each major trophic group of anaerobic bacteria in the daughter reactor and the mother reactor.

a. Epifluorescence microscopy direct count results

Epifluorescence microscopy using acridine orange or DTAF as fluorescent dyes is used worldwide to determine the total number of microorganisms in environmental samples (Schimdt et al., 1982; Bratbak, 1985; Bitten, et al., 1993). Fluorescent dyes can be used to improve the visualization of individual microorganisms by binding to specific cell components, such as protein and DNA, and fluorescing under UV light. The living cells

stained by acridine orange (DNA stain) fluoresced orange under UV light, while the living cells stained by DTAF (protein stain) fluoresced green under UV light. Samples taken from the mother and the daughter reactors were diluted to 1 x 10^{-4}, and analyzed for total bacterial number by using acridine orange and DTAF direct counting methods (Appendix C).

One of the DTAF direct counting results for the mother and the daughter reactor cultures is presented in Table 4-8. Based on the experimental results, the total number of living cells in the re-established daughter reactor was twice the number found in the mother reactor culture.

Table 4-8. DTAF direct counting results for the mother and the daughter reactor cultures

Mother reactor (x 10^8/ml)	Daughter reactor (x 10^8/ml)
2.74	4.48
2.17	5.74
2.38	5.36
2.07	4.90
2.66	5.15
2.47	4.41
2.42 ±0.24	4.96 ±0.53

One of the acridine orange direct counting results for the mother and daughter reactor cultures are shown in Table 4-9. Higher values for the total number of living cells in both of the mother and the daughter reactor cultures were estimated by the acridine orange direct counting method. However the ratio of the total number of living cells in the daughter and the mother reactor cultures was close (ca. 2:1) to the value estimated by DTAF direct counting method.

Table 4-9. Acridine orange direct counting results for the mother and the daughter reactor cultures

Mother reactor (x 10^8/ml)	Daughter reactor (x 10^8/ml)
3.10	5.31
3.23	6.36
3.04	6.64
2.71	5.27
2.95	4.65
2.83	5.84
3.44	5.76
3.04 ±0.23	5.69 ±0.63

The total number of living cells in the mother and the daughter reactor cultures was estimated by two independent tests using DTAF and acridine orange direct counting methods. The total number of living cells estimated in this experiment are summarized in Table 4-10. As illustrated by the experimental results, the culture in the daughter reactor contained ca. two times more living cells than the culture in the mother reactor. The enumeration results suggest that the microorganisms in the daughter reactor culture were relatively small in size since the average VSS concentration in the daughter reactor was just slightly higher than the VSS concentration in the mother reactor (< 1.2 times). This was confirmed by direct microscope observation.

Table 4-10. Summary of DTAF and acridine orange direct counting results for the mother and the daughter reactor cultures

	Mother reactor (x 10^8/ml)	Daughter reactor (x 10^8/ml)	D/M
DTAF	2.42 ±0.24	4.96 ±0.53	2.05
	2.44 ±0.27	5.05 ±0.34	2.07
AO	3.04 ±0.23	5.69 ±0.37	1.87
	4.01 ±0.34	6.54 ±0.53	1.63
Average	2.98	5.56	1.87

Blank runs, using D.I. water, were performed with each experiment. The total bacterial number estimated from the blank was 1,000 times lower than the number obtained from reactor culture samples.

b. MPN enumeration results

In order to estimate the bacterial distributions of the major trohpic groups, a MPN enumeration was performed for the daughter reactor culture according to the procedure provided in Appendix I. The MPN enumeration results are presented in Table 4-11.

Based on the MPN values, the major anaerobic microorganisms in the periodically perturbed daughter reactor were fermentative bacteria. They contributed to 78% of the total culturable microbial populations presented in the anaerobic reactor. H_2- and acetate-utilizing methanogens contributed about 10.7% of the population. Sytrophic acetogens contributed ca. 11% of population. The proportion of methanogens present in the total culturable anaerobic bacteria population were in the range reported previously, 1 to 10%, in MPN enumeration tests (Anderson et al., 1994; Zhang and Noike, 1994)

Table 4-11. MPN values of anaerobic bacteria in the re-established daughter reactor culture estimated using 5 tube dilution (x10^8/ml)

Substrate	MPN (x10^8/ml)	95% confidence limits (x10^8/ml) lower	upper
Glucose	1.70	0.70	4.80
Acetate	0.17	0.07	0.48
Butyrate	0.17	0.08	0.41
Propionate	0.07	0.03	0.21
Hydrogen	0.06	0.03	0.18

A comparison of the MPN enumeration results from the mother and the daughter reactors shows some differences between these two cultures. The total number of culturable anaerobic bacteria in the daughter reactor was significantly higher (ca. 1.4 times) than the number in the mother reactor. Differences could also been observed in the distribution of the major trophic groups in the total culturable microbial populations.

MPN enumeration results were in good agreement with results obtained from epifluorescence microscopy direct counting experiments. Both enumeration results indicate a higher number of anaerobic bacteria in the daughter reactor culture. Based on the total number of anaerobic bacteria estimated by epifluorescence microscopy direct counting methods, the MPN enumeration method cultured ca. 38% to 52% of viable anaerobic bacteria present in the anaerobic cultures.

4.3.7 Microscopic observations

Differences in the microbial composition of the daughter reactor and the mother reactor cultures were easily observed using phase-contrast microscopy. Cultures from the daughter reactor were white in color with mostly dispersed cells. The microbial community in the daughter reactor appeared more homogeneous with less diversity. The predominant morphologies were short rods and cocci, with some long spirillum type bacteria (Figure 4-16a, scale bar in the photo represents 2 μm). In contrast, the microbial community in the mother reactor appeared to be more diverse, being comprised of more different morphotypes (Figure 4-16b). The predominant morphologies were long filamentous rods and short rods.

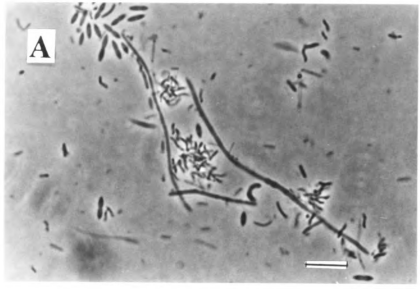

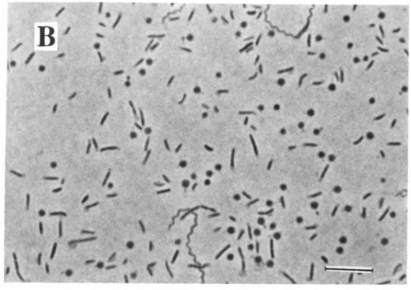

Figure 4-16. Microscopic observation of the mother (a) and daughter (b) reactor cultures.

4.4 DISCUSSION

For complete conversion of carbohydrates, such as glucose, to methane, five groups of bacteria: fermentative bacteria, propionate- and butyrate-utilizing acetogens and hydrogen- and acetate-utilizing methanogens are required (Mosey, 1983; Novaes, 1986; Pavlostathis and Giraldo-Gomez, 1991). These bacteria must work syntrophically as they are linked physiologically, kinetically and thermodynamically. Sudden environmental changes can cause changes in individual groups which eventually affect the whole microbial community (McCarty, 1964; Fongastitkul, 1994). Changes in the concentrations of intermediate volatile fatty acids during the perturbation period indicate that all the major groups of the anaerobic microbial community were impacted by the application of a substrate perturbation to the anaerobic chemostat. A change in the fermentation pattern was accompanied by a shift in the predominant microbial populations.

Typically, acetate-utilizing methanogens are responsible for the majority of COD removal and organic compound stabilization. (McCarty, 1964; Mosey 1981). The acetate-utilizing methanogens function at relatively high saturation levels (the ratio of steady-state substrate utilization rate V_t to the maximum substrate utilization rate V_{max}) compared to other anaerobic bacteria. Kaspar and Wuhrmann (1978) observed that the saturation level for acetate decarboxylation was about 43%. Similar results were reported by Valcke and Verstraete (1983) in their study of sludge fermentation. In the present study, a saturation level of 45 % was estimated under the baseline steady-state (constant feed) conditions. This indicates that the acetate-utilizing methanogens have limited additional capacity to handle sudden substrate increases. The acetate-utilizing methanogens are also among the slowest growing bacteria in the anaerobic microbial community with an experimentally observed growth yield of ca. 0.025 to 0.04 g VSS/g acetate (Lawrence and McCarty, 1967; Ahring and Westermann, 1987; Aivasidis et al., 1988). Consequently, these organisms are sensitive to environmental changes, and long periods are likely to be

required for this group of bacteria to adjust to new environmental conditions. This expectation was confirmed by the results.

Gas production on "famine days" (when glucose was not present in the feed) was a useful indicator of acetate-catabolizing methanogenic activity. After initiating the substrate perturbation, gas production on such days declined rapidly (Figure 4-7). This indicates a significant reduction in methanogenic acetate-catabolizing activity. Gas production on famine days decreased to less than 5 ml/d (detection limit) for about 30 days. Subsequently, limited gas production resumed on famine days, indicating a shift in the predominant acetate-utilizing population and/or an adaptation of the original acetate-catabolizing methanogenic bacteria. It took about 90 days for the complete recovery of acetate-catabolizing methanogenic activity.

The optimum pH for methane fermentation is between pH 6.5 to 7.4 (McCarty, 1964; Zehnder et al., 1981; Aivasidis et al., 1988; Attal, et al. 1988). At a pH value of 7.0, the methanogens could tolerate an acetate concentration as high as 6,000 to 7,000 mg/L without loss of normal acetate metabolic capacity, but they were quite sensitive to pH change (Duarte and Anderson, 1982; van den Berg et al., 1976; Yang and Okos, 1987). Yang and Okos (1987) published a study on a pure culture of methanogens utilizing acetate at pH 7 and 35 ^{o}C. In their study, the optimum acetate concentrations for the methanogenic bacteria *Methanosarsina barkeri* and *Methanosarsina mazei* were 7,000 and 6,800 mg/L, respectively. van den Berg et al (1976) reported similar results for an acetate enrichment culture operated at pH 7 and 35 ^{o}C, in which acetate conversion rates were not significantly affected by acetate concentration up to 6,000 mg/L, but when the reactor pH dropped to below 6.5, methanogenic activity decreased rapidly. In a pilot study, Duarte and Anderson (1982) found that a pH level of 6.4 was critical for a continuously fed acetate catabolizing digester operated at a 4.5 day hydraulic retention time and 35 ^{o}C. When reactor pH decreased from 6.5 to 6.3, methane production decreased by 65%, even though the digester had previously operated successfully at the same acetate concentration

(ca. 2,500 mg/L). This pH inhibition of acetate metabolism was attributed to either the pH drop itself or to the increased unionized acetic acid concentration at the lower pH.

McCarty (1964b) emphasized that a decrease in pH in anaerobic reactors should be considered as a sign of a imbalance between the different anaerobic trophic groups rather than the cause of the imbalance. This conclusion was also conformed with our experimental results. In the beginning of the perturbation experiment, due to the sudden change of the substrate feeding pattern, VFAs, especially acetate, were formed more rapidly than they were removed. The accumulated VFAs destroyed the reactor buffering capacity resulting in a decrease in reactor pH (Figure 4-5). The lower pH then, in turn, discouraged the growth of methanogens and, therefore, seriously prolonged the recovery process of the acetate-utilizing methanegons. This may help to explain why such a protracted period was required for the anaerobic community to adapt to the periodic substrate feeding conditions.

Although glucose accumulation was not observed throughout the whole experimental period, the fermentative bacteria were also affected by the periodic substrate perturbation. The most evident sign of this was the dramatic change in glucose fermentation products. For glucose, two complementary fermentation routes can occur (Cohen et al, 1979; Zoetemeyer et al, 1982a; McCarty and Mosey, 1991; Fongastitkul et al, 1994). Butyrate type fermentation is characterized by production of acetate, butyrate, carbon dioxide and hydrogen as the main fermentation products. Propionate type fermentation is characterized by the formation of acetate, propionate, and carbon dioxide, with much lower hydrogen concentrations.

Based on thermodynamic calculations, Duarte and Anderson (1982) proposed that under normal conditions (pH 7 and temperature 35 °C), the butyrate type fermentation is thermodynamically favored over the propionate type fermentation. Normally, the butyrate fermentation route is predominant in anaerobic reactors (McCarty and Mosey, 1991). This is indirectly supported by observations that anaerobic systems usually have limited

capacity for propionate metabolism but can metabolize butyrate at relatively high rates (Bae and McCarty, 1994). Thus, in anaerobic systems, butyrate is only present in trace amounts. This phenomenon was also observed in this experiment for the steady-state mother reactor and the daughter reactor prior to the start of the substrate perturbation (Table 4-4). Compared with the maximum butyrate degradation rate of 250 mg/g VSS-d, the maximum propionate degradation rate of 4.8 mg/g VSS-d possessed by the culture in the mother reactor is negligible.

During the perturbation period, glucose fermentation quickly shifted from the butyrate fermentation to a mixed butyrate-propionate fermentation. Propionate accumulation occurred immediately after initiating the perturbation (Figure 4-3). Since the propionate degradation ability of the microbial community was extremely limited, the observed propionate accumulation rate could be considered to approximate the actual propionate production rate from glucose. Mass balance calculations based on COD, indicated that during Stage 1a of the substrate perturbation, propionate fermentation accounted for as much as 37% of substrate flow. Prior to the initiation of the perturbation, propionate accumulation was observed to be less than 3% of substrate flow.

Subsequently, accelerated butyrate accumulation (Stage 1b) and a mixed butyrate-propionate type fermentation (Stage 2) were observed. During this period propionate accumulated continuously but at a reduced rate. The substrate flow through propionate fermentation decreased from ca. 37% to 12%. The molar ratio of accumulated butyrate to propionate was 1.8:1. This mixed butyrate-propionate type fermentation continued for about 70 days during the metastable steady-state. As the final transition period began, the butyrate type fermentation again became predominant.

The lithotropic H_2-utilizing methanogens were the organisms least affected in the anaerobic community. H_2 turnover rate appeared was affected over only a short period of time (the first 20 days). Mosey and Fernandez (1989) reported that the H_2-utilizing methanogens are relatively fast growing species, with an estimated doubling time of 6

hours. Kasper et al (1978) reported that under steady-state condition the saturation level of the H_2 utilizing methanogens was only about 1%. There is, therefore, a vast extra utilization capacity available for increased hydrogen oxidation during the substrate perturbation. The hydrogen-utilizing methanogens have also been found to be quite resistant to environmental changes. Hobson and Shaw (1978) found that at a pH of 7.1, an acetate or butyrate concentration up to 10,000 mg/l and propionate concentration up to 1,000 mg/L (as acetic acid) did not inhibit *M. formicicum*, the principal hydrogen-utilizing bacterium in a piggery-waste digester. Results of the present study indicate that the H_2 utilizing-methanogens in the mother reactor were resistant to changes in VFA concentration and pH (See Appendix V). The maximum H_2 utilization rate changed by only ca. 15% over a pH range of 5.5 to 7.5. These findings are in good agreement with the work of Attal et al. (1988) who reported an optimum pH range of 5.4 to 7.4 for hydrogen-utilizing methanogens. These characteristics apparently endow the H_2-utilizing methanogens with the ability to quickly and effectively respond to changes in substrate levels.

Results of protein analysis show that the average protein concentration in the mother and the daughter reactor cultures were essentially the same, but a much larger fluctuation in VSS concentration was observed in the daughter reactor. It appears that microorganisms in the daughter reactor acquired the ability to produce "stress products" during the feast period and then consume the stored products during the following famine period. This apparent storage ability acquired by the daughter reactor community allowed likely it to better tolerate the periodic substrate feed condition. The substrate storage capacity was most likely possessed by the acidogens, because: (1) this trophic group constituted the majority of the anaerobic population (79% based on MPN enumeration), and (2) the acidogens are the only major trophic group which could quickly respond to the substrate concentration change. This interpretation was supported by the decay test results. Based on results in Table 4-5 and 4-6, the decay of biomass in the daughter

reactor culture was faster than the mother reactor culture (K_{d1}). However, the maximum glucose utilization activiity of the daughter reactor culture decreased more slowly than that of the mother reactor culture (K_{d1}). A reasonable explain is that the stored substrate was consumed during the first stage of the starvation period of the daughter reactor culture resulting in a "faster" decay based on volatile solids concentration; while more acidogens remained alive due to the consumption of the stored substrate resulting in "slower" decay based on maximum substrate utilization rate. Substrate storage by acidogens has also being observed by the other researchers in glucose fed anaerobic reactors (Bae and McCarty, 1994).

The results in the perturbation experiment indicate that the structure of the anaerobic community gradually changed, enabling more effective utilization of substrate fed in a cyclic pattern. The remarkable morphological differences between the cultures in the mother and the daughter reactors suggest that the ability of the daughter reactor to adapt to the periodic substrate perturbation was most likely the result of a shift in the predominant species. Kinetic and enumeration results indicated that through a long-term selection the originally dominant microorganisms were replaced by some new/or adapted species which were smaller in size (in average) and were capably of higher substrate utilization rates and reduced decay rate. DNA and FAME (see Chapter 7 and 8) analyses support this interpretation.

4.5 SUMMARY

This study establishes that the initial steady-state anaerobic microbial community was sensitive to fluctuations in the pattern of organic loading rate of the carbon source. The rapid accumulation of VFAs reflects an apparent decrease in the number or activity of acetate-utilizing methanogens and acetogens during the initial 110 days.

Fermentative bacteria were also impacted by the substrate perturbation. A shift in the products of glucose fermentation occurred during the first and the second stages of the perturbation.

The pH decrease associated with VFA accumulation appeared to be, in-part, responsible for inhibiting acetate-utilizing methanogenic activity and prolonged the system recovery process.

The anaerobic system did gradually adapt to the perturbation conditions through a long term change in community structure as evidenced by changes in the kinetics of substrate utilization and decay, microbial composition and morphological changes.

Chapter 5

RESPONSE OF ANAEROBIC COMMUNITY TO THREE DAY FEAST-THREE DAY FAMINE LONG-TERM PERIODIC SUBSTRATE PERTURBATION

5.1 INTRODUCTION

Conversion of carbohydrates, fats and proteins to methane requires the combined activity of fermentative, acetogenic, and methanogenic bacteria (McCarty, 1981; Novaes, 1986; Pavlostathiand Giraldo-Gomez, 1991). Many studies have examined the response of anaerobic systems to environmental perturbations, especially changes in organic loading (Cohen et al., 1981; Smith and McCarty, 1989; Hickey and Switzenbaum, 1991b, c; Gupta, et al., 1994). Essentially all of the perturbation experiments described to date were performed over a relatively short time period (from a few days to a few weeks). Little is known about the effects of long-term, continuous periodic substrate perturbations on anaerobic community structure and function.

In order to determine whether long-term adaptive changes might occur in such systems, a series of long-term periodic substrate perturbations with different cyclic frequencies were applied to anaerobic chemostats. In Chapter 4, the response of an anaerobic chemostat subjected to an one day feast-one day famine cyclic feeding pattern was examined. This chapter extends the conditions evaluated to a long-term (>400 days) three day feast-three day famine feeding pattern. The response of the anaerobic chemostat population to the 3/3 day perturbation, especially the thermodynamic changes during the perturbation period, were investigated.

5.2 MATERIALS AND METHODS

5.2.1 Anaerobic reactor

A schematic representation of the experimental apparatus used for the perturbation experiment is shown in Figure 5-1. The experimental system consisted of a 1,500 ml working volume all glass reactor, timer controlled pumps for substrate and mineral media feed, and provisions for effluent liquid and gas effluent collection. Two Watson-Marlow 101 U/R pumps (Watson-Marlow, Inc., Wilmington, MA) were used to alternately supply glucose plus mineral media and mineral media alone (no glucose) at a flow rate ca. 150 ml/d. Power to the Watson-Marlow 101 U/R pumps was channeled through a electronic ChronTrol XT timer (ChronTrol Co., San Diego, CA). This programmable timer was used to control on/off operation of the two substrate feed pumps to obtain the desired substrate feed schedule. The contents of the anaerobic reactor were kept completely mixed with a magnetic stir bar driven by a Corning magnetic stir plate (Model PC-310, Corning Inc., Corning, New York). The entire apparatus was located in a constant temperature chamber (Nor-Lake Scientific, Hudson, WI) at 35 ± 0.5 °C.

5.2.2 Substrate and nutrients

Glucose was supplied as the sole carbon and energy source. Analytical reagent grade granular glucose (Mallinckrodt Specific Chemical Co., Paris, KE) was used to prepare the 16 g/L glucose solutions. A buffer solution, prepared with reagent grade powder sodium bicarbonate (J, T. Baker Inc., Philipsburg, NJ), was mixed with the glucose solutions to obtain 7 g/L $NaHCO_3$ in the feed solution. The mineral nutrient solution was selected based on the compounds and their concentrations used by several researchers worked on anaerobic digestion (Cohn et al. 1982; Zoetemeyer et al. 1982a; Zehnder et al. 1987). The concentration of the various components in the nutrient solution was described in detail previously (Chapter 4). Both the feed substrate solution and the feed nutrient solution were prepared with deionized water.

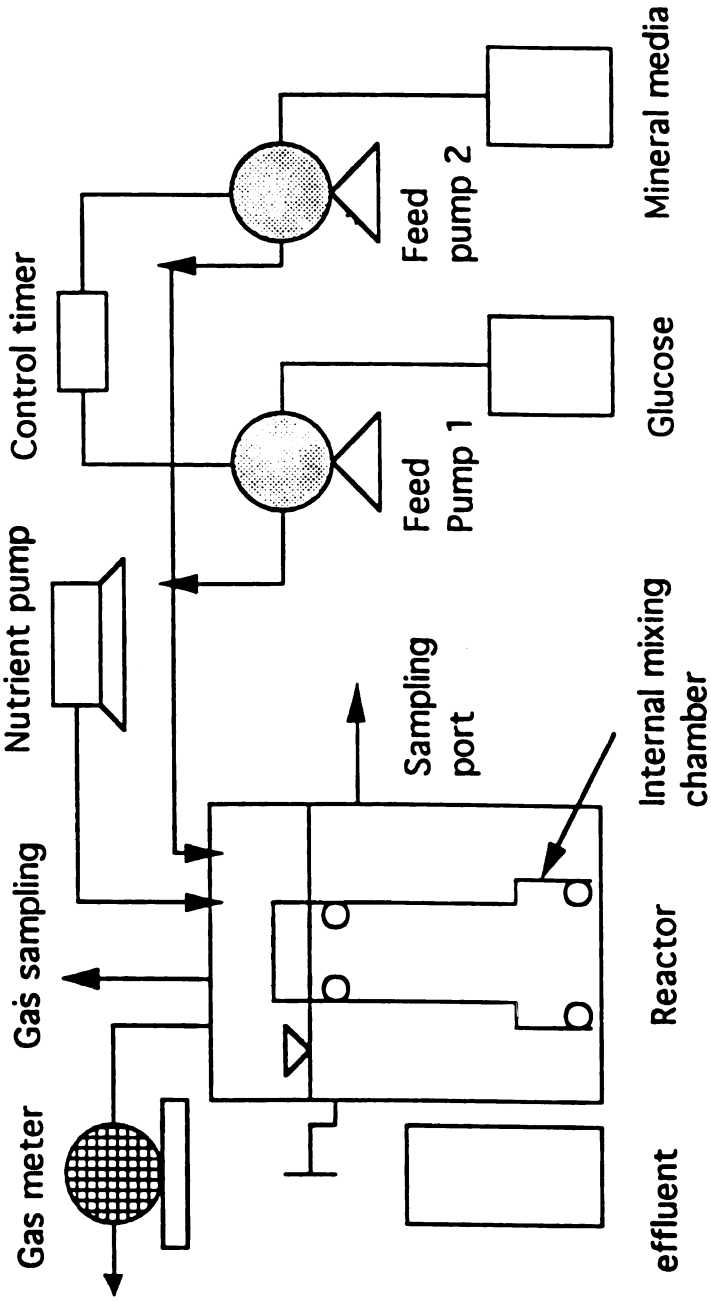

Figure 5-1. Schematic of the experimental set up.

5.2.3 Analytical methods

Reactor performance was monitored daily for effluent pH, total gas production and composition, and gas-phase hydrogen partial pressure. COD, VFA, ethanol and VSS analysis were performed on a daily to weekly basis, depending on reactor performance. Total gas production was measured with a digital gas meter based on liquid displacement. Procedures and equipment used for performing the above analyses are provided in Appendix A.

5.2.4 Free energy calculations

Free energy changes were calculated using a modified equation (Appendix F) which allows the effect of reactor pH to be counted for compared to standard physiological conditions (T = 35 °C and pH = 7).

$$\Delta G' = \Delta G^{o'} + m\,RT \ln([H^+]/10^{-7}) + RT \sum Vi \ln Ai \qquad (5\text{-}1)$$

where:

$\Delta G'$ = free energy change under operation conditions, KJ/mol

$\Delta G^{o'}$ = the increment of free energy under standard physiological conditions (25 °C, 1 atm and pH 7)

m = net number of protons in the reaction (m is negative when more protons are consumed than formed)

R = gas constant, 8.3143 J/K-mol

T = temperature, K

$[H^+]$ = proton concentration in the reactor solution, mol

Vi = the stoichiometric coefficient for component Ai in a biological reaction (i = 1,2,3,...) and is negative for reactants and positive for products

Ai = the physiological concentration of the component i in the reaction, mol.

Under experimental conditions, the reactor temperature was maintained at 35 °C (308 K), therefore equation (5-1) can be rewritten as:

$$\Delta G' = \Delta G^{o'} + 5.9\,[\log([H^+]/10^{-7})^m + \sum Vi \log Ai] \qquad (5\text{-}2)$$

TABLE 5-1. Free energy associated with the anaerobic oxidation of glucose fermentation intermediates.

Equation	$\Delta G^{o'}$ (KJ/mol)
(1) $CH_3CH_2COO^- + 2\ H_2O = CH_3COO^- + 3\ H_2 + CO_2$	+76.1
(2) $CH_3CH_2CH_2COO^- + 2\ H_2O = 2\ CH_3COO^- + 2\ H_2 + H^+$	+48.1
(3) $CH_3CH_2OH + H_2O = CH_3COO^- + H^+ + 2\ H_2$	+9.6
(4) $CH_3COO^- + H^+ = CH_4 + CO_2$	- 35.8
(5) $4H_2 + CO_2 = CH_4 + 2H_2O$	- 135.8

Equations used to calculate standard free energies for anaerobic oxidation of glucose metabolic intermediates at pH 7 are presented in Table 5-1. Free energy values were calculated according to Thauer et al. (1977).

5.2.5 Reactor inoculation

The inoculum (1,500 ml) for the daughter reactor was obtained from a 15 L laboratory-scale "mother" reactor operated under steady state conditions with a 10 day HRT and a constant 8 g/L glucose feed. The mother reactor was inoculated with digester sludge taken from Jackson Wastewater Treatment Plant (Jackson, Michigan). The inoculated "daughter" reactor was initially operated under the same conditions as the mother reactor (10 day HRT with continuous input of 8 g/L glucose) for 50 days. Once

steady-state was reached and sufficient baseline information obtained, a square wave substrate perturbation was applied to the daughter reactor.

5.2.6 Experimental design

In this study, a long term periodic substrate perturbation was applied to an anaerobic "daughter" reactor. The response of the system to the perturbation was then investigated. During the perturbation, the reactor influent glucose concentration was alternately changed in amplitude from 16 g/L to 0 g/L (mineral media only) on a 6 day square wave cycle (Figure 5-2), i.e. the reactor was fed 16 g/L glucose solution for three days followed by glucose-free mineral media at the same flow rate for the next three days. A 10 day hydraulic retention time (dilution rate of 0.1 d^{-1}) was maintained throughout the experiment. The perturbation loading pattern was chosen so that the average influent glucose concentration during the perturbation period was equal to the steady-state concentration of 8 g/L applied to the control "mother" reactor. The daughter reactor was continuously operated for a period of 450 days including ca. 50 days under steady-state baseline conditions and ca. 400 days under perturbation conditions.

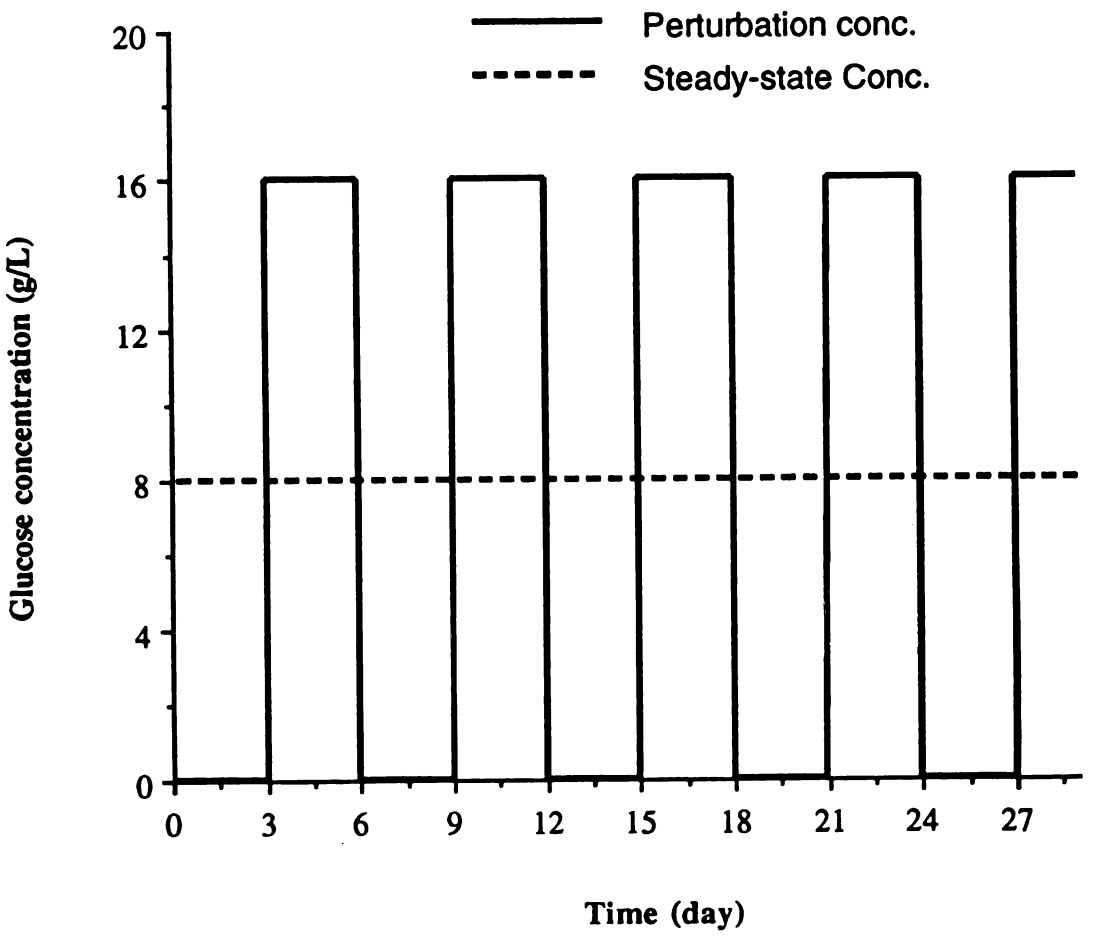

Figure 5-2. Substrate feeding pattern used for perturbation experiment.

5.3 RESULTS

5.3.1 Effects of the periodic substrate perturbation.

The response of the daughter reactor community to the periodic substrate perturbation can be broken down into four distinct stages (Figure 5-3): 1. rapid accumulation of metabolic intermediates of glucose fermentation (acetate, propionate, hydrogen and ethanol) and COD accumulation; 2. establishment of a metastable "steady-state" at reduced COD removal efficiency (Figure 5-4); 3. rapid VFA degradation; and (4) re-establishment of steady-state with high COD removal efficiency. Stage 1 can be further divided into two distinct sub-stages: stage 1a. rapid acetate and propionate accumulation, and stage 1b. rapid ethanol and hydrogen accumulation while acetate and propionate concentrations stabilized. Stage 2 also can be divided into two sub-stages: stage 2a. a cyclic pattern of acetate and butyrate concentration changes and stage 2b. all the major glucose degradation intermediates become more stabilized. Each of the above stages is discussed in greater detail in the following sections.

Stage 1a (day 0 to day 18)

As shown in Figures 5-3 and 5-4, the initial microbial community was highly sensitive to variation in organic feed concentration. A rapid accumulation of glucose metabolic intermediates including acetate, propionate, as well as ethanol and hydrogen, occurred nearly immediately after initiation of the substrate perturbation. Effluent COD concentration quickly increased from 370 mg/L to ca. 6,000 mg/L during the first 18 days (three complete perturbation cycles), accumulating at an average rate of 310 mg/L-d (Figure 5-4).

The acetate-utilizing methanogens were immediately impacted by the substrate perturbation as evidenced by a sharp increase in the effluent acetate concentrations. Effluent acetate concentration increased from 150 mg/L to ca. 3,000 mg/L during the first 18 days, accumulating at an average rate of 158 mg/L-d. Acetate contributed ca. 50% of

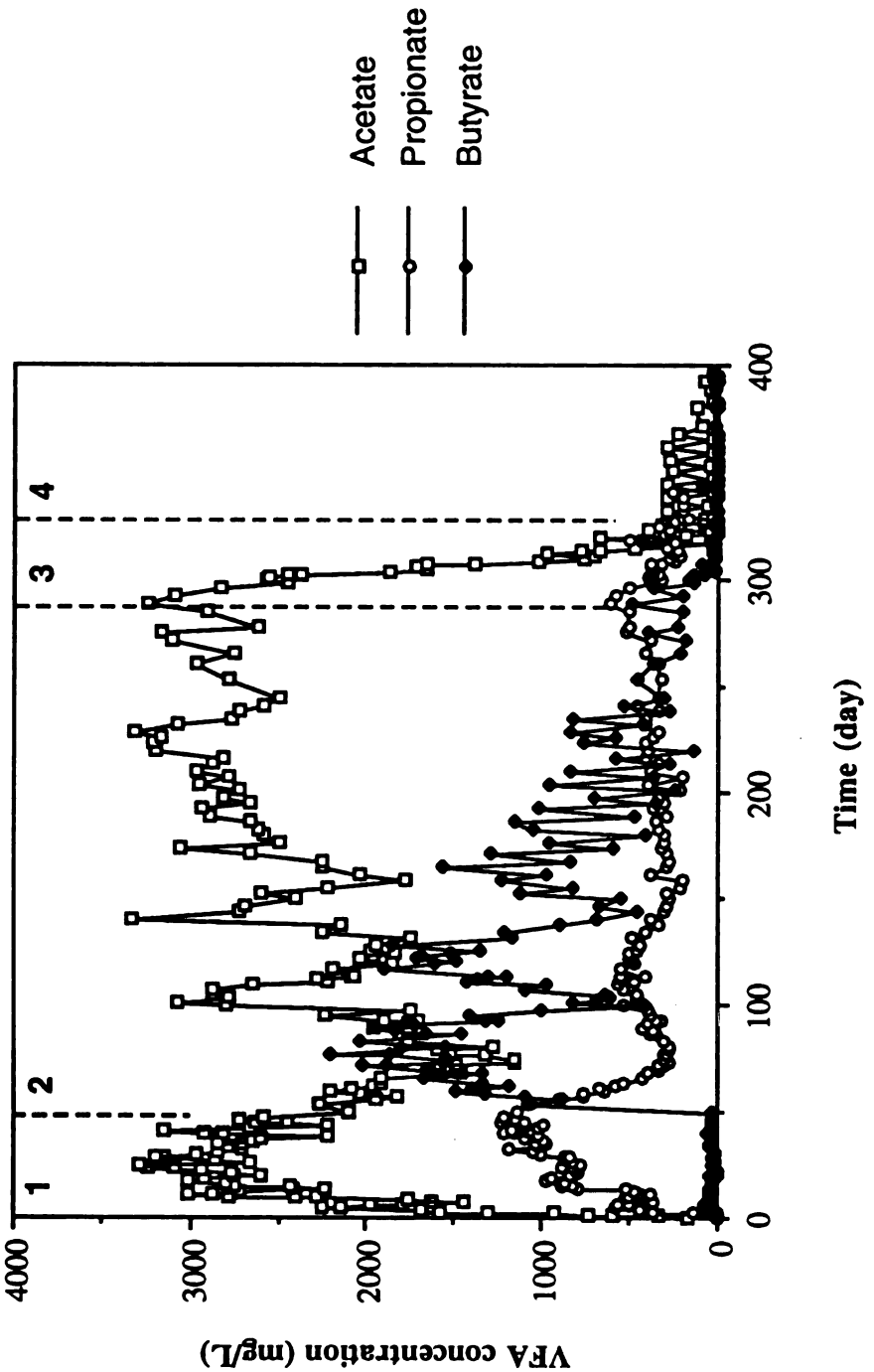

Figure 5-3. Changes in VFA concentrations in during the perturbation period.

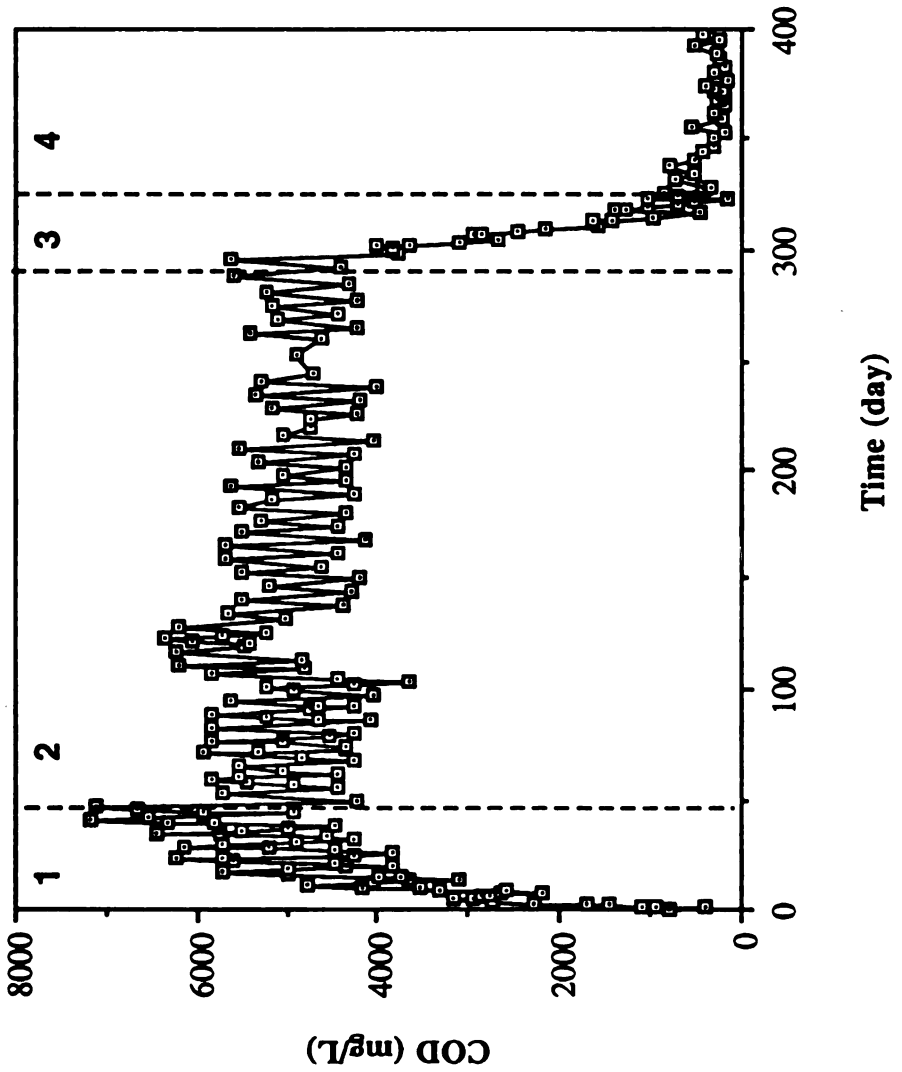

Figure 5-4. Changes in COD concentrations during the perturbation period.

the total increase in COD observed during this period, with acetate concentration fluctuating around 3,000 mg/L.

A rapid accumulation of propionate was also observed during the initial 18 days of the substrate perturbation. Effluent propionate concentration increased from less than 30 mg/L to a level of ca. 1,000 mg/L, at an average daily accumulation rate of 53 mg/L-d. Propionate contributed about 26% of the total COD accumulated during this period.

Ethanol and gas phase hydrogen concentrations increased appreciably during the glucose feed period. Although the accumulated ethanol and hydrogen degraded during the following fasting periods (mineral media only), peak concentrations of accumulated ethanol and hydrogen during the feed periods gradually increased.

Butyrate did not accumulate during this period. Effluent butyrate concentration remained at ca. 30 mg/L.

Stage 1b (day 19 to day 48)

During this period, the acetate and propionate concentrations stabilized while an accelerated accumulation of hydrogen and ethanol was observed. (Figure 5-5a). The accumulation of hydrogen suggests a significant decrease in hydrogen-utilizing methanogenic activity. As shown in Figure 5-5a, hydrogen accumulated immediately after initiation of the substrate perturbation. A maximum hydrogen partial pressure of ca. 6.6 x 10^{-2} atm (6.6% headspace gas composition) was observed at day 45. Subsequently, hydrogen concentrations decreased rapidly.

Ethanol accumulation was coincident with the periodic hydrogen accumulation (Figure 5-5b). The peak values of accumulated ethanol quickly increased to ca. 800 mg/l within four complete perturbation cycles (24 days). Thus, ethanol contributed as much as 23% of the accumulated COD during this period. In contrast to the accumulation pattern of the VFAs, the ethanol that accumulated during the three day glucose feed period was quickly metabolized during the following three day fasting period. Periodic ethanol accumulation

70000

60000

50000

40000

30000

20000

10000

10

Years

P

P

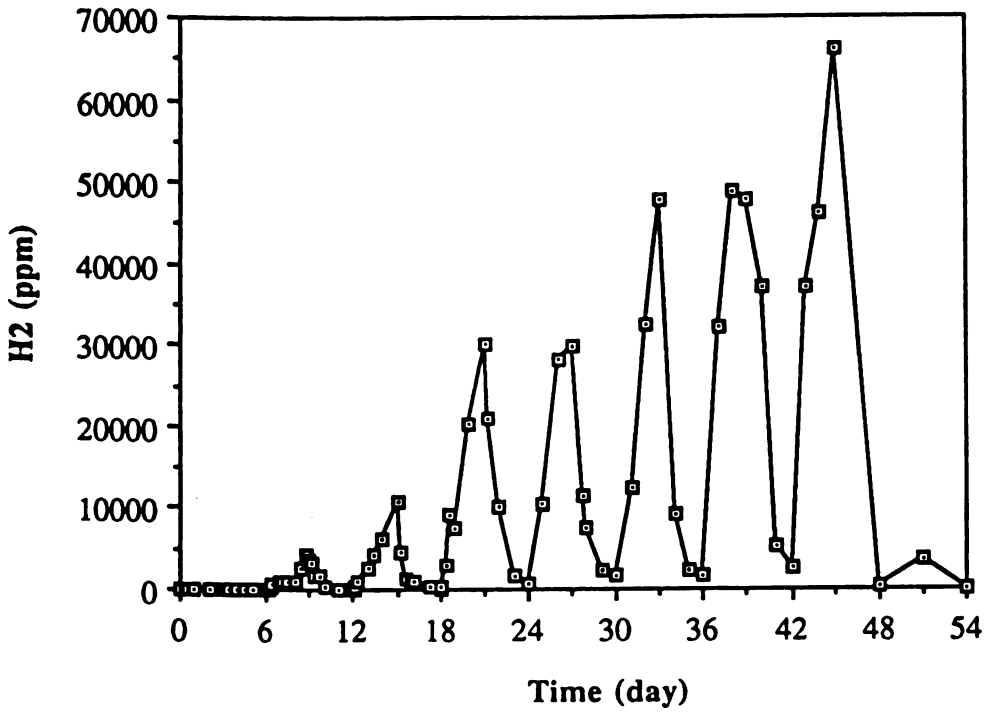

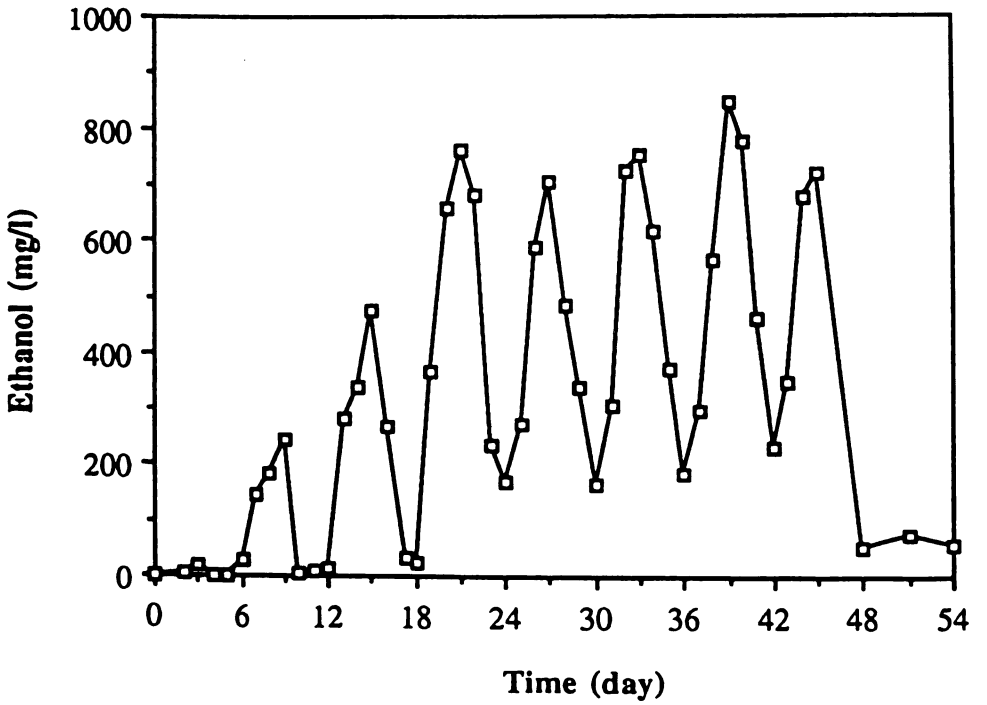

Figure 5-5. Changes in hydrogen and ethanol concentrations during the first stage of the perturbation period.

continued, until a complete recovery of hydrogen-utilizing methanogenic activity was observed. No significant ethanol accumulation was observed thereafter.

During the first stage of the substrate perturbation, pH decreased from a steady-state value of 7.0 to ca. 6.2 with large fluctuations (Figure 5-6). Daily gas production rate (average value for the 6-day cycle) decreased from about 430 ml/L-d to a minimum level of ca. 135 ml/L-d at the end of this period (Figure 5-7). Most of the gas was produced during the glucose feeding period. The average gas production during the famine period decreased from ca. 80 ml/L-d to ca. 10 ml/L-d within about 50 days. Effluent butyrate and iso-butyrate concentrations remained low (less than 50 mg/L and 90 mg/L, respectively) during the first stage of the substrate perturbation. No VFAs, other than acetate and propionate, accumulated during this period. No glucose (< 0.5 mg/l) was detected in the reactor liquid phase during the glucose feed period.

Stage 2. (day 49 to 289)

When the average effluent COD concentration reached ca. 5,000 mg/L, a metastable "steady-state" was established. During this period, the peak hydrogen concentrations observed during the glucose feed period soon returned to near their prior perturbation levels of less than 50 ppm, and remained stable at this level thereafter. COD removal efficiency averaged about 41%, compared to ca. 95% during the baseline period. Average daily gas production decreased to 54 % of the baseline value, and CH_4 content in the reactor headspace was 26% compared to 50% prior to the perturbation. Although effluent COD remained relatively stable during the metastable steady-state, significant changes in the composition of the VFAs were observed.

2a. (day 49 to 189)

For the period of from day 49 to 189, a dramatic accumulation of butyrate was initially observed. Between days 49 and 52, butyrate concentration quickly increased

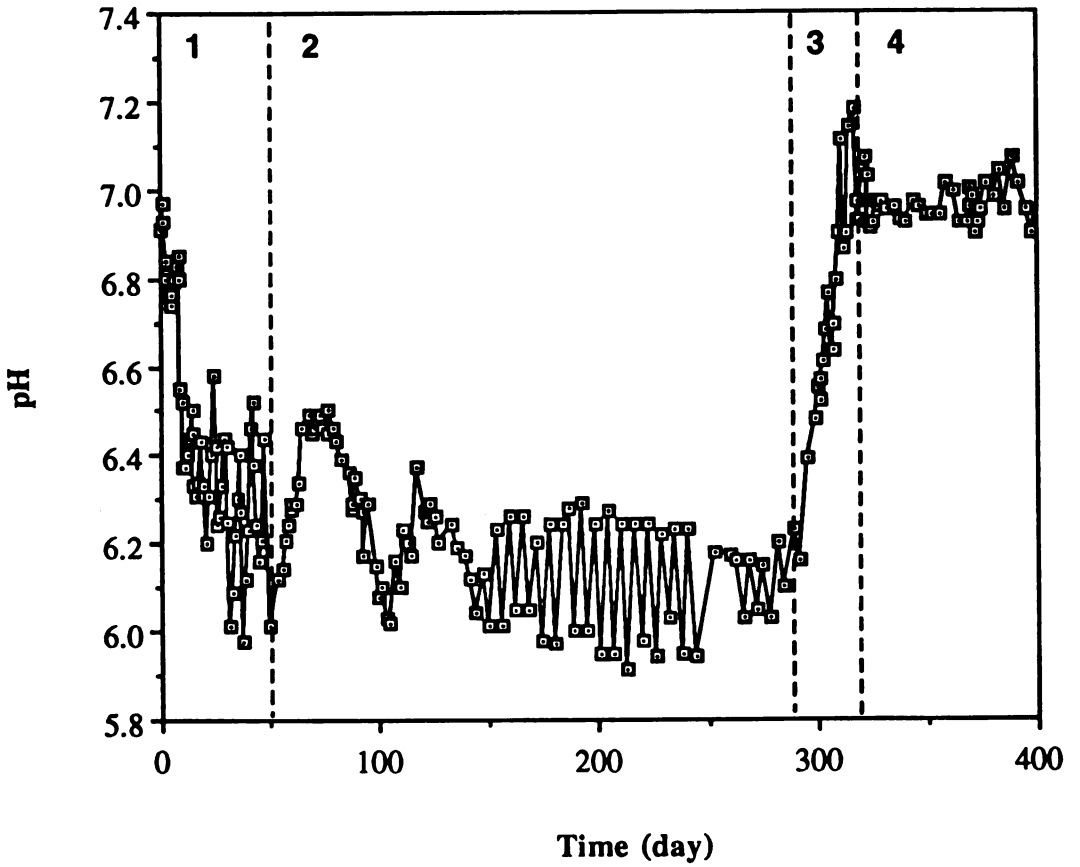

Figure 5-6. Changes in pH during the perturbation period.

Gas (mL/L-d)

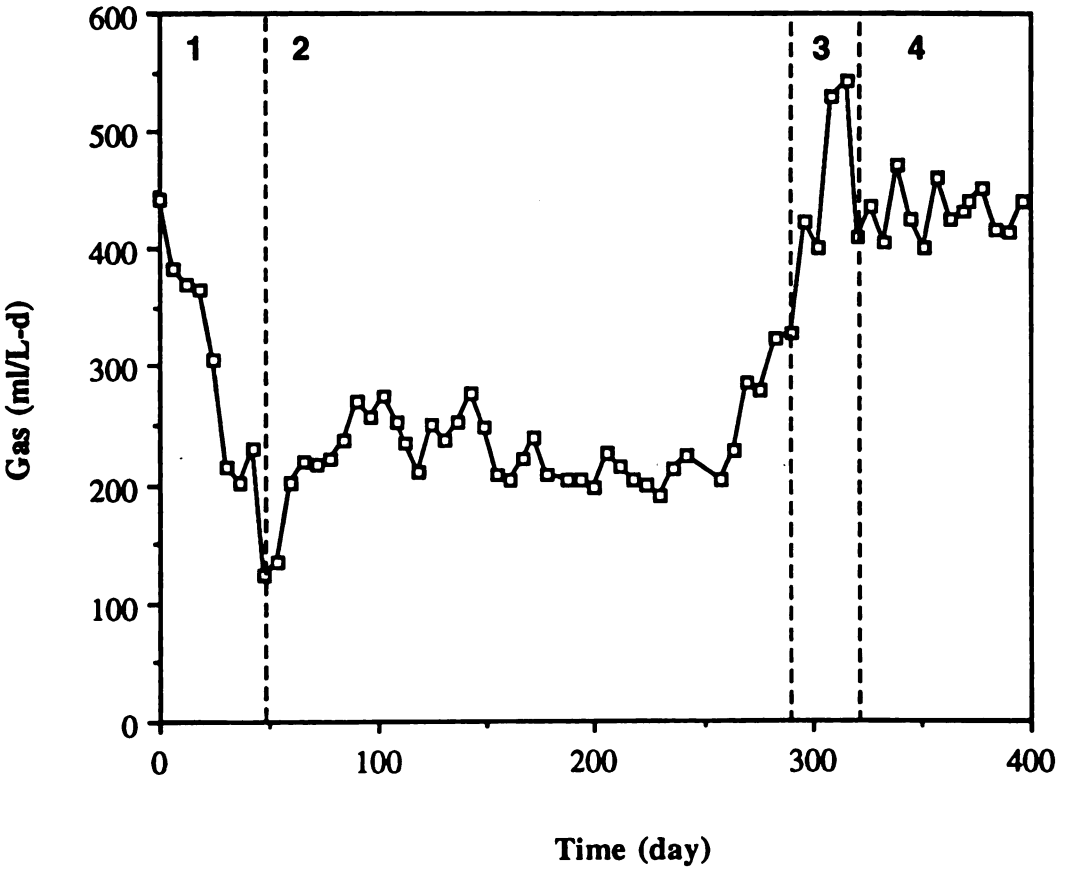

Figure 5-7. Gas production during the perturbation period.

from less than 50 mg/L to ca. 1,100 mg/L, and in the following 20 days, butyrate concentration further increased to a peak level of ca. 2,200 mg/L, accounting for as much as 65% of the accumulated COD during this period. Acetate concentration varied concurrently with butyrate concentration in a cyclic pattern, when butyrate levels increased acetate levels decreased and vice-versa. In each cycle, the acetate and butyrate concentrations varied concurrently with amplitudes from ca. 1,700 mg/L to ca. 3,400 mg/L and from ca. 2,000 mg/L to ca. 500 mg/L, respectively. The cyclic pattern of acetate and butyrate concentration changes had a frequency of approximating 48 days for three complete cycles.

Propionate concentration decreased steadily from ca. 1,200 mg/L to a minimum level of ca. 300 mg/l. It then increased slightly to an average value of ca. 400 mg/L, accounting for about 12% of the accumulated COD during this period.

2b. (day 190 to day 289)

During this period, the 50 day butyrate-acetate concentrations cyclic variation pattern was broken. Butyrate concentration steadily decreased within several mini cycles in two apparent steps. First the butyrate concentration steadily decreased from ca. 1,200 mg/L to a minimum level of ca 150 mg/L. Acetate concentration concurrently increased to levels of over 3,200 mg/L. This peak acetate concentration apparently temporarily blocked butyrate degradation, as a result butyrate concentration quickly increased until a peak level of ca. 1,100 mg/L was reached. In the following ca. 60 days, the butyrate concentration again continuously decreased and stabilized at a level of ca. 300 mg/L. The acetate concentration fluctuated around ca. 2,800 mg/L.

Stage 3 (day 290 to day 340)

A rapid decrease in VFA concentrations began on day 290. As shown in Figure 3a, during this period a sharp decrease in acetate concentration was observed. Within about

30 days, the acetate concentration decreased from ca. 3,200 mg/L to less than 200 mg/L. Meanwhile, butyrate and iso-butyrate concentrations quickly decreased from ca. 450 and 250 mg/l to their pre-perturbation concentrations of less than 30 mg/L each, respectively. Propionate concentration decreased steadily from 600 mg/L to ca. 300 mg/L, and effluent COD decreased from ca. 5,500 mg/L to less than 800 mg/L. The pH quickly increased from 6.2 to about 7.1, and the gas production rate also reflected a drastic change in VFA utilization. Average gas production rate peaked at 560 ml/L-d on the same day what acetate concentration began to fall (Figure 5-7).

Stage 4 (day 340 to day 400)

With the exception of propionate, all VFAs stabilized at new steady-state levels within ca. 30 days subsequent to the start of rapid acetate degradation. After another 20 days, a new steady-state was re-established in the anaerobic reactor. During this period the average COD concentration, pH and biogas production rate were similar to those observed before the substrate perturbation. A comparison of the reactor performance during the pre-perturbation steady-state condition, the metastable steady-state condition, and the new steady-state condition established during the substrate perturbation, is presented in Table 5-2.

5.3.2 Changes in gas production rate during substrate perturbation period

Gas production directly represented the effect of the periodic substrate perturbation on the anaerobic microbial community. During the first stage of the substrate perturbation, a period marked by rapid VFA accumulation, the average daily gas production (average value for the 6-day cycle) concurrently decreased from about 430 ml/L-d to a minimum level of ca. 130 ml/L-d. The average daily gas production increased slightly and fluctuated around a level of 230 ml/L-d (Figure 5-7). As observed in previous one day feast-one day famine perturbation, most of the gas was produced on days when glucose was provided

Table 5-2. Summary of reactor operation results during the different stages of the perturbation experiment[1]

	Baseline steady-state	Metastable steady-state	New steady-state
COD_{in} (mg/l)	8500	8500	8500
COD_e (mg/l)	370 ± 53[2]	4970 ± 630	280 ± 103
VSS (g/l)	1060 ± 160	720 ± 160	1000 ± 180
Gas (ml/L-d)	430 ± 20	230 ± 30	440 ± 260
CH_4 (%)	50 ± 2.0	26 ± 6.0	49 ± 2.0
pH	7.02 ± 0.04	6.14 ± 0.17	6.97 ± 0.04
Acetate (mg/l)	150 ± 30	2320 ± 570	120 ± 100
Propionate (mg/l)	26 ± 15	403 ± 110	18 ± 9.0
Butyrate (mg/l)	24 ± 8.0	1030 ± 550	8 ± 4.0
Iso-butyrate (mg/l)	17 ± 10	90 ± 60	2 ± 0.8

1: All the data shown in the columns of transient steady-state and new steady-state are averaged values for six day cycle during substrate perturbation period.
2: Standard deviation.

(440 to 460 ml/L-d). Average gas production for three famine days in each cycle decreased steadily from ca. 100 ml/L-d to a minimum level of ca. 10 ml/L-d within ca 50 days, indicating a significant decrease in the number or activity of acetate-utilizing methanogens. Subsequently, gas production on famine days increased slightly and fluctuated around a level of ca. 25 ml/L-d for about 190 days. After day 240, gas production on famine days increased (Figure 5-8), and by day 270, it had increased to near pre-perturbation levels. A sudden increase in the gas production rate was then observed on famine days. On day 315, a peak gas production of ca. 448 ml/L-d was observed on a famine day. This peak coincided with a sharp drop in acetate concentration of the reactor effluent. Gas production on famine days stabilized at a level of ca. 100 ml/L-d thereafter.

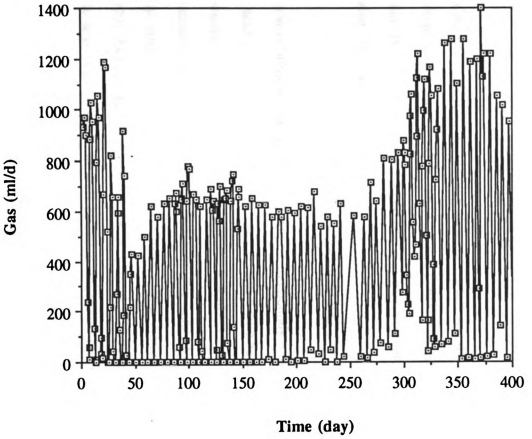

Figure 5-8. Daily gas production during the perturbation period

5.3.3 Changes in un-ionized VFA concentrations during the substrate perturbation period

No special pH control means other than routine bicarbonate addition was employed. Under these conditions, accumulated VFA concentration (as acetic acid) correlated with reactor pH throughout the experiment.

Accumulation of acetic or other volatile fatty acids will neutralize mineral alkalinity in the reactor, causing the pH to decrease. A pH-dependent equilibrium exists between the ionized and un-ionized volatile acids is illustrated for acetate in Equation 5-3:

$$CH_3COOH = CH_3COO^- + H^+ \qquad (5\text{-}3)$$

As the pH decreases, equilibrium shifts to the left and the un-dissociated acetic acid concentration increases. At 35 °C the ionization constant (K_{ca}) has a value of 1.73×10^{-5} (Kroeker, 1979). The un-ionized acetic acid concentration can be calculated by using the following equation:

$$[CH_3COOH] = [CH_3COO^-][H^+]/K_{ca} \qquad (5\text{-}4)$$

Because of the passive diffusion of neutral compounds across the bacterial membrane, acetic acid and other VFAs in their un-ionized form would be expected to cross penetrate the bacteria cell membrane without resistance. Un-ionized VFA level is a function of VFA concentration and environmental pH, and is directly linked to inhibition of methanogenic activity (Attal et al, 1988; Duarte and Anderson, 1982; Anderson et al., 1982; Kroeker et al., 1979). As illustrated in Figure 5-9, the un-ionized VFA concentration (as acetic acid) is usually less than 10 mg/L in well operated anaerobic reactors. An un-ionized VFA concentration above 30 mg/L tends to result in reactor failure. Therefore, an increase in VFA concentration or a decrease in pH may increase un-ionized VFA concentration to levels at which acetate-metabolizing methanogenic activity is significantly inhibited or even stopped.

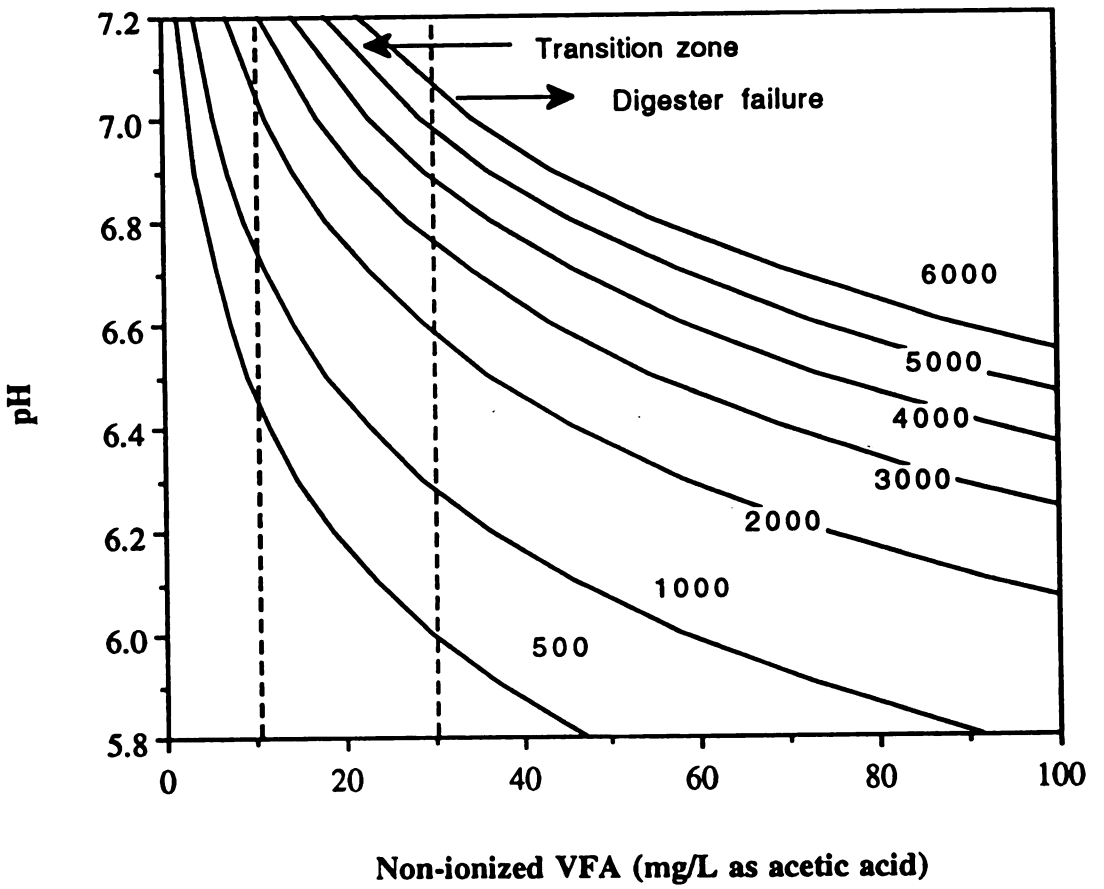

Figure 5-9. Relationship of un-ionized volatile fatty acids, pH and anaerobic reactor performance (after Attal et al, 1988; Duarte and Anderson, 1982; Kroeker et al., 1979).

The changes in un-ionized VFA concentrations (as acetic acid) in the present study and in the one day feast-one day famine perturbation (1/1 day perturbation) are presented in Figure 5-10, and summarized in Table 5-3. Experimental data show that although the average VFA concentrations were essentially the same in the metastable steady-state in both perturbation tests, due to a combined effect of lower pH value and larger fluctuations in VFA concentrations, much higher un-ionized acetate and un-ionized VFA concentrations were observed during the 3/3 day perturbation test.

Table 5-3. Summary of un-ionized acetate and un-ionized VFA concentrations (as acetic acid) observed during the 3/3 day and 1/1 day substrate perturbations[1]

	Steady-state	Metastable steady-state	New steady-state
Reactor 3/3:			
pH	7.2	6.14	6.97
un-ionized Ac (mg/L)	0.3	97.10	0.74
un-ionized VFA (mg/L)	1.04	142.90	0.86
Reactor 1/1:			
pH	7.2	6.34	7.02
un-ionized Ac (mg/L)	1.05	65.64	1.44
un-ionized VFA (mg/L)	1.43	93.36	1.61

1: Data used for un-ionized VFA calculation were taken from Tables 4-3 and 5-2 respectively.

Un-ionized VFA (mg/L as acetic acid)

Fig
Sub

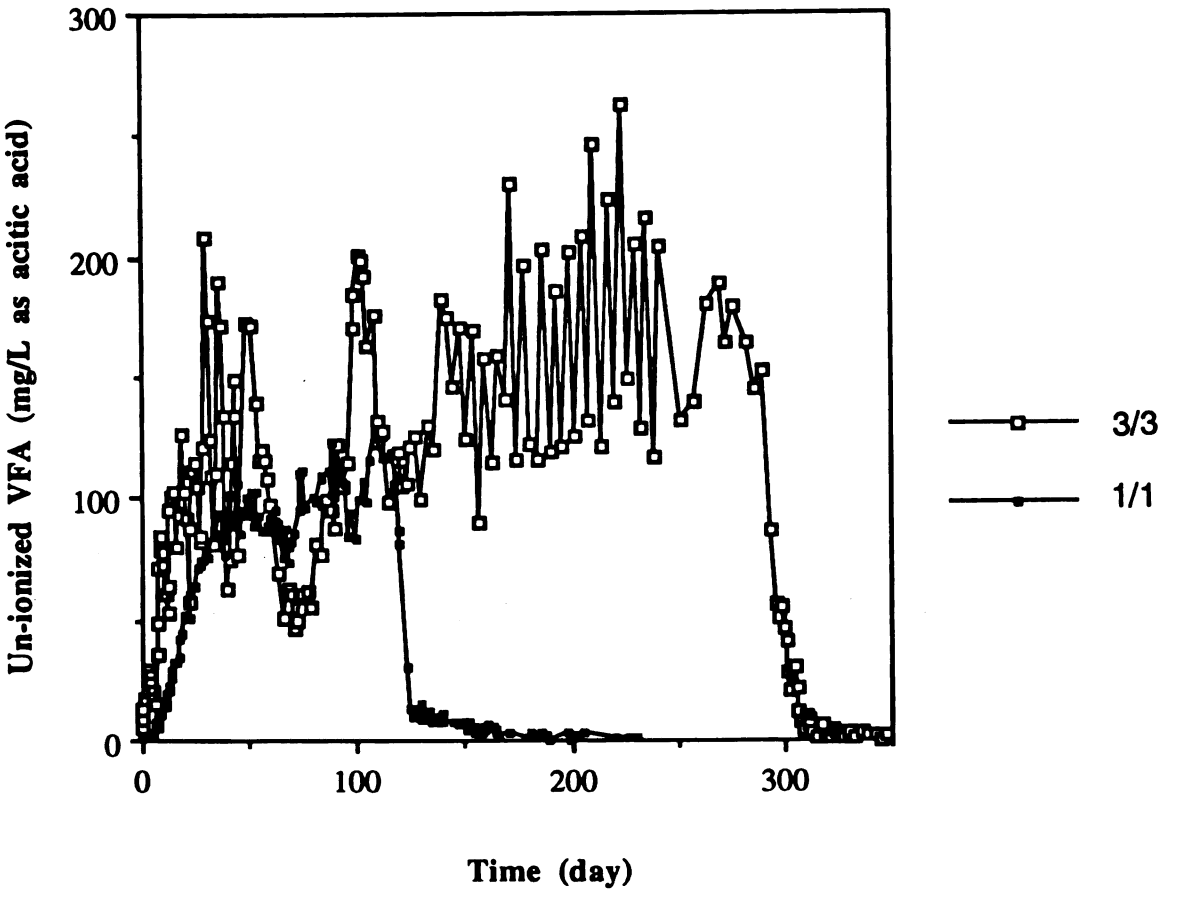

Figure 5-10. Changes in non-ionized VFA concentrations during the 1/1 day and 3/3 day substrate perturbations.

5.3.4 Free energy calculations for anaerobic oxidation of glucose metabolic intermediates.

Free energy available for hydrogen and carbon dioxide conversion to methane during the pre-perturbation period varied between -3.3 to -6.2 KJ/mol of H_2 (Figure 5-11a). This value increased to between -25 and -27 KJ/mol of H_2 during the first stage of the perturbation period indicating that the removal of hydrogen was not thermodynamically limited. These values decreased to levels approaching pre-perturbation values during the beginning of the second stage.

During the first two stages of the long-term substrate perturbation, acetate concentration rapidly increased and then stabilized at levels of around 3,000 mg/L. The free energy available for acetate catabolism concurrently increased from ca. -24 KJ/mol to -37 KJ/mol during this period (Figure 5-11b), indicating that acetate accumulation was the result of a kinetic and not thermodynamic limitation. Production of acetate exceeded the ability of the acetate utilizing methanogens to metabolize acetate by a considerable amount.

This does not appear to be the situation for the accumulation of the higher molecular weight VFAs. The free energy available for oxidation of propionate and butyrate dramatically changed during the first two stages. Results of free energy calculation show that during the first stage of the substrate perturbation, free energy available for propionate and butyrate catabolism concurrently decreased from ca. -5.1 KJ/mol and -13.1 KJ/mol to average levels of 40 KJ/mol and 34 KJ/mol, respectively (Figure 5-12a and b). This was caused by significant hydrogen accumulation. As a result, oxidation of propionate and butyrate was thermodynamically impossible. During the second stage, when hydrogen concentration returned to pre-perturbation levels (< 50 ppm), the free energy for oxidation of propionate and butyrate again became favorable. Free energy available for propionate and butyrate oxidation fluctuated around -7.5 KJ/mol and -5.0 KJ/mol, respectively. When steady-state conditions were re-established, the free energy available for propionate and butyrate oxidation increased to ca. -14.2 KJ/mol and - 16.2 KJ/mol, respectively.

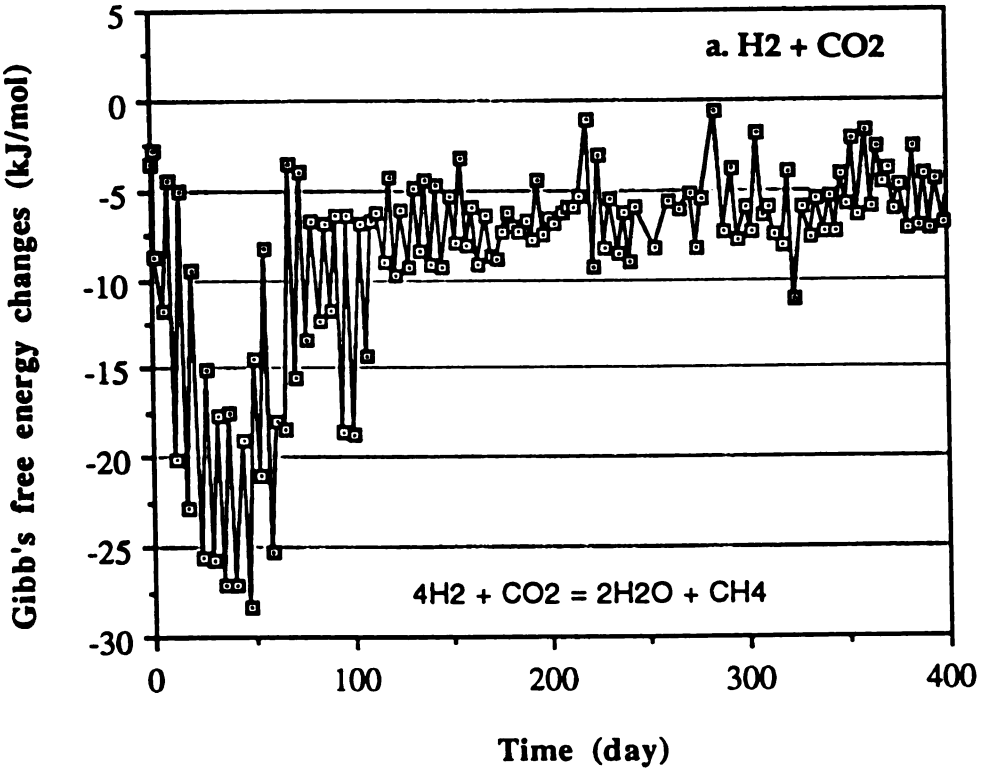

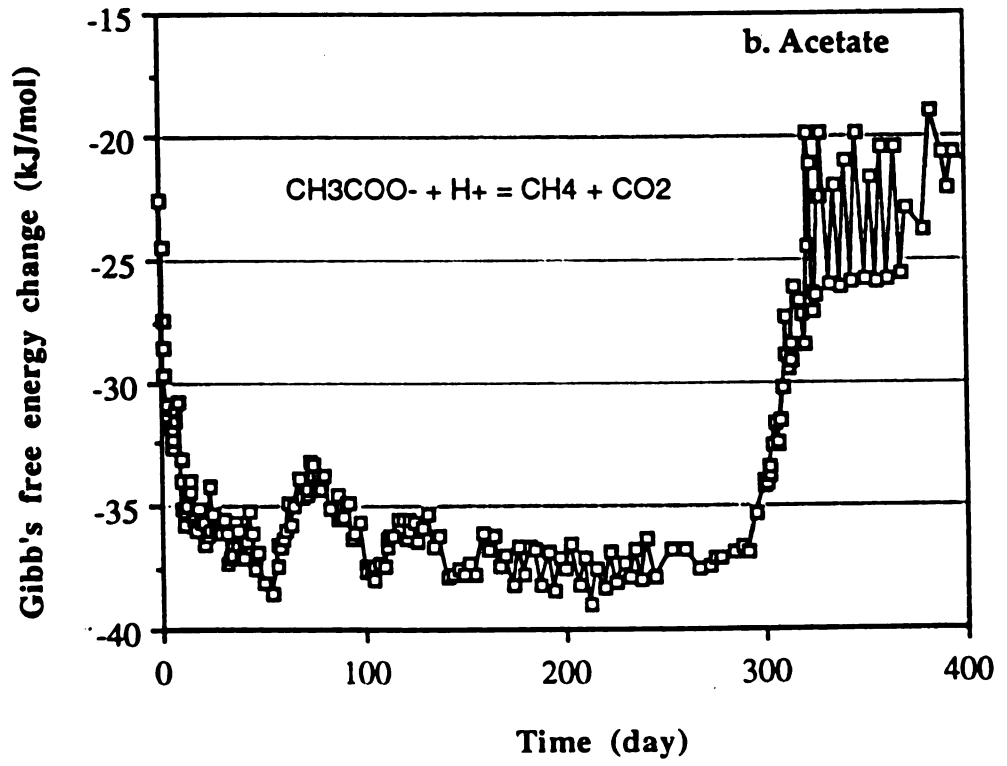

Figure 5-11. Free energy available for hydrogen and carbon dioxide, and acetate conversion to methane during the substrate perturbation period.

Gibb's free energy Change (kJ/mol)

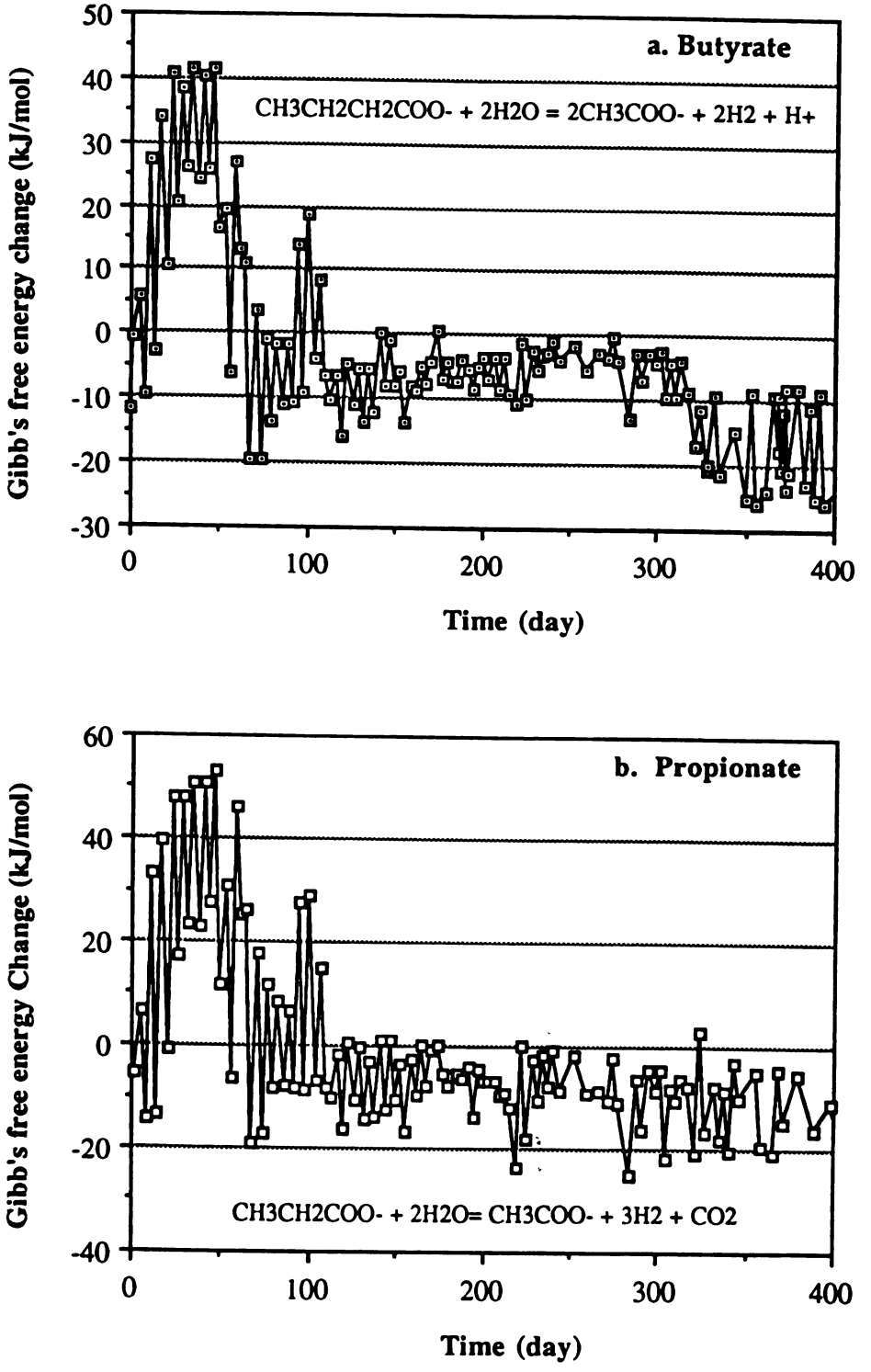

Figure 5-12. Free energy available for the anaerobic oxidation of butyrate and propionate during the substrate perturbation period.

Free energy calculations for ethanol oxidation show that during the first stage of the substrate perturbation the free energy available for ethanol oxidation changed dramatically within each perturbation cycle (Figure 5-13). A cyclic pattern of free energy changes, driven by the pattern of hydrogen accumulation (Figure 5-5), was observed. Although the free energy available for ethanol oxidation was negative most of the time, the average free energy in each perturbation cycle decreased quickly from ca. -28 KJ/mol to ca. -5 KJ/mol in the end of the first stage. When the hydrogen concentration returned to normal (< 50 ppm) in the beginning of the second stage, free energy available for ethanol oxidation increased to near pre-perturbation values and stabilized thereafter.

Free energy changes calculated for oxidation of glucose metabolic intermediates under steady-state pre-perturbation and perturbation conditions are summarized in Table 5-4.

Table 5-4 Free energy values (KJ/mol) observed for the anaerobic oxidation of glucose metabolic intermediates during substrate perturbation.

Substrate	Baseline Steady-state	Transient Steady-state[1]	New Steady-state
Acetate	-24.3 ± 3.1[2]	-37.4 ± 0.7	-23.6 ± 2.8
Propionate	- 5.1 ± 1.7	-7.5 ± 5.6	-14.2 ± 4.9
Butyrate	-13.1 ± 3.7	-5.0 ± 2.7	-16.2 ± 6.2
Ethanol	-29.8[3] ± 3.7	-17.9[3] ± 6.4	-35.6[3] ± 4.0
Hydrogen	-6.3 ± 4.0	-21.3 ± 4.5	-5.6 ± 4.1

1. Calculated based on data from day 80 to day 290.
2. Standard deviation
3. Estimated based on ethanol detection limit of 0.5 mg/l.

Gibbs free energy change (KJ/mol)

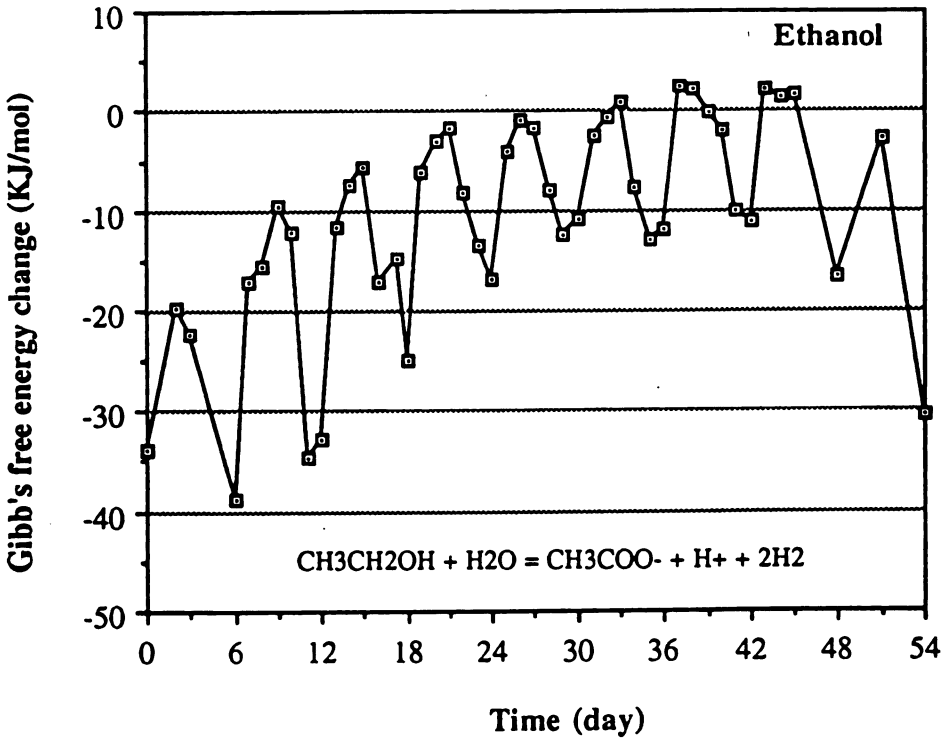

Figure 5-13. Free energy available for the anaerobic oxidation of ethanol during the substrate perturbation period.

5.3.5 Electron equivalents mass balance

An electron balance that accounts for influent and effluent organics, cells and methane production can be used to demonstrate the relative importance of each reaction product. Electron equivalents that are derived from the complete oxidation of key substrates to carbon dioxide were determined from the following half reactions:

$$C_6H_{12}O_6 + 6H_2O = 24e^- + 24H^+ + 6CO_2 \quad (5\text{-}5)$$

$$CH_3COOH + 2H_2O = 8e^- + 8H^+ + 2CO_2 \quad (5\text{-}6)$$

$$CH_3CH_2COOH + 4H_2O = 14e^- + 14H^+ + 3CO_2 \quad (5\text{-}7)$$

$$CH_3CH_2CH_2COOH + 6H_2O = 20e^- + 20H^+ + 4CO_2 \quad (5\text{-}8)$$

$$CH_3CH_2OH + 3H_2O = 12e^- + 12H^+ + 2CO_2 \quad (5\text{-}9)$$

$$CH_4 + 2H_2O = 8e^- + 8H^+ + CO_2 \quad (5\text{-}10)$$

$$H_2 = 2e^- + 2H^+ \quad (5\text{-}11)$$

$$CH_{1.7}O_{0.4}N_{0.2} + 1.6H_2O = 4.3e^- + 4.3H^+ + CO_2 + 0.2NH_3 \quad (5\text{-}12)$$

Based on the above half reactions, the electron equivalents of the glucose substrate, fermentation intermediates, methane and biomass are summarized in Table 5-5. Here, one mole of cells is assumed to be equal to 22.9 grams of VSS, based on the empirical cell formula of $CH_{1.7}O_{0.4}N_{0.2}$ obtained in Chapter 3.

An electron equivalents balance was performed using data for the entire periodic substrate perturbation period (Figure 5-14). The distribution of the electron equivalents in reactor effluent during the different stages of the substrate perturbation is summarized in Table 5-6. These data demonstrate that under steady-state condition, most of the electrons generated from glucose oxidation quickly flowed through the fermentation intermediates, such as VFAs and hydrogen, ending up in methane (75%) and biomass (19%). In contrast, under unstable perturbation conditions (stage one to stage three), a significant amount (ca. 65 to 70%) of electrons generated from glucose oxidation ended up in fermentation intermediates, mainly as acetate, propionate, butyrate and ethanol. Electron

Table 5-5. Electron equivalents (eq) of the anaerobic reactor substrate, fermentation intermediates and products

Organics	MW	mol eq/mol mass	g mass/mol eq
Glucose	180	24	7.50
Acetic acid	60	8	7.50
Propionic acid	74	14	5.29
Butyric acid	88	20	4.40
Ethanol	46	12	3.83
Hydrogen	2	2	1.00
Methane	16	8	2.00
Biomass	22.9	4.3	5.33

Table 5-6 Electron equivalents distribution (mmol) in anaerobic reactor effluent during the 3/3 substrate perturbation (Total input electron equivalents = 104)

Organics	Steady-state	Stage 1	Stage 2	New steady-state
Methane	77.9 ±1.8	22.6 ±9.3	17.9 ±4.9	79.8 ±1.3
Biomass	19.4 ±0.7	9.8 ±1.4	13.7 ±1.8	18.4 ±0.3
Acetate	1.3 ±0.4	32.0 ±0.9	33.0 ±6.7	1.3 ±0.4
Propionate	0.2 ±0.2	19.3 ±2.4	8.4 ±3.1	0.1 ±0.03
Butyrate	0.7 ±0.4	2.1 ±1.3	25.5 ±11.0	0.1 ±0.04
Ethanol	ND[1]	11.4 ±4.0	ND	ND
Total	99.5	97.2	98.5	99.7

1: ND, not detectable

equivalents in hydrogen were negligible throughout the perturbation period. The electrons in the measured products accounted for 93.6% of the input electrons in the feed glucose.

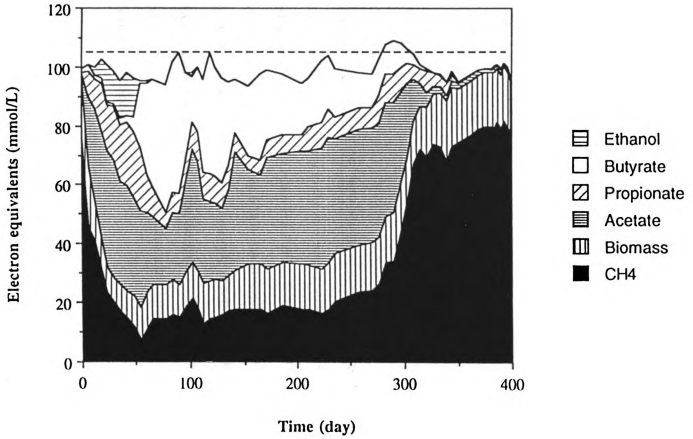

Figure 5-14. Electron mass balance during the perturbation period.

5.3.6 Microscopic observations

Cultures from the control mother reactor and the daughter reactor (after acclimation to the perturbation) were both white in color with mostly dispersed cells. Differences in the microbial composition of these two cultures were easily observed using phase-contrast microscopy. The microbial community in the mother reactor appeared to be more diverse, being comprised of more different morphotypes (Figure 5-15a, scale bar in the photo represents 2 μm). The predominant morphologies were long filamentous rods and short rods. By contrast, the microbial community in the daughter reactor after steady-state was re-established (Figure 5-15c) appeared more homogeneous with less diversity. The predominant morphologies were short rods and cocci, with some long spirillum type bacteria.

Microscopic observations performed during the metastable "steady-state" showed that a unique community structure existed in the daughter reactor during this period. This community was morphologically different from both of the community structures in the stable control mother reactor and in the new steady-state daughter reactor (Figure 5-15b). The predominant morphologies observed during this time were long thick filamentous rods and cocci. There appeared to be much less diversity compared with either original or re-established populations. Routine microscopic observations also revealed that the shifts of the predominant morphologies in the daughter reactor occurred within relatively short time period. This corresponds well with other experimental observations such as changes in COD and VFA concentrations.

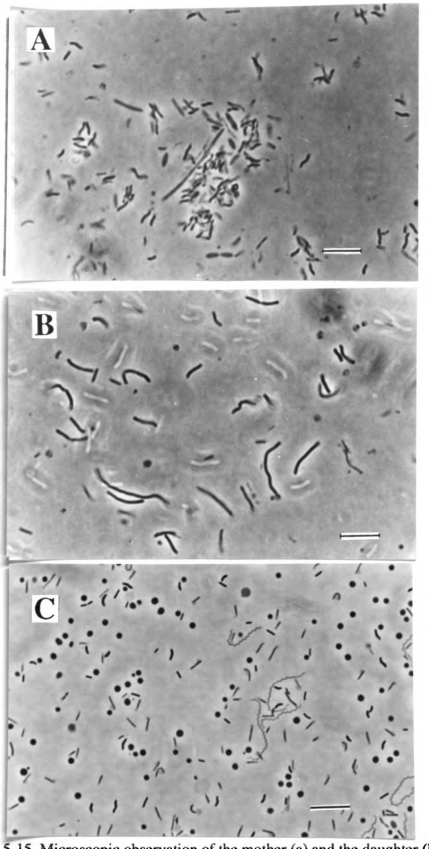

Figure 5-15. Microscopic observation of the mother (a) and the daughter (b, c) reactor cultures.

5.4 DISCUSSION

The acetate-utilizing methanogens were significantly impacted species in the anaerobic microbial community in the present study. Although the response of the acetate-utilizing methanogens to the 3/3 day perturbation was similar to those observed in the 1/1 day perturbation, the more protracted adaptation period indicates that more serious inhibition took place under the 3/3 day perturbation conditions.

Thermodynamic calculations (Figure 5-11) indicate that the inhibition of the acetate-utilizing methanogenic activity in the 3/3 day perturbation was not likely due to thermodynamic limitations. van den Berg et al. (1976) reported that a gas phase hydrogen concentration up to 0.8 atm had no effect on the conversion rate of acetate to methane. Boone et al. (1987) reported similar results. Therefore the elevated hydrogen concentration with a peak level of ca 0.07 atm during the first stage of the 3/3 day perturbation was not likely to significantly affect the acetate-metabolizing methanogenic activity. As mentioned in chapter 4, at a pH level about 7.0, the methanogens could tolerate an acetate concentrations as high as 6,000-7,000 mg/L. But they were found to be quite sensitive to pH change (Duarte and Anderson, 1982; van den Berg et al., 1976; Yong and Okos, 1987). This pH related inhibition of methanogenic activity was mainly attributed to the increase in un-ionized VFA concentration at lower pH (Kroeker et al., 1979; Anderson et al, 1982). The increase in the concentration of un-ionized VFA may cause a decrease in intercellular pH. The excess protons would have to be extruded out to maintain a functional proton gradient. The process of proton extrusion from the cell would require hydrolysis of ATP, resulting a decrease in ATP availability for growth and metabolism of the organism (Fukuzaki et al., 1990; Attal et al., 1988).

Because the un-ionized VFA is the likely inhibitor of the acetate-utilizing methanogenic activity, a comparison based on this parameter was performed on the data obtained from the 1/1 day and 3/3 day perturbations. Calculation results show that after initiation of the substrate perturbations, the un-ionized VFA concentrations quickly increased to levels far above the empirically derived "critical" un-ionized VFA

concentration range of 10 to 30 mg/L (Kroeker et al., 1979; Anderson et al, 1982) in both reactors (Figure 5-9). During the metastable steady-state, the average un-ionized VFA concentrations (as acetic acid) for reactors under 3/3 day and 1/1 day perturbations were around 143 mg/L and 93 mg/L respectively. Thus, although the average total VFA concentrations in these two reactors were essentially the same (Table 4-3 and 5-2) during the metastable steady-state, the un-ionized VFA concentrations (as acetic acid) were ca. 1.5 times higher in the 3/3 than in the 1/1 day fed system due to larger fluctuation in VFA concentrations and lower pH. A much larger amplitude in the fluctuation of un-ionized VFA concentrations was also observed during the 3/3 day perturbation, which might be the other major inhibitory factor effect the recovery of methanogenic activity. These observations may help to explain in part why a more protracted period was required for the anaerobic community to adapt to the 3/3 periodic substrate feed condition.

After ca. 270 day adaptation, acetate catabolizing methanogenic activity significantly recovered as indicated by a rapid increase in the gas production on days when glucose was not fed. It is interesting to note that complete recovery of acetate-metabolizing methanogenic activity occurred at a pH value of ca. 6.1 and an un-ionized VFA concentration of 175 mg/L (as acetic acid). This observation illustrates that through a long-term adaptation or shift in the predominant acetate-utilizing methanogens, the anaerobic population did acquire the ability to effectively metabolize acetate under previously inhibitory conditions.

The hydrogen-utilizing methanogens appeared to be significantly impacted by the 3/3 periodic substrate perturbation. Measurable accumulation of hydrogen occurred immediately after the initiation of the substrate perturbation. Although the accumulated hydrogen was subsequently metabolized during fasting periods, the peak concentration of the accumulated hydrogen during the glucose feed period continuously increased for each subsequent cycle. This indicates an apparent decrease in the population size or metabolic activity of the hydrogen-utilizing methanogens. As illustrated by the results of the free

energy calculations, the decrease in the hydrogen metabolic activity was not due to thermodynamic limitations.

The hydrogen-utilizing methanogens are relatively fast growing species and appear to be resistant to environmental changes (Mosey and Fernandes, 1989; Hobson and Shaw, 1978; Attal et al., 1988). Attal et al. (1988) reported an optimum pH range of 5.5 to 7.4 for hydrogen-utilizing methanogens. Hydrogen-utilizing methanogens were also able to tolerate extremely high VFA concentrations. An acetate or butyrate concentration up to 10,000 mg/L, and a propionate concentration up to 1,000 mg/L (as acetic acid) at a pH of 7.1, did not inhibit *M. formicicum*, the principal hydrogen-utilizing bacterium in a piggery-waste digester (Hobson and Shaw, 1978). Results of the present study also indicate that the H_2-utilizing methanogens in the mother reactor were quite resistant to high VFA concentrations (see Appendix E). In view of this, the temporary decrease in H_2 utilization capacity observed during this period was most likely due to a population decrease caused by hydraulic "wash out" and decay during the prolonged fasting period.

As mentioned above, in spite of the increase in VFA concentrations and the decrease in pH, the environmental conditions in the perturbed reactor appeared to be still within the tolerable range for hydrogen-utilizing methanogens. This allowed the hydrogen-utilizing methanogens to quickly adapt to perturbation conditions. Within ca. 60 days, the hydrogen-utilizing methanogens appeared to have fully adapted to the substrate loading pattern as indicated by a sudden decrease in the level of accumulation of hydrogen during the glucose feed period. This recovery also made oxidation of propionate and butyrate thermodynamically favorable.

Ethanol is one of the major intermediates produced during carbohydrates fermentation (Smith and McCarty, 1989). The microbial population in the steady-state control mother reactor possessed a relatively high ethanol degradation capacity. Under normal operation conditions, the ethanol produced from glucose fermentation was rapidly and completely converted to acetate and hydrogen, resulting in no detectable ethanol (< 0.5 mg/L). Even

under perturbation conditions, ethanol accumulation is usually not observed (Cohen et al., 1981; McCarty and Mosey, 1991; Gupta et al., 1994; this study, Chapter 4). Ethanol degradation is, therefore, not considered to be a rate limiting step in methane production from organic materials. The relatively high accumulation of ethanol observed in this study appears to be directly linked to the high hydrogen concentrations.

Free energy calculations (Figure 5-13) indicate that hydrogen accumulation significantly decreased the free energy available for oxidation of ethanol. Experimental results show that when the free energy available for anaerobic oxidation of ethanol (based on headspace H_2 concentrations) decreased to less than ca. -5 KJ/mol, ethanol degradation was thermodynamically inhibited.

Over the course of this study, a dramatic change in glucose fermentation route was observed. As mentioned in Chapter 4, under methanogenic conditions two major, complementary glucose fermentation routes exist: the butyrate type fermentation and the propionate type fermentation (Cohen et al., 1979; Zoetemeyer et al., 1982a; 1982b; Fongastitkul et al., 1994). Under normal conditions (pH 7 and temperature 35 ^{o}C), the butyrate type fermentation is thermodynamically more favorable and, therefore, the butyrate fermentation route predominates in anaerobic reactors (Duarte and Anderson, 1982; McCarty and Mosey, 1991). In the present study, thermodynamic data supports the conclussion that a shift occurred in the glucose fermentation route.

During the first stage of the 3/3 day substrate perturbation, the fermentation of glucose appeared to quickly switch from a butyrate type to a propionate type fermentation. Propionate accumulation occurred immediately after initiating the perturbation. Since degradation of propionate was thermodynamically impossible during this time period (Figure 5-12), the observed rate of propionate accumulation can be considered to approximate the actual propionate production rate from glucose. Propionate formation from glucose is described by the following reaction (Thauer. et al., 1977):

$$C_6H_{12}O_6 = 4/3CH_3CH_2COO^- + 2/3CH_3COO^- + 2/3HCO_3^- + 8/3H^+ \quad (5\text{-}13)$$

A COD balance indicates that during the first stage, substrate flow through propionate contributed as much as 34% of the total COD accumulation. Prior to the initiation of the substrate perturbation, no propionate accumulation was observed. Based on maximum propionate oxidation rate, less than 5% of substrate flow was due to propionate formation. No butyrate or iso-butyrate accumulated even though oxidation of butyrate and iso-butyrate was thermodynamically inhibited during this period (Figure 5-11). This suggests that the fermentation route of glucose had nearly completely shifted from the butyrate type to the more reduced propionate type. Such a change was driven by the accumulation of reducing equivalents in the system (hydrogen and likely formate).

The results also show that once the thermodynamic condition changed, the fermentative bacteria can quickly shift the fermentation route to the more favorable butyrate type. A dramatic accumulation of butyrate occurred when the reactor hydrogen concentration returned to near its normal level. Butyrate accounted for as much as 65% of the accumulated COD during this period (Figure 5-3), while substrate flowing through the propionate fermentation was reduced from ca. 34% to about 11%.

Inhibition of butyrate metabolism by acetate has been reported by several researchers. Dwyer *et al.* (1988), using a butyrate-degrading co-culture, found that removal of acetate from the butyrate rich media increased the butyrate degradation rate. Ahring and Westerman (1989) reported that an acetate concentration of ca. 2,000 mg/L could completely block butyrate degradation. Based on a theoretical analysis, Kaspar and Wuhrmann (1978) found that this kind of product inhibition was due to a thermodynamic limitations. Hickey and Switzenbaum (1991c) pointed out that under transient loading conditions acetate accumulation could reduce the available free energy for oxidation of butyrate and propionate to low levels, slowing down or stopping the reactions.

In the present study, thermodynamically linked product inhibition was observed for butyrate degradation. A cyclic butyrate-acetate accumulation occurred during the second

stage of the substrate perturbation. A plausible explanation for this cycle is as follows. When the acetate concentration fell to less than ca. 2,000 mg/L, a corresponding decrease in butyrate concentration was observed, indicating renewed butyrate degradation. Each mole of butyrate can be converted into two moles of acetate by butyrate degrading organisms (Thiele and Zeikus, 1988). This resulted an acetate accumulation because degradation was impaired. When the acetate concentration increased to above ca. 3,000 mg/L, free energy available for butyrate oxidation was approximately zero (Figure 5-12), and the butyrate degradation rate decreased due to a thermodynamic limitation. A new cycle of butyrate accumulation was then observed. This cyclic butyrate-acetate accumulation was broken when acetate degradation increased presumably due to acclimation of the acetate-utilizing methanogenic population.

The above scenario underscore the critical role of acetate during the metastable steady-states. The free energy available for oxidation of butyrate and other intermediate long chain volatile fatty acids, could be reduced to levels at which the oxidation of these VFAs could not proceed (Mawson et al, 1991). Acetate associated inhibition can persist for a much longer time than H_2 inhibition because of the slow growth rate of acetate-utilizing methanogens.

The experimental results indicate that through a long-term adaptation, the structure of the anaerobic community gradually changed, enabling more effective utilization of substrate fed in a three day feast-three day famine cyclic pattern. The remarkable morphological differences observed between the mother and the daughter reactor cultures suggests that the ability of the daughter reactor to adapt to the periodic substrate perturbation was most likely the result of a shift in the predominant species. DNA (Chapter 6) and FAME (Chapter 8) analyses support this interpretation.

5.5 SUMMARY

This study establishes that the anaerobic microbial community from a continuously fed chemostat was sensitive to the three day feast-three day famine substrate feeding pattern. The rapid accumulation of glucose fermentation intermediates reflects an apparent decrease in the number or activity of methanogens and acetogens during the first and second stages of the substrate perturbation.

The pH related un-ionized VFA inhibition was likely in part responsable for the decrease in methanogenic activity and for the extremely long recovery period observed under the 3/3 day perturbation condition.

The H_2-utilizing methanogens appeared to be affected by the three day feast-three day famine periodic substrate feeding pattern during the first stage (48 days) of the substrate perturbation. A significant accumulation of H_2 was observed during this period, with adaptation occurring shortly thereafter.

Fermentative bacteria were impacted by the substrate perturbation: a shift in the glucose fermentation route during the first and the second stages of the substrate perturbation was observed.

Thermodynamics appeared to play a significant role in the accumulation of propionate and butyrate. A cyclic acetate-butyrate accumulation pattern indicates that a build-up of acetate can seriously reduce the available free energy for the anaerobic oxidation of butyrate to levels at which the oxidation of the VFA thermodynamically cannot proceed.

The anaerobic system did gradually adapt to the perturbation conditions through extremely long-term changes in microbial community structure as evidenced by remarkable morphological change, as well as genetic and biophysical changes.

Chapter 6

RESPONSE OF ANAEROBIC COMMUNITY TO A LONG-TERM FIVE DAY FEAST-FIVE DAY FAMINE PERIODIC SUBSTRATE PERTURBATION

6.1. INTRODUCTION

Many studies have examined the response of anaerobic systems to environmental perturbations, especially changes in organic loading (Cohen et al., 1981; Gupta, et al., 1994; Hickey and Switzenbaum, 1991b, 1991c; Smith and McCarty, 1989). The effects of long-term, continuous periodic substrate perturbations on anaerobic community structure and function have not been well demonstrated. This is despite the fact that long-term periodic substrate loadings are common in nature and in engineered systems.

In order to determine whether long-term adaptive changes might occur in such systems, a series of long-term periodic substrate perturbations with different cyclic frequencies were applied to anaerobic chemostats. Chapters 4 and 5 describe experimental results for one day feast-one day famine and three day feast-three day famine cyclic feeding patterns. This chapter extends the perturbation conditions evaluated to a five day feast-five day famine feeding pattern, to investigate response of anaerobic systems under longer perturbation intervals.

6.2 MATERIALS AND METHODS

6.2.1 Anaerobic reactor

A schematic representation of the experimental apparatus used for the perturbation experiment is shown in Figure 6-1. The experimental set-up was the same as described in Chapter 4.

6.2.2 Substrate and nutrients

Glucose was supplied as the sole carbon and energy source. Analytical reagent grade granular glucose (Mallinckrodt Specific Chemical Co., Paris, KE) was used to prepare the 16 g/L glucose solutions. A buffer solution, prepared with reagent grade powder sodium bicarbonate (J, T. Baker Inc., Philipsburg, NJ), was mixed with the glucose solutions to obtain 7 g/L $NaHCO_3$ in the feed solution. The mineral nutrient solution was selected based on the compounds and their concentrations used by several researchers (Cohn et al. 1982; Zoetemeyer et al. 1982a; Zehnder et al. 1987). The concentration of the various components in the nutrient solution was described in details previously (Chapter 4).

6.2.3 Analytical methods

Reactor performance was monitored daily for effluent pH, total gas production, gas composition, and gas-phase hydrogen partial pressure. COD, VFAs and VSS analysis were performed on a daily to weekly basis, depending on reactor performance. Procedures and equipment employed for the above analyses are provided in Appendix A.

Cell density of anaerobic protozoa were determined by direct microscopic counts on Hy-lite counting chamber (Fisher Scientific, Pittsburgh, PA).

Liquid samples (15 ml each) were collected and centrifuged for DNA extraction from the steady-state control mother reactor and the re-established daughter reactor contents. Genomic DNA extraction was performed as described by Zhou et al. (1995) with the following modifications. The bacterial samples were ground with a mortar and pestle in the presence of liquid nitrogen and sterile sand, the mortar and pestle were washed with

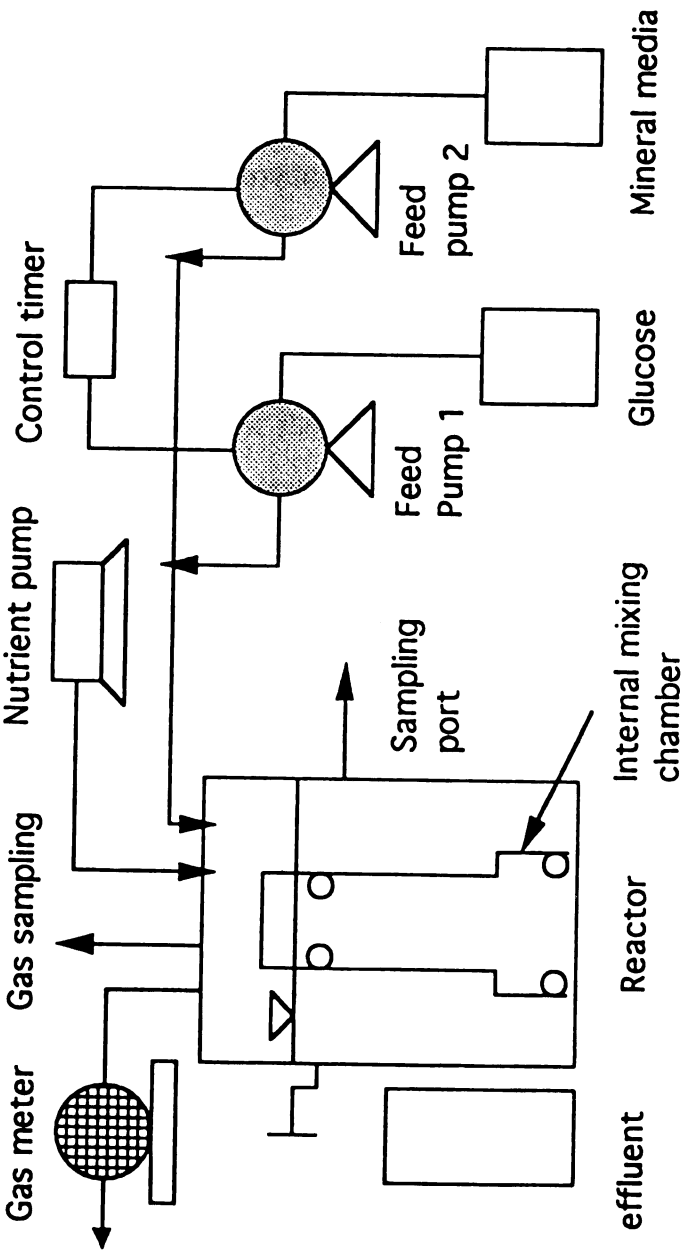

Figure 6-1. Schematic of the experimental set up.

extraction buffer (18 ml) and the samples were transferred to 50 ml tubes. The preparations were then frozen at -70 °C and thawed by microwave heating until brief boiling a total of three times. The DNA was extracted by following the SDS-based high salt and high temperature extraction protocol (Zhou et al., 1995). To compare the microbial community structures between the two reactors, the fingerprinting method was used to analyze the intergenic region between 16S and 23S rRNA genes. The primers for amplifying this region and the conditions for PCR amplification were described by Massol-Deya et al. (1995).

6.2.4 Reactor inoculation

The inoculum (1,500 ml) for the daughter reactor was obtained from a 15 L laboratory-scale "mother" reactor operated under steady state conditions with a 10 day HRT and a constant 8 g/L glucose feed (Chapter 5). The mother reactor was inoculated with digester sludge taken from Jackson Wastewater Treatment Plant (Jackson, Michigan). The mother reactor also served as a stable control by which to compare changes in activity levels and in microbial community with the daughter reactor. The inoculated "daughter" reactor was initially operated under the same conditions as the mother reactor (10 day HRT with continuous input of 8 g/L glucose) for ca. 50 days. Once steady-state was reached and sufficient "base-line" information obtained, a square wave substrate perturbation was applied to the daughter reactor.

6.2.5 Experimental design

In this study, a long term periodic substrate perturbation was applied to the anaerobic daughter reactor. The response of the system to the perturbation was then investigated. During the perturbation, the reactor influent glucose concentration was alternately changed in amplitude from 16 g/L to 0 g/L (mineral media only) on a 10 day square wave cycle (see Figure 6-2), i.e. the reactor was fed 16 g/L glucose solution for five days followed

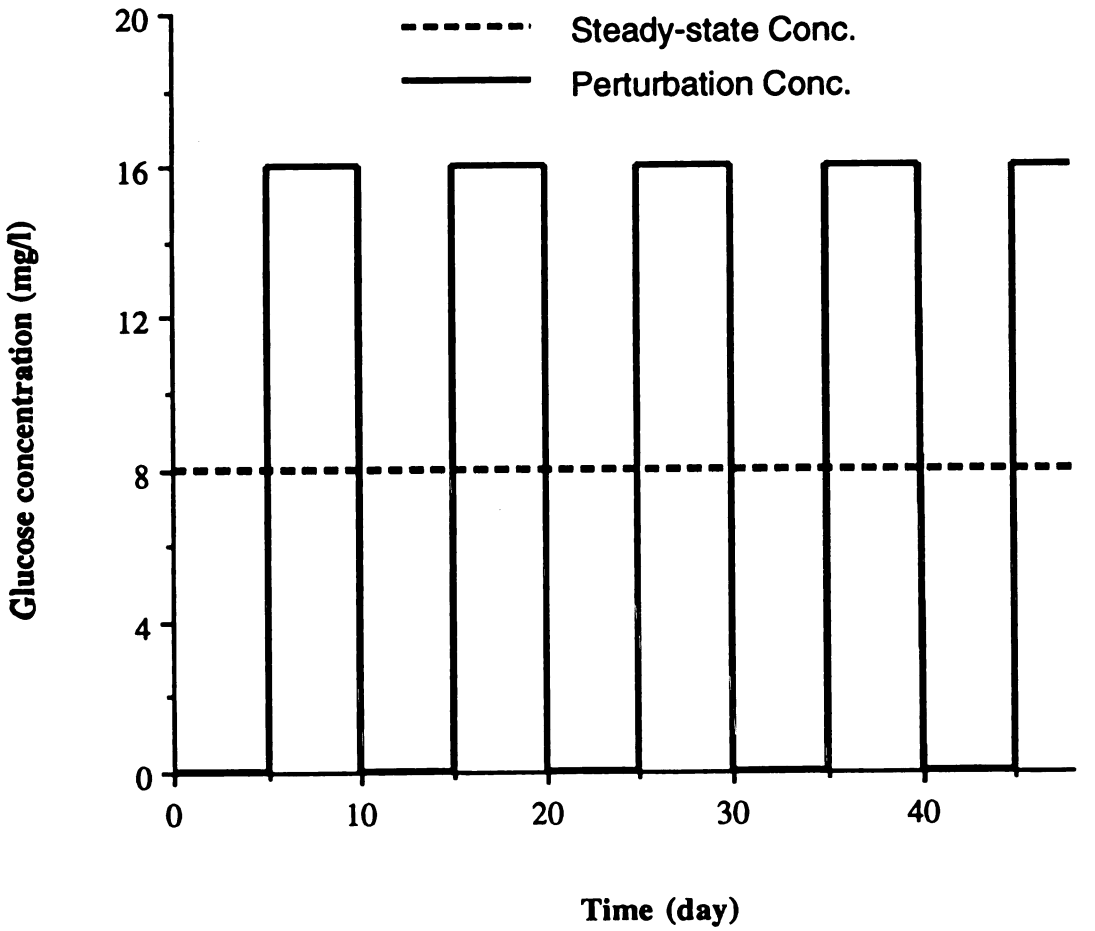

Figure 6-2. Substrate feeding pattern for the 5/5 perturbation experiment.

by glucose-free mineral media at the same flow rate for the next five days. A 10 day hydraulic retention time (dilution rate of 0.1 d^{-1}) was maintained throughout the experiment. The perturbation loading pattern was chosen so that the average influent glucose concentration during the perturbation period was equal to the steady-state concentration of 8 g/L applied to the control "mother" reactor. The daughter reactor was continuously operated for a period of 350 days including ca. 50 days under steady-state baseline conditions and ca. 300 days under perturbation conditions.

6.3 RESULTS

6.3.1 Effects of the periodic substrate perturbation.

The response of the daughter reactor community to the five day feast-five day famine periodic substrate perturbation (5/5 day perturbation) can be divided into two stages: 1. rapid accumulation of glucose metabolic intermediates and recovery, and 2. long-term cyclic fluctuations in effluent COD and VFA concentrations after a pseudo steady-state was re-established in the perturbed anaerobic reactor. Each of the two stages will be discussed in greater detail in the following sections.

Stage one (day 1 to day 80)

The steady-state microbial community in the chemostat was sensitive to the sudden changes in glucose feed concentration. A rapid accumulation of glucose metabolic intermediates, mainly acetate and propionate, occurred immediately after the initiation of the substrate perturbation. Effluent COD quickly increased from 400 mg/L to 2,900 mg/L during the first 5 days of the glucose feed period, accumulating at an average rate of 500 mg/L-d (Figure 6-3a). During the following five day of fast, the accumulated COD decreased rapidly. The peak COD in each subsequent perturbation cycle decreased rapidly, indicating a quick adaptation of the microbial community to the perturbation conditions. After five complete perturbation cycles (50 days) the average effluent COD

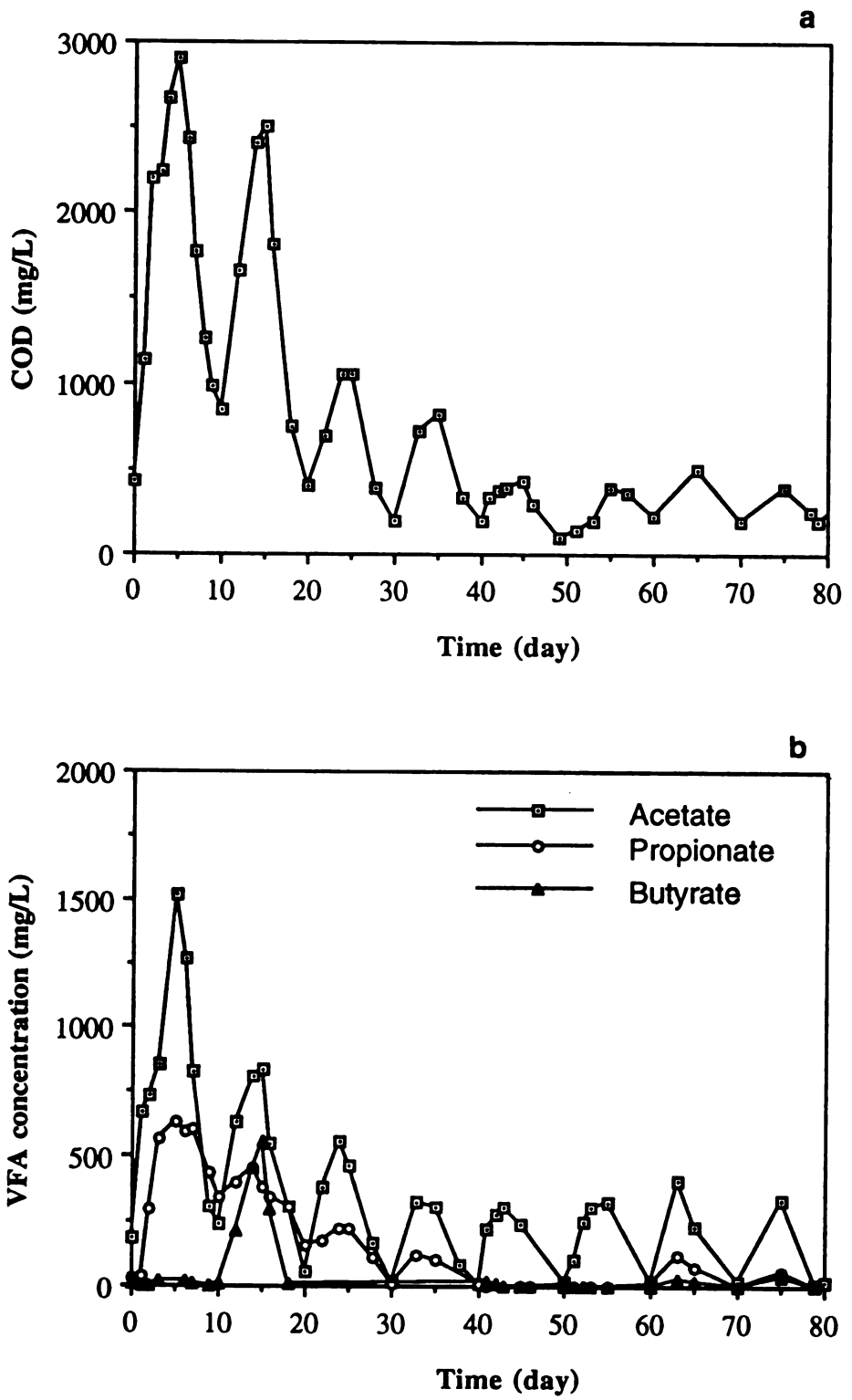

Figure 6-3. COD and VFA concentration changes during the first stage of the 5/5 perturbation experiment

during each perturbation cycle returned to near the levels observed before the initiation of the perturbation.

The acetate-utilizing methanogens were immediately impacted by the substrate perturbation as evidenced by a sharp increase in effluent acetate concentrations (Figure 6-3b). Effluent acetate concentration increased from 150 mg/L to ca. 1,500 mg/L during the first 5 day glucose feed period, accumulating at an average rate of 270 mg/L-d. Acetate contributed to ca. 57% of the total increase in COD observed during this period. The acetate concentration decreased from 1,500 mg/L to ca. 250 mg/L during the following five day no glucose fed period. Based on mass balance calculations, biological degradation accounted for about 50 percent of the total acetate reduction during this period (50% was due to hydraulic "washout"). The peak acetate concentration observed decreased rapidly during the subsequent perturbation cycles, indicating an increase in acetate-utilizing methanogenic activity and/or population. After four complete perturbation cycles (40 days), the peak concentration of acetate observed during each perturbation cycle became relatively stable with an average value of ca. 330 mg/L (± 50 mg/L). Meanwhile, the average effluent acetate concentration during each perturbation cycle returned to near the pre-perturbation level of 190 mg/L, indicating a recovery of the acetate-utilizing methanogens from the initial impact of the periodic substrate perturbation.

A rapid accumulation of propionate was also observed initially. During the first 5 day glucose fed period, effluent propionate concentration increased from less than 30 mg/L to a peak level of ca. 630 mg/L, accumulating at an average rate of 120 mg/L-d. Thus propionate contributed to as much as 36% of the total COD accumulated during this period. During the following five day non glucose feed period, the previously accumulated propionate decreased from 640 mg/L to ca. 340 mg/L. Mass balance calculations indicate that the decrease in propionate concentration was mainly due to hydraulic dilution, which contributed as much as 85% of the total propionate removal during this period. During the following three perturbation cycles the peak concentration of propionate decreased steadily from ca. 450 mg/L to less than 150 mg/L. Mass balance calculations show that

Table 6-1 Apparent propionate degradation rate changes during the first four substrate perturbation cycles (40 days)

Cycle	Propionate degradation rate (mg/L-d)
B[1]	4.7
1	8.4
2	14.3
3	25.6
4	30.4

1: Base-line value obtained before initiation of the substrate perturbation.

the apparent propionate degradation rate increased during each subsequent perturbation cycle as shown in Table 6-1. After the fourth cycle no significant accumulation of propionate was observed.

Significant butyrate accumulation was only observed during the second cycle of the substrate perturbation. At that time, the butyrate concentration increased from 5 mg/L to a peak level of 560 mg/L by the end of the five day glucose feed period, contributing ca. 55% of the net COD accumulation. Accumulated butyrate decreased to less than 10 mg/L during the following five day fasting period. No significant butyrate accumulation was observed thereafter.

As shown in Figure 6-4, the hydrogen-utilizing methanogens appeared to be only slightly affected by the 5/5 day substrate perturbation. Elevated hydrogen concentrations with a peak of ca. 280 ppm were observed in the reactor headspace during the first cycle of the substrate perturbation. The peak hydrogen levels decreased to about 60 ppm during the following two perturbation cycles, returning to its normal level (< 30 ppm) thereafter.

A temporary accumulation of ethanol, with a peak level up to 200 mg/L, was observed during the first three days of the glucose feed period in the first cycle of the substrate

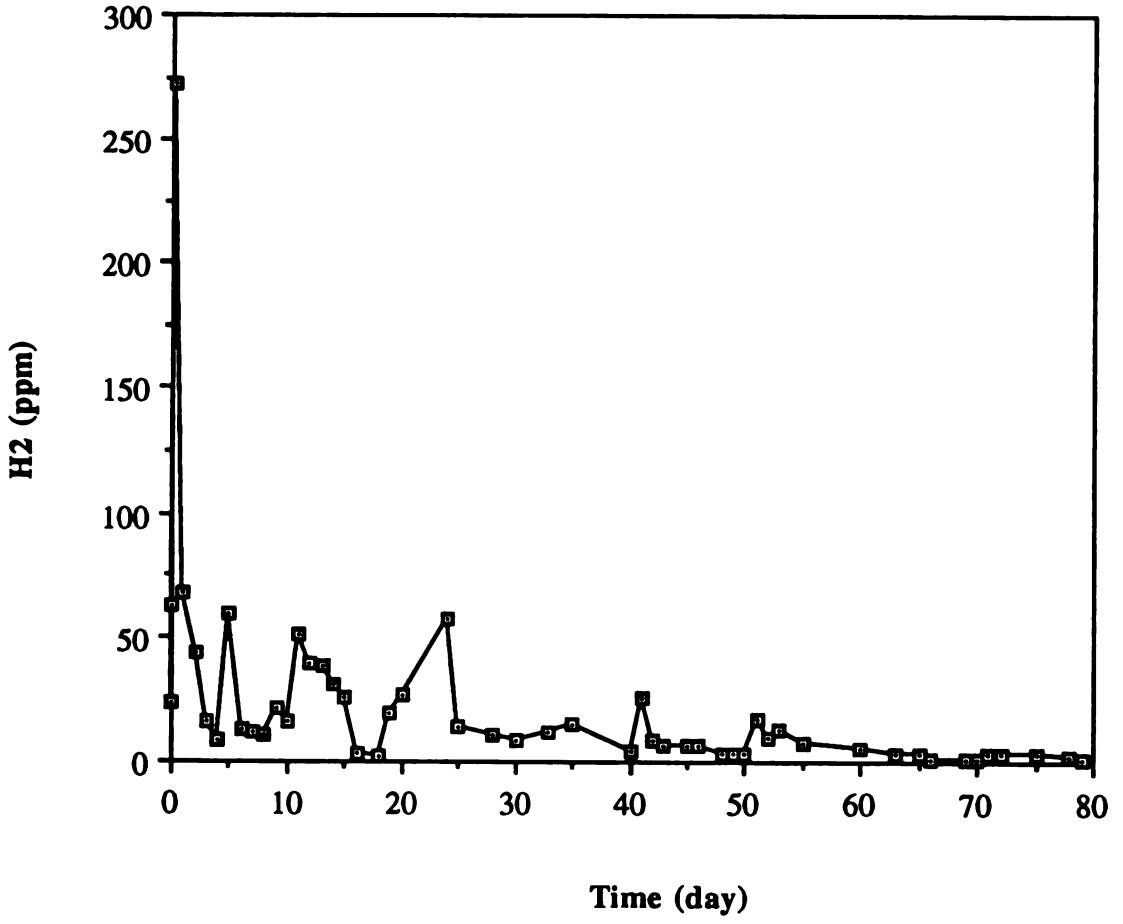

Figure 6-4. Hydrogen concentration change during the first stage of the 5/5 perturbation period.

perturbation (results not shown). The accumulated ethanol was soon degraded to levels below detection limit (< 0.5 mg/L) by the end of the five day glucose feed period. This short term ethanol accumulation occurred coincidentally with the increase in hydrogen concentration during the first cycle of the substrate perturbation. Subsequently, no ethanol accumulation was observed.

The changes in pH during the first stage of the substrate perturbation also reflected the adaptive changes. During the first 50 days of the substrate perturbation (Figure 6-5a), a large fluctuation in pH was observed . Thereafter, a relatively stable pH (pH = 7.00 ± 0.06) was observed. The changes in pH were related to non-ionized VFA concentration (as acetic acid) during the first stage of the substrate perturbation, as shown in Figure 6-5b.

Thermodynamic calculations indicate that during the first cycle of the substrate perturbation, the free energy available for propionate and butyrate anaerobic oxidation decreased to approximately zero, due to the effect of the elevated hydrogen concentration. Subsequently the free energy available for propionate and butyrate oxidation gradually increased, remaining negative at all times (Figure 6-6). Therefore, propionate and butyrate degradation was not thermodynamically limited, except during the first cycle of the substrate perturbation.

The above observations illustrate that the anaerobic microbial community was able to quickly recovered from the initial impact of the 5 day feast-five day famine substrate perturbation. After ca. 50 days (5 complete cycles) a "pseudo steady-state" microbial community was re-established in the perturbed anaerobic reactor. A comparison of the reactor performance during the pre-perturbation steady-state conditions and the new steady-state conditions established during the substrate perturbation, is presented in Table 6-2.

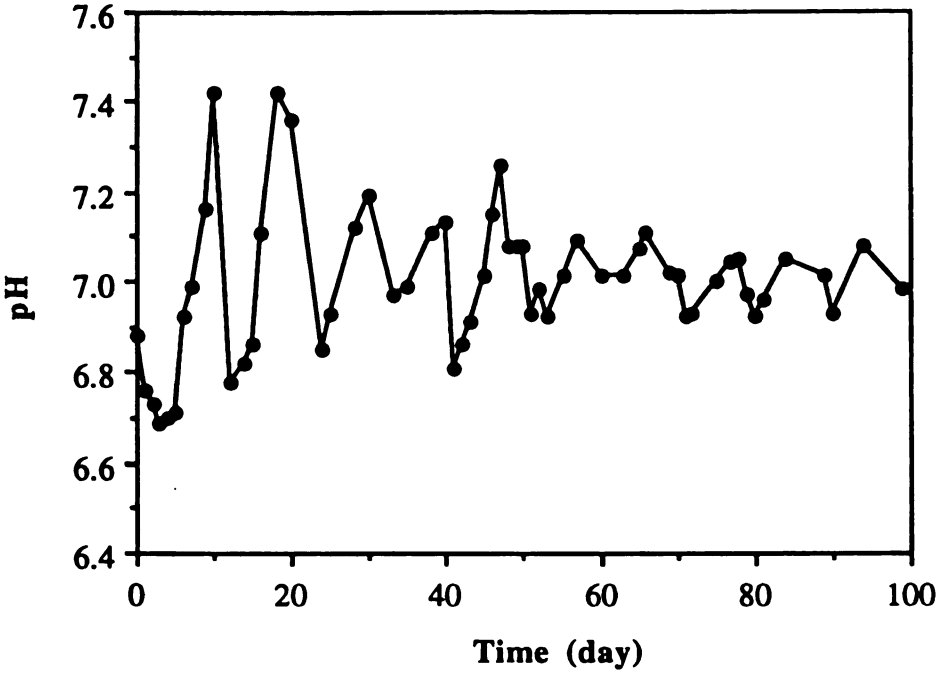

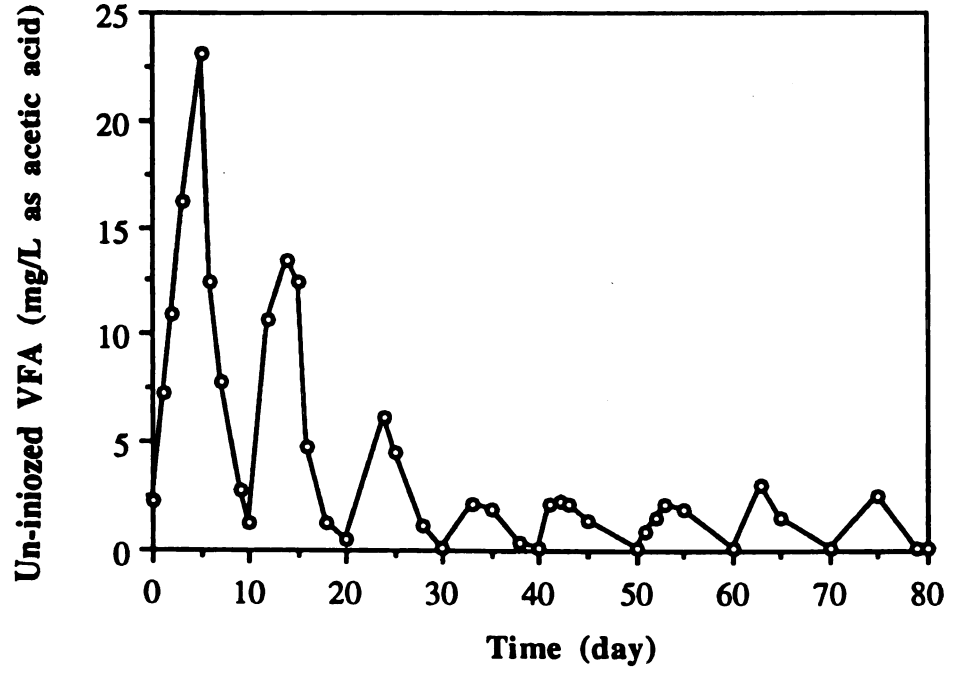

Figure 6-5. pH and un-ionized VFA concentration changes during the first stage of the 5/5 perturbation period.

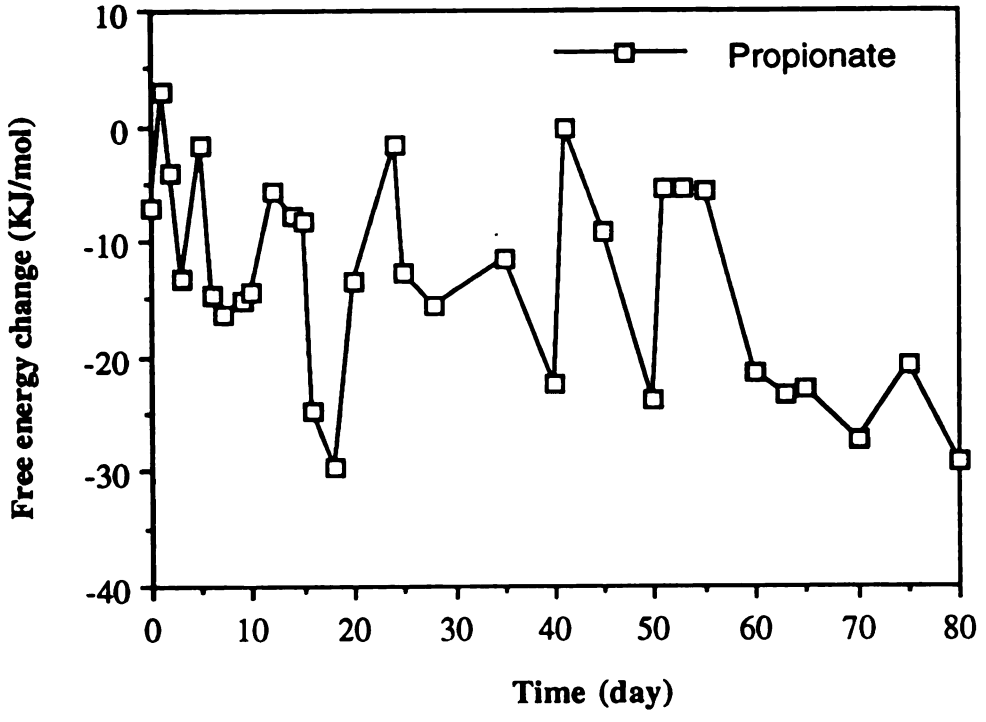

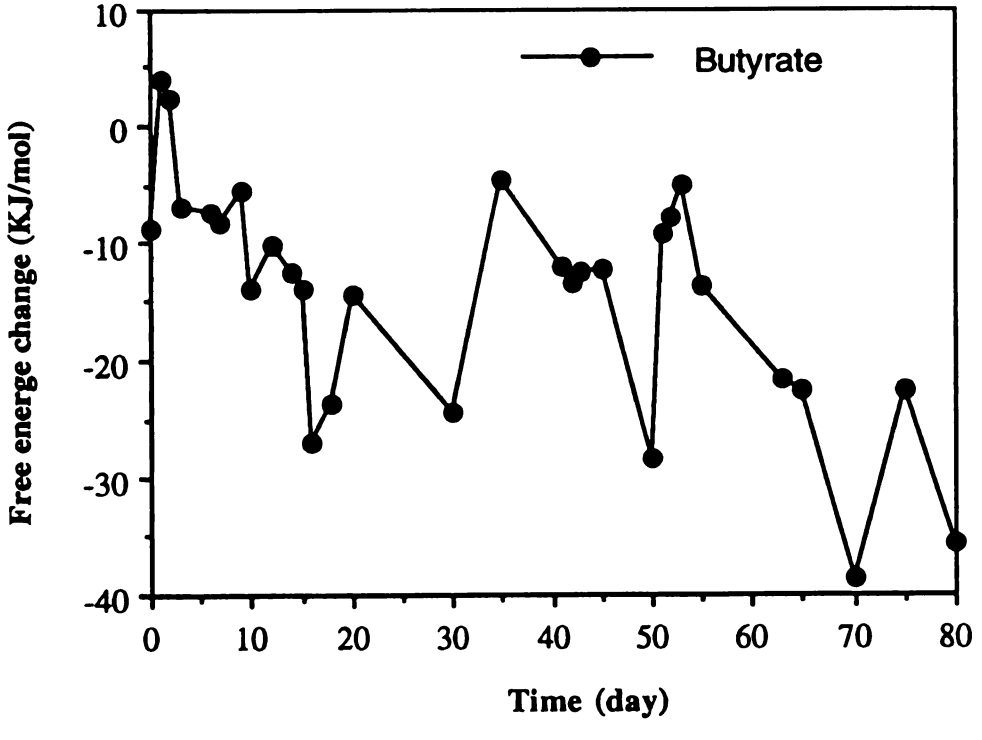

Figure 6-6. Free energy available for the oxidation of butyrate and propionate during the first stage of the 5/5 perturbation period.

Table 6-2. Summary of reactor operational performance during the baseline steady-state and new established pseudo steady-state

	Baseline steady-state	New steady-state[1]
COD_{in} (mg/l)	8500	8500
COD_e (mg/l)	370 ± 53[2]	290 ± 200
VSS (mg/l)	1060 ± 160	1230 ± 370
Gas (ml/L-d)	430 ± 20	410 ± 330
CH_4 (%)	50 ± 2	48 ± 5
pH	7.02 ± 0.04	7.00 ± 0.06
Acetate (mg/l)	190 ± 30	160 ± 135
Propionate (mg/l)	26 ± 15	20 ± 35
Butyrate (mg/l)	24 ± 8.0	7 ± 11
Iso-butyrate (mg/l)	17 ± 10	12 ± 18

1: All the data shown in the columns of new steady-state are averaged values for ten day cycle during substrate perturbation period.
2: Standard deviation.

Stage two (day 81 to day 300)

Long term operational results revealed that performance (i.e. COD removal efficiency) and the community structure established under 5/5 day perturbation conditions was not stable. Large fluctuations in effluent COD and VFA concentrations, as well as in reactor biomass concentration were observed. As shown in Figure 6-7a, the reactor effluent COD concentration varied in a cyclic pattern. From day 100 to day 220, the peak effluent COD in each perturbation cycle gradually increased from ca. 400 mg/L to 1,500 mg/L. After another 120 days, the peak COD in each perturbation cycle began to decrease until a minimum level of ca 500 mg/L was achieved. This long-term cyclic change in effluent COD continued throughout the substrate perturbation period.

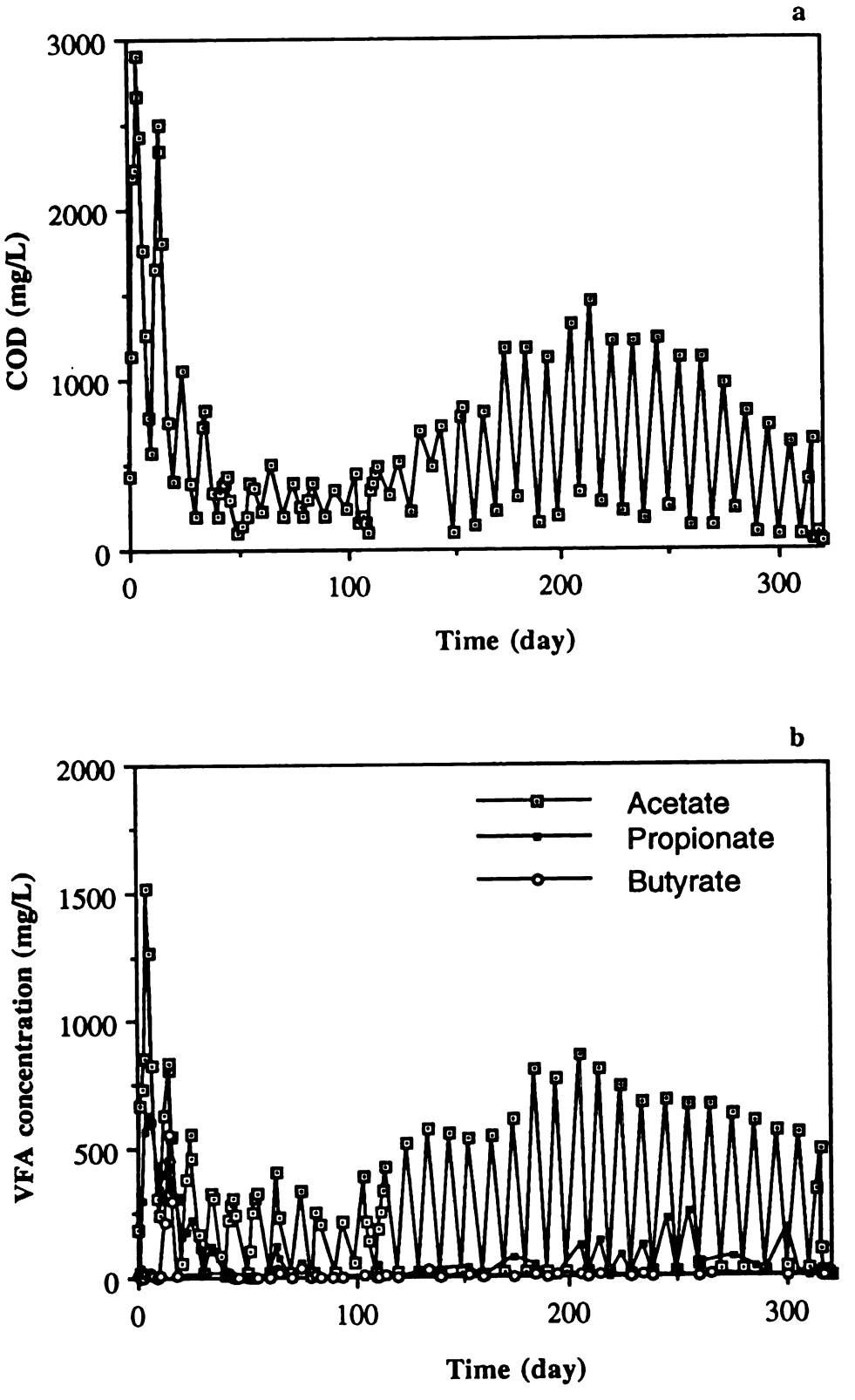

Figure 6-7. COD and VFA concentration changes during the entire 5/5 perturbation period.

Results of VFA analysis show that the effluent COD fluctuation was mainly due to changes in acetate concentration (Figure 6-7b). The long-term acetate change in concentration coincided with the change in COD, both in frequency and in amplitude. This indicates a change in acetate-utilizing methanogenic activity. An occasional fluctuation in propionate concentration was also observed during this period.

The fluctuation in effluent COD and VFA concentration was accompanied by a concurrent change in reactor biomass concentration. As shown in Figure 6-8, a long-term biomass concentration change which had a similar frequency with the periodic COD and acetate concentration changes was observed. Average biomass concentration during each perturbation cycle gradually decreased from ca. 1.2 g/L to ca. 0.7 g/L and then again increased to ca. 1.2 g/L over the period of a complete cycle. This suggests that the reactor effluent COD and VFA concentration changes were affected by the biomass concentration change.

During this period no significant changes in reactor pH or reactor headspace hydrogen concentration were observed.

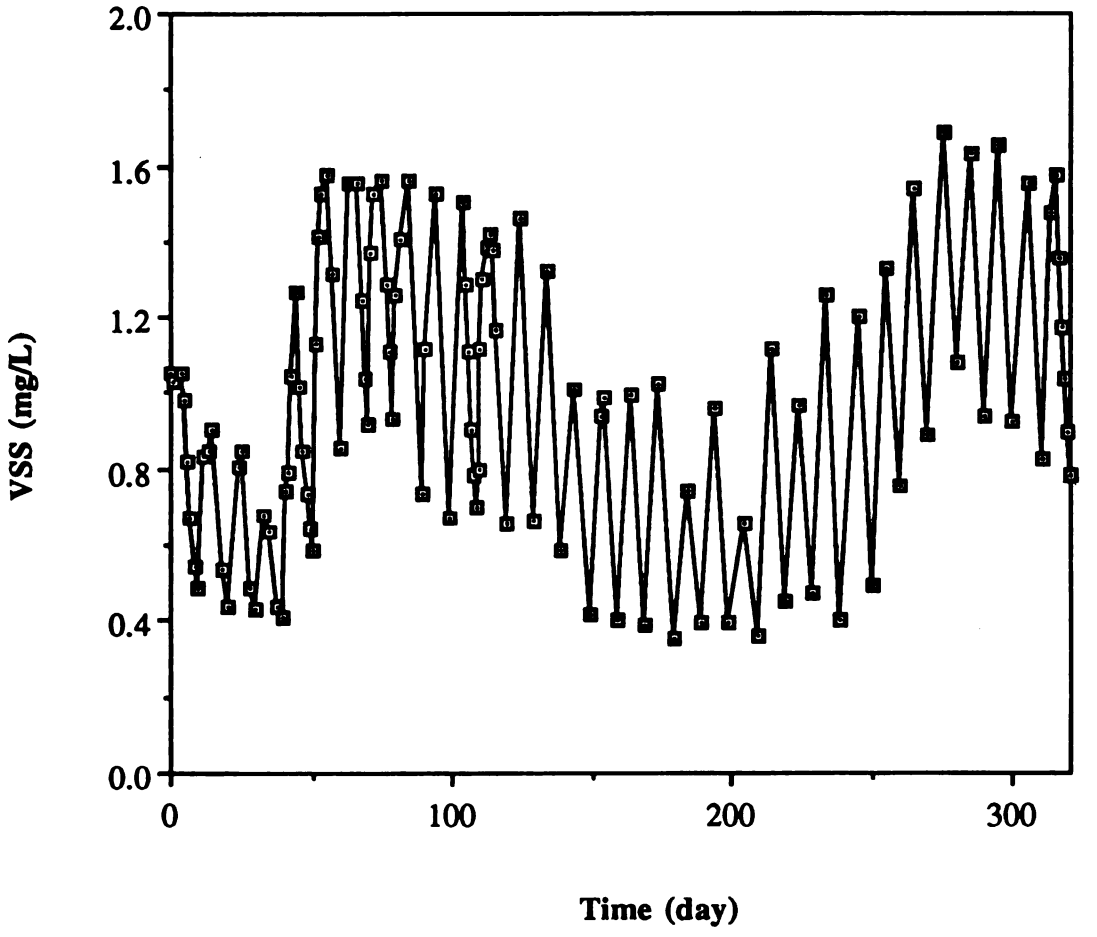

Figure 6-8. Biomass concentration change during the substrate perturbation period.

6.3.2 Observation of protozoa density changes

During the perturbation period occasionally bursts in the protozoa population were observed. As shown in Figure 6-9, the protozoa observed in the 5/5 day anaerobic reactor were round in shape with one or two flagella and could move around freely. Based on the scale of the hemacytometer checks, the protozoa observed in this experiment were estimated to have a diameter (or length) of ca. 9 to 10 μm. According to Fenchel (1987), protozoa displaying enormous variation in size, the size range covered by protozoa is from ca. 2 μm to 10 cm. Therefore the protozoa observed in the anaerobic reactor were relatively small in size. During the perturbation period the protozoa population usually fluctuated around a level of ca. 4.0×10^2 /ml, which might be equivalent to a bacterial density of 4.0×10^5/ml, assuming that a single protozoan was approximately 1,000 times larger than a single bacterium. Therefore, the protozoa normally only contributed ca. 1/1000 or less of the total biomass present in the anaerobic reactor.

Several peaks in protozoa density were observed during the experimental period. The largest burst in protozoa density observed in this experiment is presented in Figure 6-10. During this period the protozoa population quickly increased from less that 1.5×10^2/ml to a peak level of ca. 8.32×10^4/ml, which would be equivalent to a bacteria density of 8.32×10^7/ml. Therefore, at that time the protozoa population represented as much as 10 to 15 percent of the total biomass. A decay curve of protozoa density was obtained using a batch test (Figure 6-11a). Under starvation conditions, the protozoa density decreased linearly with time. The protozoa decay rate was similar to the first stage biomass decay rate (6-11b).

No attempt was made to further investigate the behavior of the anaerobic protozoa. Therefore, the metabolic and kinetic characteristics and the effect of the protozoa on the anaerobic microbial community are not clear. Morphologically similar protozoa were also observed in all the other anaerobic reactors but their density usually fluctuated around levels of ca. 4×10^1 to 3×10^2 /ml, which is about 200 to 1,000 times lower than the peak value observed in the 5/5 reactor culture. Based on the available data, no valid links

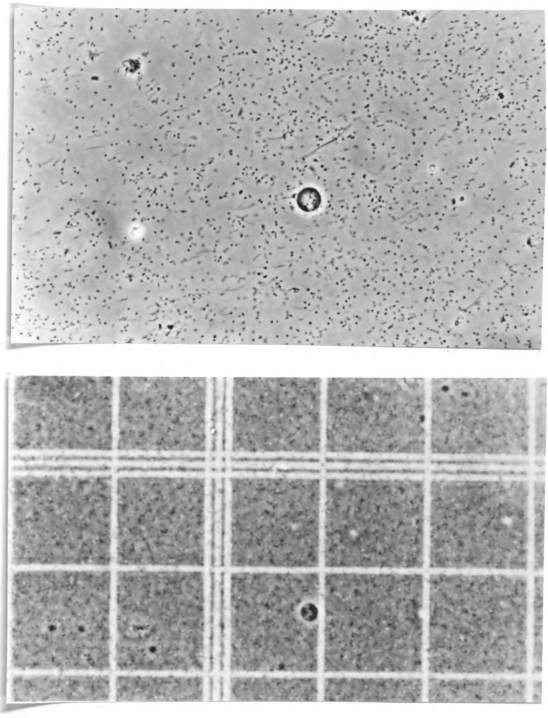

Figure 6-9. Microscopic observation of the protozoa in the 5/5 reactor culture.

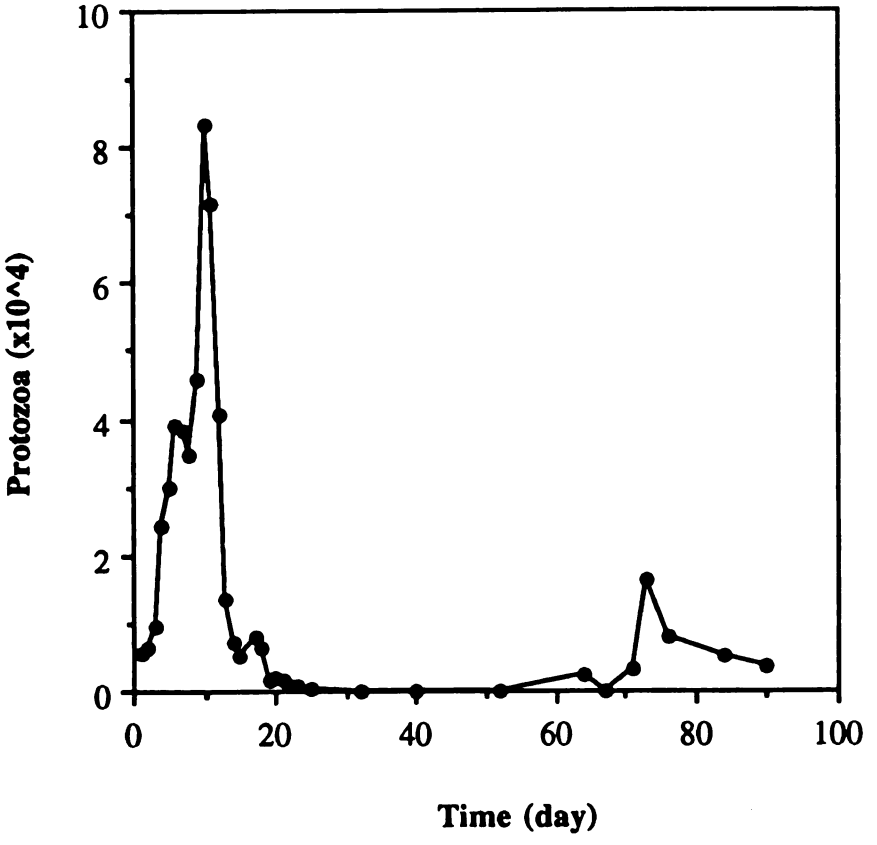

Figure 6-10. Protozoa density changes during observation period.

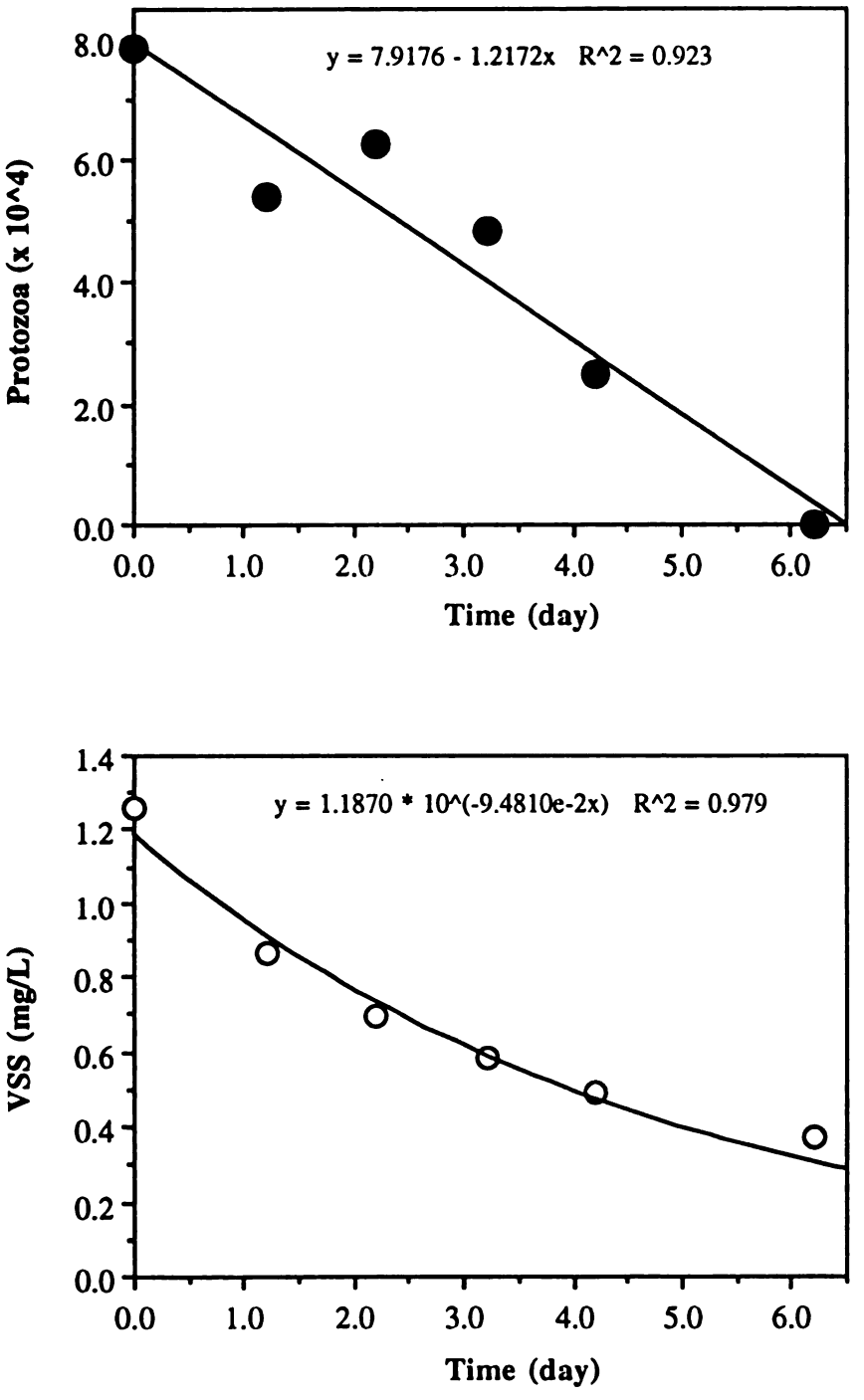

Figure 6-11. Changes in protozoa density and total biomass concentration under starvation condition.

between the protozoa population and the reactor operation performance were obtained. However, a significant fluctuation in COD concentration did correspond to one of the increases in protozoa concentration.

6.3.3 Microscopic observations

Cultures from the established daughter reactor were white in color with mostly dispersed cells. Differences in the microbial composition of the daughter reactor culture with the mother reactor culture were easily observed using phase-contrast microscopy. The microbial community in the mother reactor appeared to be more diverse, being comprised of more different morphotypes (Figure 6-12a, scale bar in the photo represents 2 μm). By contrast, the microbial community in the daughter reactor after steady-state was re-established (Figure 6-12b) appeared more homogeneous with less diversity. The predominant morphologies were short rods and cocci, with some long spirillum type bacteria.

A comparison of the microbial compositions in the re-established daughter reactor cultures show some interesting results. As presented in Figure 6-12 (b, c and d), with some recognizable differences, all of the re-established daughter reactor cultures had similar microbial morphologies, regardless of the recovery processes they experienced. This observation suggests that under perturbation conditions some "basic" microbial community structure is necessary, especially when all the inocula came from the same source.

In the cultures taken from the mother and the daughter reactors, a number of bacteria that autofluoresced blue-green under UV light were observed. Differences in bacteria morphologies were also observed under UV light for the mother and the daughter reactor cultures. In the mother reactor culture, a larger part of these bacteria were rods, with less long filaments and cocci. Scattered clusters of sarcina were also observed. These metanogen-like bacteria were morphologically similar to *Methanobacterium*-, *Methanococcus*- and *Methanoscina* , respectively (Zeikus, 1979). In the daughter reactor

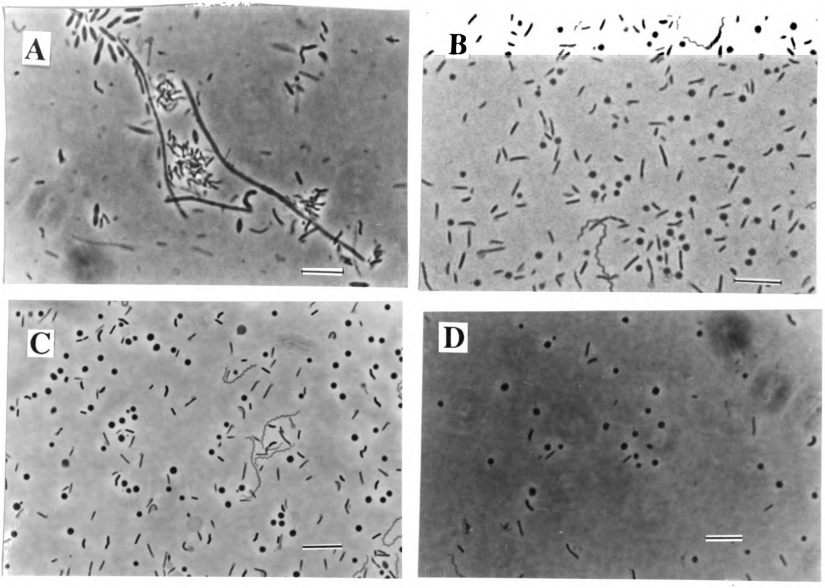

Figure 6-12. Microscopic observations of the mother (a), the 5/5 (b), 1/1 (c) and 3/3 (d) daughter reactor cultures.

cultures, a majority of the autofluoresced bacteria consisted of long curved filaments with fewer rods and cocci. These methanogen-like bacteria in the daughter reactor cultures were mophologically similar to *Methanobacterium thermoautotrophicum-*, *Methanothrix-* and *Methanococcus,* respectively (Zeikus, 1979). Although differences between daughter reactor cultures were recognizable, this differences were not as pronounced as the mophological differences between the mother and the daughter reactor cultures.

6.3.4 Results of genetic analysis

Once the daughter reactors attained the new quasi-steady-state, genetic analyses were performed to document changes in community structure. The results of the Hpa II restriction endonuclease digest of 16S rRNA polymerase chain reaction (PCR) amplified from the mother and the daughter reactor cultures are shown in Figure 6-13. Differences in microbial community can be observed from distinctive restriction fragment patterns between the mother and each of the daughter reactor cultures, as well as between each pair of the daughter reactor cultures. The results indicate changes in community structure did occur in the re-established daughter reactor cultures. A more detailed discussion of changes in the community structure in the perturbed daughter reactors is provided in Chapter 8.

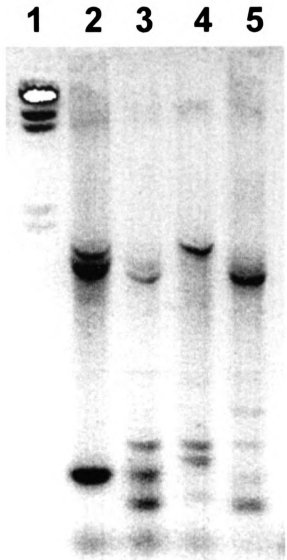

Figure 6-13. DNA analysis results for the mother and the daughter reactor cultures. Lane 1, DNA standard (123 bp); lane 2, mother reactor culture; lane 3, 1/1 reactor culture; lane 4, 3/3 reactor culture; lane 5, 5/5 reactor culture.

6.5 DISCUSSION

The 5/5 day perturbation had less impact on the anaerobic system performance than the 1/1 or 3/3 day perturbations. Although VFA and COD accumulation in the 5 day glucose fed period were similar to those observed during the early stages of the 1/1 and 3/3 day perturbations (Table 6-3), the following 5 day fasting period apparently allowed sufficient time for the microbial community, and especially the acetate-utilizing methanogens, to degrade the accumulated VFAs. The considerable hydraulic dilution was also likely a reason for the system response. Surprisingly a rapid recovery was observed under the 5/5 day perturbation conditions. Based on the experimental results, a new pseudo steady-state established in the anaerobic chemostat within ca. 50 days (5 full perturbation cycles). This adaptation period was much shorter than those required for the 1/1 day and 3/3 day perturbation experiments (see Chapter 4 and 5). This observation illustrates that the perturbation frequency is an important parameter which could directly affect the recovery progress of perturbed anaerobic system.

Table 6-3 COD and VFA accumulation rates in the beginning of the substrate perturbations

Parameter	1/1	3/3	5/5
COD (mg/L-d)	530	560	500
Acetate (mg/L-d)	304	340	270
Propionate (mg/L-d)	122	88[1]	120

1: Significant ethanol accumulation was observed during the same period.

Although the adaptation period was relatively short in the present five day feast-five day famine perturbation test, a shift in glucose fermentation route was still observed. As shown in Figure 6-3, immediately after the initiation of the substrate perturbation, rapid

propionate accumulation was observed. Assuming the following propionate fermentation reaction from glucose (Thauer. et al., 1977):

$$C_6H_{12}O_6 = 4/3CH_3CH_2COO^- + 2/3CH_3COO^- + 2/3HCO_3^- + 8/3H^+ \quad (6\text{-}1)$$

the substrate flowing through propionate fermentation contributed as much as 46% of the total COD that accumulated during this period. Prior to the initiation of the perturbation, no propionate accumulation was observed and based on maximum propionate oxidation rate, less than 3% of substrate flow was due to propionate formation (Table 6-1). In the meantime, no butyrate accumulation was observed although anaerobic oxidation of butyrate was thermodynamically inhibited. It appears, therefore, that accumulation of reducing equivalents in the system (hydrogen and likely formate) shifted the glucose fermentation route from the butyrate type (Duarte and Anderson, 1982; McCarty and Mosey, 1991) to the more reduced propionate type fermentation (Palns Sam-Soon et al., 1987).

In the second cycle of the substrate perturbation, a rapid accumulation of butyrate was observed. Butyrate accounted to as much as 55% of the net accumulated COD during this period. Simultaneously, the percentage of the substrate flowing through propionate fermentation route decreased to ca. 11% of the net accumulated COD, indicating that the butyrate fermentation had again become the predominant fermentation route. Although an increased propionate degradation capacity was observed (Table 6-1), the rapid decrease in accumulated propionate concentration during each perturbation cycle appeared to be mainly due to a shift in the glucose fermentation route.

This observation indicates that the fermentative bacteria can shift their fermmentation route promptly in response to unfavorable environmental changes, especially elevated hydrogen partial pressure. With a sudden increase in hydrogen partial pressure, about 45% of the substrate flow can be shunted to the propionate fermentation route. This ratio was quite constant for all the three of the perturbed daughter reactor communities. At higher hydrogen partial pressure, some of the glucose was converted to ethanol. Under

these conditions substrate flow through the butyrate fermentation was completely blocked thermodynamically. Once thermodynamic conditions were again suitable for butyrate formation, the fermentation bacteria could instantly shift the fermentation route back to butyrate production, resulting in a peak substrate flow of ca. 55% through this route. This phenomenon was observed in all the daughter reactors.

The microbial community that become re-established under the 5/5 day perturbation condition did not appear to be as stable as the communities developed under the 1/1 day and 3/3 day perturbation conditions. This was evidenced by the large fluctuation in the reactor effluent COD, VFA and biomass concentrations. A possible reason for this apparent cyclic fluctuation in reactor operation performances is instability in the acetate-utilizing methanogen population. As discussed before, the relatively long starvation period employed in the 5/5 day perturbation mode may help to reduce adverse environmental conditions during the early stage of the perturbation due to hydraulic dilution. This hydraulic "washout" can also cause considerable biomass loss under the pseudo steady-state condition. At the end of the glucose feed period, the substrate available for the anaerobic bacteria in the following starvation period became very limited. Therefore a considerable portion of the biomass was lost due to hydraulic wash out. If the number of acetate-utilizing methanogens in the reactor was less than a certain minimum at the end of the famine period, acetate would accumulate during the next perturbation cycle. This process would stop at a certain point when the accumulated acetate at the end of the feast period had reached a level which could support enough methanogens to survive the following starvation period and therefore, more effectively to handle the following substrate pulse. Although the same course could also occurred for other groups of anaerobic bacteria, experimental results show that this was most pronounced for acetate-utilizing methanogens. This hypothesis, however, needs to be further evaluated.

Several sudden bursts in the size of the protozoa population were observed during this experiment. At least one of these coincided with a larger COD fluctuation. Although the kinetic and metabolic characteristics of the observed protozoa are unknown, some impact of the protozoa on the anaerobic community is likely. The sudden increase in the protozoa in population could reduce available substrate for the bacterial community or the protozoa could be predators of any or all of trophic groups present in the anaerobic reactor.

As discussed before, under 5/5 day perturbation conditions, the balance between anaerobic trophic groups was relatively unstable. The occasional burst in the protozoa population could be a sign, and/or a factor which reflected or caused the anaerobic community upset. From an ecological point of view, the so called "predominant species" have a strong affinity for existing carbon and energy sources under given environmental conditions. If a ecosystem, such as an anaerobic reactor, is occupied by "native" microorganisms, a stranger which under normal conditions find it hard to invade. The observation that protozoa populations increased significantly in several occurring may indicate that the substrate perturbation did create a strong impact on existing microbial population.

6.6 SUMMARY

This study illustrates that the five day feast-five day famine substrate perturbation had less impact on the anaerobic population than the 1/1 and 3/3 frequency. The anaerobic microbial community could adapt to the 5/5 day substrate perturbation within a relatively short time period (ca. 50 days) through a change in community structure as evidenced by changes in the kinetics of substrate utilization, genetic and morphological changes. The long-term performance of this population was, however, less stable than the populations in the 1/1 and 3/3 perturbed systems.

Experimental results confirmed that the fermentative bacteria could response to environmental changes by quickly adjusting their fermentation route so that maximum free energy could be obtained under the changed environmental conditions.

The perturbation frequency is an important parameter for anaerobic systems operated under periodic substrate fed conditions. It could directly affect the systems recovery process and the long-term operation stability.

Chapter 7

OPERATIONAL CHARACTERISTICS OF THE RE-ESTABLISHED MICROBIAL POPULATIONS UNDER STEADY-STATE AND SHOCK LOADING CONDITIONS

7.1 INTRODUCTION

Many perturbation experiments have been performed to investigate response of anaerobic systems to sudden increase in organic loading rate and other environmental shocks. These experiments mainly focused on inhibitory effects, recover processes and thermodynamic changes in the anaerobic systems that resulted from the perturbations (Cohen et al., 1981; Smith and McCarty, 1989; Hickey and Switzenbaum, 1991b, c; Gupta, et al., 1994). For these substrate perturbations, usually only the negative effects of the environmental perturbations on anaerobic systems were emphasized. However, some of the experimental results indicated potential benefits from perturbations on anaerobic systems. For example, researchers noted that when an anaerobic system was repeatedly subjected to organic overload, the perturbed systems eventually became less and less seriously affected by the perturbations (Cohen, et al., 1986). Although some of the perturbation results indicated microbial community changes, little effort was directed towards studying the effects of environmental perturbations on the microbial communities.

In this chapter the stability and operational characteristics of the microbial communities that became established in the periodically perturbed daughter reactors, especially in the 1/1 day daughter reactor, were investigated and compared with performance of the control mother reactor under both steady-state and shock loading conditions.

7.2 MATERIALS AND METHODS

7.2.1 Anaerobic reactors

Three 1.5 liter working volume anaerobic reactors which received 1/1, 3/3 and 5/5 day periodic glucose feed were used for the steady-state operational performance observation. The set up and operational conditions of these periodically perturbed reactors were described in detail in the previous chapters (Chapter 4, 5, and 6).

A 1.5 liter working volume anaerobic reactor (reactor m-1) inoculated with 1,500 ml culture taken from the control mother reactor and operated under the same conditions as the mother reactor (10 day HRT and 8 g/L glucose feed) was used to perform organic loading rate and temperature shock experiments. Before initiation of the shock loading experiments, this reactor had operated under steady-state conditions for more than 100 days.

7.2.2 Substrate and nutrient solutions

Analytical reagent grade granular glucose (Mallinckrodt Specific Chemical Co., Paris, KE) was used to prepare the 8 g/L and 16 g/L glucose solutions. A buffer solution, prepared with reagent grade powder sodium bicarbonate (J, T. Baker Inc., Philipsburg, NJ), was mixed with the above glucose solutions to obtain 7 g/L and 14 g/L N_aHCO_3 in the reactor feed solutions respectively. Both the glucose solution and the sodium bicarbonate buffer solution were prepared with deionized water. The composition of mineral nutrient solution used in this study was the same as described in Chapter 4.

7.2.3 Analytical methods

Analyses of COD, VSS, pH, optical density (OD), glucose, volatile fatty acids, gas composition and gas-phase hydrogen partial pressure were carried out as described in Appendix A.

7.2.4 Experimental procedures

The operational characteristics of the daughter reactor populations after recovery from the perturbations were investigated under periodic feeding conditions for an extended operational period, ca. 150 days. During this period the reactor effluent COD, VFA, VSS, gas production and gas composition were measured and compared with values obtained from the steady-state control mother reactor.

The stability and resistance of the daughter reactor (1/1) and the constantly fed reactor (m-1) populations to sudden environmental changes were examined under substrate and temperature shock conditions. For the glucose shock loading rate experiment, the glucose concentration in the reactors was increased suddenly to 4,000 mg/L by pulse addition of glucose while normal feeding continued. For the temperature shock experiment, the reactor temperature was temporally decreased to 25 °C for 24 hours and then returned the normal operating temperature of 35 °C. Following application of the perturbations, reactor operational parameters such as COD, VFA, pH were monitored until steady-state operation was again achieved. The experimental conditions used in the glucose and temperature shock experiments are listed in Table 7-1.

Table 7-1 Experimental conditions used in the glucose and temperature shocks.

	m-1	1/1
Glucose shock experiment		
Glucose shock loading (g/L)[a]	4	4
Glucose feed (g/L-d)	0.8	1.6/0
Temperature (°C)	35	35
HRT (day)	10	10
Temperature shock experiment		
Shock temperature (°C)[b]	25	25
Glucose feed (g/L-d)	0.8	1.6/0
HRT (day)	10	10

a: Pulse injection amount.
b: Duration of 24 hours.

7.3 Results

7.3.1 Operational performance of the daughter reactors

The changes in effluent COD concentrations of the three daughter reactors during the entire perturbation period (upset and recovery) are presented in Figure 7-1. Remarkable differences were observed in the time required for recovery. After recovery, the operational performance of these reactors were further monitored for a period of ca. 150 days. Experimental results illustrate that the re-established microbial communities in the 1/1 and 3/3 day daughter reactors were relatively stable. These two reactors could maintain long-term stable and effective operation under periodic feed conditions. The performance of microbial community in the 5/5 day daughter reactor was not stable.

Significant fluctuations in effluent COD and VFA were observed during the extended operation period after recovery of the 5/5 day reactor recovered.

In respond to the cyclic pattern in the feed regime, cyclic patterns were observed for operational parameters, such as COD, VSS, gas production and hydrogen partial pressure (Figures 7-2 to 7-5), in the daughter reactors after recovery. Based on experimental results, the most significant change in operational parameters always occurred during the first day following the substrate feeding pattern shift. Compared with changes in other operational parameters, the cyclic pattern in VSS concentrations were more gradual. The operational performance of the three daughter reactors and the mother reactor are summarized in Table 7-2. Experimental data illustrate that compared with the control reactor, similar operational results were achieved in the daughter reactors. These data also show that with a longer perturbation interval, the fluctuation in operational parameters increased.

Specific maximum substrate utilization rates of glucose and glucose fermentation intermediates in the mother and the daughter reactor cultures are summarized in Table 7-3. From this table it can be seen that the daughter reactor cultures possessed higher specific substrate utilization rates than the mother reactor culture. The differences in the specific maximum substrate utilization rate indicate changes in microbial community and/or

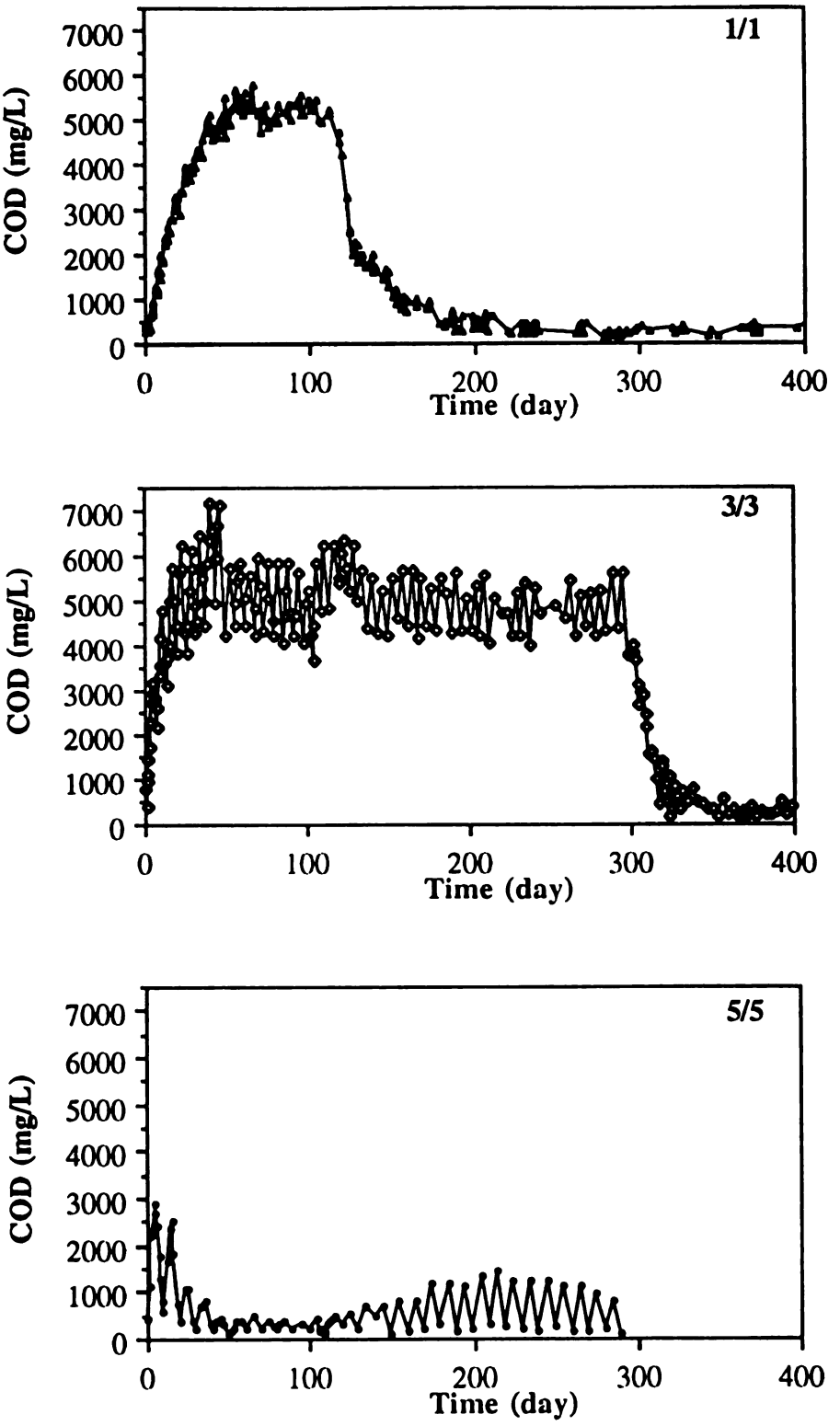

Figure 7-1. Recovery processes of the 1/1, 3/3 and 5/5 day daughter reactor populations.

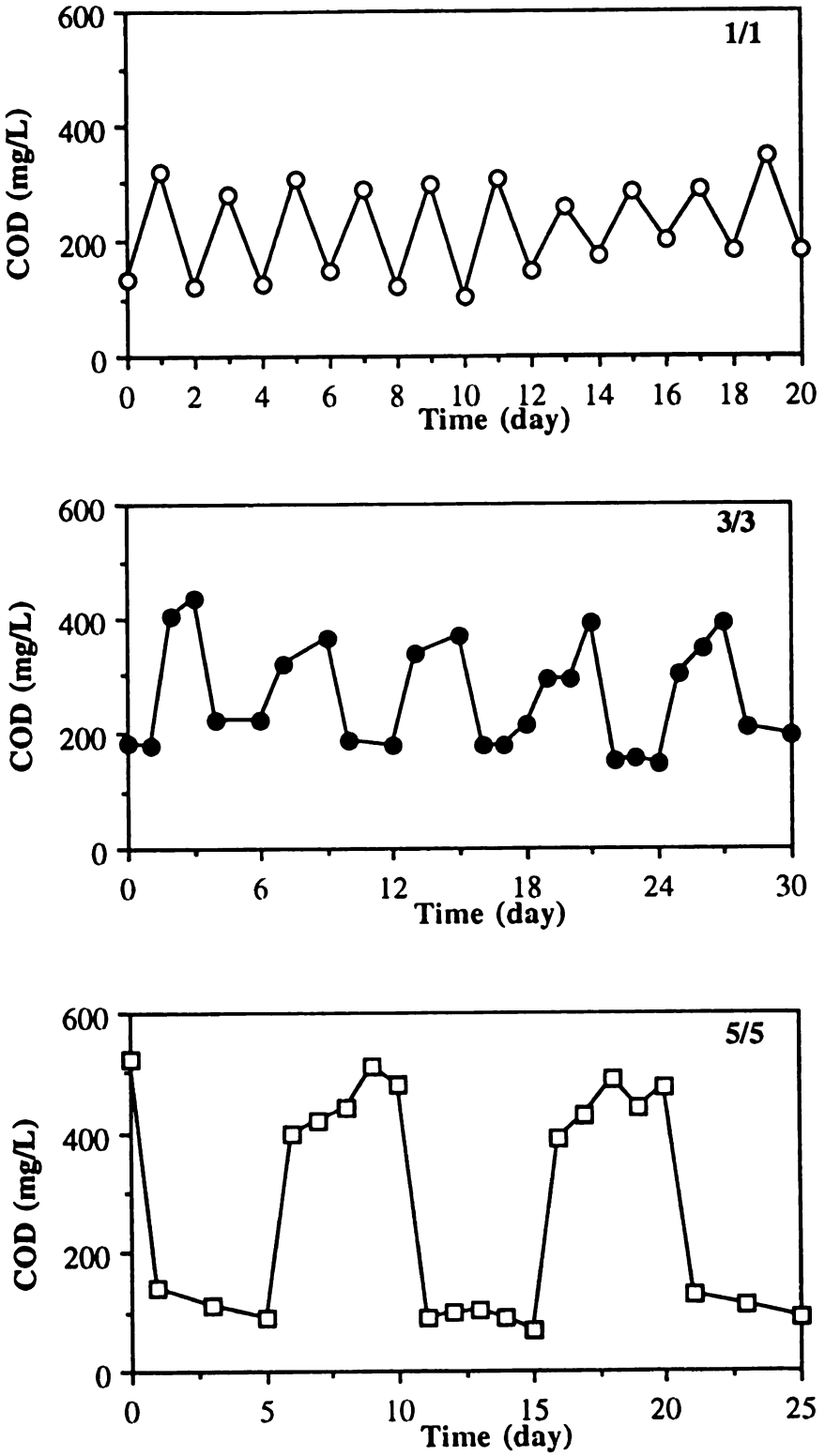

Figure 7-2. COD concentration changes in the re-established daughter reactors.

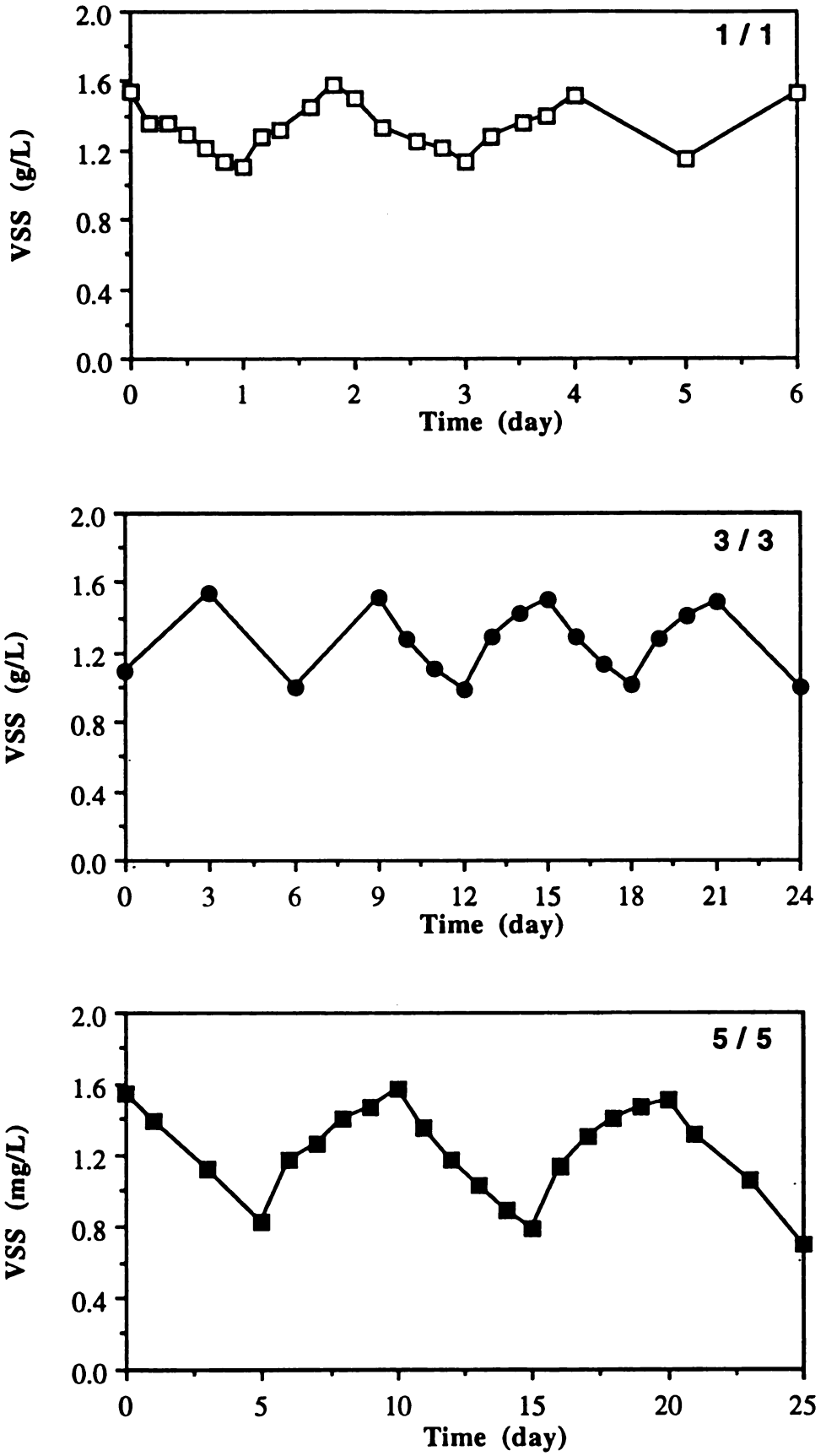

Figure 7-3. VSS concentration changes in the re-established daughter reactors.

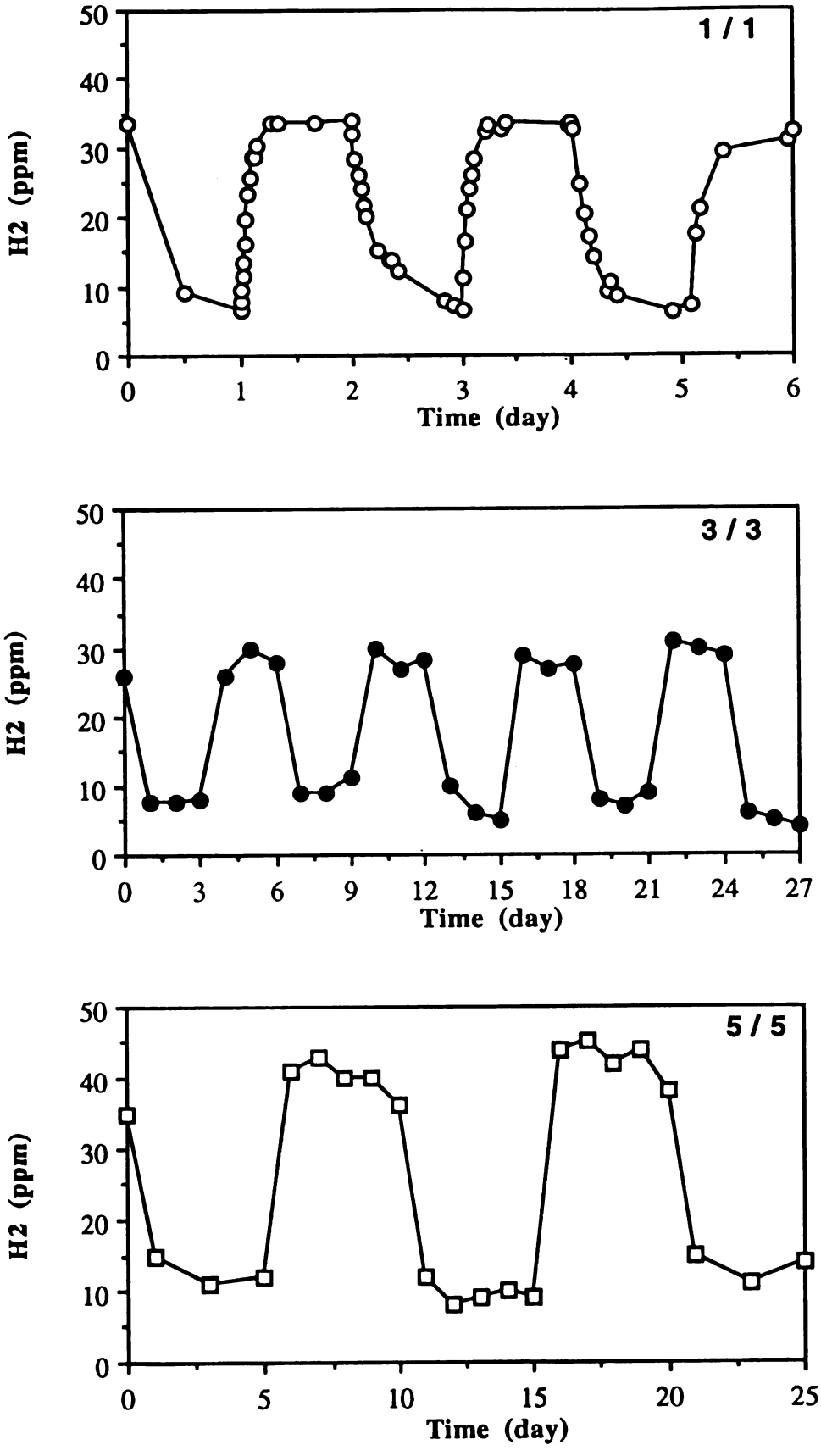

Figure 7-4. Hydrogen concentration changes in the re-established daughter reactors.

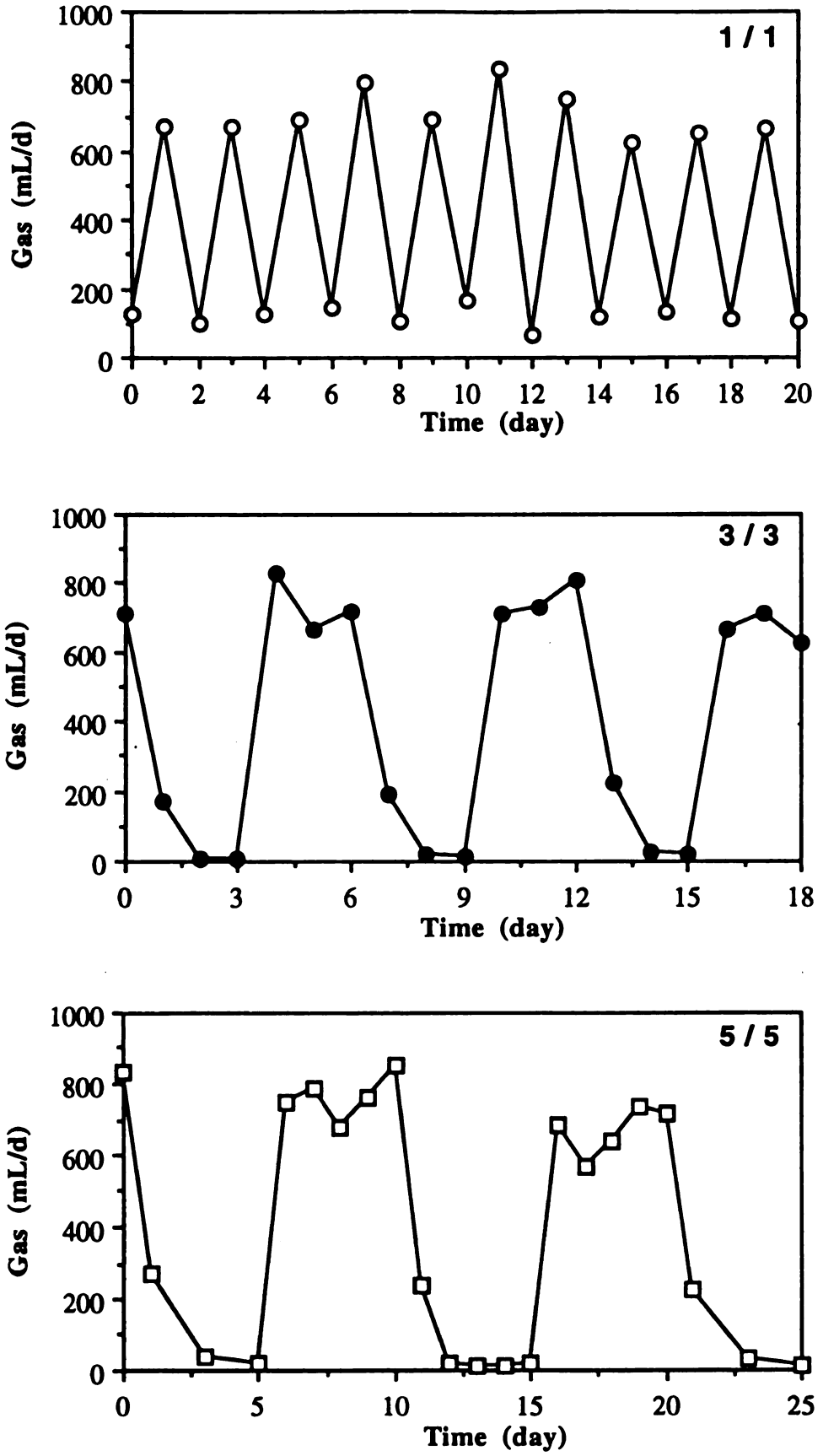

Figure 7-5. Gas production changes in the re-established daughter reactors.

7-2 Summary of operational performance of the mother and the daughter reactors

Parameters	M	1/1[1]	3/3[2]	5/5[3]
CODin (mg/l)	8500	8500	8500	8500
CODe (mg/l)	320 ±40[4]	250 ±60	280 ±100	430 ±350
VSS (mg/l)	1260 ±110	1300 ±170	1200 ±180	1190 ±380
Gas (ml/L-d)	430 ±60	410 ±230	440 ±260	410 ±360
CH_4 (%)	51 ±2	50 ±2	49 ±2	48 ±5
pH	7.03 ±0.05	7.02 ±0.06	6.97 ±0.04	7.03 ±0.09
Acetate (mg/l)	120 ±50	110 ±40	120 ±100	250 ±220
Propionate (mg/l)	12 ±5	20 ±13	18 ±9	34 ±50
Butyrate (mg/l)	4 ±3	7 ±2	8 ±4	14 ±20

1: Average value for two day cycle,
2: Average value for six day cycle,
3: Average value for ten day cycle,
4: Standard deviation.

TABLE 7-3. Maximum specific substrate utilization rates for the mother and the daughter reactor cultures

	M	1/1	3/3	5/5
V_{Glu} (mg/g vss. d)	3790 ±180[1]	4140 ±180	3870 ±160	10800 ±230
V_{Ac} (mg/g vss. d)	780 ±73	1050 ±78	1120 ±78	900 ±85
V_{Pr} (mg/g vss. d)	4.8 ±1.0	61 ±9.9	160 ±12	240 ±25
V_{Bt} (mg/g vss. d)	250 ±28	350 ±40	470 ±35	290 ±35
V_{H2} (mmole/g vss . d)	81 ±14	155 ±16	113 ±25	90 ±25

1: Standard deviation.

fermentation intermediate distribution in the perturbed anaerobic reactors. The changes in the maximum specific substrate utilization rates was apparently related to substrate perturbation intervals. The maximum specific utilization rate of propionate, as well as glucose, increased with increasing perturbation intervals (Figure 7-6); the maximum specific utilization rate of acetate, butyrate and hydrogen increased for the 1/1 perturbation intervals and then declined with further increase in the length of the perturbation intervals. (Figure 7-7).

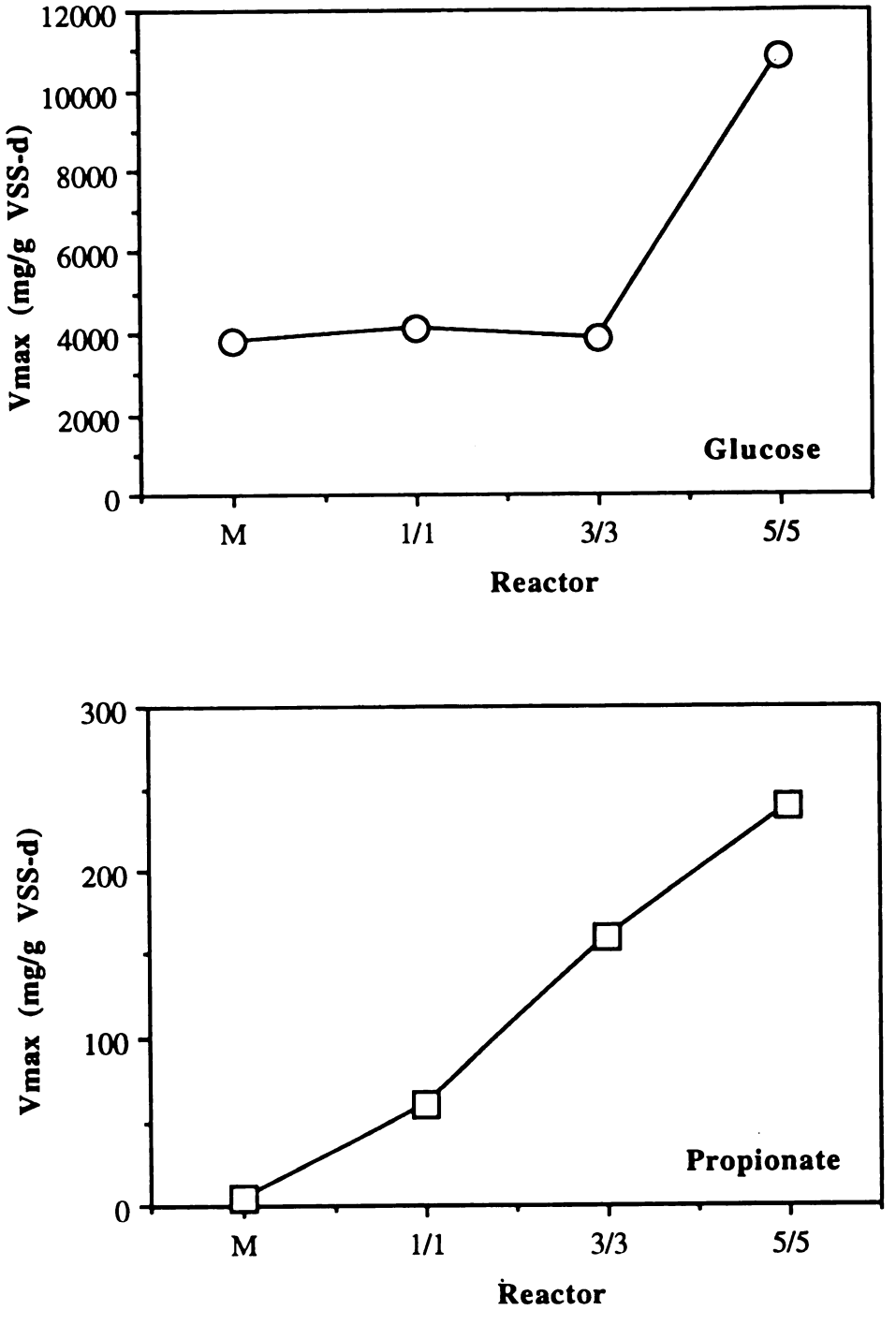

Figure 7-6. Effect of perturbation interval on maximum glucose and propionate utilization rates.

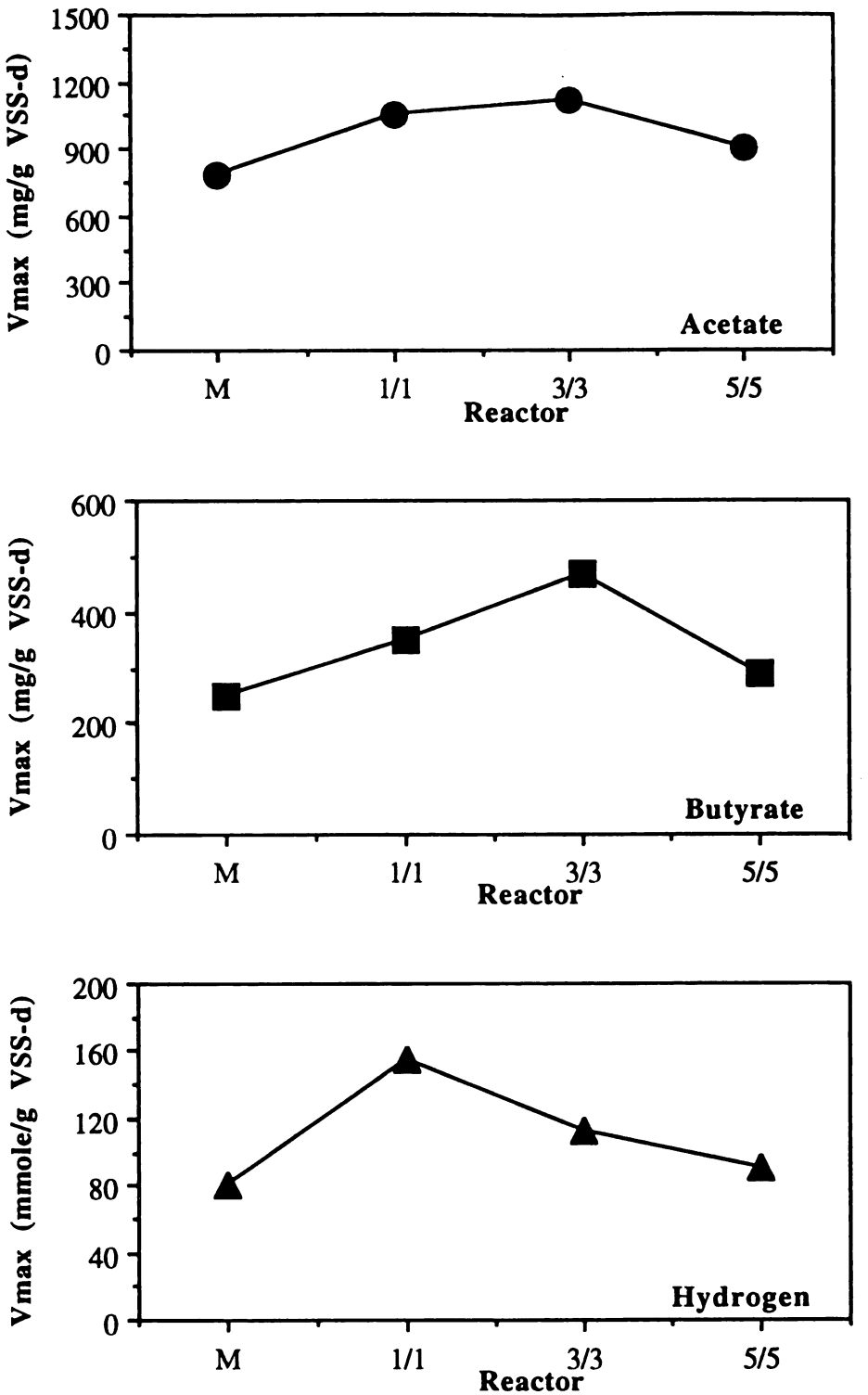

Figure 7-7. Effect of perturbation interval on maximum acetate, butyrate and hydrogen utilization rates.

7.3.2 Response of anaerobic populations to glucose and temperature shocks

Both glucose and temperature shocks were performed on the 1/1 daughter reactor and the constant feed chemostat (m-1) which was used as the representative of the control mother reactor. For both experiments, the shock was applied at the beginning of the change in the feed for the 1/1 reactor. Before initiation of the glucose and temperature shocks, samples were intensively collected from the daughter reactor 1/1 and the constantly fed anaerobic reactor m-1 for three weeks to obtained baseline operational performance (Table 7-4).

7-4 Baseline operation results for reactor 1/1 and m-1.

parameters	1/1[1]	m-1
CODe (mg/L)	248 ±78[2]	427 ±56
pH	6.90 ±0.07	6.97 ±0.02
VSS (g/L)	1.15 ±0.18	0.94 ±0.11
H_2 (ppm)	19.7 ±9.4	29.4 ±4.9
CH_4 (%)	50 ±2.0	50 ±1.0
Gas (ml/L-d)	430 ±31	417 ±20

1: average value for two day cycle
2: Standard deviation.

a. Results of glucose shock loading test

After pulse injection of the concentrated glucose stock solution, the effluent COD concentration in reactor m-1 immediately increased to level of ca. 4,600 mg/L and then gradually decreased to near its pre-perturbation level over the next 4 days (Figure 7-8a). The glucose injected into reactor m-1 was completely degraded within 11.5 hours at an

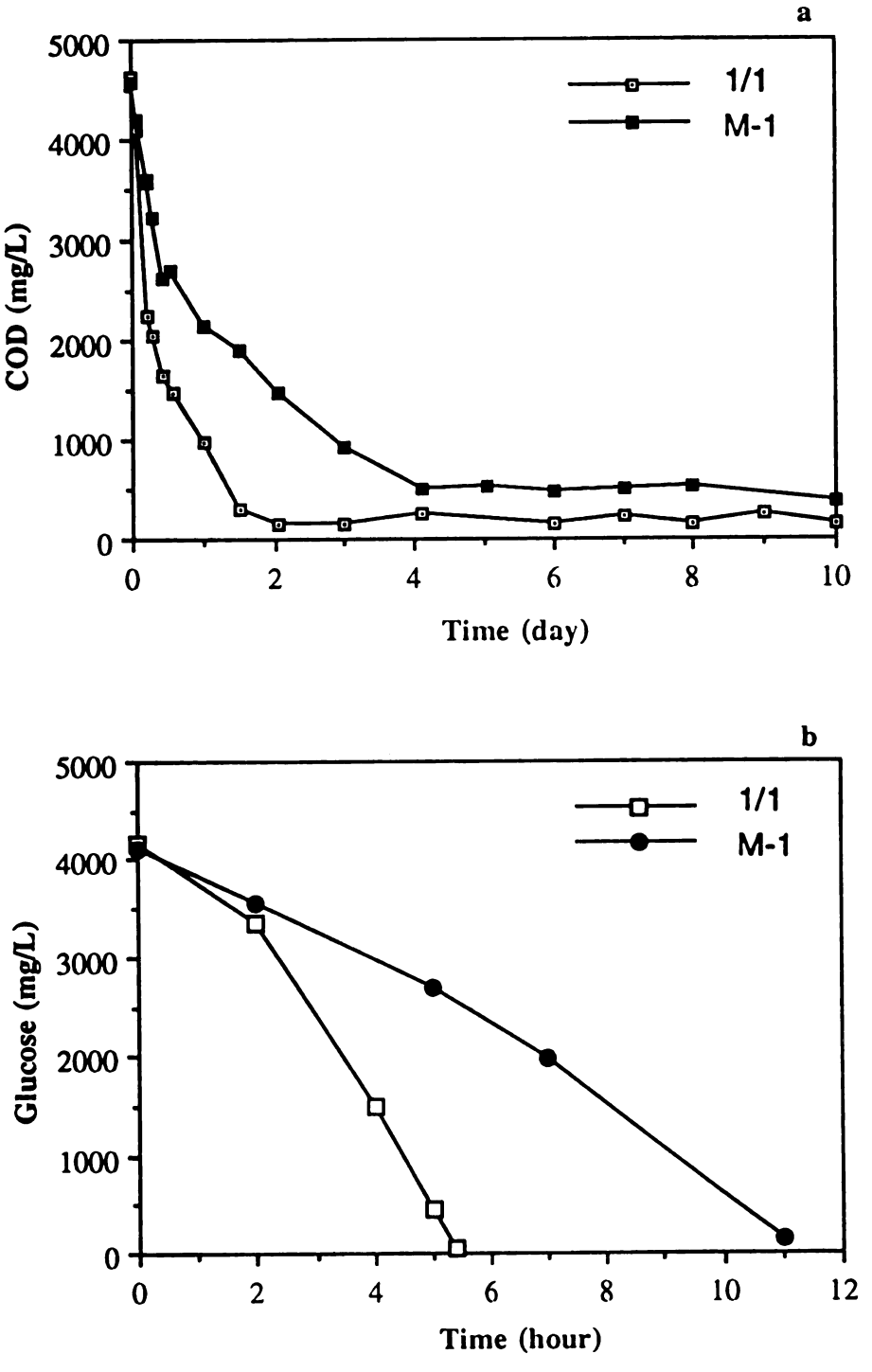

Figure 7-8. Changes in a) COD and b) glucose concentrations during the glucose shock loading experiments.

average degradation rate of 360 mg glucose/L-h (Figures 7-8b). A rapid accumulation of glucose metabolic intermediates was observed immediately after the glucose was added. Acetate, ethanol and propionate concentrations reached their peak levels of ca. 1,100 mg/L, 500 mg/L and 300 mg/L, respectively, at the same time when glucose was observed to decrease to below detection limits (< 0.5 mg/L) (Figure 7-9a). Concurrently, a rapid accumulation in hydrogen up to 1,600 ppm was observed in the reactor headspace (Figure 7-10a). No significant butyrate accumulation was observed throughout the experimental period. The hydrogen and ethanol that accumulated were metabolized within ca. 0.5 and 1.5 days, respectively. For acetate and propionate, ca. 4 days was needed before their concentrations returned to near the pre-shock levels. During the shock loading period a remarkable change in biomass concentration was also observed (Figure 7-10b). Reactor pH decreased concurrently from 6.98 to 6.62 with the significant accumulation of the glucose fermentation intermediates and returned to near its normal levels within ca. 4 days (Figure 7-11).

The anaerobic population in the 1/1 daughter reactor appeared to be more resistant to the glucose shock. The pulse injection of glucose resulted a peak COD concentration of ca. 4500 mg/L. The effluent COD concentration returned to near its pre-shock levels within about 2 days (Figure 7-8a). The injected glucose was completely metabolized within ca. 5.5 hours at an average disappearance rate of ca. 760 mg glucose/L-h (Figure 7-8b). This rapid degradation of glucose caused a significant accumulation of acetate, butyrate and propionate concentrations up to 760 mg/L, 150 mg/L and 70 mg/L, respectively (Figure 7-9b). After the pulse injection of glucose, ethanol accumulated up to 470 mg/L within ca 5 hours and then completely degraded during the following 24 hours. An accumulation of hydrogen with a peak level of ca. 350 ppm, was observed in the 1/1 reactor headspace (Figure 7-10a). The changes in biomass and pH observed during the glucose shock loading test are presented in Figure 7-10b and 7-11 respectively. The perturbed daughter reactor returned to its normal condition within ca. 1.5 days.

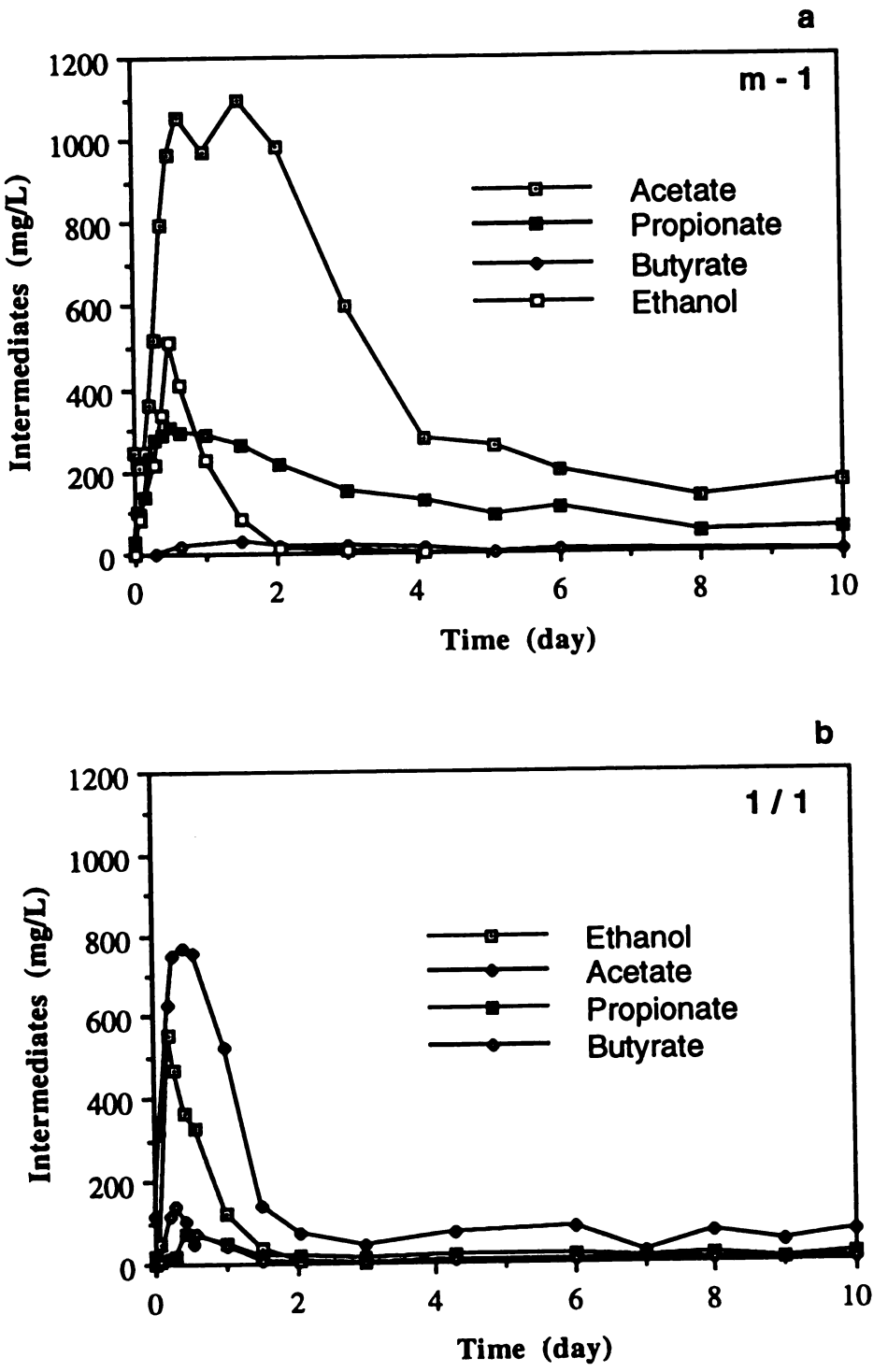

Figure 7-9. Changes in concentrations of glucose fermentation intermediates for the a) m-1 and b) 1/1 reactors during the glucose chock loading experiments.

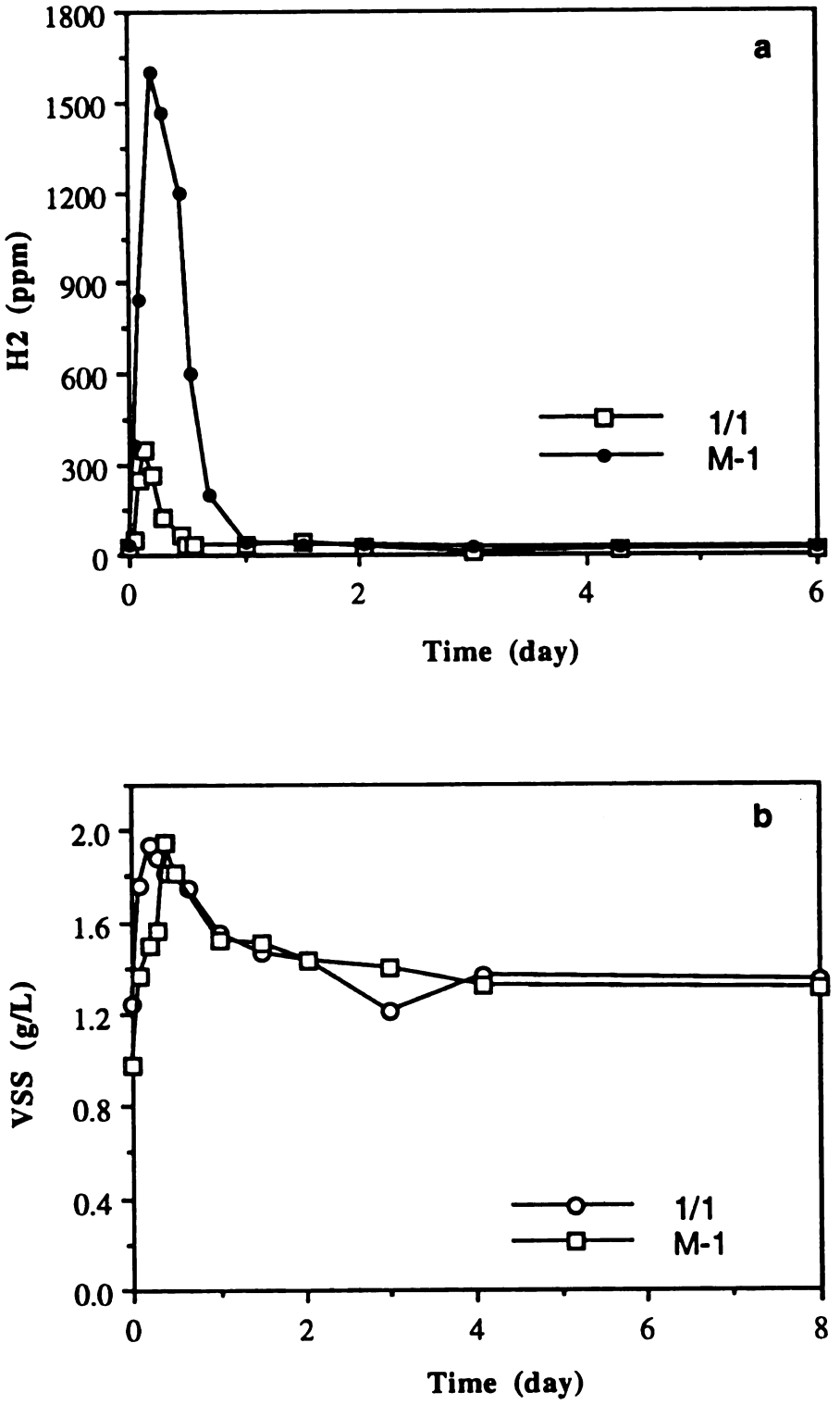

Figure 7-10. Changes in a) hydrogen and b) biomass concentrations during glucose shock loading experiments.

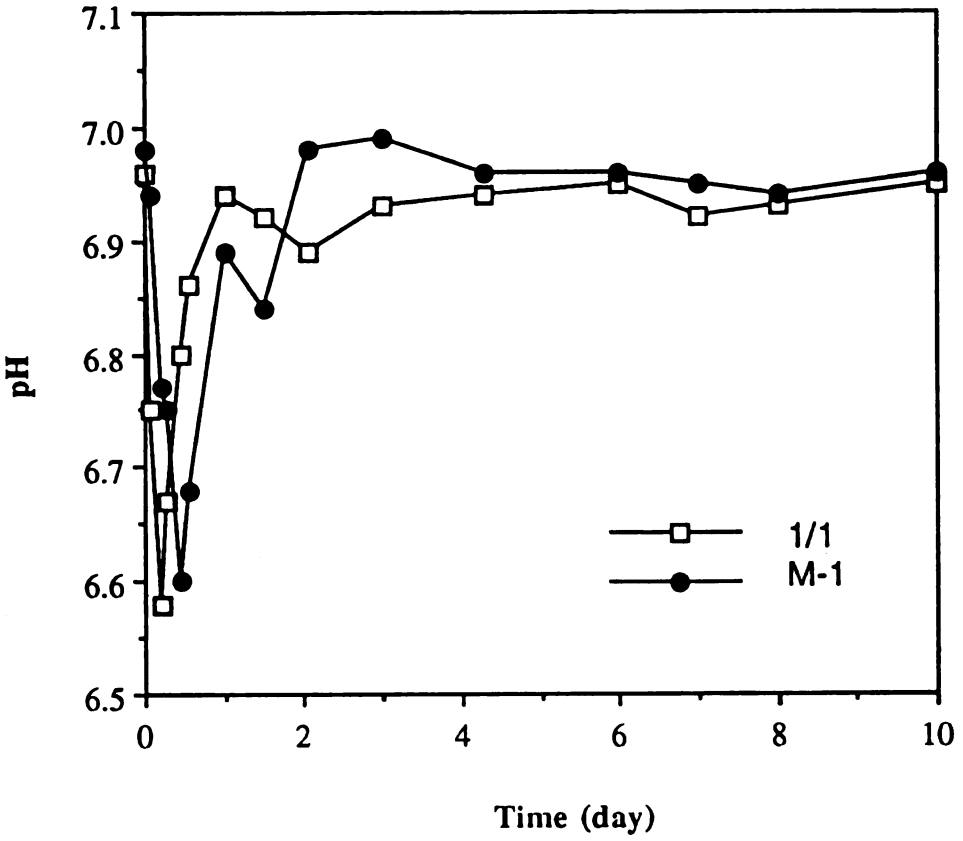

Figure 7-11. Changes in pH observed during the glucose shock loading experiments.

Table 7-5. Peak levels of glucose fermentation intermediates and other operational parameters in reactor 1/1 and m-1 during glucose shock loading tests

Parameters	1/1	m-1
Hydrogen (ppm)	350	1600
Acetate (mg/L)	770	1100
Ethanol (mg/L)	560	510
Propionate (mg/L)	70	310
Butyrate (mg/L)	140	30
pH	6.58	6.60
VSS (g/L)	1.94	1.87
Recovery time (day)	1.5	4.0

The peak levels of glucose fermentation intermediates and other operational parameters during the glucose shock loading test are summarized in Table 7-5.

b. Results of temperature shock

The temperature shock was performed by temporally shutting off the reactor heating system for 24 hours. Reactor temperatures decreased from 35 °C to ca. 25 °C within ca. 3 hours and remained at this level until heating resumed (Figure 7-12a).

The response of the m-1 and the periodically fed 1/1 reactors to the 24 hour temperature shock is presented in Figure 7-12b. In the reactor m-1, a slight increase in effluent COD during the 24 hour temperature shock period was followed by a continuous increase in effluent COD over the following 15 days. A peak COD level of ca. 1100 mg/L was observed. Subsequently, COD decreased to its normal level within 5 more days. A slight decrease in reactor pH was also observed in reactor m-1. Although the effluent

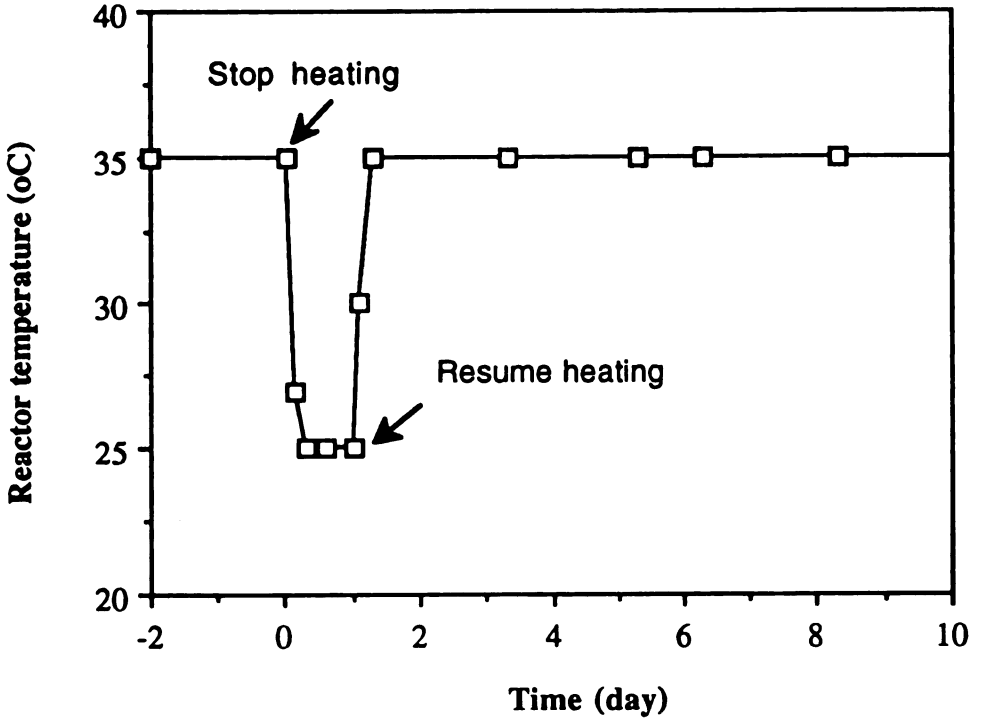

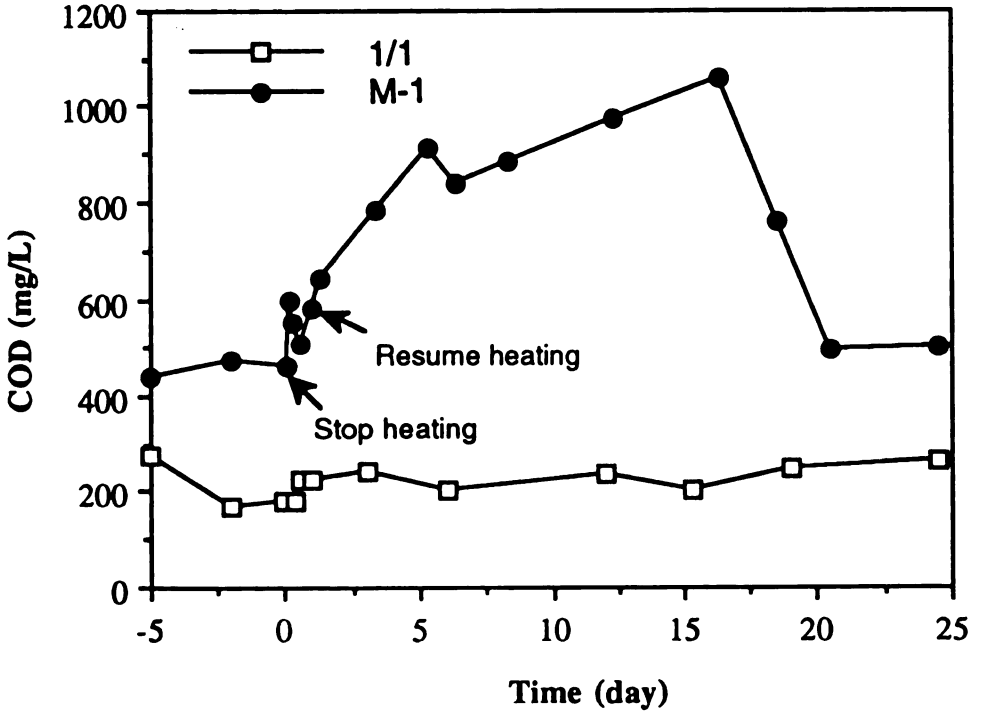

Figure 7-12. Changes in temperature (a) and COD concentrations (b) during the temperature shock experiments.

COD concentration in reactor m-1 increased to twice its normal value, no significant increase in effluent VFA (acetate, propionate and butyrate) concentrations was observed. Analytical results also demonstrated that the COD increase was not the result of accumulation of common glucose metabolic intermediates ethanol and lactic acid. The elevated COD concentration observed during the temperature shock period were not identified.

In contrast, the community in the 1/1 reactor was not significantly affected by the short-term temperature shock. No significant change in COD or other operational parameters was observed either during the temporary temperature decrease or thereafter (Figure 7-12b).

No changes in headspace hydrogen partial pressure was observed for either system.

7.4 Discussion

Experimental results presented in previous chapters illustrate that the anaerobic populations could gradually recover from the initial impacts of the periodic substrate perturbations. Additional experimental results obtained from this study demonstrate that the re-established anaerobic populations could maintain stable and effective operation under long-term periodic substrate feed conditions. The average COD removal efficiency and gas production, as well as other operational parameters, obtained in the re-established daughter reactors were similar to those obtained in the control mother reactor which operated under constant substrate feed conditions. The only major difference in daily operational performance between the mother and the periodically fed daughter reactors, was the cyclic changes in the operational parameters of the daughter reactors. This study established that periodic substrate feeding mode could be used as an operational strategy to enhance reactor stability.

In addition to high organic removal efficiency, the re-established daughter reactor population appeared to be more resistant to sudden environmental changes. Short recovery time and less serious impacts were observed for the daughter reactor community. The characteristics possessed of the daughter reactor community are most likely due to changes in microbial community. As indicated by the maximum specific substrate utilization rates, more active or "robust" species became predominant in the perturbed daughter reactor populations presumably because of a long-term selection/adaptation processes (Table 7-3). To achieve effective organic degradation, the entire anaerobic community must work syntrophically. The enhanced substrate utilization capacity in the daughter reactor population does not only benefit individual trophic groups, but is also advantageous to the entire system. Remarkable differences in the distribution of glucose fermentation intermediates were observed in reactor 1/1 and m-1 after glucose shocks (Table 7-5). Much less propionate was produced in the daughter reactor. This was most likely due to reduced hydrogen accumulation in the 1/1 system which, as discussed in Chapter 4 and 5, could dramatically change glucose fermentation routes. As usually

observed in perturbed anaerobic reactors (Mosey and Fernandez, 1989), a large amount of propionate was produced in the m-1 reactor, indicating a significant shift in the fermentation route. Due to poor propionate utilization capacity possessed by the constantly fed anaerobic community, propionate contributed a large portion of the accumulated COD during the following recovery period in the m-1 reactor.

Usually, operators of anaerobic reactor systems for wastewater treatment strive to achieve a constant feed. Under such conditions, the number of electrons channeled through propionic and butyric acids is greatly decreased (Palns, 1987; Mosey 1981). This causes a decrease in the relative population of the associated acetogens. Consequently, the resulting system is susceptible to acid accumulation from influent substrate variations (Duarte and Anderson, 1982; Fongastitkul et al, 1994). Although this drawback has long been recognized (Harper and Pohland, 1985), no suitable resolution has been reached to date. This appears to be due to the paradox that to maintain high organic removal efficiency constant feed is desirable, but in order to change substrate distribution (i.e. let more substrate flow through butyrate-propionate fermentation) some kind of perturbation is necessary. Experimental results presented in this thesis suggest a reasonable resolution -- introducing properly controlled periodic substrate perturbations. This procedure could effectively change substrate distribution so as to maintain sufficient acetogens in the community, while at the same time sustaining a high efficiency of organic removal.

Maximum substrate utilization rates in the perturbed daughter reactor cultures changed with perturbation intervals. This observation shows that the maximum substrate conversion rates may be used as a group criteria to compare or estimate stability of anaerobic communities. This observation also implies that there is the possibility of adjusting the perturbation interval to achieve an "optimum" microbial community structure.

The above experimental results and discussion strongly suggest that although usually considered "harmful", substrate perturbations, if properly controlled, can be used as a tool to improve operational performance of anaerobic systems.

7.5 Summary

The re-established daughter reactor populations could maintain stable and effective operation under long-term periodic substrate feed conditions. There reactors possessed higher substrate utilization capacities, and appeared to be more resistant to environmental shocks.

These experimental results suggest the potential use of the substrate perturbation as a tool to optimize anaerobic microbial community and improve system operational performance.

Chapter 8

CHARACTERIZATION OF MICROBIAL COMMUNITY STRUCTURE CHANGE IN RESPONSE TO LONG-TERM PERIODIC SUBSTRATE PERTURBATIONS BY FATTY ACID METHYL ESTERS

8.1 Introduction

Methane fermentation results in the conversion of organic materials to methane and carbon dioxide in the absence of molecular oxygen. Conversion of carbohydrate, fat and protein to methane requires the combined activity of fermentative, acetogenic, and methanogenic bacteria (McCarty, 1981; Novaes, 1986; Pavlostathis, 1991). These different functional groups are composed of a large number of bacteria, of which relatively few have been isolated (Zeikus, 1979; Iannotti, 1982). Although much effort has been directed towards culturing the bacteria present in anaerobic digesters, only a small portion of the microorganisms present in anaerobic digesters have been cultured (Toerien and Hattingh, 1969; Varel, 1984; Britz et al., 1994).

The above studies highlight the difficulties in culturing bacteria from anaerobic environments where many bacteria are syntrophically associated via complex physiological, kinetic and thermodynamic interactions. Recognizing the limitations of conventional isolation techniques, White (1979, 1983) advocated new methods based on the analysis of lipids to obtain information about the community structure and nutritional status of complex microbial ecosystems, without the need for selective removal or growth of isolates. Fatty acid methyl esters (FAME) analysis can be used to obtain a characterization of the microbial community (Bobble and White, 1980). In bacterial cells, fatty acids occur mainly in the cell membranes as the acyl constituents of phospholipids

(Kandeda, 1991). Some fatty acids are unique to specific bacteria or to groups of bacteria and can serve as signatures for these bacteria (Ikemoto S. et al., 1978; Boe and Gjerde, 1980). Gillan and Hogg (1984) have used this concept to divide the bacterial community of mangrove sediments into several subgroups.

The FAME method is frequently used to assess the structure of soil and aquifer communities (Vestal and White, 1989; Rajendran N., et al., 1992; Zelles, et al., 1992). In addition, some researchers have pioneered use of FAME to estimate metabolic status and community structure of anaerobic digesters (Henson et al., 1985; Mikell et al., 1987; Schropp et al., 1988; Hedrick et al., 1991). However, little is known about the FAME characteristics for specific anaerobic systems, such as the glucose fed anaerobic chemostats evaluated in this study, or the feasibility of using FAME profiles to monitor changes in microbial community. Confirmed information is still lacking for the relationship of the FAME results with major operational parameters such as COD and VFA concentrations.

This chapter presents the results of using FAME analysis techniques to monitor changes in microbial community structure for the daughter reactors described in Chapters 4 to 6, during initial steady-state perturbation conditions and after recovery.

8.2 MATERIALS AND METHODS

8.2.1 Anaerobic reactors

A 15 L working volume anaerobic chemostat (the mother reactor), operated at 10 day HRT and 35 °C with glucose as the sole carbon and energy source, was used as a source of organisms for the inoculation of daughter reactors and as a stable control. Three 1.5 L working volume anaerobic chemostats (the daughter reactors) were inoculated with cultures taken from the mother reactor and were initially operated until a steady state was achieved under the same conditions as the control mother reactor (10 day HRT and 8 g/L glucose feed). After collection of sufficient steady state baseline information, the three daughter reactors were subjected to periodic loading patterns in which glucose feed concentration was varied from 16 g/L to 0 g/L (mineral media only) in 2 day, 6 day and 10 day cycles respectively.

System set up, nutrient supply and inoculation procedures are described in detail in Chapters 3 - 6, respectively.

8.2.2 Sample collection and storage

Samples of reactor liquid phase were transferred into clean, dry screw cap culture tubes (13 mm x 100 mm), then centrifuged at 2000 g for 10 minutes; the resulting cell pellets were stored at -35 °C for subsequent extraction and analysis.

8.2.3 FAME extraction

A complete description of the FAME extraction procedure is provided in Appendix G.

8.2.4 FAME analysis

FAME analysis was performed by using a HP 5890A gas chromatograph (Hewlett Packard, Palo Alto, CA), equipped with a flame ionization detector (FID) and a 25-m HP Ultra 2 capillary column using UHP (99.999%) hydrogen gas as carrier (50 ml/min). The oven temperature was programmed from 170 °C to 270 °C, heating for 20 min at a rate of

5 °C/min, followed by a 3.4-min isothermal period at 270 °C. The injector and detector temperatures were 250 °C and 300 °C, respectively. The analysis time for each sample was ca. 23.4 minutes.

8.2.5 Numerical analysis methods

All FAME data consisted of peak areas expressed as percentages of the total peak area of a trace. Three numerical methods were used for the analysis of the FAME data:

(1) Calculation of the overlap coefficient, S_O (Bousfield *et al.*, 1983). So is a measure of the degree of overlap of two superimposed traces, both scaled to the same total area of 100:

$$So\ (i, j) = 100 - 0.5 \sum |x_{ik} - x_{jk}| \qquad (8\text{-}1)$$

where:

x_{ik}, x_{jk} = the percentage areas of the kth peak for the ith and jth culture respectively.

The overlap coefficient attempts to mimic the way in which traces might be compared visually. In an intuitive sense, two traces which could be superimposed exactly would be considered completely similar, whereas two which showed no overlap would be completely dissimilar. Thus the value of the overlap coefficient S_O can be defined as:

$$0 \leq S_O\ (i,j) \leq 1 \qquad (8\text{-}2)$$

(2) Principal-component analysis. Principal-component analysis was performed using the SYSTAT 6.0 statistical package (SYSTAT. Intelligent software, Evanston, IL).

(3) Cluster analysis. Cluster analysis was completed using the median linkage method and using the SYSTAT 6.0 statistical package (SYSTAT. Intelligent software, Evanston, IL)

8.2.6 Experimental design

In this study, three daughter reactors were subjected to long-term periodic substrate perturbations. During the perturbation period, the influent glucose concentrations of the daughter reactors were alternately changed in amplitude from 16 g/L to 0 g/L (mineral media only) on 2 day, 6 day and 10 day square wave cycles respectively. A 10 day hydraulic retention time (dilution rate of 0.1 d^{-1}) was maintained throughout the experiment in all the perturbed daughter reactors. The daughter reactors were continuously operated for a period of 450 days including ca. 50 days under steady-state baseline conditions and ca. 400 days under perturbation and recovery conditions.

The microbial community changes in the perturbed daughter reactors and in the control mother reactor were monitored using fatty acids profiles by periodically sampling these reactors. Fatty acids profiles obtained before the initiation of the substrate perturbations served as baseline reference values. FAME samples were more frequently collected during the operational stages when rapid environmental changes occurred (as indicated by other operational parameters such as COD and VFA concentrations) to trace possible microbial community changes that occurred during these relatively short time periods. This sampling schedule allowed us to explore the relationship between FAME profiles and operational parameters.

8.2.7 Nomenclature for fatty acids configuration

The fatty acid designation sequence used in this Chapter is as follows: number of carbon atoms, number of double bonds, and the location of double bonds in relation to the omega (methyl) end of the fatty acid. The number of double bond are indicated after a colon symbol. When the location of the double bond is indicated as "w6", the double bond is in the 6 carbon, counting from the omega end. Special structures are designated: "a" for anteiso; "i" for iso; "cyc" for cyclopropane, and "OH" for hydroxyl group. A more detailed description of fatty acid nomenclature is presented in Appendix H.

8.3 RESULTS

8.3.1 Determination of minimum sample size for FAME analysis

In order to determine the minimum sample size necessary for reliable FAME analysis, 5 different sample volumes were analyzed. For each level, triplicate samples were analyzed to minimize random error. The sample volumes and the equivalent biomass (as VSS) used for determination of the minimum sampling size for the mother reactor culture are presented in Table 8-1. FAME profiles for samples with a liquid volume from 3 ml to 10 ml were essentially the same (Table 8-2).

When the liquid sample volume was reduced to 1 ml (equivalent to a biomass dry weight as VSS of ca. 1.12 mg), significant differences among the FAME profiles were observed. Some of the cell membrane fatty acids, which were present in relatively small abundance, disappeared from the FAME profile. Similar results were obtained from other parallel experiments (results not shown). Based on these results, a minimum biomass (as VSS) amount of ca. 3.5 mg was determined necessary for reliable FAME analysis. Because of the relatively large fluctuations in biomass concentrations in the perturbed daughter reactors, a liquid sample volume of 6 ml was chosen as the routine sampling size for FAME analysis. For samples which had extremely low biomass concentrations, a larger volume was used.

The accuracy and the reproducibility of the GC-FAME analysis were evaluated with triplicate samples from the different anaerobic reactors. The coefficient of variation for most fatty acids was generally below 5% for triplicate analysis. Standard deviations higher than 5% were only observed for the fatty acids with low abundance (< 4 percent).

Table 8-1. Sample volumes and equivalent biomass (as VSS) of the mother reactor culture used for minimum sampling size determination

Sample volume (ml)	Equivalent Biomass (mg)
0.5	0.56
1	1.12
3	3.36
5	5.60
10	11.20

Table 8-2. Effect of sample volume on relative abundance of fatty acids for FAME analysis.

Fatty acid	10 ml	5 ml	3 ml	1 ml	0.5 ml
a-13:0	0.26±0.03	0.18±0.02	0.22±0.02	-[a]	-
13:1	2.09±0.13	2.04±0.14	2.06±0.11	-	-
13:0	2.16±0.08	1.66±0.07	1.71±0.09	-	-
i-14:0	4.14±0.22	3.67±0.17	3.73±0.14	-	-
14:0	12.49±0.27	12.15±0.27	11.98±0.26	13.34±0.28	15.86±0.38
i-15:0	13.04±0.33	13.11±0.29	12.87±0.38	15.67±0.47	18.99±0.65
a-15:0	25.03±0.55	24.85±0.57	24.77±0.71	29.91±0.72	38.64±1.16
15:0	18.26±0.46	18.49±0.51	18.34±0.38	22.95±0.67	26.51±0.66
i-14:0 3OH	3.39±0.21	3.42±0.17	3.58±0.19	-	-
14:0 2OH	0.35±0.02	0.31±0.10	0.34±0.09	-	-
i-16:0	4.62±0.19	4.77±0.17	4.83±0.18	5.76±0.23	-
a-16:0	0.51±0.10	0.54±0.05	0.56±0.08	-	-
16:0	4.93±0.22	5.15±0.27	5.19±0.23	6.53±0.30	-
i-17:0	1.36±0.08	1.56±0.10	1.52±0.12	-	-
a-17:0	4.58±0.31	5.02±0.25	5.18±0.27	5.83±0.31	-
17:1 w6c	0.78±0.10	0.85±0.09	0.86±0.11	-	-
17:0	1.19±0.07	1.28±0.10	1.29±0.07	-	-
i-17:0 3OH	0.39±0.09	0.44±0.11	0.45±0.07	-	-
17:0 2OH	0.42±0.06	0.49±0.10	0.52±0.06	-	-

a: Not detected

8.3.2 Characterization of microbial community structure in anaerobic reactor populations by FAME analysis

Typical FAME profiles obtained from the mother and the daughter reactor populations are presented in Table 8-3. FAME profiles designated daughter 1/1-1, daughter 3/3-1 and daughter 5/5-1 were obtained from 1/1, 3/3 and 5/5 day daughter reactors under the steady-state condition that re-established after long-term perturbation; FAME profiles named daughter 3/3-2 and daughter 5/5-2 were obtained from 3/3 and 5/5 day daughter reactors during a metastable period prior to re-establishmentof a stable steady-state.

At least 41 fatty acids were identified among the different bioreactor microbial populations. Under steady-state conditions, fatty acids i-15:0, a-15:0 and 14:0 were prevalent. Significant amounts of these fatty acids were observed in all steady-state anaerobic reactor populations. Fatty acids i-14:0 3OH, 15:0 and 16:0 were also present in relatively significant amounts.

During the metastable operation periods, significantly different FAME profiles were observed. The prevalent fatty acids for the stressed metastable steady-state reactor populations were straight chain fatty acids 16:0 and 14:0; 18:0 and 16:1 w7c were observed in particular populations. As shown in Table 8-3, some fatty acids were detectable for only a particular reactor community. For example, fatty acids 10:0 and i-11:0 were found only in the 1/1 day daughter reactor, and fatty acids a-13:0 and a-19:0 were found only in the mother reactor community.

Differences in microbial communities among the anaerobic reactor populations can be recognized by comparing the abundance of the major cell membrane fatty acids and the unique fatty acids which are present only in particular reactor communities. After a stable steady-state was re-established, the mother reactor and 1/1, 3/3 and 5/5 day daughter reactor communities appeared to have similar populations. In contrast, the structures of the stressed metastable 3/3 and 5/5 day daughter reactor communities were significantly different.

Table 8-3 FAME profiles for the mother and the daughter reactor microbial populations

Fatty acid	mother	daughter 1/1-1	daughter 3/3-1	daughter 5/5-1	daughter 3/3-2	daughter 5/5-2
10:0	-a	0.11	-	-	-	-
i-11:0	-	0.28	-	-	-	-
11:0	-	0.66	0.12	-	-	-
12:00	0.10	5.11	0.12	0.99	3.96	1.31
i-13:00	0.16	1.48	2.24	0.26	-	0.85
a-13:0	0.08	0.00	-	-	-	-
13:1	2.28	1.51	-	-	0.97	4.05
13:0	0.89	0.77	0.56	-	-	0.97
i-14:0	2.58	4.92	3.06	13.58	1.10	-
14:0	10.35	10.78	10.09	12.81	10.94	14.07
i-13:0 3OH	-	0.12	-	-	-	-
i-15:1	-	0.17	-	-	-	-
i-15:0	16.36	27.06	25.34	2.46	1.25	2.96
a-15:0	26.54	10.78	11.50	37.22	4.54	3.70
15:1 w8c	0.41	-	0.22	-	-	-
15:0	9.47	2.82	9.02	3.49	1.81	8.10
i-14:0 3OH	8.45	9.86	12.71	0.29	-	-
14:0 2OH	0.45	0.17	0.49	-	-	-
i-16:0	3.85	5.78	5.20	4.64	-	-
a-16:0	0.50	-	0.83	-	-	-
16:1 w9c	0.21	0.15	0.22	-	1.38	2.04
16:1 w7c	0.30	0.17	0.32	2.21	2.03	11.60
16:0	4.88	3.98	5.42	12.36	48.19	26.98
i-17:0 w9c	0.41	0.72	0.21	-	-	-
i-17:0	2.67	4.50	2.30	-	-	-
a-17:0	4.45	1.83	6.83	2.14	-	0.39
17:1 w8c	0.52	-	0.32	-	-	4.28
17:0 cyc	0.41	0.21	-	2.21	2.92	3.52
17:0	1.77	-	1.38	0.14	2.14	2.58
16:0 3OH	-	-	-	4.52	-	6.24
16:0 2OH	-	-	-	-	-	-
18:1 w9c	-	0.27	0.31	-	0.94	0.99
18:0	0.21	0.65	0.31	0.18	11.04	1.07
i-17:0 3OH	0.60	0.89	0.38	-	-	0.66
17:0 2OH	0.31	0.00	0.28	0.24	1.43	-
i-19:1	-	4.14	-	0.26	3.42	0.79
17:0 3OH	0.27	-	-	-	-	0.50
a-19:0	0.14	-	-	-	-	-
19:0 cyc, w8c	0.13	-	-	-	1.94	0.70
20:3 w6,9,12c	0.27	0.13	0.23	-	-	0.60
20:2 w6,9c	-	-	-	-	-	0.54

a: not detected

The percentages of saturated, branched, unsaturated and cyclopropyl fatty acids in the total cell membrance lipids have been found to be useful criteria for microbial community analysis (Guckert et al., 1986; Kaneda, 1991). In Table 8-4, these percentages are illustrasted for the different reactor populations. Distinctive differences in microbial communities existed between the steady-state and the stressed anaerobic reactor populations. Under steady-state conditions the majority (ca. 60 to 70%) of the cell wall fatty acids were branched fatty acids. Unsaturated and cyclopropyl fatty acids were both present at low levels. In contrast, under metastable steady-state conditions, the majority

Table 8-4 the abundance (%) of the saturated, branched, unsaturated and cyclopropyl fatty acids in the different reactor populations

Fatty acid	M	D1/1-1	D3/3-1	D5/5-1	D3/3-2	D5/5-2
Saturated	27.7	24.9	27.0	30.0	77.8	61.4
Branched	66.8	68.2	70.6	60.8	6.9	9.4
Unsaturated	5.0	6.7	2.4	7.0	10.4	24.9
Cyclopropyl	0.5	0.2	0.0	2.2	4.9	4.3

Table 8-5. Similarity matrix (So, %) of FAME data for reactor communities

	M	D1/1-1	D3/3-1	D5/5-1	D3/3-2
D1/1-1	69				
D3/3-1	79	81			
D5/5-1	60	46	45		
D3/3-2	29	35	27	39	
D5/5-2	38	32	36	46	60

of the cell membrane fatty acids were saturated fatty acids (ca. 60 to 80%). Unsaturated and cyclopropyl fatty acids were both present at relatively high levels. By grouping fatty acids, a similar conclusion can be achieved for the community population similarities of the various microbial populations as determined by the direct comparison of the FAME profiles.

Quantitative taxonomic techniques were used to evaluate changes in FAME profiles. Overlap correlation coefficients, principal-components and median linkage clusters are provided in Table 8-5, Figures 8-1 and Figure 8-2, respectively.

The matrix of similarity coefficients calculated for each pair of FAME profiles (Table 8-3) is presented in Table 8-5. By definition, a high percentage for So means high similarity between the two microbial communities that are being compared. Choosing the mother reactor FAME profile as the reference community (column 1 in Table 8-5), the daughter reactor communities can be ranked from most to least similar as: 3/3-1, 1/1-1, 5/5-1, 5/5-2 and 3/3-2. Based on the values of the similarity coefficients (So), the FAME profiles can be sorted into two groups: the FAME profiles obtained from steady-state reactor populations, and the FAME profiles obtained from the stressed reactor populations. From the results presented in Table 8-5 the most similar pair was 3/3-1 and 1/1-1, and the next most similar pair was the mother and daughter 3/3-1. The FAME profiles for the 3/3-2 and 5/5-2 were significantly different from the steady-state reactor FAME profiles, the similarity between these two FAME profiles was relatively high.

Significant differences in the populations were evident when the FAME profiles of the different stable steady-state and metastable reactors were compared using principal-component analysis (Figure 8-1). The stable steady-state reactor communities separated from the metastable communities by both the first and the second axes (P1 and P2), which accounted for 50.1% and 31.0% of the variation in the FAME profiles, respectively. If the mother reactor FAME profile is selected as a reference, the relatedness of FAME profiles as evaluated in P1-P2 space (Figure 8-1) has exactly the same order as previously

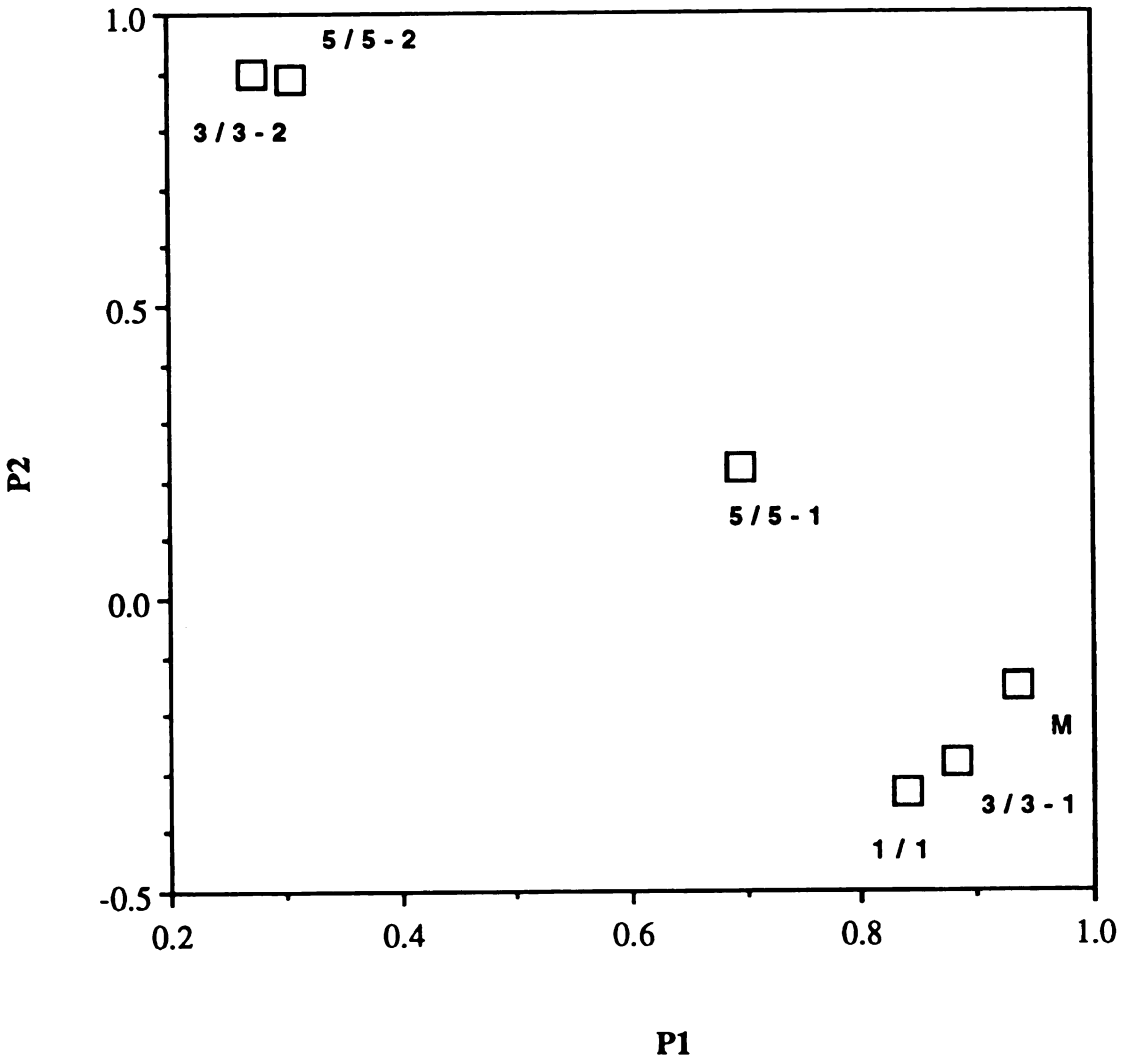

Figure 8-1. Principal-component analysis of the FAME profiles listed in Table 8-3.

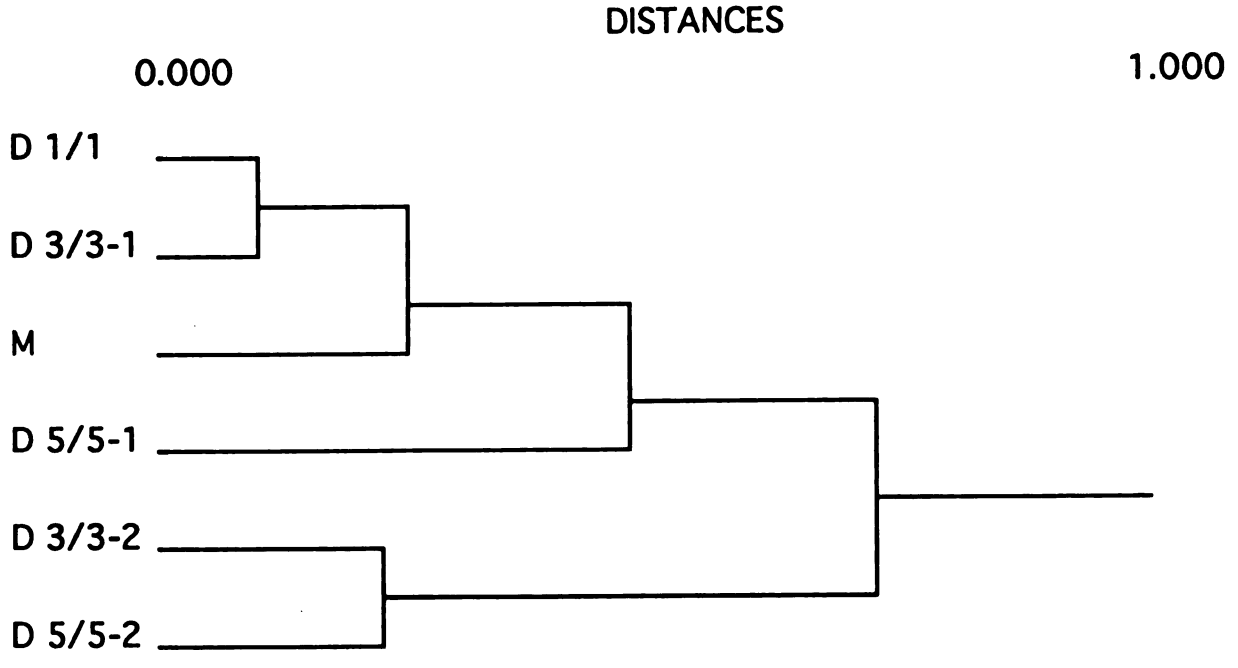

Figure 8-2. Clustering of the anaerobic reactor populations using the 1-Pearson correlation coefficient, median linkage method with FAME profiles listed in Table 8-3.

determined using the similarity coefficient. Principal-component analysis shows that the community structure in the steady-state 5/5 day daughter reactor community was considerably different from those found in the other three steady-state anaerobic reactor communities. This trend was also revealed by previous FAME results.

Using Join-cluster analysis method, the FAME profiles presented in Table 8-3 were sorted into two groups: FAME profiles from the stable steady-state reactor communities and FAME profiles from the metastable reactor communities (Figure 8-2). The communities in the first group were further divided into three sub-groups based on similarities in structures. This classification of FAME profiles was in good accordance with other FAME analyses presented previously.

8.3.3 Feasibily of Monitoring microbial community structure changes by FAME analysis

The feasibility of using FAME analysis to monitor community structure changes in anaerobic reactor populations was evaluated during the 3/3 and 5/5 day substrate perturbation experiments. These results are presented in the following two sections.

1. Experimental results for the 3/3 day perturbation conditions

As described in Chapter 5, significant microbial community changes occurred as evidenced by the physical-chemical, kinetic and genetic analyses, as well as by microscopic morphological observations. The FAME profiles obtained during this perturbation period also reflected changes in the microbial communities. As indicated by the FAME profile taken at day 28, a dramatic change in the microbial population occurred compared to the initial community (Figure 8-3). The predominant cell membrane fatty acids observed at day 28 changed from a-15:0 (28%) and i-15:0 (16%) to 16:0 (48%). Some other cell membrane fatty acids which had a relatively high abundance in the original steady-state FAME profile, such as 15:0, i-14.0 3OH and a-17:0, were absent or decreased to relatively low levels. This dramatic change in the microbial population, as

Abundance (%)

Abundance (%)

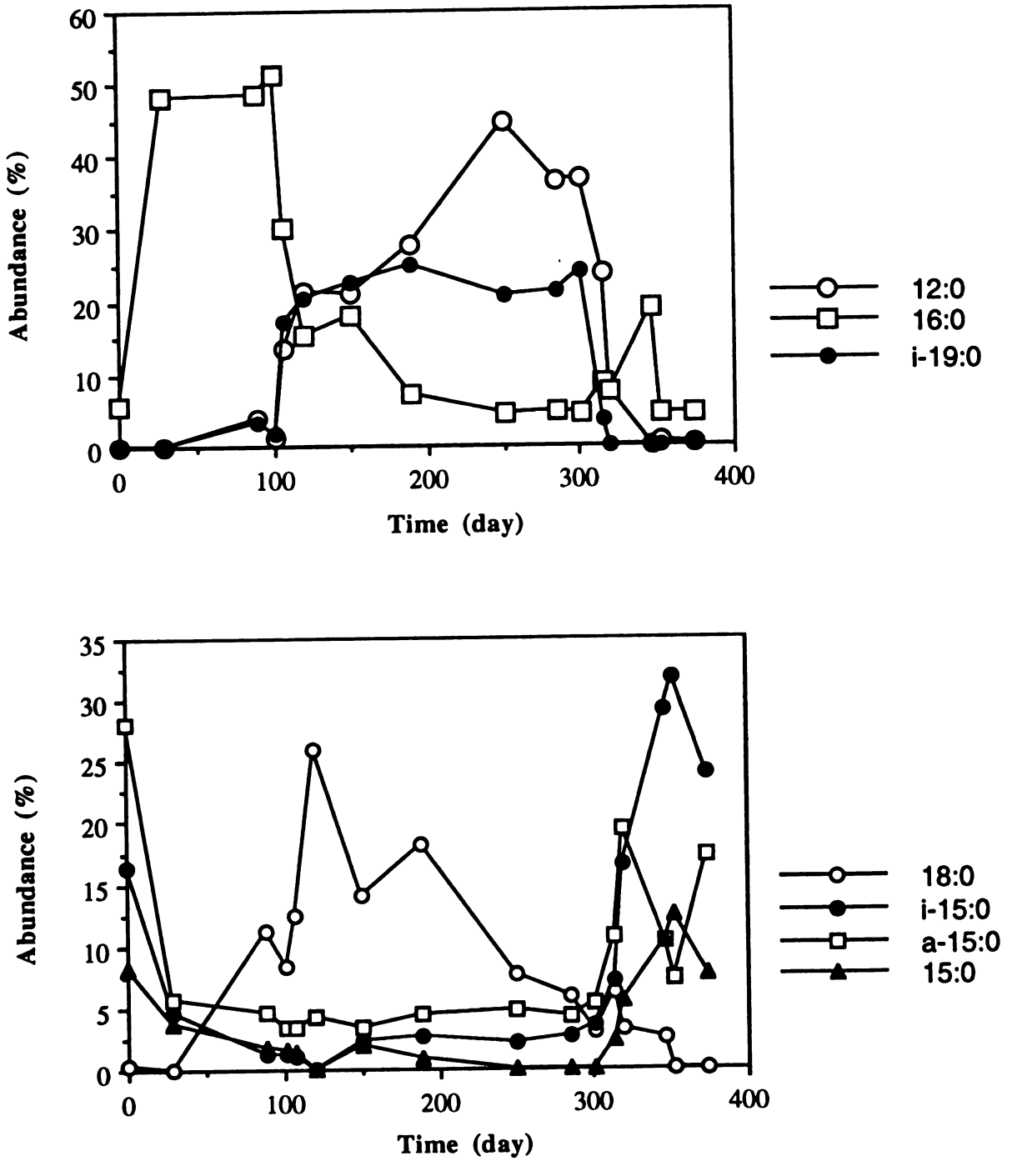

Figure 8-3. Changes in major cell membrane fatty acids abundance during perturbation period in 3/3 day reactor populations.

indicated by the FAME analysis, coincided with the rapid accumulation in COD and VFAs (stage 1a, see Chapter 5).

Subsequent FAME profiles obtained from day 88 to day 287 (the metastable steady-state) show that the structure of the perturbed daughter reactor community was not stable. The predominant cell membrane fatty acids shifted from 16:0 to 12:0, 18:0 and i-19:1. This change corresponded to changes in other parameters such as VFAs (see Chapter 5). A rapid change in FAME composition occurred between day 303 to 323. During this relatively short time period, the predominant cell membrane fatty acids shifted from 12:0 and i-19:1 to i-15:0, a-15:0, 15:0 and i-14:0 3OH, respectively, similar to what was observed in the original steady-state FAME profiles before the perturbation was applied. This change corresponded to the third stage of the 3/3 day perturbation during which time rapid degradation of the accumulated VFAs took place.

The FAME profiles during the 3/3 day perturbation were also analyzed by sorting FAME constituents into saturated, branched, unsaturated and cyclopropyl fatty acids (Figure 8-4). This grouping procedure provided additional information about changes in the microbial community structure. After initiating the substrate perturbation, the abundance of the saturated cell membrane fatty acids increased from ca. 27% to 70%, while the branched cell membrane fatty acids concurrently decreased from ca. 70% to a level of ca. 6.4%. The abundance of saturated and branched fatty acids returned to near pre-perturbation levels of ca. 30% and 63%, respectively, at which point reactor performance again stabilized with high COD removal efficiency. When high COD removal efficiency was observed, an abundance ratio of saturated fatty acids to branched fatty acids of ca 2/1 was observed. When COD removal was poor, this ratio shifted dramatically to less than 1/10.

The FAME profiles obtained from the 3/3 day reactor populations were evaluated using numerical methods. The similarity coefficients, calculated based on the initial steady-state community FAME profile, suggest changes in populations presented in the perturbed anaerobic reactor (Figure 8-5). Dramatic changes in the microbial community,

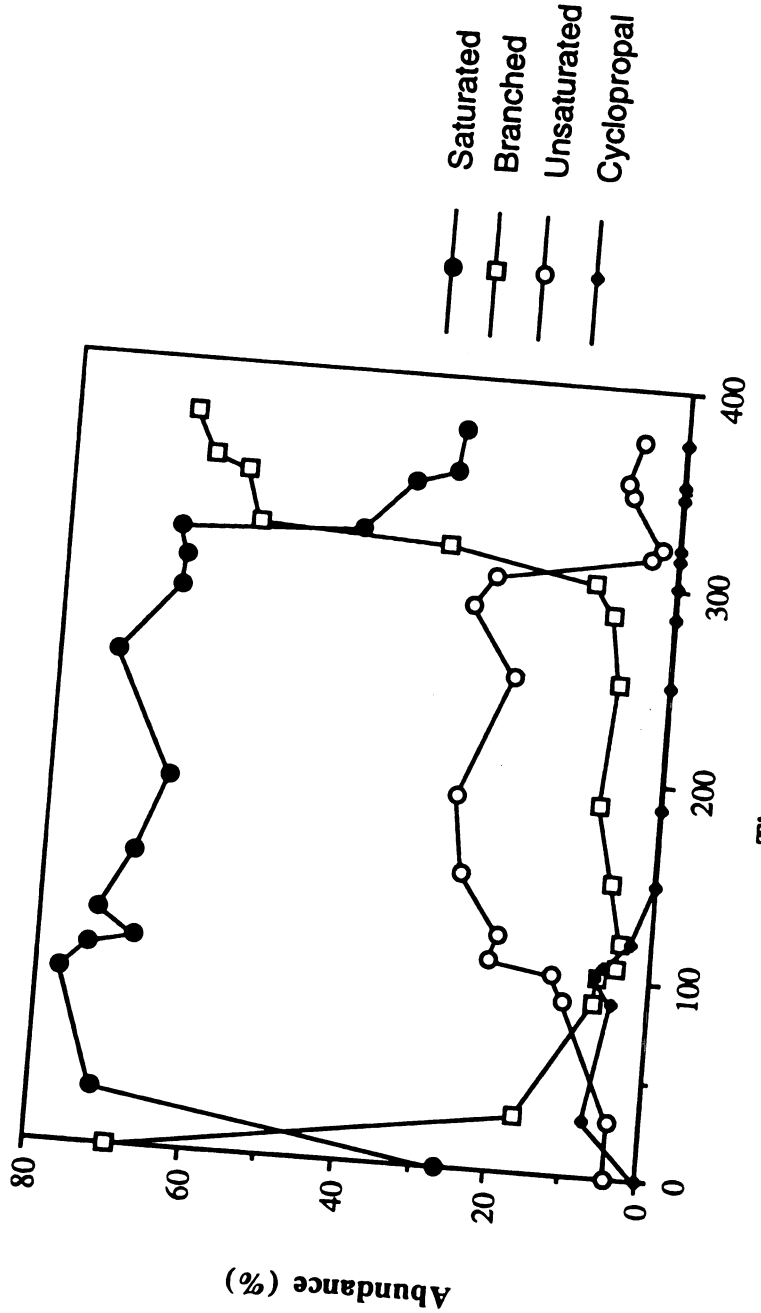

Figure 8-4. Changes in grouped cell membrane fatty acids abundance during perturbation period in 3/3 day reactor populations.

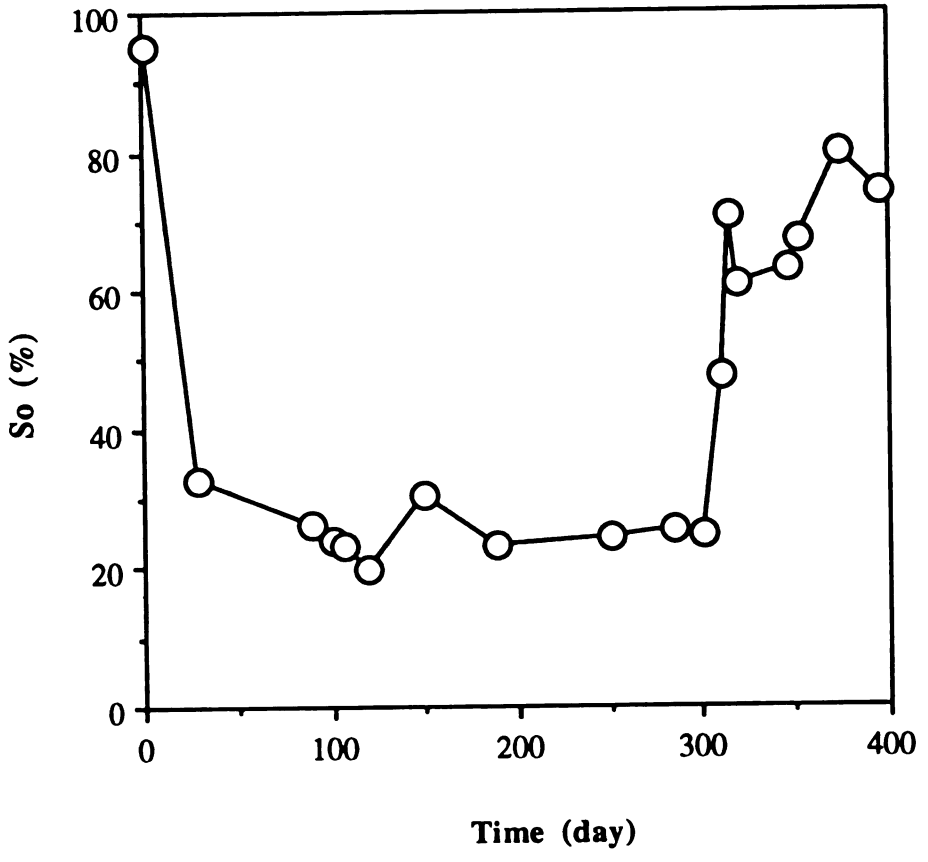

Figure 8-5. Changes in similarity coefficient So during perturbation period in 3/3 day reactor populations.

as indicated by the values of the similarity coefficient, So, were observed during the first and the third stages of the substrate perturbation experiment. FAME profiles with low So values were obtained during periods of metastable operation. This was when glucose fermentation intermediates (ie VFAs) accumulated. The correspondence between the So values and reactor effluent COD concentrations suggests that efficient COD removal was achieved by anaerobic communities which have a structure that is similar to that of the initial steady-state microbial community.

Principal-component analyses illustrate the entire sequence of changes in community structure that occurred during the 3/3 day substrate perturbation period (Figure 8-6). The FAME profiles corresponding to stable steady-state and metastable steady-state are well separated in P1-P2 space. Some of the FAME profiles belonging to the transient state lay between the steady-state and stressed FAME profiles in the P1-P2 space. A zone appears to exist in P1-P2 space corresponding to "healthy" operation and a relatively high COD removal efficiency. By contrast, FAME profiles located far from the "steady-state zone" appear to reflect stressed conditions. This trend is illustrated by the FAME profiles for the 3/3 day perturbation experiment.

Using cluster analysis, FAME profiles obtained from the 3/3 day perturbation experiment can be sorted into two groups (Figure 8-7). The first group includes the original FAME profile obtained before the perturbation initiated and the FAME profiles obtained when a high COD removal steady-state was re-established. The second group includes the FAME profiles obtained during the transient state and stressed metastable steady-state period. This group was further divided into two subgroups in which the first subgroup contains FAME profiles obtained from day 28 to day 110, and the second subgroup contains FAME profiles obtained from day 120 to day 311. The fact that two distinctive subgroups of FAME profiles existed during the metastable steady-state indicates that significant changes in the microbial population took place during this period.

The similarity coefficient (So) as well as the relative abundance of the saturated and branched fatty acids correlated well with COD removal efficiency (Figure 8-8). Similar

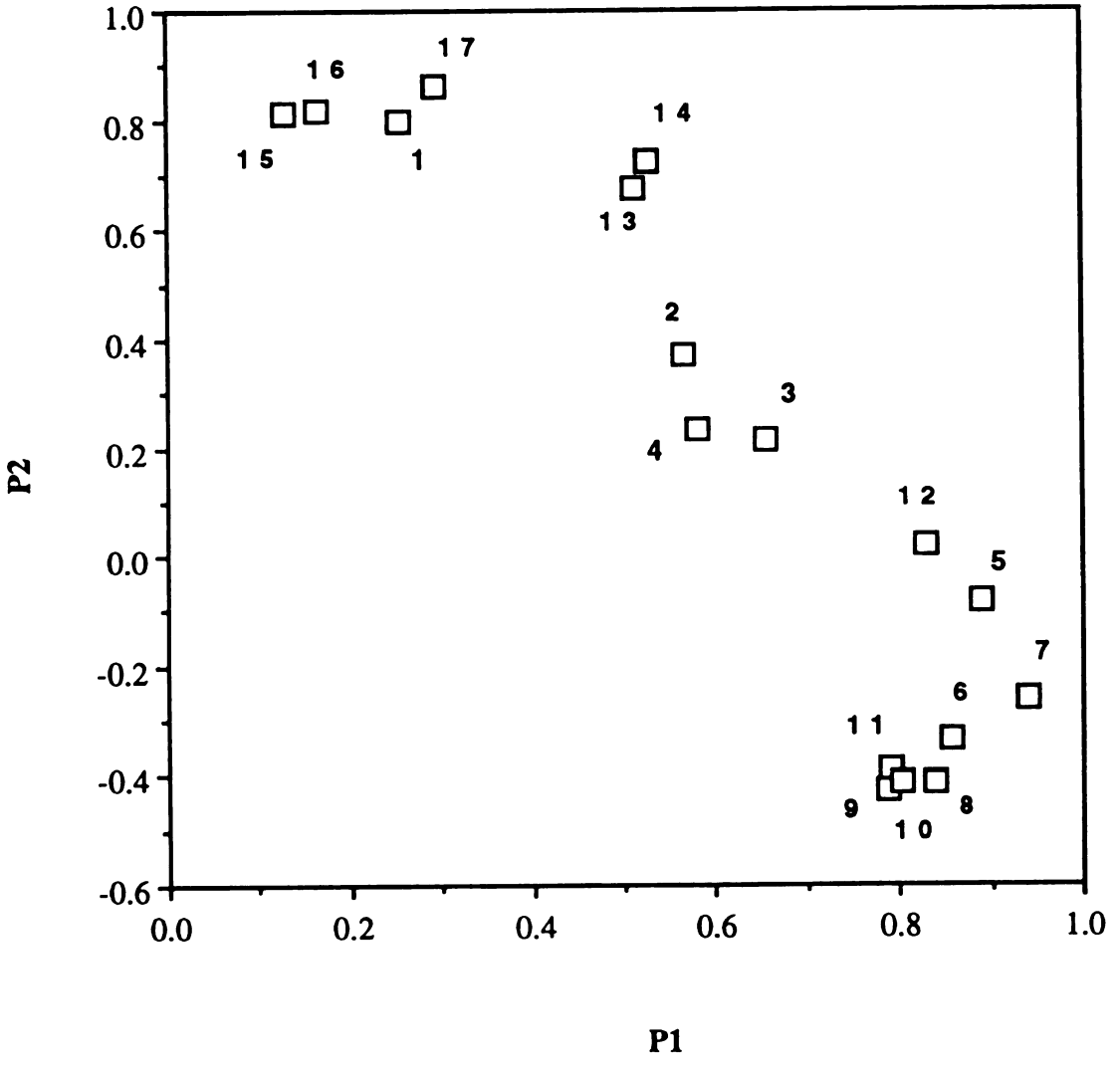

Figure 8-6. Principal-component analyses of the FAME profiles obtained from 3/3 day reactor populations.

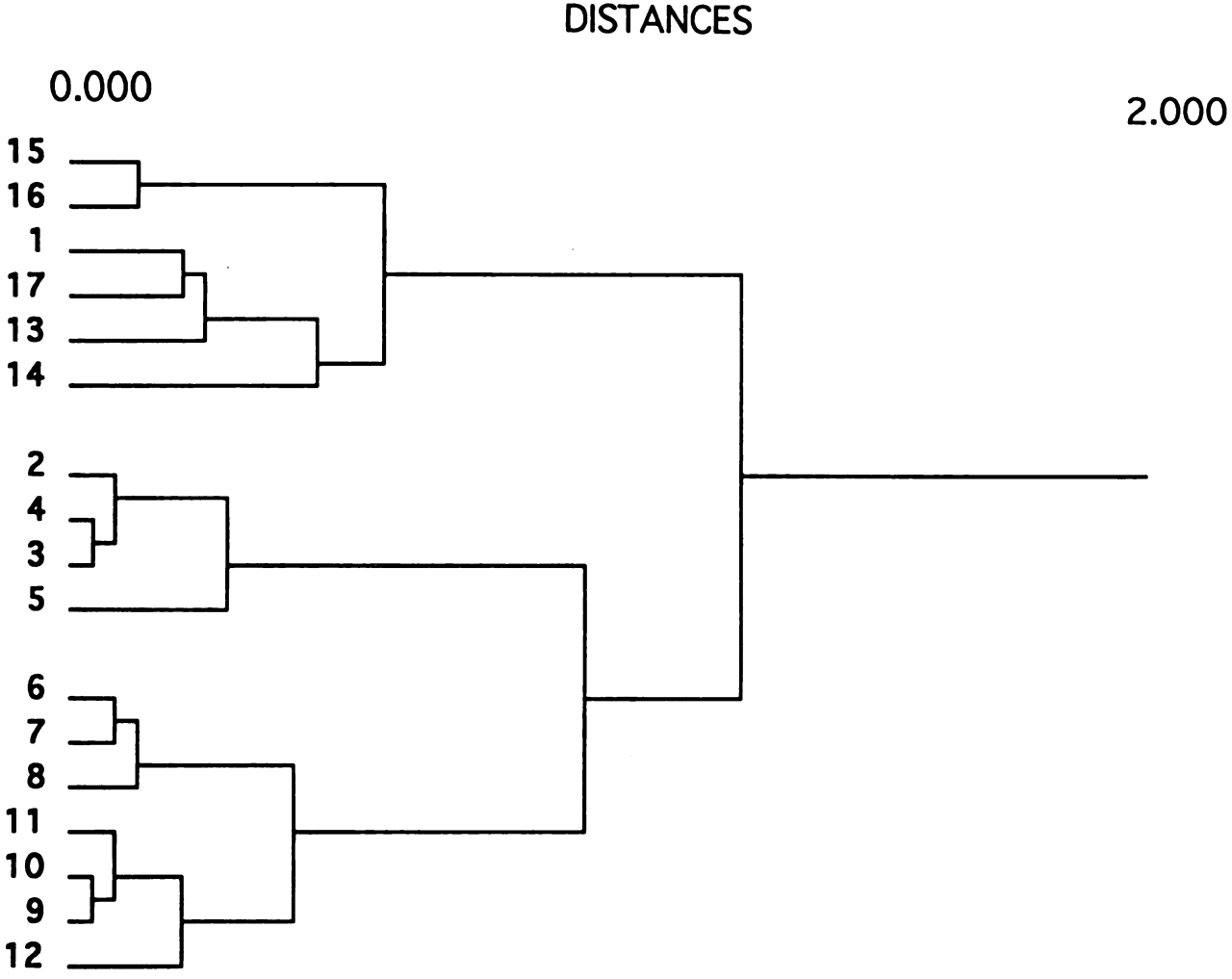

Figure 8-7. Clustering of the anaerobic reactor populations using the 1-Pearson correlation coefficient, single linkage method with FAME profiles obtained from 3/3 day reactor populations.

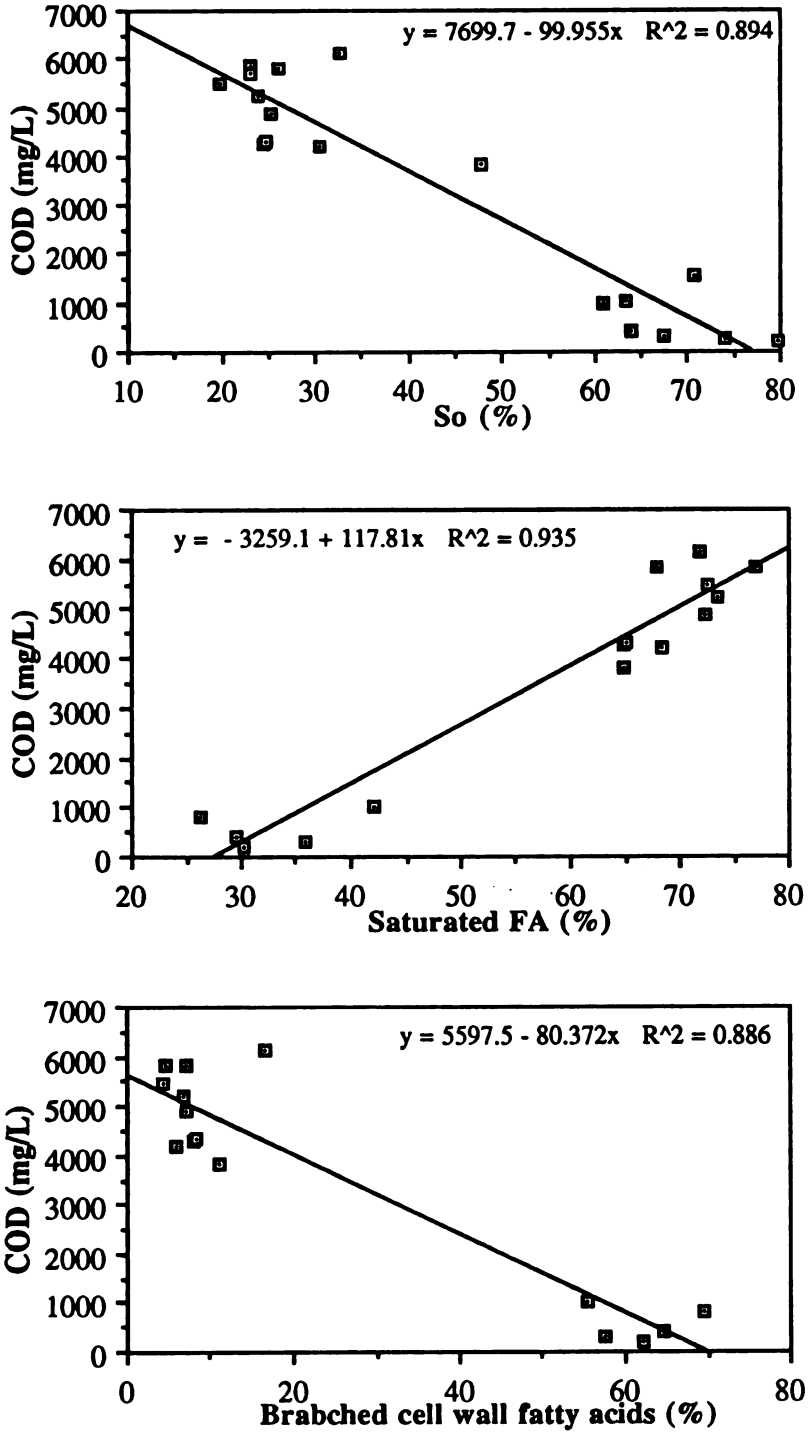

Figure 8-8. Correlation between the reactor effluent COD and the similarity coefficient So, the abundance of the saturated fatty acids and the branched fatty acids.

correlations also exist between So and the abundance of grouped membrane fatty acids as well as other operational parameters such as total effluent VFA, pH and average daily gas production (results not shown). These findings further confirm the feasibly of using FAME profiles as indicators of reactor operational performance.

2. Experimental results for the 5/5 day perturbation conditions

A shift in the predominant cell membrane fatty acids was observed during the 5/5 day substrate perturbation experiment (Figure 8-9). During the first 60 days, the abundance of the fatty acid a-15:0 (predominant prior to the perturbation was started) decreased significantly while the abundance of fatty acids 16:1 w7c and 16:0 concurrently increased. This dramatic change in the abundance of the major cell membrane fatty acids suggests that a population change occurred. The abundance of fatty acids, a-15:0 and i-15:0, subsequently increased steadily while cell wall fatty acids 16:1 w7c decreased rapidly. At day 100, fatty acids 16:0 and 14:0 suddenly increased in abundance, and the abundance of fatty acid a-15:0 stabilized. This sudden change in cell membrane fatty acids composition indicates another shift in community structure. The abundance of major cell membrane fatty acids returned to near pre-perturbation levels by around day 290.

The changes in microbial community that occurred in the 5/5 day reactor paralleled changes in the composition of the grouped cell membrane fatty acids (Figure 8-10). A dramatic change in the abundance of the saturated, branched and unsaturated cell membrane fatty acids occurred during the first 30 days. This coincided with a rapid accumulation of glucose fermentation intermediates. Subsequently, the composition of the grouped cell membrane fatty acids gradually returned to their original distribution. At day 80 another major community structure change took place, as indicated by the significant change in grouped cell membrane fatty acids.

Numerical analysis of FAME profiles also provides insight as to community changes in the 5/5 day anaerobic reactor. As illustrated by similarity coefficients referenced to the initial FAME profile, significant changes in microbial community occurred during the

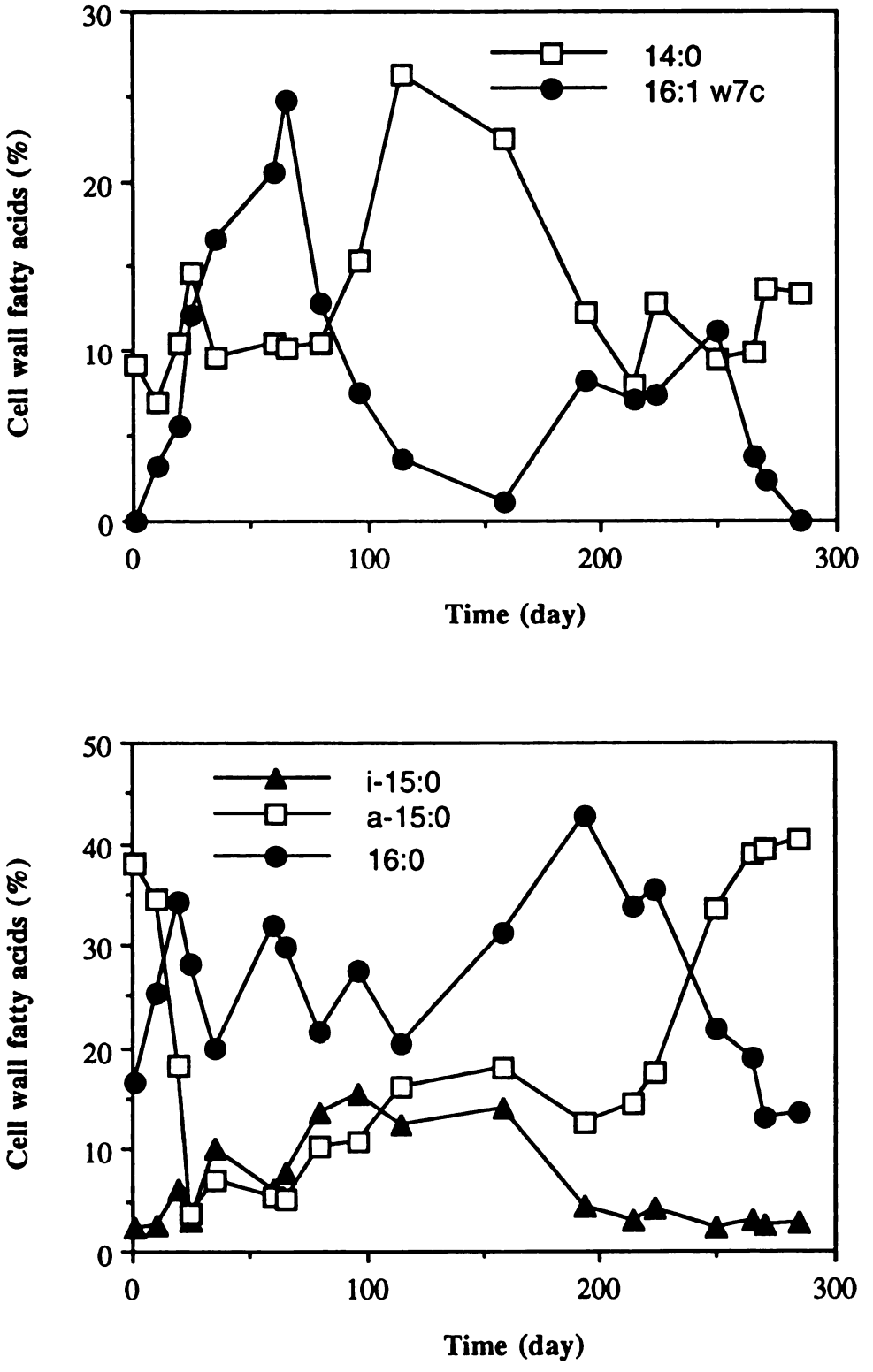

Figure 8-9. Changes in major cell membrane fatty acids abundance during the 5/5 day substrate perturbation period.

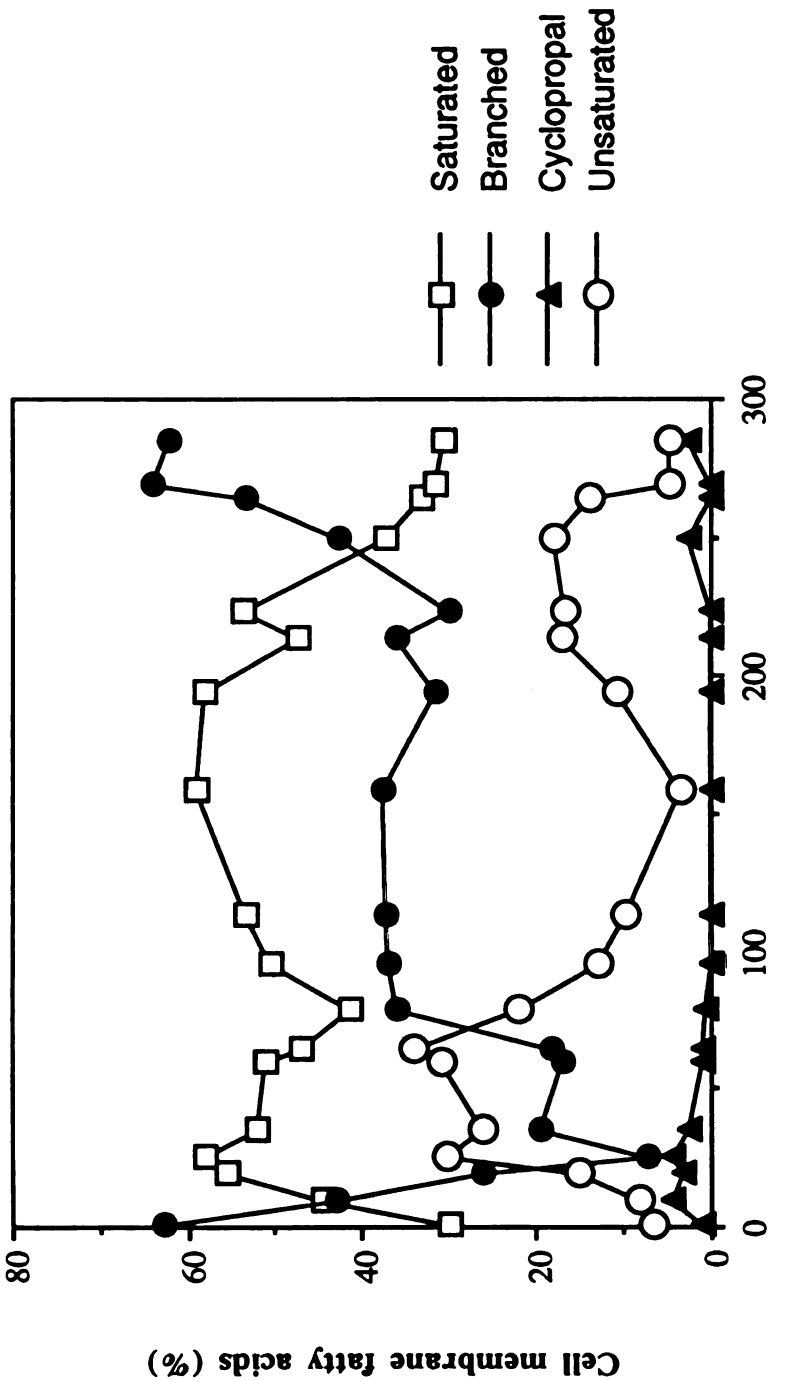

Figure 8-10. Changes in grouped cell membrane fatty acids abundance during the 5/5 day substrate perturbation period.

perturbation period (Figure 8-11). Principal component analysis separates the 5/5 day reactor FAME profiles completely in P1-P2 space (Figure 8-12). Cluster analysis sorted the 5/5 day FAME profiles into two distinct groups (Figure 8-13). The first group includes the FAME profiles at the beginning and end of the experiment. The second group is further divided into three subgroups which include all the other FAME profiles obtained during the substrate perturbation period.

The above FAME analysis results illustrate that eventhough effluent COD and VFA for the reactor subjected to 5/5 day perturbation conditions returned to pre-perturbation levels in a relatively short period (Chapter 6), the microbial community was not stable. Microbial community changes continued throughout the experimental period. This trend is reflected in the reactor effluent COD concentration. A significant cyclic fluctuation in effluent COD was observed throughout the experiment after "recovery" from the substrate perturbation.

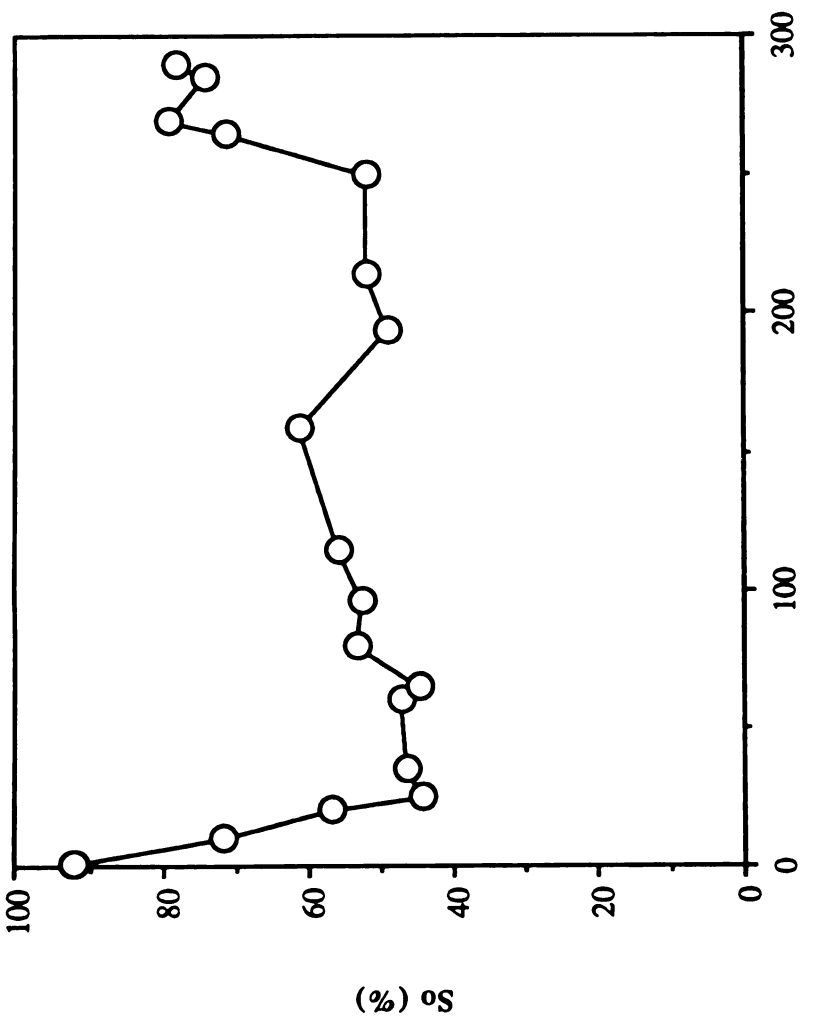

Figure 8-11. Changes in similarity coefficient So during the 5/5 day substrate perturbation period.

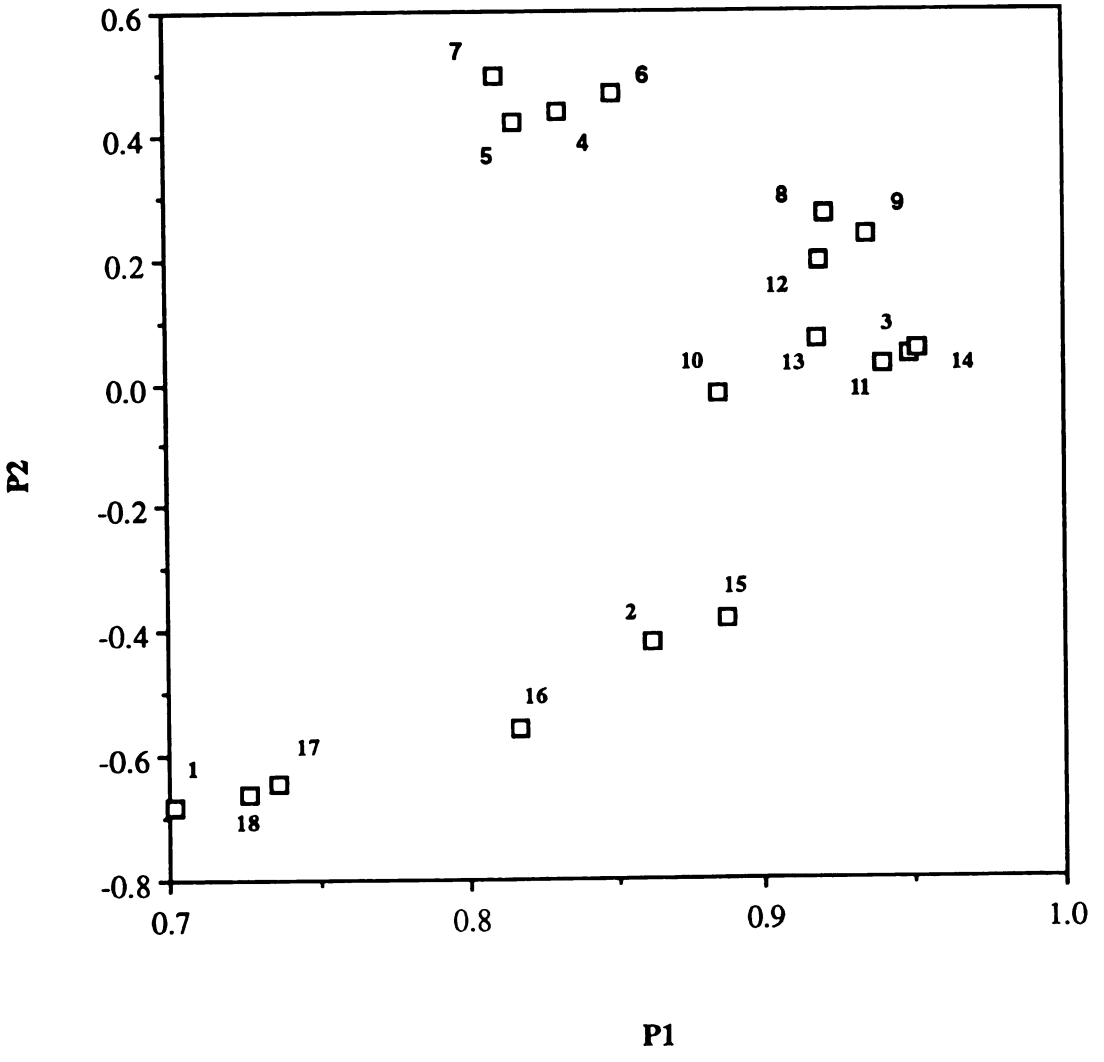

Figure 8-12. Principal component analysis of FAME profiles obtained from 5/5 day substrate perturbation experiment.

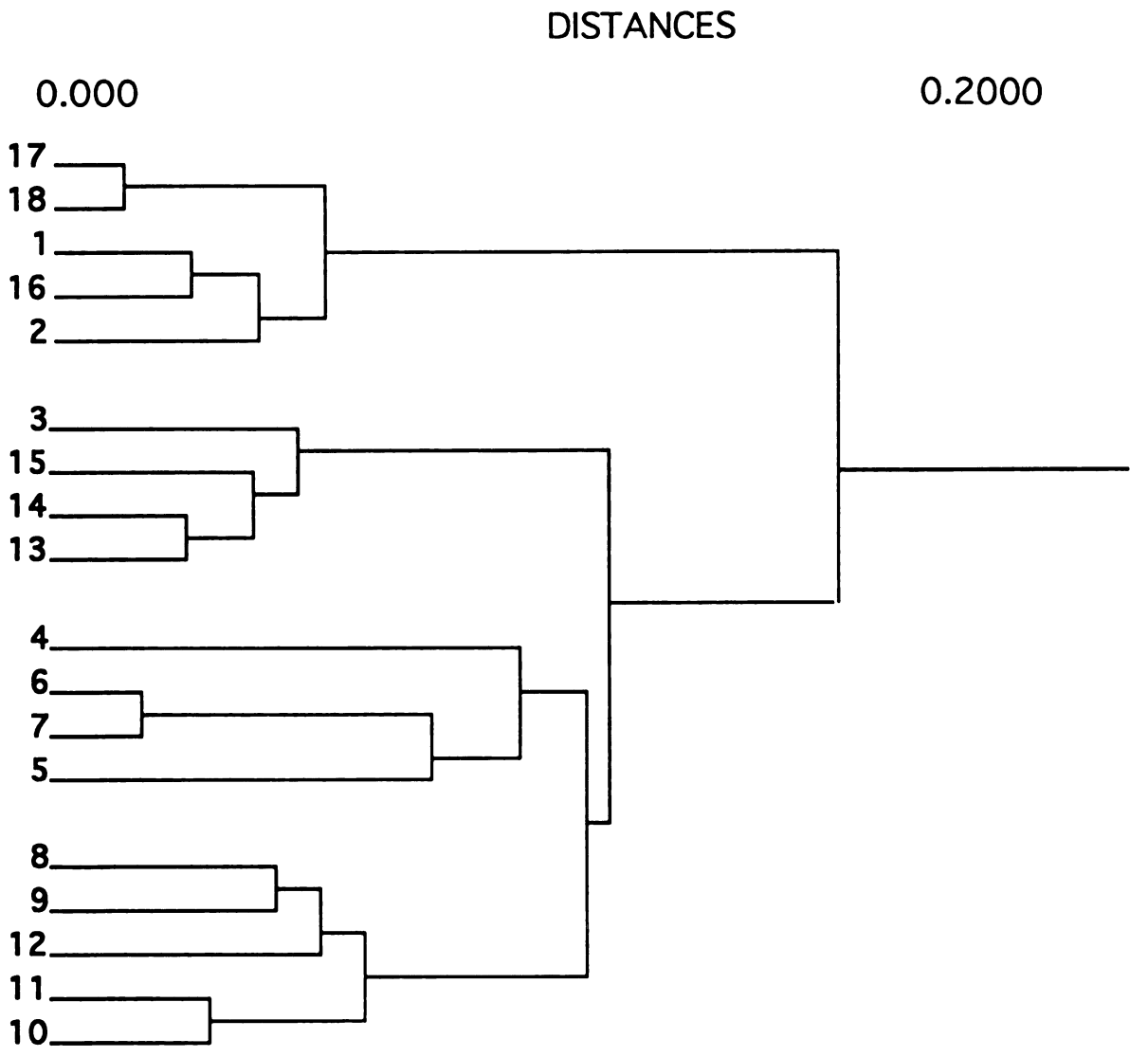

Figure 8-13. Clustering of the FAME profiles obtained from 5/5 day experiment using the 1-Pearson correlation coefficient, single linkage method.

8.3.4 Effects of starvation on FAME profiles

Changes that occurred in FAME profiles under starvation conditions were also investigated. Cultures taken from the mother and the re-established 1/1 day daughter reactors were placed in 158 ml anaerobic serum bottles and incubated at 35 °C without feed for 25 days.

During the starvation period only slight changes in the composition of the cell membrane fatty acids were observed in both the mother and the daughter reactor populations. The most noticeable changes in abundance of the cell membrane fatty acids were found to be 15:0, 16:0 and a-17:0 for mother reactor population while the most noticeable change in cell membrane fatty acids compositions were found to be i-14:0 3OH and i-19:1 for the 1/1 day daughter reactor population. In both cases these changes were negligible compared to the changes that occurred between steady-state and perturbed chemostat systems.

Results of the grouped cell membrance fatty acids illustrate that during the decay period the abundance of the saturated cell membrane fatty acids decreased slightly, while the branched cell membrane fatty acids increased slightly in both of the two anaerobic communities (Figure 8-14).

The similarity coefficients calculated based on the original FAME profiles indicate that changes in the microbial community that occurred during the starvation period in the mother and daughter reactor communities was slight (Figure 8-15).

The principal component analysis of the FAME profiles obtained during the starvation test also indicates that the changes caused by the starvation conditions were not significant for either the mother or the 1/1 reactor communities (Figure 8-16). Plotting the FAME profiles during the starvation period in the P1-P2 space, the two reactor populations could only be separated in the P2 axis which in this particular situation represents only 0.6% of the total variance (P1 represents 99% of the total variance in the FAME profiles). Based on the scattering range of the FAME profiles in the P1-P2 space, it also can be seen that

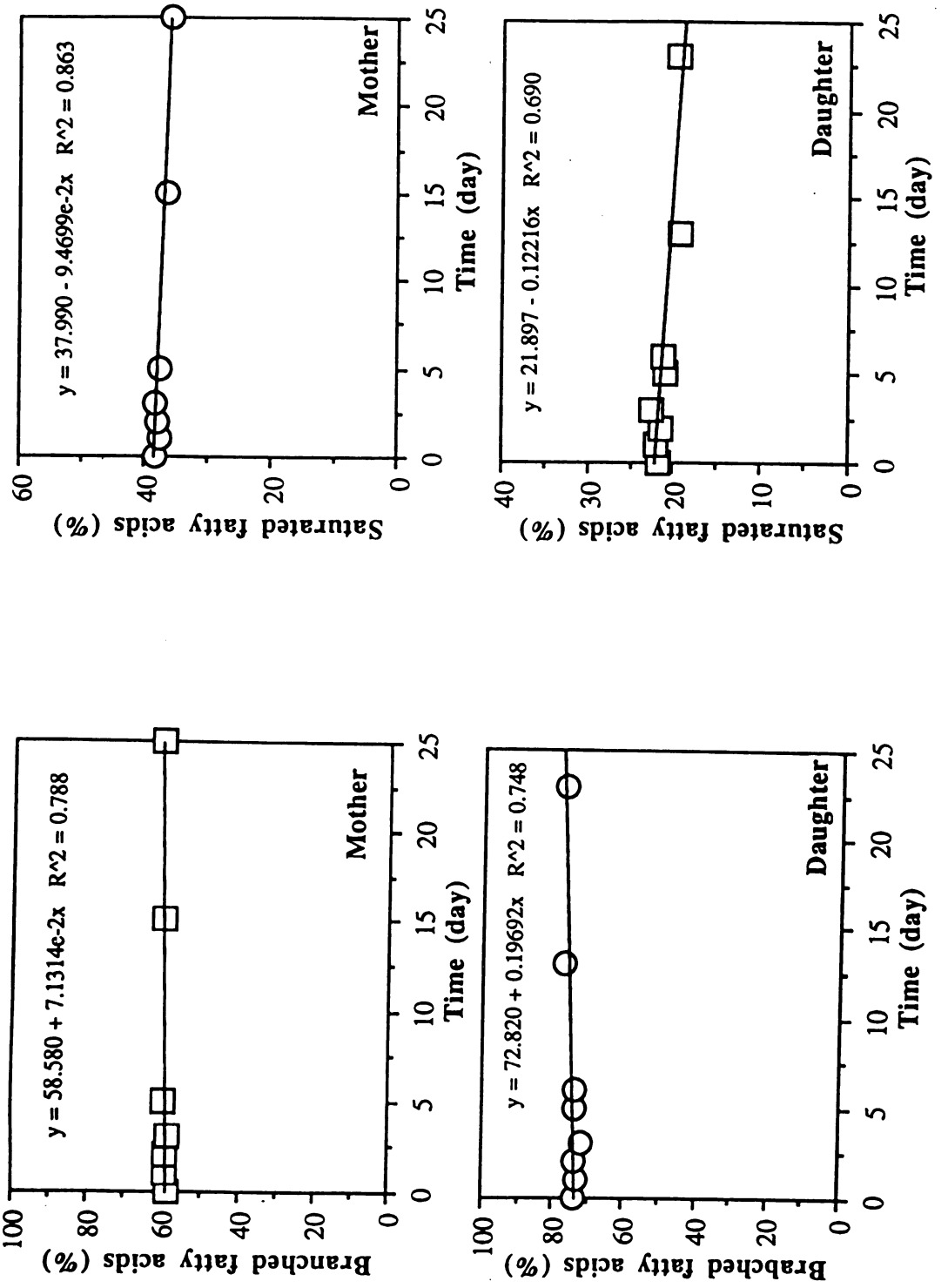

Figure 8-14. Changes in grouped fatty acids abundance during the starvation period.

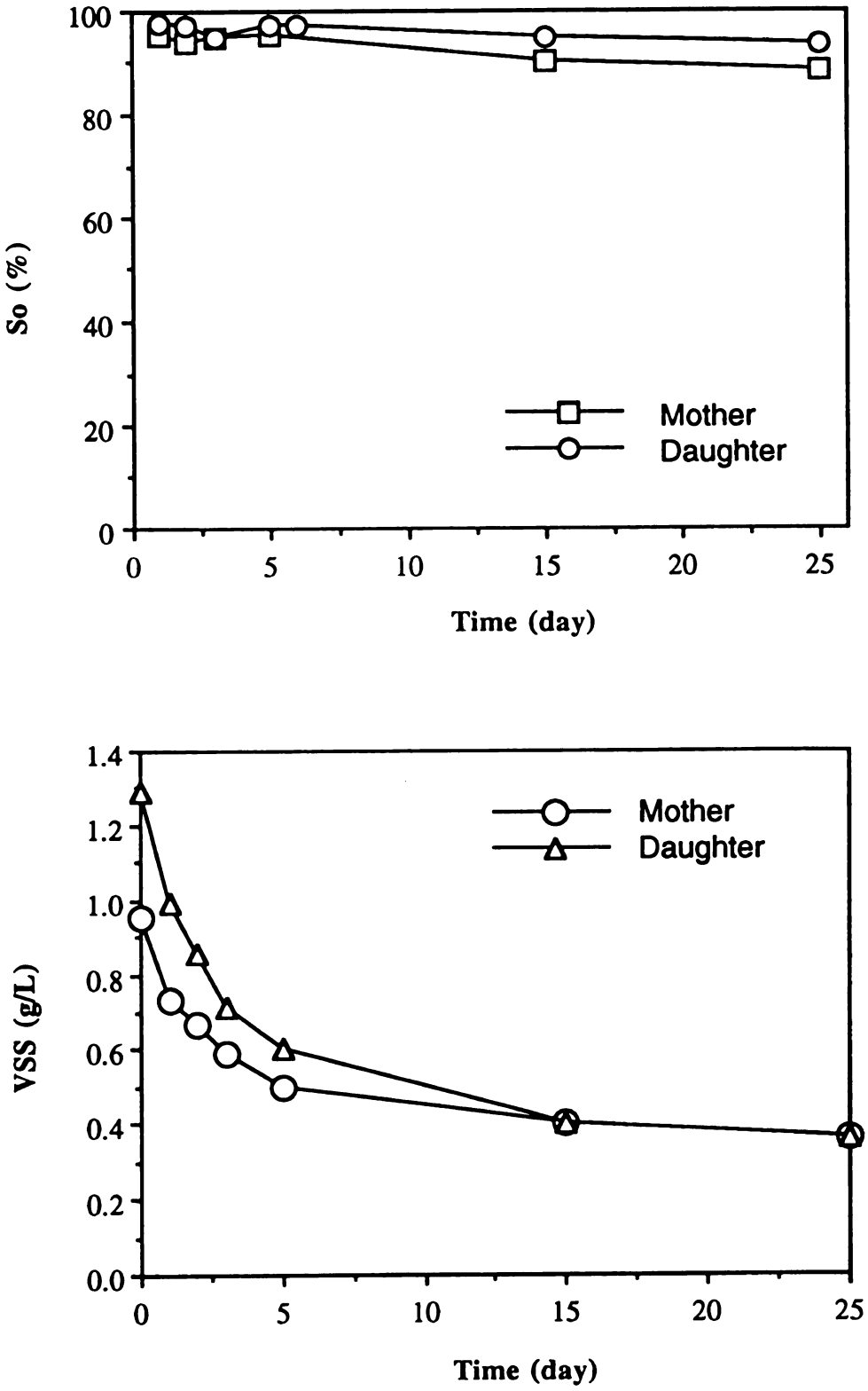

Figure 8-15. Changes in similarity coefficient So during the starvation period for the mother and the 1/1 day daughter reactor cultures.

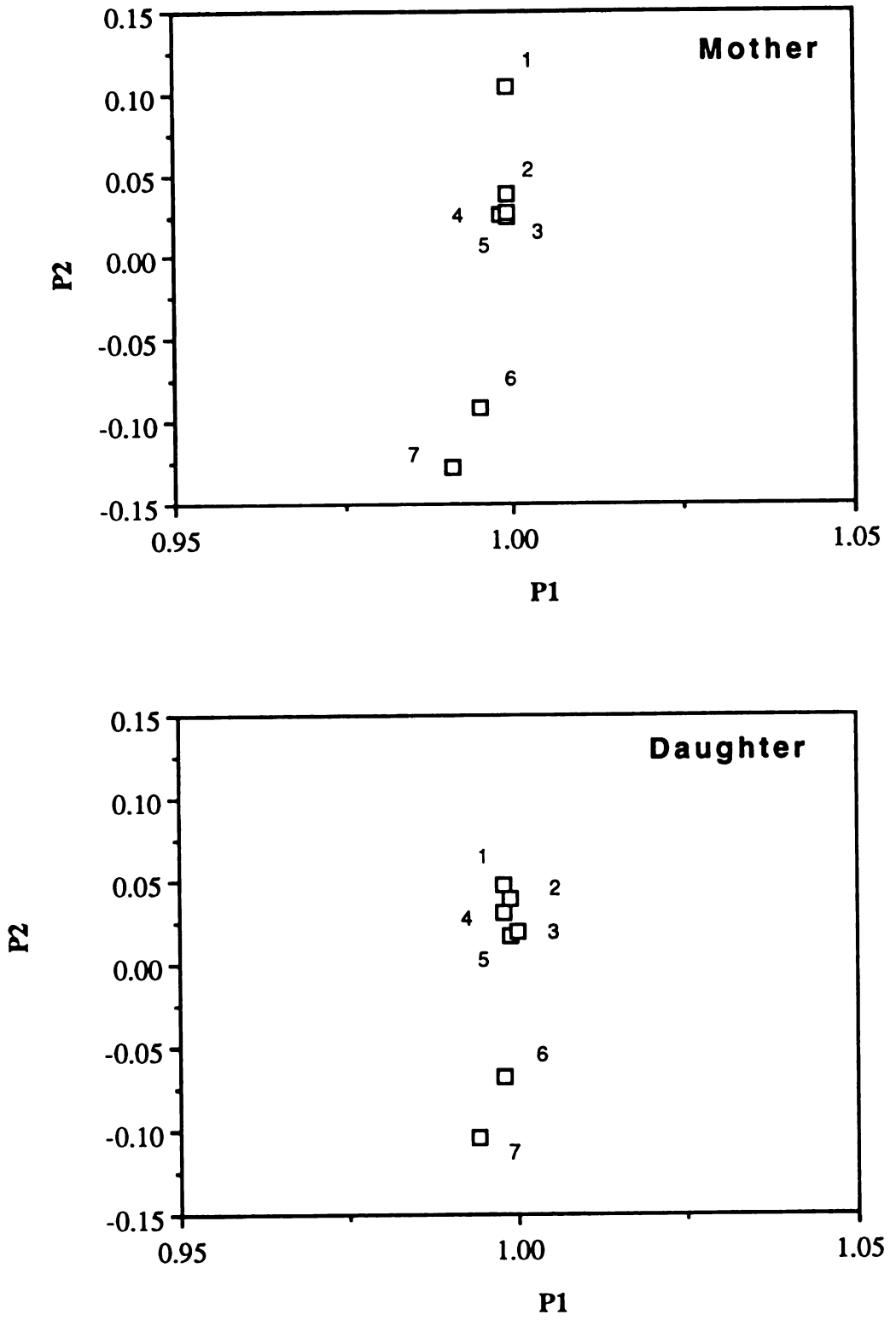

Figure 8-16. Principal component analysis results for the FAME profiles obtained during the starvation test.

during the starvation test a slightly larger change occurred in the mother reactor population.

8.3.5 Effect of shock loading on FAME profiles

The effect of shock loading conditions on FAME profiles were investigated using a constantly fed anaerobic reactor (m-1) and periodically fed daughter reactor 1/1. During this experiment, 6 grams of glucose was pulse injected into each of the two, 1.5 liter working volume anaerobic reactors while maintaining normal organic and hydraulic loading rates.

Significant changes were observed in the FAME profiles during the shock loading. The most remarkable changes were observed in the abundance of the individual cell membrane fatty acids 12:0, 15:0 and 17:1 in the constantly fed anaerobic reactor m-1. The most noticeable changes in the abundance of the individual cell membrane fatty acids in the 1/1 day daughter reactor were 13:1, a-15:0 and i-14:0 3OH (Figure 8-17).

The abundance of the total saturated, unsaturated and branched cell membrane fatty acids changed rapidly just after the initiation of the shock loading test (Figure 8-18). The largest changes in the abundance of the grouped cell membrane fatty acids occurred during the first few days, when dramatic changes in reactor glucose fermentation intermediates took place.

The similarity coefficients also reflected the changes in the microbial populations (Figure 8-19). The largest changes, as indicated by similarity coefficient (So), occurred in the first few days of the shock loading test for both anaerobic reactor populations. Based on the similarity coefficients obtained during the shock loading experiment more significant changes apparently occurred in the constantly fed anaerobic reactor population.

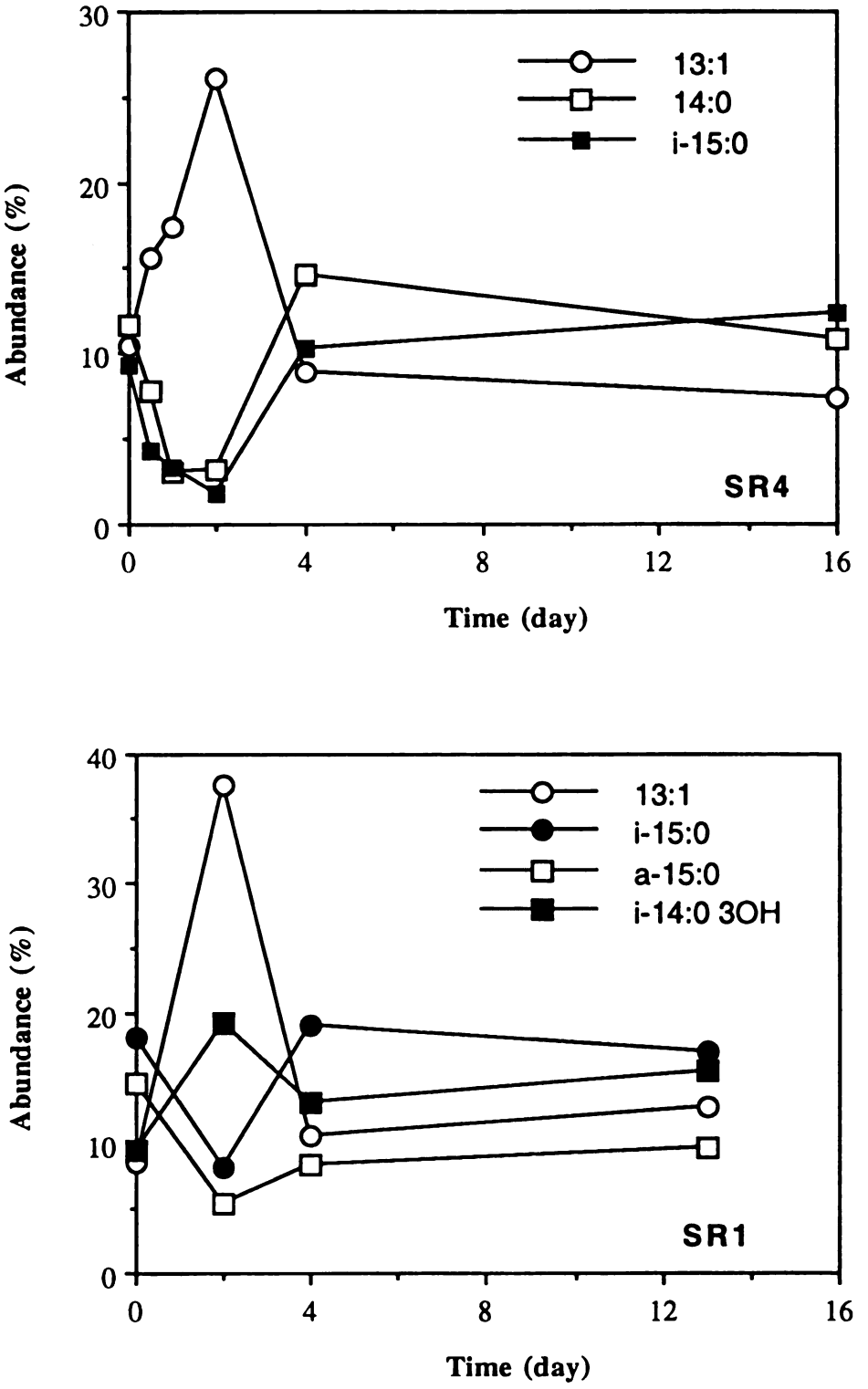

Figure 8-17. Changes in major cell membrane fatty acids abundance during shock loading experiment.

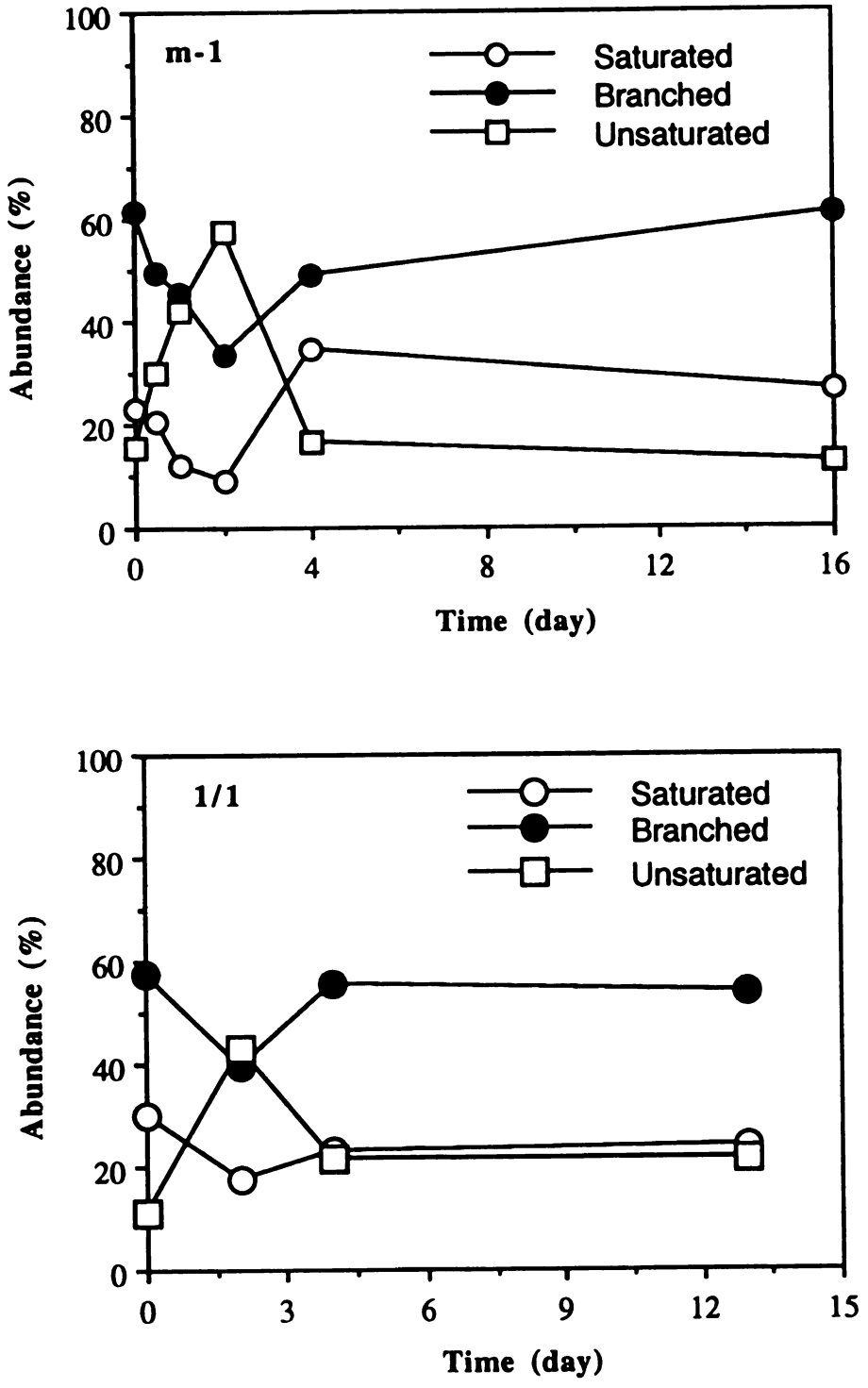

Figure 8-18. Changes in grouped cell membrane fatty acids abundance during the glucose shock loading test.

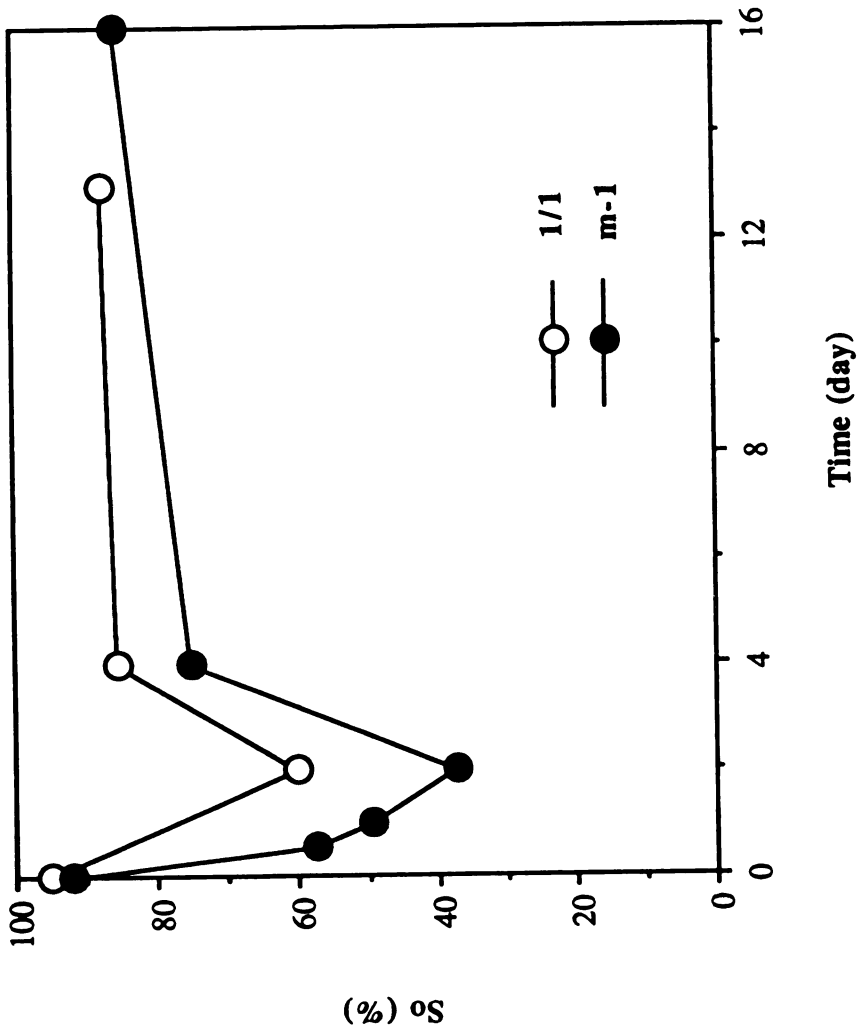

Figure 8-19. Similarity coefficient changes during the glucose shock loading test.

8.3.6 FAME analysis results for mother and 1/1 day daughter reactor MPN enrichments

In order to obtain FAME characteristics for the predominant species in each trophic group in the mother and the 1/1 daughter reactor (after steady-state was re-established) populations, MPN enrichments were analyzed. The MPN enrichments used for FAME analysis included glucose fermenting bacteria, butyrate- and propionate-utilizing acetogens, and hydrogen- and acetate-utilizing methanogens.

Due to the extremely low biomass concentrations in the MPN tubes, reliable FAME profiles were only obtained from the glucose fed MPN enrichments (Figure 8-20a). Both the mother and the daughter reactor FAME profiles, presented in Figure 8-20, came from the highest (10^{-9}) dilution glucose MPN tubes. In both these samples, the cultures appeared to be morphologically homogeneous. Although these two cultures in the glucose MPN enrichments cannot be morphologically distinguished, two different predominant fermentative bacteria did exist, as indicated by the results of FAME profiles. The major cell membrane fatty acids for the fermentative bacteria in the mother reactor MPN enrichment were 16:0 (51.4%), 16:1 w7c (14.7%), 14:0 (12.5%) respectively, while the major cell membrane fatty acids for the fermentative bacteria in the daughter reactor enrichment were 18:0 (33.3%), i19:0 (16.9%), 12:0 (16.6%), respectively. A low similarity coefficient value of 0.27 also indicated the significant difference between the two glucose fermentative populations.

The population difference indicated by FAME analysis was confirmed by the DNA analysis results. Cultures taken from the same glucose feed MPN tubes of the mother and the daughter reactors were directly used for polymerase chain reaction (PCR) amplification. The results of the Hpa II restriction endonuclease digest of 16S rRNA polymerase chain reaction (PCR) amplified from the glucose fed MPN tube cultures are shown in Figure 8-21. Population differences can be observed from the distinctive restriction fragment patterns for the two reactor MPN cultures.

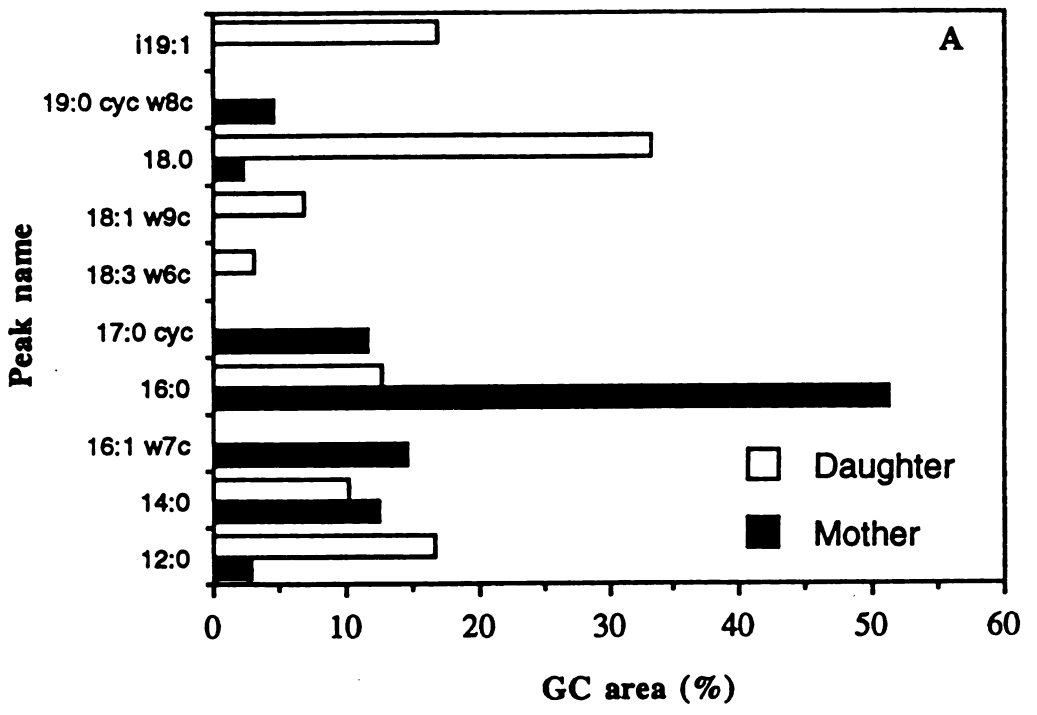

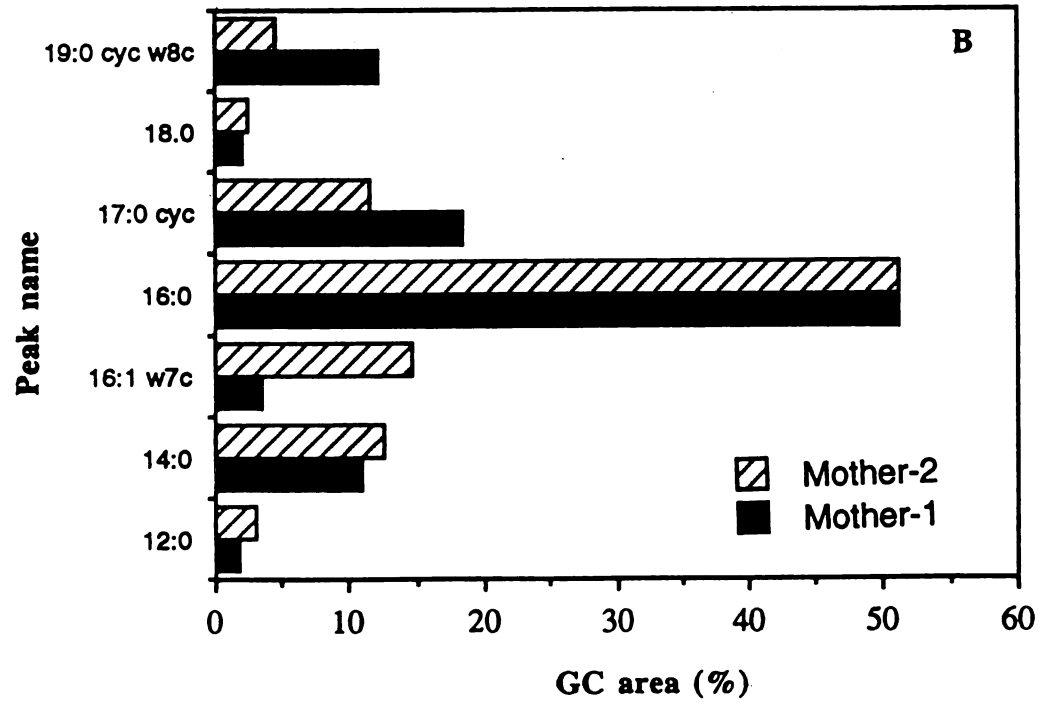

Figure 8-20. FAME profiles obtained from mother and 1/1 daughter reactor glucose MPN enrichment cultures.

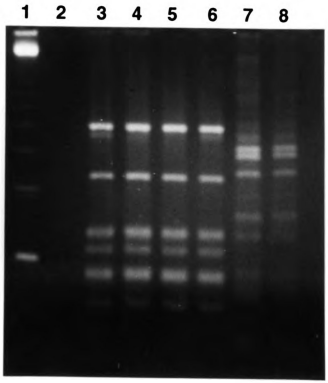

Figure 8-21. DNA analysis results for mother and 1/1 daughter reactor glucose MPN enrichment cultures. Lane 1, DNA standard (123 bp); lane 2 blank; lane 3 and 4, 10^{-7} dilution MPN tubes of the mother reactor; lane 5 and 6, 10^{-8} dilution MPN tubes of the mother reactor; lane 7 and 8, 10^{-7} dilution MPN tubes of the daughter reactor.

In contrast to the population difference observed between the mother and daughter reactor MPN enrichments, FAME profiles for the mother reactor glucose MPN enrichments from two independent MPN enumeration tests performed 8 months apart were quite similar (Figure 8-21b). A relatively high similarity coefficient value of 0.86 was obtained between these two samples. This result indicates that the predominant glucose fermentative population in the mother reactor was quite stable during the experimental period.

The above observations further confirmed the feasibility of using FAME profiles as indicator to identify or distinguish individual microbial species in the anaerobic systems.

8.4 DISCUSSION

Most of substrate perturbation experiments reported in the literature focus on anaerobic system response in terms of kinetics and operational performance, (i.e. in substrate degradation rate, accumulation of metabolic intermediates and changes in biomass concentration). Little is known about the effects of substrate perturbations on anaerobic microbial community structure. This is, in part, due to the lack of a reliable technique for monitoring of changes in microbial communities. Changes in anaerobic populations can not be effectively monitored or identified using ordinary analytical methods, such as microorganism isolation and incubation, microscopic observation or kinetic parameter evaluation.

This work establishes that the effects of environmental perturbations on microbial communities can be effectively investigated using FAME analysis. FAME analysis revealed community structure differences between the periodic feed daughter reactor and the control mother reactor communities and made it possible to monitor population changes during the entire perturbation period. In response to the periodic substrate perturbation, significant changes in microbial populations occurred in all the perturbed daughter reactor communities. This observation was in good agreement with other observations such as changes in COD and VFA concentrations, substrate degradation rates, microscopic examination and DNA analysis. For example, a solid correlation was observed between the similarity coefficient (So) or the abundance of the grouped cell membrane fatty acids and conventional reactor operational parameters, such as COD and total VFA concentrations.

The abundance of the saturated, branched and unsaturated cell membrane fatty acids were previously found to be a useful tool for the analysis of microbial community structure in aquifer and soil ecological systems (Guckert et al., 1986; Kaneda, 1991). Guckert et al. (1985) reported that the abundance of the grouped cell membrane fatty acids

were quite different among the marine sediments incubated under aerobic, facultative and anaerobic conditions.

During the present study, the abundance of the total saturated, unsaturated and branched cell membrane fatty acids was found to sensitively reflect the community structure changes in anaerobic reactor communities. Similarity in the abundance of the grouped cell membrane fatty acids was found in all the stable reactor communities. The abundance of the saturated, branched and unsaturated cell membrane fatty acids accounted to ca. 30%, 65% and 5% of the total cell membrane lipids under normal operational conditions. This ratio significantly changed during the unbalanced transient and metastable steady-state conditions indicating dramatic changes in the microbial communities.

FAME profile is known as a multivariant description of a viable microbial community structure (White, 1983). Each trophic group of bacteria usually has its own special composition and predominant cell membrane fatty acids (Ikemoto et al., 1978; Kaneda, 1991). The similar abundance of the grouped cell membrane fatty acids observed for the steady-state anaerobic populations illustrates that under given operating conditions, a certain microbial community structure is required to achieve effective glucose conversion to methane. To effectively carry out methane fermentation, the fermentative, acetogenic and methanogenic bacteria must work syntrophically, and sufficient organisms from each group (or guild) of bacteria must be present in the total community. Any significant changes in microbial composition will directly change the abundance of the grouped cell membrane fatty acids.

Theoretically, two different kind of population changes may occur in anaerobic systems. The first is the community structure changes caused by imbalance among different major trophic groups of anaerobic bacteria. The second is community structure changes resulting from a shift of predominant species within a major trophic group or guild of anaerobic bacteria. These two kinds of community structure changes may occur

individually or simultaneously. The first kind of changes can be easily observed using ordinary analysis methods because it is often accompanied by large changes in conventional operational parameters. The second type of change in community structure may not be easily observed by ordinary analysis. This is because a shift in the predominant species within the same trophic group may result in only slight changes in kinetics of substrate utilization.

Both of the above changes in community structure may be identified using FAME analysis. Considering the fact that each major group of anaerobic bacteria has its own unique abundance in grouped cell membrane fatty acids (Kaneda, 1991), large changes in abundance of the grouped cell wall fatty acids may indicate imbalance among the major trophic groups of anaerobic populations. On the other hand, changes in the abundance of individual cell membrane fatty acids, which do not largely change the abundance of the grouped cell membrane fatty acids, may indicate a shift in predominant species within the same trophic groups of the anaerobic communities. However, this speculation will need additional experimental verification.

The abundance of cyclopropyl fatty acids is a stress marker in many FAME related biosystem studies (Knivett and Cullen, 1965; Lepage et al., 1987; Hedrick, 1991). Hedrick (1991) reported that the abundance of the cell membrane fatty acid cyc 17:0 was much more variable in disturbed samples and was significantly greater in an overfed reactor population than in a healthy population. During an acetone-butanol fermentation study, Lepage et al., (1987) found that the abundance of cyclopropyl fatty acids considerably increased when the studied population was exposed to high concentration of solvents or cultivated under decreased temperature conditions. In the present study, a higher abundance of the cyclopropyl fatty acids was often observed during the transient stage of the substrate perturbations. At that time, the most significant change in environmental conditions and microbial population imbalance often took place. These

results indicate that the increased abundance of cyclopropyl fatty acids may also have some use as a stress marker for anaerobic reactor communities.

Results of FAME analysis obtained from the mother and the daughter reactor MPN enrichments show that FAME profiles can be used to distinguish changes within a trophic group in anaerobic systems. Considering the fact that the anaerobic community is composed of several specific sub-groups of fermentative, acetogenic and methanogenic bacteria and that each group of bacteria may possess its own unique composition of cell membrane fatty acids, then mathematical analysis of anaerobic microbial communities should be possible if the FAME composition (the fingerprint of anaerobes) can be obtained for the predominant anaerobic microorganisms present in specific metabolic groups.

Procedures for numerical FAME profile analysis have been developed and verified in this experiment for effective study of microbial population changes in the anaerobic reactors. One of the major advantages of using numerical methods to treat raw FAME data is that quantitative comparisons of the individual microbial communities can be performed. By this method, the information contained in the raw FAME profiles can be more accurately interpreted and represented for further analysis. This essentially avoids subjective error and uncertainty resulting from using "vassal" or other semi-empirical methods for FAME data interpretation. This was verified by using the similarity coefficient (So), clustering and principal component analysis methods to treat FAME profiles. Highly consistent conclusions were reached using these three different numerical treatments of the same FAME profiles.

Clustering analysis results indicated that perturbed anaerobic communities underwent several different structural changes. Clear evidence has been visually presented, using principal-component analysis, that the perturbed microbial communities tend to return to their original steady-state composition after adaptation to the environmental perturbation.

This is reasonable because only under conditions where the substrate supplied to the anaerobic community can be completely metabolized does the maximum free energy become available for the entire anaerobic community. This is likely the major driving force for the disturbed anaerobic system to return to its steady-state (or attractor) condition. Through principal component analysis, it has also been observed that a zone of "good health" apparently existed in the P1-P2 space which was valid for all the anaerobic reactor populations examined in this study. This zone will likely change to some degree depending upon the substrate fed to the system. This was not examined herein.

Although FAME analysis cannot answer all experimental questions regarding anaerobic reactor microbial community structure changes and operational performance, it does represent an additional set of tools for studying the anaerobic systems. Based on the findings in this work, FAME analysis can be effectively used to identify and monitor anaerobic reactor population community structure changes. If enough steady-state baseline information has been obtained to develop comparison standards (the "heath zone" in P1-P2 space, the "heath ratio" of the abundance of grouped cell wall fatty acids, ect.), it may be possible to use FAME profiles to assess anaerobic reactor operational performance. Analysis techniques for FAME profiles can obviously be extended for use in other biological treatment systems.

This is reasonable because only under conditions where the substrate supplied to the anaerobic community can be completely metabolized does the maximum free energy become available for the entire anaerobic community. This is also the major driving force for the disturbed anaerobic system to return to its steady state for sustaining condition. Through principal component analysis, it has also been observed that a zone of "good health" appeared existed in the P1-P2 space which was valid for all the anaerobic reactor populations examined in this study. This zone will likely change to some degree depending upon the substrate fed to the system. This was not examined herein.

Although PAME analysis cannot answer all experimental questions regarding anaerobic reactor microbial community structure changes and operational performance, it does represent an additional set of tools for study the anaerobic systems. Based on the findings in this work, PAME analysis can be effectively used to identify and monitor anaerobic reactor population community structure changes. If enough steady-state baseline information has been obtained to develop comparison standards (the "heath zone" in P1-P2 space, the "heath ratio" of the abundance of syntrophs cell wall fatty acids, ect.), it may be possible to use PAME profiles to assess anaerobic reactor operational performance. Analysis techniques for PAME profiles can obviously be extended for use in other biological treatment systems.

8.5 SUMMARY

Cell membrane fatty acids are widely studied group of lipids with sufficient taxonomic diversity that can be used in defining microbial community structure. Experimental results presented in this chapter illustrate that FAME analysis can be successfully used as a tool to identify and monitor microbial community structure changes in anaerobic reactors.

The abundance of the grouped cell membrane fatty acids was an important indicator of changes in anaerobic reactor community structure and reactor performance. A relatively stable "health" ratio among these grouped cell membrane fatty acids exist under specific operational conditions. Large changes in these ratios indicated community structure changes which were related to unbalanced operational performance.

Using numerical analysis methods, the information contained in the raw FAME profiles can be more accurately and quantitatively interpreted and used for identifying and monitoring microbial community structure changes. By using principal-component analysis it is possible to "visually" trace microbial community structure changes in the P1-P2 space. Based on comparison with other operation parameters, a 'health' zone can be established in the P1-P2 space. In this manner, FAME profiles can be used to graphically ascertain whether the reactor is operating well or not.

The microbial community structure changes illustrated by FAME analysis were in good accordance with other experimental observations such as chemical-physical, kinetic, genetic and morphological analysis results.

Chapter 9

CONCLUSIONS AND ENGINEERING SIGNIFICANCE

A. Conclusion

1. The microbial communities from steady-state anaerobic chemostats were sensitive to an applied periodic substrate feeding pattern. The rapid accumulation of glucose fermentation intermediates indicates an apparent decrease in the number or activity of methanogens during the transient and metastable steady-state periods.

2. The acetate-utilizing methanogens were seriously affected by the periodic substrate feeding pattern. Under the 1/1 and 3/3 day perturbation conditions, extremely long recovery times were observed for the acetate-utilizing methanogens. Experimental results suggest that in addition to the inherent slow growth rate of the acetate utilizing methanogens, pH related un-ionized VFA inhibition may be partially responsible for the protracted period required for the anaerobic communities to adapt to the 1/1 and 3/3 day perturbation conditions.

3. Through a long-term adaptation, the acetate-utilizing methanogens apparently acquired the ability to effectively metabolize acetate at pH as low as 5.9 to 6.2 and VFA concentration up to ca. 4,000 mg/L (as acetate), a level that was highly inhibitory for the original acetate-utilizing methanogens.

4. H_2-utilizing methanogens were impacted by the periodic substrate perturbations, especially under 1/1 and 3/3 day perturbation conditions. However, the adaptation time for the hydrogen-utilizing methanogens was relatively quick compared to that of the acetate-utilizing methanogens.

5. The fermentative bacteria were affected by the periodic substrate perturbation with dramatic changes in the glucose fermentation pathway. Under elevated hydrogen partial pressure, the electrons flowing through the propionate fermentation route increased from less than 5 percent to ca. 40 percent, indicating that the fermentative bacteria responded to the environmental changes by quickly shifting the pathway of fermentation to maximize free energy under the altered environmental conditions.

6. A cyclic and alternating accumulation of acetate and butyrate was observed during the 3/3 day perturbation test. Results of thermodynamic calculations indicate that accumulated acetate reduced the available free energy to levels at which anaerobic oxidation of butyrate could not proceed. Once acetate concentrations decreased and butyrate concentrations increased, the cycle reversed, and acetate accumulated.

7. The anaerobic systems did gradually adapt to the periodic substrate perturbations through changes in the microbial communities as evidenced by changes in kinetics of substrate utilization, FAME and DNA analysis and morphological observations.

8. The populations that became established in the 1/1 and 3/3 reactors could maintain long-term stable and effective operation. One of the reactors (1/1) was evaluated to assess its resistance to environmental impact. This reactor community appeared to be more resistant to environment shocks, such as pulse organic loading and a short term temperature decrease, compared to the control mother reactor community.

9. The perturbation interval is an important control parameter for anaerobic chemostat systems operated under periodic feeding conditions. It can directly affect recovery and operational stability of the perturbed anaerobic systems. Based on results of this study, stable communities can likely only be established and maintained for a certain range of perturbation intervals.

10. FAME analysis can be effectively used as a tool to identify and monitor changes in anaerobic microbial communities. Using numerical analysis methods, the information contained in raw FAME profiles can be accurately and quantitatively interpreted for comparison of microbial communities.

11. Well controlled periodic substrate perturbations can be used as a tool to improve operational performance and robustness of anaerobic systems..

b. Engineering importance of this study.

Many perturbation experiments have been performed to investigate the response of anaerobic systems to increased organic loading rate and other environmental shocks. These experiments have mainly focused on inhibitory effects, recovery processes and thermodynamic changes that resulted from the perturbations. In this sense, environmental perturbations, on engineered biological systems, are usually considered as having only negative effects. The results of this study, however, suggest potential benefits of perturbations on engineered systems. For example, others have reported a tendency toward gradually increased maximum substrate utilization rates when an anaerobic system was subjected to successive shock loadings (Cohen, et al., 1982). Although perturbation results often indicated microbial community changes (Harper and Poland, 1985; Fongastitkul, 1994), little effort was directed at evaluating the effects of environmental perturbations on microbial communities.

This study demonstrates that anaerobic communities can be selected or "optimized" by well controlled periodic substrate perturbations. Controlled substrate perturbations can therefore be used as a tool to improve operational performance and robustness. Substrate perturbations can create "hostile" or harsh environmental conditions. This can break down the existing dynamic balance among the specific trophic groups (guilds) of the anaerobic community. Only the "robust" species which possessed or can develop the requisite ability for survive are retained under such conditions. Less competitive species, which may dominate the original community will eventually be eliminated or their population size reduced. Long-term periodic substrate perturbations selected for these populations possessing higher substrate utilization capacities. Periodic substrate perturbations also changed fermentation intermediate distribution, resulting in more stable microbial

communities. The adaptive communities are better able to cope with unfavorable environmental changes.

The above observation has ecological and engineering implications. Unlike microbial communities in nature which are always exposed to unstable environments (and are subjected to natural selection thereby), microbial communities in engineered biological systems are for most part developed and maintained under carefully controlled, steady-state conditions. Operational conditions in engineered biological systems are controlled so that the microbial communities can achieve "optimum performance", but, paradoxically, this practice may result in the selection of population with reduced ability to cope with unfavorable environmental conditions, such as temperature drop, pH change, pulse loading and other impacts resulting from operational errors. The situation is worse for anaerobic populations due to the inherent slow growth rates possessed by the key microorganisms in these systems. Results presented in this thesis suggest that properly controlled perturbations might be used to select for robust populations to replace "idle" or less competitive ones and to keep the population "strong" and "vigorous". This method might be viewed as an ecological method or technique to distinguish itself from other physical, chemical or biological methods which used to improve biological system operational performance.

This new operational strategy is, obviously, not only applicable for anaerobic chemostats. Through more experiment and practice, its application can be expected to benefit other biological treatment systems.

Chapter 10

RECOMMENDATIONS FOR FUTURE RESEARCH

. Perform long-term periodic substrate perturbations under pH controlled conditions to investigate the extent of the effect of the perturbation with the role of pH eliminated, and to observe adaptation and the resultant population changes.

. Isolate and identify predominant microorganisms in each individual subgroups of the mother and the daughter reactor populations during different stages of the perturbation. This will allow better understanding of the microbial community changes during the perturbation periods.

. Determine if a unique microbial community is established under given perturbation conditions by simultaneously initiating perturbations on replicate anaerobic reactors under identical conditions.

. Examine the response of periodic substrate perturbations on other anaerobic systems such as UASB or anaerobic FBR which are often employed for full-scale anaerobic treatment.

. Conduct pilot or full scale substrate periodic feeding experiment. Before use of periodic substrate feeding as a practical operational strategy, a pilot or full scale experiment should be performed.

APPENDIX A

APPENDIX A

GENERAL ANALYTICAL METHODS

1. Sample collection and storage

Gas samples were taken from the reactor gas sampling port using 1,000 µl Unimetrics gas-tight valve syringes (Unimetrics Corp., Shorewood, IL) equipped with 25 gauge needles, and were analyzed immediately after taken from the reactor.

Liquid samples were withdrawn from the reactor liquid phase using 10 ml syringes equipped with 22 gauge needles, centrifuged using a Hermle compact centrifuge (Model Z203, National Labnet Co., Woodbridge, NJ) at 3,500 x g for 10 minutes, and either analyzed immediately or frozen at -35 °C and stored for further analysis.

2. Analytical methods

i. COD, pH, SS, VSS and alkalinity

Chemical oxygen demand (COD), pH, suspended solids (SS), volatile suspended solids (VSS) and alkalinity were determined in accordance with procedures from Standard Methods for the Examination of Water and Wastewater (APHA, 1989).

COD was analyzed using Hach COD glass vials and a Hach COD reactor (Model 45600 Hach Company, Loveland, CO). The COD values of the digested samples were determined using the ferrous ammonium sulfate titration method.

pH was measured using an Orion Model 720 pH meter equipped with an Orion glass Ag/AgCl combination pH electrode (Orion Research Inc., Boston, Ma).

SS were analyzed using 0.45 µm glass fiber filtration disc (Whatman International Ltd, Maidstone, England). VSS were determined by ignition in a muffle furnace at 550 °C.

ii. Volatile fatty acids

Volatile fatty acids (acetate, propionate, butyrate and iso-butyrate) and ethanol were measured using a Perkin-Elmer 8700 GC (Perkin-Elmer Co., Palo Alto, CA) equipped with a flame ionization detector (FID). VFAs and ethanol were separated at 125 °C using GP 10% SP-1200/1% H_3PO_4 on 80/100 Chromosorb in a glass column (6' x 2 mm ID) using nitrogen (50 ml/min.) as a carrier. The temperature of injector and detector were 180 and 250 °C respectively. After centrifuged at 3500 g for 10 minutes, the supernatant was acidified using concentrated H_3PO_4 (1/20, vol. acid/sample). Injection volumes were 0.1 to 0.4 ul depending on sample concentration.

iii. Methane and carbon dioxide

Methane and carbon dioxide were determined using a Varian model 3700 GC (Varian Associates Inc., Norwalk, CT) equipped with a thermal conductivity detector (TCD). CH_4 and CO_2 were separated at 130 °C on 80/100 carbonsphere in a stainless steel column (6' x 1/8" ID) using helium (40 ml/min.) as a carrier. The temperatures of the injector and detector were 180 and 250 °C, respectively. An injection volume of 0.2 ml was used for all analyses.

iv. Gas phase hydrogen partial pressure

Gas phase hydrogen partial pressure was measured using a RGA3 Reduction Gas Analyzer (Trace Analytical, Menlo Park, CA). The reduction gas detector was operated at temperature of 265 °C with 30 ml/min of helium as carrier gas. The reaction bed temperature was 90 °C. An injection volume of 1 ml was used for all analyses.

v. Optical density

The optical density of anaerobic reactor culture was determined by using a Perkin Elmer LAMBDA 6 UV/VIS spectrophotometer (Perkin-Elmer Co., Palo Alto, CA) at waveleght of 650 nm against DI water.

vi. C, H, N elemental contents

The elemental contents of biomass carbon, hydrogen and nitrogen were determined by using a P-E 2400 CHN elemental analyzer equipped with a P-E AD-4 Ultramicrobalance (Perkin-Elmer Co., Norwalk, CO).

APPENDIX B

APPENDIX B

MPN ENUMERATION METHOD

The five tube per dilution MPN method (APHA, 1989) was used to estimate the population distribution in the anaerobic reactors. Glucose-fermenting bacteria, propionate- and butyrate-utilizing acetogenes, and acetate- and H_2-utilizing methanogens were examined.

1. Medium and substrate preparation

a. Phosphate buffered basal media (PBBM) composition

NaCl	2.7 g
$MgCl_2$. $6H_2O$	0.6 g
$CaCl_2.2H_2O$	0.3 g
NH_4Cl	3.0 g
Resazurin solution	3 ml
trace mineral II	30 ml
Double distilled water	3000 ml

After dissolving the above chemicals in D. I. water, the media solution pH was adjusted to 7.2 - 7.4 by adding 4 N NaOH or 4 N HCl.

b. Amount of substrate solutions

10% Glucose solution	100 ml
1 M Propionate solution	100 ml
1 M Butyrate solution	100 ml
1 M Acetate solution	100 ml

c. Stock chemical solutions:

(1) 10% sodium bicarbonate solution

10 g $NaHCO_3$ dissolved in 100 ml DI water.

(2) Vitamin solution

The vitamin solution used in this study was adopted from Wolin *et al.* (1963). It contained (mg /1000 ml DI water):

Biotin	2
Forlic acid	2
Pyridoxine-HCl (B6)	10
Thiamine-HCl (B1)	5
Riboflavin (B2)	5
Nicotinic acid	5
Pantothenic acid	5
Cyanocobalamin (B12)	0.1
P-aminobenzoic acid (PABA)	5

The above compounds were added in the listed order to ensure complete dissolution. The solution was then filter sterilized (0.25 μm filter) and stored in vacuum and N_2 gas flushed, and autoclaved serum bottles.

(3) 2.76 M phosphate buffer solution:

Dissolve 15 g KH_2PO_4 and 29 g K_2HPO_4 in 100 ml DI water.

(4) 2.5% $Na_2S{\cdot}9H_2O$ solution:

Sulfide solution was prepared under an oxygen free N_2 atmosphere. Double distilled water was boiled for 15 min in a flask under N_2 gas atmosphere and cooled for 5 min. Subsequently, 25 g of $Na_2S{\cdot}9H_2O$ crystal were transferred into the flask containing 1,000 ml DI water and dissolved by stirring. After the solution had cooled to room temperature (25 °C), concentrated HCl was used to adjust pH to 9.5 under a N_2 atmosphere.

(5) Trace metal solution, it contained (g/1000 ml):

$FeCl_2 \cdot 4H_2O$	1.5
$ZnCl_2$	0.07
$MnCl_2 \cdot 4H_2O$	0.1
H_3BO_3	0.06
$CoCl_2 \cdot 6H_2O$	0.19
$CuCl_2 \cdot 2H_2O$	0.002
$NiCl_2 \cdot 6H_2O$	0.024
$Na_2MoO_4 \cdot 2H_2O$	0.36
HCl (12N)	6.4 ml

The $FeCl_2 \cdot 4H_2O$ was first dissolved in the HCl, then this solution was mixed with 950 ml DI water. Subsequently all the other salts were dissolved into this solution. pH was adjust to 6.0 with 1 N NaOH. Final solution volume was adjusted to 1 L with deionized water.

Substrate and chemical stock solutions were transferred into serum bottles(1/3 full), sealed with rubber stoppers and aluminum crimpers, there alternately evaluated under vacuum and flashed with N_2 gas at 14 psig three times. Serum bottles were autoclaved at 121 °C for 25 min.

2. Dilution used for each substrate

Glucose fermenters	10^{-5} - 10^{-11}
H_2-utilizing methanogens	10^{-4} - 10^{-10}
Acetate-utilizing methanogens	10^{-4} - 10^{-10}
propionate-utilizing acetogens	10^{-4} - 10^{-10}
Butyrate-utilizing acetogens	10^{-4} - 10^{-10}

For each dilution 5 tubes were used.

3. MPN tube preparation protocol

(1) Boil and dispense media solution under a N_2 gas purge.

(2) Dispense 9 ml solution into each pressure tube and seal the tube with rubber stopper and aluminum ring.

(3) After autoclaving at 121 °C for 25 min, add the following amounts of autoclaved chemical agents to each tube:

10% HCO_3^- solution	0.1 ml
Vitamin solution	0.1 ml (after filtering through 0.2 μm glass fiber filter)
Phosphate buffer	0.1 ml
2.5% $Na_2S \cdot 9H_2O$	0.1 ml

(4) Pressurize the tubes by 5% CO_2 + 95% H_2 mixture at 14 psig except the tubes for H_2 degraders

(5) Add proper substrate to pressure tube as follows:

10% glucose	0.2 ml
1 M acetate	0.2 ml
1 M propionate	0.2 ml
1 M butyrate	0.2 ml
80% H_2 + 20% CO_2 mixture	20 psig

4. Incubation

After preparation, MPN tubes were incubated at 35 °C. The incubation time used for glucose fermenters was 14 days. The incubation time for all other microorganisms was 60 days.

5. Test result determination

Test results reported here were based on CH_4 detection for acetogens and methanogens. Tubes that had a CH_4 concentration above 0.5 mM were evaluated as positive. The results for glucose-utilizing fermentative bacteria were recorded on the basis of increase in optical density compared to non-inoculated control tubes. Tubes with an optical density > 0.2 at 650 nm were scored as positive.

APPENDIX C

APPENDIX C.

EPIFLUORESCENCE MICROSCOPY DIRECT COUNTING METHODS

Fluorescent dyes can improve the visualization of individual microorganisms by binding to specific cell components (Bratbak, 1985; Bitton, et al., 1993). Acridine Orange has affinity for DNA, RNA, acidic polysaccharides; while DTAF has affinity for protein.

1. Acridine orange direct count (DNA stain)

Materials

(1). 0.2 um pore size 25 mm diameter polycarbonate membrane filters (Fisher No. 11021);

(2). 1% Formaldehyde solution;

(3). 0.1% Acridine Orange (Sigma C. I. 46005) solution;

(4). 0.1% Polyoxyethylene sorbitan mono-oleate(Tween 80, Sigma No. P-1754) solution;

(5). 80% ethanol solution;

(6). 80% isopropanol solution;

(7). Sterilized distilled water;

(8). TWA-30 Microscope.

Procedure

1. Take 1 ml sample from the reactor and immediately mix with 1 ml of 1% formaldehyde solution and 8 ml water in a 14 ml sterilized falcon tube and store at 4 ^{o}C for further analysis.

2. Serially dilute sample so that about 30 - 60 cells per grids can be observed.

3. Add 1 ml of 0.1% AO solution into the sample (1 ml sample 8 ml water), mix well and store in the dark for 30 min.

4. Wash filtration glass column with water first and then and 80% ethanol.

5. Put filtration membrane on the filter.

6. Wash the membrane with 1 ml of the 0.1% Tween 80 solution.

7. Add 2 ml sample and 8 ml sterilized DI water into the filtration column for filtration.

8. Add 2-3 ml 25% isoproponol solution to the filter column to wash the membrane.

9. Remove the membrane from the fitter and place on a microscope slide (add a drop of oil on the slide first).

10. Count the orange spots under UV light on the observation grids. In order to get reliable results, repeated counting 5-10 times should be performed for each sample.

Calculation:

Effective filter area is 231 mm^2. Using the 63 X objective the graticule field is 156 X 156 um, the total area is 0.024336 mm^2. Therefore the effective filter area contains:

231 / 0.024336 = 9492.1 graticule field

The total bacteria number in the sample can be calculated:

Bacteria No./ml = 9492.1 x N_f x N_d

Where:

N_f: Average bacteria number observed on graticule field

N_d: sample dilution.

2. DTAF direct count (protein stain)

Reagents:

1. Phosphate Buffered Saline

0.05M Na_2HPO_4 (7.8 g/L)

0.85% NaCl (8.5 g/L)

The Na_2HPO_4 is diluted in 0.85% NaCl and adjusted to pH 9.0 and filtered through 0.2 µm membrane prior to use.

2. DTAF fluorescent stain: 5-(4, 6-dichlorotriazin-2-yl) aminofluorescein dissolved 2 mg in 10 ml of PBS immediately prior to use. Stain is stable for several hours.

3. Distilled water (from CME lab)

4. 25% isopropanol-250 ml

   Filter through a 0.2 μm membrane prior to use.

5. Immersion Oil - Type FF.

6. 0.1% formaldehyde solution.

Materials

1. Falcon tubes - 17 x 100 mm;
2. Dispo tube - 12 x 75 mm;
3. Plain microscope slides;
4. Cover glass - 22 mm sq.;
5. Filter - Black - 25 mm, 0.2 μm;
6. Warring Blender;
7. Stop Watch;
8. Adjustable pipettes with tips to deliver 0.5, 1.0 and 5 ml;
9. Filter Apparatus;
10. Forceps;
11. Fluorescent Microscope;
12. 400/27° Kodak slide film (MSU Biochemical Store 36-roll 1442355, 24-roll 1442351).

Procedure

1. Dilute the sample properly so that in the microscope grid about 100 cells can be observed.

2. In the dilution tube add 1 ml of 0.1 % formaldehyde solution plus 8 ml filtered water.

3. Add 0.5 ml of the diluted culture in 12 * 75 mm glass tubes (No in duplicate.

4. Add 0.5 ml of DTAF stain, mix well by vortexing.

5. Place sample in the dark for 30 min.

6. After 30 min. mix all tubes on vortex again.

7. Place black filter on filter apparatus and Attach filter cylinder.

8. Add 5 ml of PBS in the cylinder.

9. Add all the stained sample to the PBS (5 ml)

10. Rinse the tube with a little PBS and pour into the cylinder.

11. Turn on the vacuum pump, open the valve to the cylinder, until filter is dry.

12. Add 5 ml of PBS-twice, applying vacuums until filter is dry between each 5 ml.

13. Add 5 ml of distilled water - applying vacuum until dry.

14. Add 5 ml 25% isopropanol - applying vacuum until dry.

15. Close valve and turn off vacuum pump.

16. Remove filter and place on microscope slide, add one drop of immersion oil to filter, cover with cover glass. Cover glass may be sealed with fingernail polish.

17. Examine under the fluorescent microscope using the grid to facilitate counting.

Calculation:

Effective filter area is 231 mm^2. Using the 63x objective the graticule field is 156 X 156 μm, the total area is 0.024336 mm^2. Therefore the effective filter area contains:

231 / 0.024336 = 9492.1 graticule field

The total bacteria number in the sample can be calculated:

Bacteria No./ml = $9492.1 \times N_f \times N_d$

Where:

N_f: Average bacteria number observed on graticule field,

N_d: sample dilution.

APPENDIX D

APPENDIX D

PROTEIN MEASUREMENT PROCEDURE

Protein analysis was performed according to the MBS method (Bradford, 1976; Sedmak and Grossberg, 1977). In this method the diluted samples were first digested with 10 N NaOH for two hours. Then 5 N HCl was added to neutralize the solution. Coomassie protein assay reagent was added to the neutralized samples and reacted for 20 min. The mixed liquor was transferred into 1.5 ml 1 cm path light polystyrene curettes and the absorbence obtained using on spectrophotometer at a wavelength of 595 nm compared to a blank.

Materials:

1. 10 N NaOH solution (Cat No SS255-1, Fisher scientific, Pittsburgh, PA);
2. 5 N HCl solution (Cat No LC15360-2, Fisher scientific, Pittsburgh, PA);
3. Coomassie protein assay reagent (Cat No 23200, Pierce, Rockford, IL);
4. 10 ml glass tube with screw cap;
5. 1.5 ml, 1 cm path polystyrene curette (Cat No LS-2410-100, Life Science Productes, Inc., Denver, CO);
6. Perkin-Elmer Lambda 6 UV/VIS spectrometer (Perkin-Elmer Corporation, Norwalk, CT).

Procedure:

1. Add 1 ml diluted sample (1/10 of the original concentration) into 10 ml glass tube.
2. Add 0.5 ml 10 N NaOH solution into the tube mixing well with the diluted sample and digest for 2 hours.
3. Add 1 ml 5 N HCl solution into the tube to neutralize the solution.
4. Add 2 ml Coomassie protein assay reagent into the tube and react for 20 min.

5. Read absorption at wavelength 595 nm against Coomassie protein assay reagent blank (use 1 ml D.I. water to replace diluted sample).

6. Calculate protein concentration by using standard absorption curve.

7. In this experiment the standard calibration curve was prepared by using standard protein solution with the following protein concentrations: 10, 20, 40, 60, 80 and 100 ug/ml.

APPENDIX E

APPENDIX E

EFFECT OF pH AND VFAS ON MAXIMUM HYDROGEN UTILIZATION RATES

The effect of pH and VFAs on the maximum hydrogen utilization rates of the mother reactor culture was investigated using batch experiments. The effect of VFA concentration on conversion of H_2-CO_2 was tested in 158 mL serum bottles containing 60 ml of the mother reactor culture. The bottles were pressurized by addition of 20 psig of H_2-CO_2 gas (80:20) into headspace. VFA concentrations examined using duplicate samples for each test are listed in Table E-1.

Table E-1. VFA concentrations examined in the H_2-CO_2 degradation experiment

Acids	Concentrations (mg/L)					
Acetate	200	1000	1500	2000	3000	4500
Propionate	100	500	1000	1600	3000	4000
Butyrate	100	1600	3200	4600	6200	

The effect of pH on conversion rates of H_2-CO_2 by the mother reactor culture was evaluated using 158 ml serum bottles. Culture conditions were similar to the VFA studies. The pH of the culture was adjusted to 5.0, 5.5, 6.3, 6.8, 7.6 and 8.2 by adding different amount of 5N NaOH or 5N HCl solutions into liquid phase.

Bottles were incubated in a shaking bed at 35 °C. H_2-CO_2 conversion rates were calculated based on methane production. Results reported were averages of duplicate samples.

The effect of pH on the conversion rates of H_2-CO_2 is presented in Figure E-1. The optimum pH for maximum hydrogen conversion by the mother reactor culture was ca. 5.5 to 6.8. When the pH was increased or decreased beyond this range, a significant decrease in hydrogen utilization rate was observed.

The effects of VFA concentrations on the maximum hydrogen utilization rate are presented in Figure E-2 (a-c). When acetate, propionate and butyrate concentrations were less than 2,000, 1,500 and 2,000 mg/L, respectively, the H_2-CO_2 utilization rates were not effected. When the VFAs concentrations were increased to ca. 4,500, 3,500 and 6,000 mg/L, respectively, the H_2-CO_2 utilization rates were decreased to ca. 87%, 89% and 87%, respectively, of the maximum utilization rates measured under normal operation conditions (VFAs < 200 mg/L).

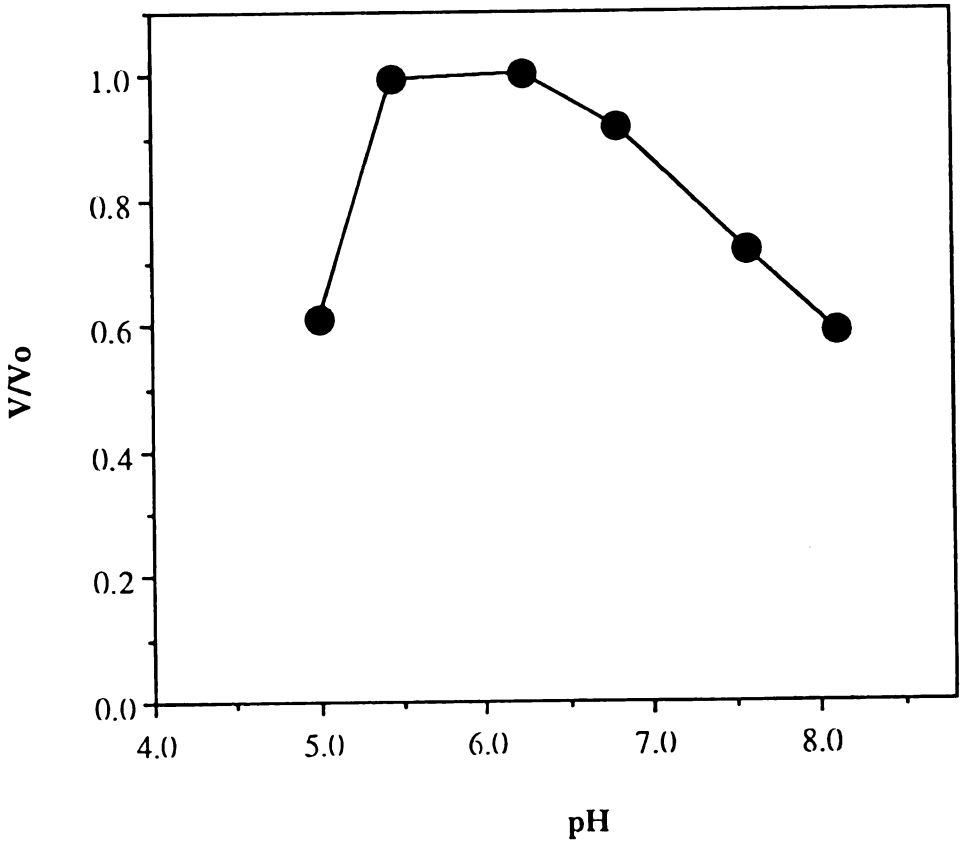

Figure E-1. pH effect on hydrogen conversion rates.

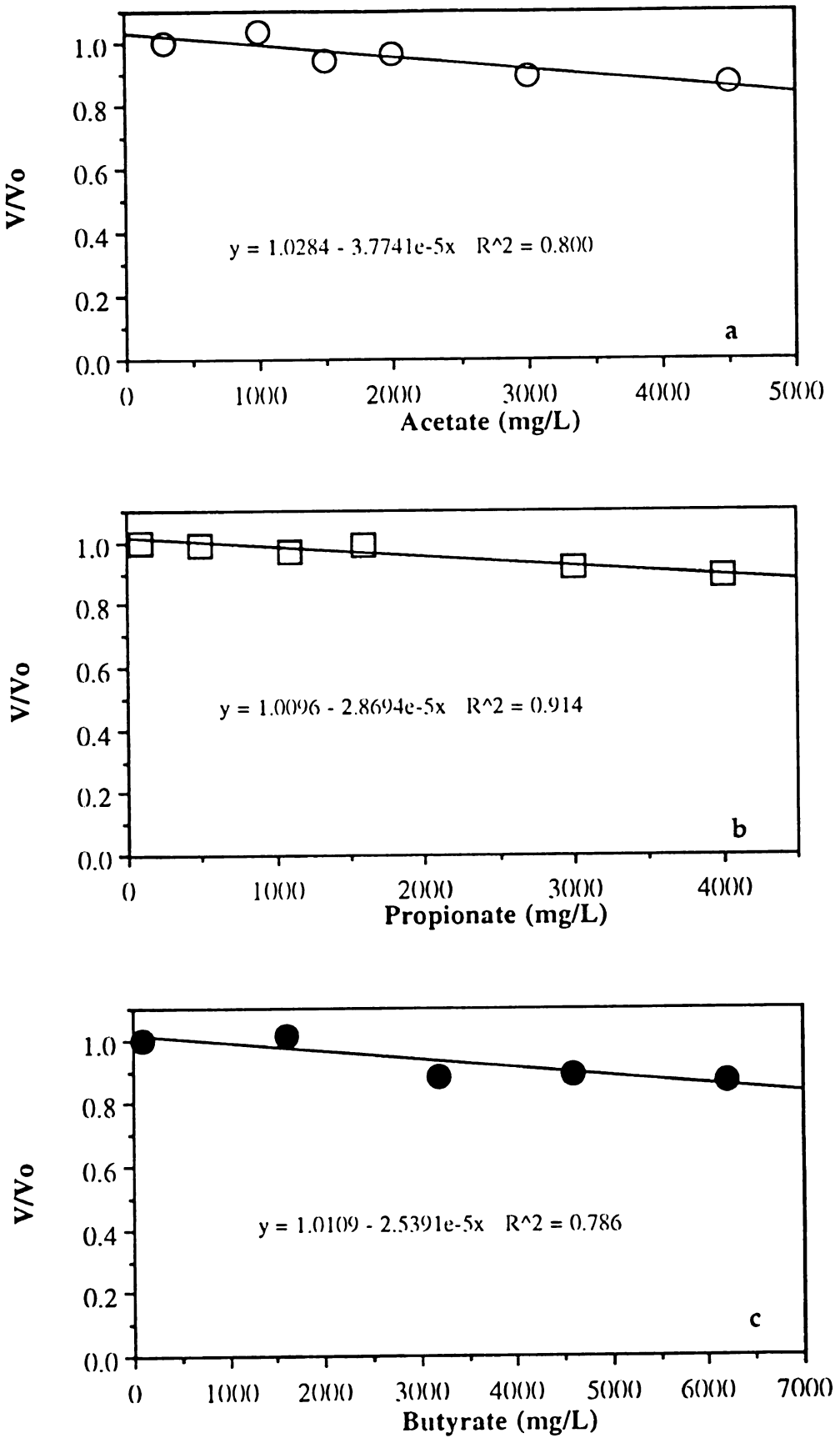

Figure E-2. VFA effect on hydrogen conversion rates at pH 7.4. (a) acetate; (b) propionate; (c) butyrate.

APPENDIX F

APPENDIX F

DEVELOPMENT OF FREE ENERGY EQUATION USED FOR ACTUAL OPERATION CONDITIONS

Based on Thauer *et al* (1977), the free energy change under physiological conditions (pH 7 and 25 °C) can be calculated as:

$$\Delta G' = \Delta G^{o'} + RT \sum Vi \ln Ai \qquad (F\text{-}1)$$

where:

R = gas constant, 8.3143 J/K mol,

T = Temperature, K,

Vi = The stoichiometric coefficient for component Ai in a biological reaction (i = 1,2,3,...) and is negative for reactants and positive for products,

Ai = the physiological concentration of the component i in the reaction, mol,

$\Delta G^{o'}$ = the increment of free energy at standard physiological conditions (25 °C, 1 atm and pH 7), KJ/mol.

$\Delta G^{o'}$ was calculated from ΔG^{o} according to the following equation:

$$\Delta G^{o'} = \Delta G^{o} + m\, \Delta f'(H^{+}) \qquad (F\text{-}2)$$

Where:

ΔG^{o} = free energy change under standard condition (25 °C, 1 atm and unit solutes concentrations), KJ/mol,

m = net number of protons in the reaction (m is negative when more protons are consumed than formed),

$\Delta f'(H^{+})$ = the free energy of formation of a proton at pH 7.

$\Delta f'(H^{+})$ in equation (F-2) can be written as:

$$\Delta f'(H^{+}) = RT \ln 10^{-7} \qquad (F\text{-}3)$$

Substitute $\Delta f'(H^+)$ from equation (F-3) to equation (F-2), get:

$$\Delta G^{o'} = \Delta G^o + m\ RT \ln 10^{-7} \qquad \text{(F-4)}$$

To use the same principle, the "standard free energy change" under operation pH other than pH 7 can be calculated as:

$$\Delta G^{o'}_{op} = \Delta G^o + m\ \Delta f'(H^+)$$
$$= \Delta G^o + m\ RT \ln(H^+) \qquad \text{(F-5)}$$

Where:

$\Delta G^{o'}_{op}$ = Standard free energy change at operating pH, KJ/mol,

$[H^+]$ = Proton concentration in the reactor solution, mol/L.

Resolve ΔG^o from equation (F-4) and substitute it to equation (F-5), get:

$$\Delta G^{o'}_{op} = \Delta G^{o'} + m\ RT \ln([H^+]/10^{-7}) \qquad \text{(F-6)}$$

Under operation conditions, the free energy change can be calculated using following equation:

$$\Delta G'_{op} = \Delta G^{o'}_{op} + RT \sum Vi \ln Ai \qquad \text{(F-7)}$$

Substitute equation (F-6) into equation (F-7) and rearrange it, get:

$$\Delta G'_{op} = \Delta G^{o'} + m\ RT \ln([H^+]/10^{-7}) + RT \sum Vi \ln Ai$$
$$= \Delta G^{o'} + 2.303\ RT\ [\log([H^+]/10^{-7})^m + \sum Vi\ Log\ Ai] \qquad \text{(F-8)}$$

where the free energy units are KJ, the substrate concentrations are in mole and the gas pressure is atm.

APPENDIX G

APPENDIX G

FAME EXTRACTION PROCEDURE

1. Saponification

Samples were treated by strong methanolic base combined with heat to lyse the cells. Fatty acids were cleaved from the cell lipids and were converted to their sodium salts.

(1). First add 1.0 ml methanolic base into each of the culture tubes.

(2). Tightly seal each tube with a clean Teflon-lined screw cap.

(3). Vortex the tubes for 5-10 seconds.

(4). Place a rack of the sample tubes into a boiling water bath at 100 ± 2 °C.

(5). After 5 minutes, remove the tubes from the boiling water and cool them slowly.

(6). Vortex the tubes for 5-10 seconds then return the tubes to the water bath and continue heating the tubes for additional 25 minutes.

(7). After a total of 30 minutes of saponification in the water bath, remove and set the rack of tubes in a pan of room temperature water.

2. Methylation

Methylation converts the fatty acids (as sodium salts) to fatty acids methyl esters which increases the volatility of the fatty acids for the GC analysis.

(1). Add 2 ml methylation reagent to each tube.

(2). Tightly cap the tube and vortex the solution for 5-10 seconds.

(3). Heat the tube at 80 °C water bath for 10 minutes.

(4). Cool the tubes to room temperature by place the tubes in a tray of room temperature water.

3. Extraction

Fatty acid methyl esters are removed from the acidic aqueous phase and transferred to an organic phase with a liquid-liquid extraction procedure.

(1). Add 1.25 ml hexane/MTBE extraction solvent to each tube.

(2). Place batch of tubes in a laboratory rotator and mix end-over-end for 10 minutes.

(3). Use clean Pasteur pipette to remove and discard the lower aqueous phase.

(4). Add 3 ml base wash solution to each tube and rotate the tubes end-to-end for 5 minutes.

(5). Centrifuge at 2000 rpm for 3 minutes to clarify the interface between phases.

4. Base wash

(1). Add 3.0 ml of reagent 4, the base wash, into each tube.

(2). Tightly cap and rotate the tubes end-over-end for five minutes.

(3). Brief centrifugation (three minutes at 2000 rpm) is recommended to clarify the interface between the phases when an emulsion is presented.

5. Transfer extract

Transfer of the extract to sample bottle. After that remove the upper solvent phase to GC autosampler bottle for run GC analysis.

APPENDIX H

APPENDIX H

NOMENCLATURE OF FATTY ACIDS

A. Straight Chain

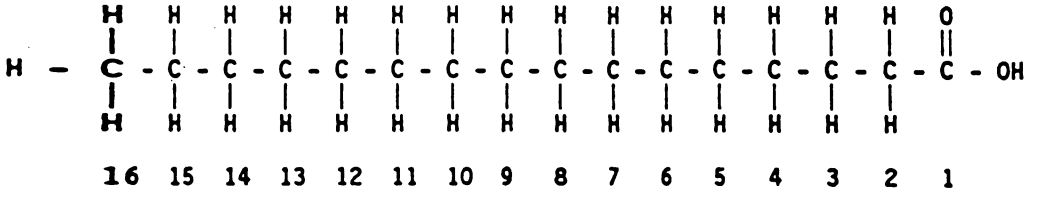

The above represents the straight chain fatty acid palmitic acid, written as 16:0, where the "16" represents the number of carbons in the compound, and the number after the colon indicates the number of double bonds in the carbon chain (in this case, none). Note the carboxyl group(COOH) at the right.

Note that these compounds may also be written with the letter C in front of the number, such a C16:0. The letter "C" stands for "carbons" in the compound, and a compound written C16:0 is the same as one written 16:0.

B. Unsaturated

1. cis conformation

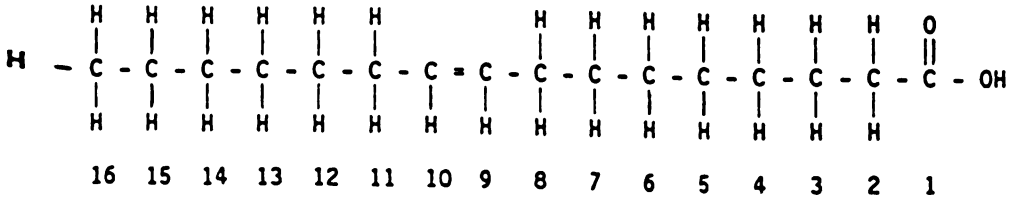

The designation 16:1 indicates that the compound has 16 carbons and 1 double bond. The above represents the unsaturated fatty acid 16:1 cis 9. Note that both hydrogens at the double bond are on the same side.

2. trans conformation

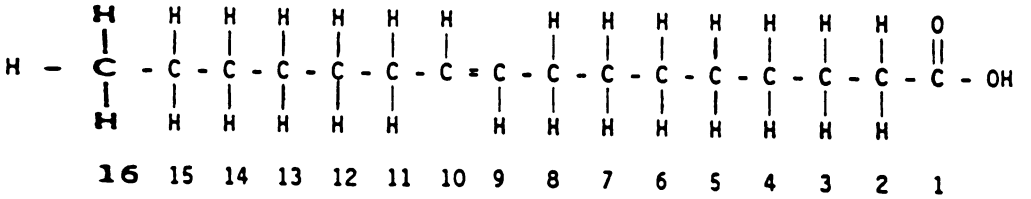

The above represents the unsaturated fatty acid 16:1 trans 9. Note that the hydrogens at the double bond are on opposite sides of the compound.

C. Iso

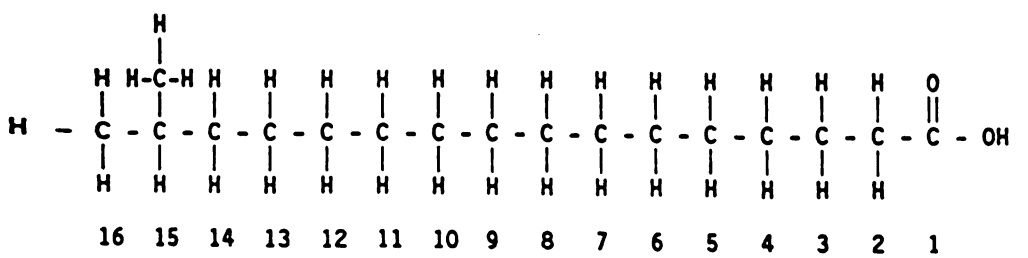

The above represents the fatty acid 17:0 ISO. A methyl group occurs at the second to the last carbon in the chain.

D. Anteiso

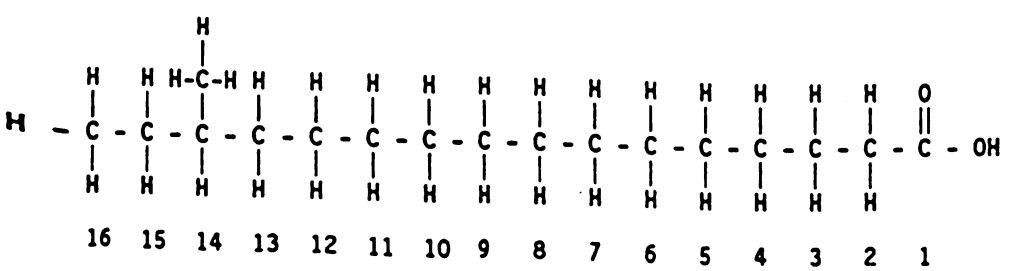

The above represents the fatty acid 17:0 ANTE. A methyl group occurs at the third to the last carbon in the chain.

E. Cyclopropane

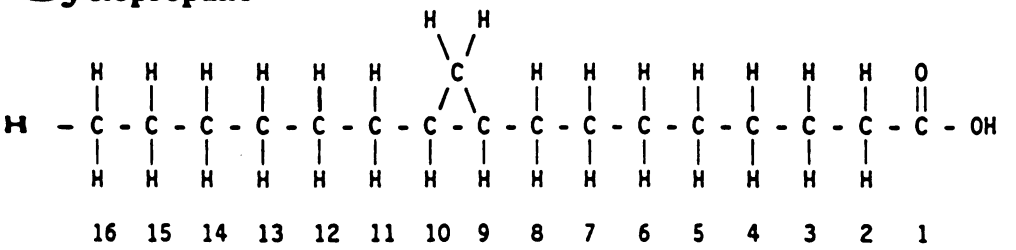

The above represents the fatty acid 17:0 CYCLO 9-10. In this case, this compound is made from 16:1 cis 9 with the addition of the carbon group at the double bond position.

F. Hydroxy

1. The 2-hydroxy

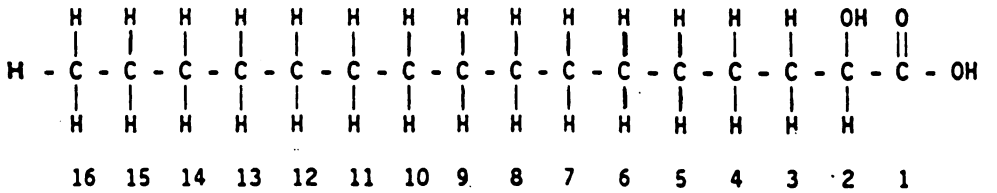

The above represents the fatty acid 16:0 2OH, where a hydroxyl group is added at the 2 (alpha) position.

2. The 3-hydroxy

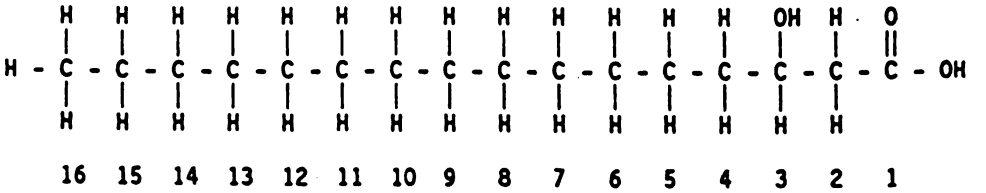

The above represents the fatty acid 16:0 3OH, where a hydroxyl group is added at the 3(beta) position.

3. Other hydroxys

Hydroxyl functional groups may occur at other positions besides the second and third carbon. These are not common across the numerous species of bacteria which have been looked at to-date.

G. Mixed functional groups

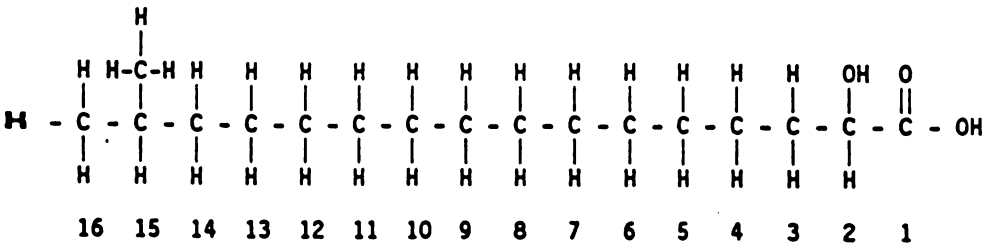

Combinations of the various functional groups also occur. The above represents the fatty acid 17:0 ISO 2OH

H. Fatty acid methyl ester

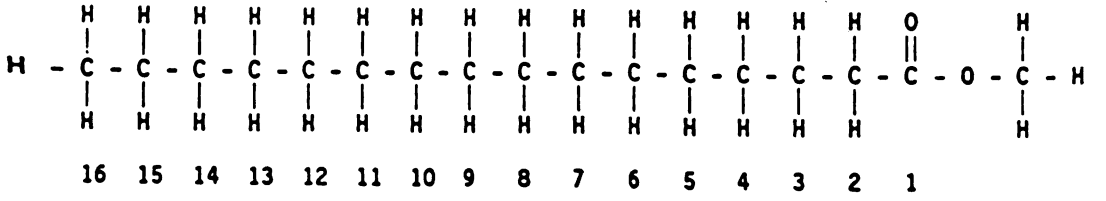

The above represents the fatty acid methyl ester 16:0, written as 16:0 FAME on the MIS printed reports. A methyl group is added to the carboxyl group to increase volatility for GC analysis.

I. Dimethyl acetal

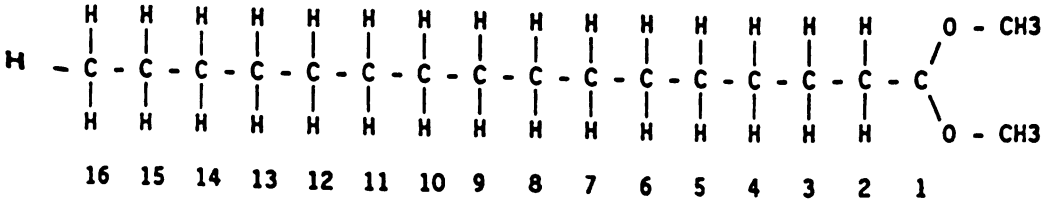

The above represents dimethyl aldehyde 16:0, written as 16:0 DMA on the MIS printed reports. Dimethyl acetals occur as analogs of the fatty acids present in anaerobic bacteria, and can contain any of the above functional groups. They result form the ether-linked lipids in plasmologens.

J. Normal hydrocarbon

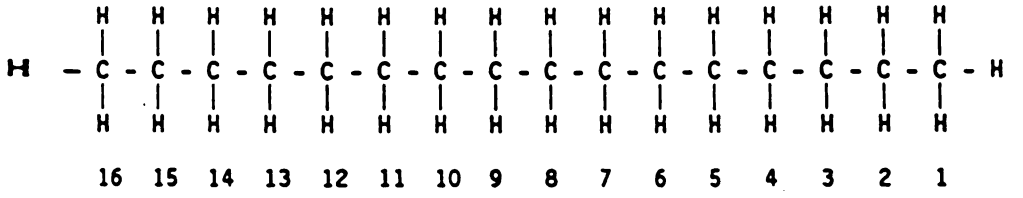

The above represents normal hydrocarbon 16:0, also written as n 16:0.

K. Aldehyde

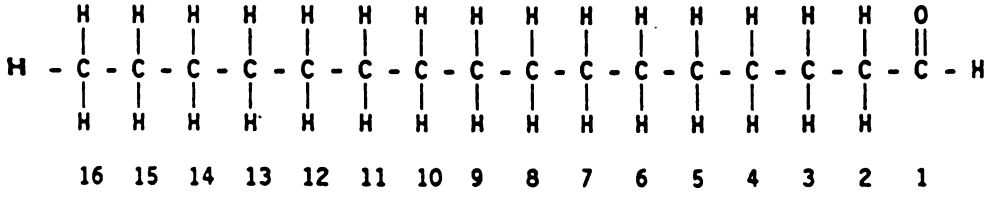

The above represents aldehyde 16:0.

L. Alcohols

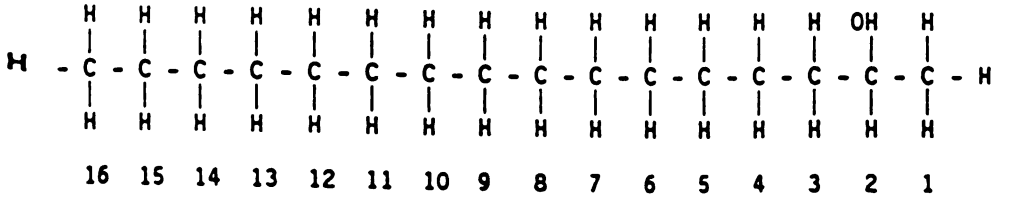

The above represents the alcohol 2-octadecanol. This compound, as well as 2-eicosanol (20 carbons long), occur in some species of Mycobacterium.

LIST OF REFERENCES

LIST OF REFERENCES

Agargy, F. J., Cole, R. D. and E. A. Pearson (1963) Kinetic and activity parameters of anaerobic fermentation systems, SEAL Report 63-2, Sanitary Engineering Research Laboratory, University of California, Berkeley.

Ahring, B. K. and P. Westermann (1987) Kinetics of butyrate, acetate, and hydrogen metabolism in a thermophilic, anaerobic, butyrate-degrading triculture. Appl and Environ Microbiol 53: 434-439.

Ahring, B. K. and P. Westermann (1988) Product inhibition of butyrate metabolism by acetate and hydrogen in a thermophilic coculture. Appl Environ Microbiol 54: 2393-2397.

Aivasidis, A., K.-H. Bastin and C. Wandrey (1988) Optimization of selection stress in a chemostat, Proceedings of the Fifth International Symposium on Anaerobic Digestion, held on Bologna, Italy, 22-26 May, Pergamon Press, Oxford, P35-46.

Alphenaar, P. A. (1993) Phosphorus requirement in high-rate anaerobic wastewater treatment, Was. Res. 27:749-756.

American Public Health Association (1989) Standard methods for the examination of water and wastewater. 17th ed. (A. D. Eaton, L. S. Clesceri and A. E. Greenberg, ed.) American Public Health Association, Washington, D.C.

Anderson, G. K., T. Donnelly and K. J. McKeown (1982) Identification and control of inhibition in the anaerobic treatment of industrial wastewaters, Proc. Biochem. 13:28-32.

Anderson, G. K. and G. Yang G (1992) Determination of bicarbonate and total volatile acid concentration in anaerobic digesters using a simple titration, Water Environ. Res. 64: 53-64.

Anderson, G. K., B. Kasapgil and O. Ince (1994) Microbiological study of two-stage anaerobic digestion during start-up Was. Res. 28:2383-2392.

Archer, P. B. and G. E. Powell (1985) Dependence of the specific growth rate of methanogenic mutualistic cocultures on the methanogens. Arch. Microbiol., 141:133-137.

Atlas, R. M. and R. Bartha, Microbial Ecology, The Benjamin/Cummings Publishing Company, Inc. Menlo Park, CA 94025, 1987.

Attal, A., F. Ehlinger, J. M. Audic and G. M. Faup (1988) pH inhibition mechanisms of acetogenic, actoclastic and hydrogenophilic populations. Proceedings of the Fifth International Symposium on Anaerobic Digestion, Bologna, Italy, 22-26 May, Pergamon Press, Oxford, 71-78.

Bae J. and P. L. McCarty (1993) Variation of carbon monoxide production during methane fermentation of glucose, Wat. Environ. Res. 65:890-898.

Barford, J. P. (1989) Start-up, Dynamics, and Control of Anaerobic Digesters, Handbook on Anaerobic fermentations, Larry E. Erickson and Daniel, Yee-Chak F. (ed), Marcel Dekker, Inc., New Work.

Barnes T., Influence of organic shock loadings on the performance of an anaerobic fluidized bed system, paper presented at the 37th Purdue Industrial Waste Conference, Purdue, IN, April 1983.

Benefield L. D. and C. W. Randall, Biological Process Design for Wastewater Treatment, Prentice-Hall, Inc., Englewood, NJ. 1980.

Bitton, G., B. Koopman, K. Jung, G. Voiland and M. Kotob (1993) Modification of the standard epifluorescence microscopic method for total bacterial counts in environmental samples, Wat. Res. 27:1109-1112.

Bobble, R. J. and D. C. White (1980) Characterization of benthic microbial community structure by high-resolution gas chromatography of fatty acid methyl esters, Appl. Environ. Microbiol. 39:1212-1222.

Boe, B. and J. Gjerde (1980) Fatty acid pattern in the classification of some representatives of the families *Enterobacteriaceae* and *Vibrionaceae* , J. of Gen Microbiol 116:41-49.

Boone, D. R. (1987) Effects of hydrogen pressure during growth and effects of pregrowth with hydrogen on acetate degradation by *Methanosarcina* species, Appl. Environ. Microbiol. 53: 83-87.

Bousfield, I. J. (1983) Numerical analysis of total fatty acid profiles in the identification of coryneform, noncoryneform and some other bacteria, J. Gen Microbiol 129: 375-394.

Bradford, M (1976) A rapid and sensitive method for the quantitation of microgram quantities of protein utilizing the principle of protein dye-binding. Anal. Biochem. 72:248-253.

Bratbak, G. (1985) Bacterial biovolume and biomass estimations, Appl Environ Microbiol 49:1488-1493.

Britz, T. J. (1994) Acidogenic microbial species diversity in anaerobic digesters treating different substrates, Wat. Sci. Tech. 30:55-61.

Bryant, M. P. (1959) Bacterial species of the rumen. Bacteriol. Rev. 23: 39-66.

Bryant, M. P., (1977) Microbiology of the rumen, in M. J. Swenson (ed) Dukes physiology of domestic animals, 9th revised edition. Cornell University Press, Ithaca, N. Y. P287-304.

Callander, I. J., and J. P. Barford (1983) Recent advances in anaerobic digestion technology. Proc. Biochem. 18:24-30.

Chang J. T., T. Noike and J. Matsumoto (1982) Effect of retention time and feed substrate concentration of methanogenisis in anaerobic digestion. Proc. of JSCE No. 320, 67-76.

Chynoweth, D. P. and R. A. Mah (1977) Bacterial populations and end products during anaerobic sludge fermentation of glucose, J. WPCF 49: 405-412.

Cohen, A., R. J. Zoetemeyer, A. ven Deursen and J. G. ven Andel (1979) Anaerobic digestion of glucose with separated acid production and methane formation. Wat. Res. 13: 371-379.

Cohen, A., B. Distel, A. van Deursen and J. G. van Andel (1981) Role of anaerobic spore forming bacteria in the acidogenesis of glucose: changes induced by discontinuous or low-rate feed supply. Wat. Res. 15:59-68.

Cohen, A., A. M. Breure, J. G. van Andel and A. van Deursen (1982) Influence of phase separation on the anaerobic digestion of glucose-II stability and kinetic responses to shock loadings. Wat. Res. 16:254-263.

Cohen, T., Optimization of anaerobic digestion of soluble carbohydrate containing wastewater by phase separation. Ph. D dissertation, University van Amsterdam, Nieuwe Achtergracht 127, 1018 WS Amsterdam, The Netherlands, 1983.

Cord R. (1988) The capacity of hydrogenotrophic anaerobic bacteria to compete for traces of hydrogen depends on the redox potential of the terminal electron acceptor, Arch. Microbiol. 149:350-357.

Costello, D. J., P. F. Greenfield and P. L. Lee (1991) Dynamic modeling of a single-stage high rate anaerobic reactor-I. model development, Wat. Res. 25:847-858.

Dinopoulou, G., R. M. Sterritt and J. N. Lester (1988) Anaerobic acidogenesis of a complex wastewater: II. kinetics of growth, inhibition and product formation, Biotech Bioeng 31:969-978.

Dolfing, J. and R. A. Prins (1996) Methanogenic "Food Chains", American Society for Microbiology News, 62:117-118.

Duarte, A. C. and G. K. Anderson (1982) Inhibition modeling in anaerobic digestion. Wat Sci Tech 14: 749-763.

Dwyer, D. F., E. Weeg-Aressens, D. R. Shelton and J. M. Tiedje (1988) Bioenergetic conditions of butyrate metabolism by a syntrophic, anaerobic bacterium in coculture with hydrogen-oxidizing methanogenic and sulfidogenic bacteria. Appl Environ Microbiol 54:1354-1359.

Ehrlich, T., Bacteria in Nature, ed. J. S. Poindexter and E. R. Leadbetter, Plenum Press, New York, 1985.

Fenchel, T., Ecology of Protozoa, Science Tech Publishers, Madison, Wisconsin, 1987.

Fongastitkul, P., D. S. Mavinic and K. V. Lo (1994) A Two-phased anaerobic digestion process: concept, process failure and maximum system loading rate. Wat Environ Res J 66:243-254.

Fox, P., and M. T. Suidan (1996) Shock and transient loading on anaerobic reactor coupled with adsorber, J. of Environ. Eng. 68:18-24.

Fukuzaki, S. (1990) Inhibition of the fermentation of propionate to methane by hydrogen, acetate, and propionate, Appl. Environ. Microbiol. 48:719-723.

Ghosh, S. and F. G. Pohland (1974) Kinetics of substrate assimilation and product formation in anaerobic digestion, J. WPCF. 46:748-754.

Gillan, F. T. and R. W. Hogg (1984) A method for the estimation of bacterial biomass and community structure in mangrove-associated sediments. J. of Microbiological Methods 2:275-293.

Guckert, J. B. (1985) Phospholipid easter-linked fatty acid profiles as reproducible assays for changes in prokaryotic community structure of estuarine sediments. FEMS Microbiol. Ecol. 31:147-158.

Guckert, J. B., M. A. Hood and D. C. White (1986) Phospholipid easter-linked fatty acid profile changes during nutrient deprivation of *Vibrio cholerae*: increases in the *trans /cis* ratio and proportions of cyclopropyl fatty acids, Appl Environ Microbiol 52:794-801.

Gujer, W. and A. J. B. Zehnder (1983) Conversion processes in anaerobic digestion, Wat. Sci. Tech. 15:127-167.

Gupta, A. J. R. V. Flora, M. Gupta, G. D. Sayles and M. T. Suidan (1994) Methanogenesis and sulfate reduction in chemostats-1. kinetic studies and experiments. Wat. Res. 28:781-793.

Harper S. R. and F. G. Poland (1985) Recent developments in hydrogen management during anaerobic biological wastewate treatment, Biotechnol. Bioeng. 28:585-602.

Hattingh, H. J. W., J. P. Kotze, P. G. Thiel, D. F. Toerien and M. L. Siebert (1967) Biological changes during the adaptation of an anaerobic digester to a synthetic substrate, Wat. Res. 1:255-277.

Hedrick, D. B. (1991) Disturbance, starvation, and overfeeding stresses detected by microbial lipid biomarkers in high-solids high-yield methanogenic reactors. J. of Ind. Microbiol. 8: 91-98.

Heijnen, J. J., M. C. M. van Loosdrecht and L. Tijhuis (1991) A black box mathematical model to calculate auto- and heterotrophic biomass yield based on Gibbs energy dissipation, Biotechnol. Bioeng. 40:1139-1154.

Henson, J. M., P. H. Smith and D. C. Which (1985) Examination of thermophilic methane-producing digesters by analysis of bacteria lipids, Appl. Environ. Microbiol. 50:1428-1433.

Herbert, D. (1975) Stoichiometric aspects of microbial growth: Continuous culture 6. *Applications and New Fields* (Edited by Dean A. C. R., Ellwood P. C., Evans C. G. T. & Meling J.). Ellis Horwood Ltd, Chichester, U.K.

Heyes, R. H. and R. J. Hall (1981) Anaerobic digestion modeling-the role of H_2, Biotechnology Letters, 3:431-436.

Heyes, R. H. and R. J. Hall (1983) Kinetics of two subgroups of propionate-using organisms in anaerobic digestion, Appl. Environ. Microbiol., 46:710-715.

Hickey, R., W. Wu and R. Jones (1991a) The start-up, operation and monitoring of high-rate anaerobic treatment systems, Water Sci. Tech. 24:207-231.

Hickey, R. F. and M. S. Switzenbaum (1991b) The response and utility of hydrogen and carbon monoxide as process indicators of anaerobic digesters subject to organic and hydraulic overloads. Res J WPCF 63:129-140.

Hickey, R. F. and M. S. Switzenbaum (1991c) Thermodynamics of volatile fatty acid accumulation in anaerobic digesters subjected to increases in hydraulic and organic loading. Res J WPCF 63:141-144.

Hill D. T. and C. L. Barth (1974) A dynamic model for simulation of animal waste digestion, J. WPCF 49:2129-2143.

Hobson, P. N. and B. G. Shaw (1978) Inhibition of methane production by *Methanobacterium formicicum* . Wat. Res. 10:849-852.

Hungate, R. E. (1975) The rumen microbial ecosystem, Arch. Microbiol. 70: 39-66.

Iannotti, E. L., (1982) Characterization of bacteria from a swine manure digester. Appl. Environ. Micriobiol. 43: 136-143.

Ikemoto, S. (1978) Cellular fatty acid composition in *Pseudomonas* species, Gen. Appl. Microbiol. 24:199-213.

Jain M. K., J. G. Zeikus and L. Bhatnagar, Methanogens, Anaerobic Microbiology (P. N. Levett, ed.) Oxfoed University Press, New York, 1991, pp223-245.

Jeris, J. S. and P. L. McCarty (1962) The biochemistry of methane fermentation using C^{14} traces, Proceedings of 17th Industrial Waste Conference, Puedue University, P 181-197.

Kaneda, T. (1991) Iso- and Anteiso-fatty acids in bacteria: Biosynthesis, function, and taxonomic significance, Microbiol. Rev. 55:288-302.

Kaspar, H. F. and K. Wuhrmann (1978) Kinetic parameters and relative turnovers of some important catabolic reactions in digesting sludge. Appl Environ Microbiol 36:1-7.

Kisaalita, W. S., K. V. Lo and K. L. Pinder (1989) Influence of dilution rate on the acidogenic phase products distribution during two-phase lactose anaerobiosis, Biotech. Bioeng. 34:1235-1250.

Knivett, V. A. and J. Cullen (1965) Some factors affecting cyclopropyl acid formation in *Escherichia Coli*. Biochem. J. 96:771-776.

Kroeker, E. J. (1979) Anaerobic treatment process stability, J. WPCF. 51:718-727.

Krumholz, L. R. and C. W. Forsberg (1983) Association of methanogenic bacteria with rumen protozoa, Can. J. Microbiol. 29:676-680.

Labib, F., J. F. Ferguson, M. M. Benjamin, M. Merigh and N. L. Ricker (1993) Mathematical-modeling of an anaerobic butyrate degrading consortia-predicting their response to organic overloads, Environ Sci Tech 27:2673-2684.

Lawrence, A. W. and P. L. McCarty (1969) Kinetics of methane fermentation in anaerobic treatment. J. WPCF 41: Res. Suppl. R1-R17.

Lawrence, A. W. and P. L. McCarty (1970) United basis for biological treatment design and operation, J. Sanitary Engineering Division, Proceedings of the American Society of Civil Engineers, 34:757-778.

Lepage, C. (1987) Changes in membrane lipid composition of *Clostridium acetobutylicum* during acetone-butanol fermentation: effects of solvents, growth temperature, and pH. J. Gen. Microbiol. 133: 103-110.

Lettinga, G., S. W. Hobma, L. W. Hulshoff Pol, de Zeeuw, W., de Jong, P., Grin, p., and R. Roersma (1983) Design operation and economy of anaerobic treatment. Wat. Sci. Tech. 15: 177-195.

Levenspiel, O. Chemical reaction engineering, John Wiley & Sons, New Tork, 1972.

Li, Y. Y., H. H. Fang and T. Noike (1994) Recent developments in microbiology and biochemistry of homoacetogens and sytrophic acetogens. Proc. Posters of the 7th International Symposium on Anaerobic Digestion. 23-27 Jauary, 1994, Cape Town, South Africa, pp. 54-57.

Linden, C. James, Industrially important strains and pathways, in Handbook on Anaerobic Fermentations, ed. Erickson, E. Larry and Daniel Y-C Fung, Marcel Dekker, Inc., New York, 1989.

Lovely, D. R. (1985) Minimum threshold for hydrogenmetabolism inmethanogenic bacteria, Appl. Environ. Microbiol. 56:1598-1607.

Maestrojuan, G. M. and D. R. Boone (1991) Characterization of *Methanosarcina barkeri* MS^T and 227, *Methanosarcina mazei* S-6^T, and *Methanosarcina vacuolalata* Z-761^T. Int. J, Syst. Bacteriol. 41:267-274.

Massol-Deya, A., D. Odelson, R. Hickey and J. Tiedje (1995) Bacterial community fingerprinting of amplified 16S and 16-23S ribosomal DNA gene sequences and restriction endonuclease analysis (ARDRA). In *Molecular Microbial Ecology Manual* (A. D. L. Akkermans, J. D. van Elsas, and F. J. deBruijn, eds) . Kluwer Academic Publishers, Netherlands. pp. 3.3.2:1-8.

Mawson, A. J., R. L. Earle and V. F. Larsen (1991) Degradation of acetic and propionic acids in the methane fermentation, Wat. Res. 25: 1549-1554.

McCarty, P. L (1964) Anaerobic waste treatment fundamentals-part one, Public Works. 95: 107-112.

McCarty, P. L (1964) Anaerobic waste treatment fundamentals-part two. Public Works. 95: 123-126.

McCarty, P. L (1965) Thermodynamics of biological synthesis and growth, Second International Conference on Water Pollution Research, Permagon Press, New York, P169-199.

McCarty, P. L (1966), Kinetics of waste assimilation in anaerobic treatment, In Developments in Industrial Microbiology, Vol. 7, American Institute of Biological Sciences, Washington D.C.

McCarty, P. L (1981) One hundred years of anaerobic treatment. Proceedings of the Second International Symposium on Anaerobic Digestion, held on Travemunde, Federal Republic of Germany, Elsevier Biomedical Press, Amsterdam, P3-22.

McCarty, P. L., One hundred years of anaerobic treatment, in Anaerobic digestion 1981, ed. D. E. Hughes et al., Elsevier Biomedical Press, New York, 3, 1983.

McCarty P. L. and D. Smith, Effect of hydrogen concentration on population distribution and kinetics in methanogenesis of propionate, Paper presented at the First Symposium on Biotechnological Advances in Processing Municipal Wastes for Fuels and Chemicals, August 15-17, 1984, Minneapolis, Minnesota.

McCarty, P. L. and F. E. Mosey (1991) Modeling of anaerobic digestion process (a discussion of concepts). Wat Sci Tech 24:17-33.

McInerney, M. J., M. P. Bryant, and D. A. Stafford (1979) Anaerobic bacterium that degrade fatty acids in syntrophic association with methanogens. Arch. Microbiol. 122:129-135.

Meakin, S. A., S. A., J. H. E. Hash, W. D. Murry, K. J. Kennedy and G. D. Sportt (1991) A generally applicable technique for the extraction of restrictable DNA from methanodenic bacteria, J Microbiol Meth 14: 119-126.

Moletta, R., D. Verrier and G. Albagnac (1986) Dynamic modeling of anaerobic digestion, Wat. Res. 20:427-434.

Mosey, F. E (1981) Anaerobic biological treatment of food industry waste water. Wat Pollut Control 80: 273-289.

Mosey, F. E (1983a) Mathematical modeling of the anaerobic digestion process: regulatory mechanisms for the formation of short-chain volatile acids from glucose. Wat Sci Tech 15:209-232.

Mosey, F. E (1983b) Kinetic descriptions of anaerobic digestion, Proceedings of the third international symposium on anaerobic digestion, Boston, MA. pp37-44.

Mosey, F. E. and X. A. Fernandez (1989) Patterns of hydrogen in biogas from the anaerobic digestion of milk-sugars, Wat. Sci. Tech. 21:187-196.

Novaes, R. F. V (1986) Microbiology of anaerobic digestion. Wat Sci Tech 18:1-14.

Novak, J. T. and D. A. Carlson (1970) The kinetics of anaerobic long chain fatty acids degradation, J. WPCF 42:1932-1943.

Odelson, D. A. and J. A. Breznak (1985) Nutrition and growth characteristics of *Trichomitopsis termopsis*, a cellulolytic protozoa from termites, Appl. Environ. Microbiol. 49:614-621.

O'Rourke, J. T. (1968) Kinetics of anaerobic treatment at reduced temperatures, Ph. D. Dissertation, Stanford University.

Palns, Sam-soon (1987) Hypothesis for pelletization in the upflow Anaerobic sludge bed reactor. Water SA, 13:69-80.

Pavlostathis, S. G. and E. Giraldo-Gomez (1991) Kinetics of anaerobic treatment. Wat Sci Tech 24:35-59.

Peck, M. W., J. M. Skilton, F. R. Hawkes and D. L. Hawkes (1986) Effects of temperature shock treatments on the stability of anaerobic digesters operated on separated cattle slurry, Was. Res. 20:453-462.

Rajendran, N. (1992) Variation in Microbiol biomass and community structure in sediments of eutrophic bays as determined by phospholipid ester-linked fatty acids. Appl. Environ. Microbiol. 58:562-571.

Ross, R. W. and M. Smollen (1981) Engineering problems with the anaerobic digestion of soluble organic wastes. Proceedings of the Second International Symposium on Anaerobic Digestion, held on Travemunde, Federal Republic of Germany, Elsevier Biomedical Press, Amsterdam, P89-106.

Rozzi, A., S. Merlinio and R. Passino (1985) Development of a four population model of the anaerobic degradation of carbohydrates, Environ. Technol. Letters 6:610-619.

Schimdt, E. L. and E. A. Paul, Microscopic methods for soil microorganisms, P. 803-814. A. Page (ed.), Methods of soil analysis, Part 2. Chemical and microbiological properties. ASA-SSA Inc., Madison, WI. 1982.

Sedmak, J. J. and S. E. Grossberg (1977) A rapid sensitive, and versatile assay for protein using Coomassie brilliant blue G250. Anal. Biochem. 79:544-552.

Shea, T. G., W. A. Pretorius, R. D. Cole and E. A. Pearson (1968) Kinetics of hydrogen assimilation in the methane fermentation, Wat. Res. 2:833-848.

Smith, M. R. and R. A. Mah. (1978) Growth and methanogenesis by methanosarcina strain 227 on acetate and methanol, Appl. Environ. Microbiol. 44: 870-879.

Smith, P. Daniel, Hydrogenotrophic control in methanogenic processes, Ph D dissertation, Stanford University, 1987.

Smith, P. D. and P. L. McCarty (1989) Energetics and rate effects on methanogenesis of ethanol and propionate in perturbed CSTR's, Biotechnol. Bioeng. 34:39-54.

Smith, P. D. and P. L. McCarty (1990) Factors governing methane fluctuations following shock loading of digesters, J. WPCF. 62:58-64.

Speece, R. E. & P. L. McCarty (1964) Nutrient requirements and biological solids accumulation in anaerobic digestion, In "Advances in Water Pollution Research", Pergamon Press, Oxford, II, 305-322.

Steven J. S., J. P. Tommy, T. M. Al and D. C. White (1986) The relationship of eubacterial and methanogic community structure in anaerobic digesters, Procedings of 10th annual conference on energy from biomass and waste, Washington D. C. April 7-10, 1986.

Steward, M. J. (1958) Reaction kinetics and operation parameters of continuous-flow anaerobic-fermentation processes, I. E. R. Series 90, Report No. 4, Sanitary Engineering Research Laboratory, University of California, Berkeley.

Thauer, R. K., K. Jungermann and K. Decker (1977) Energy conservation in chemotrophic anaerobic bacteria. Bacteriol. Rev. 41: 100-180.

Thiele, J. H. and J. G. Zeikus (1988a) Control of interspecies electron flow during anaerobic digestion: the role of formate versus hydrogen transfers during syntrophic methanogenesis in flocs. Appl. Environ. Microbiol. 54:20-29.

Thiele, J. H. and J. G. Zeikus (1988b) Interactions between hydrogen- and formate-producing anaerobic bacteria and methanogens during anaerobic digestion. In Handbook on Anaerobic Fermentations, ed. L. E. Erickson and D. Y.-C. Fung. Dekker, Amstterdam, pp 537-595.

Tiedje, J. S. Simkins and S. Groffman (1995) Redefining the concept and scope of detrital food chains, unpublished paper.

Tijhuis, L., M. C. M. van Loosdrecht and J. J. Heijnen (1991) A thermodynamically based correlation for maintenance Gibbs energy requirements in aerobic and anaerobic chemotrophic growth, Biotechnol. Bioeng. 42:509-519.

Toerien, D. F. (1966) Enrichment culture studies on aerobic and facultative anaerobic bacteria found in anaerobic digesters, Wat. Res. 1: 147-155.

Toerien, D. F. and W. H. J. Hattingh (1969) Anaerobic digestion I. the microbiology of anaerobic digestion, Was. Res. 3:385-416.

Tsai, Y.-l. and B. H. Olson (1991) Rapid method for direct extraction of DNA from soil and sediments. Appl Environ Microbiol 57: 1017-1024.

Valcke, D and W. Verstraete (1983) A practical method to estimate the acetoclastic methanogenic biomass in anaerobic sludges. J WPCF 55:1191-1195.

van Bruggen, J. J. (1984) Methanobacterium formicicum, an endosymbiont of the anaerobic ciliate Metopus striatus McMurrich. Arch Microbiol. 139:1-7.

van den Berg, L., G. B. Patel, D. S. Clark and C. P. Lentz (1976) Factors affecting rate of methane formation from acetic acid by enriched methanogenic culture. Can. J Microbiol. 22: 1312-1319.

Varel, V. H. (1984) Characteristics of some fermentative bacteria from a thermophilic methane-producing fermenter. Microb. Ecol. 10:15-24.

Vestal, J. R. and D. C. White (1989) Lipid analysis in microbial ecology. BioScience 39:535-541.

Visser, A. Y. Gao and G. Lettiga (1993) Effects of short-term temperature increases on the mesophilic anaerobic breakdown of sulfate containing synthetic wastewater, Was. Res. 27:541-550.

Vogels, G. D. (1980) Association of methanogenic bacteria with rumen Ciliates. Appl. and Envir. Micriol. 40:608-612.

Weast, R. C. (ed.) CRC Handbook of Chemstry and Physics, 51th ed. CRC Press, Inc. Boca Raton, FL, 1979.

White, D. C., Analysis of microorganisms in terms of quantity and activity in natural environments, in Slater J. H. et al., (ed.), Microbes in their natural environments. p. 37-66. Cambridge University Press, New York, 1979.

White, D. C. (1983) Lipid analysis of sediments for microbial biomass and community structure. ASTM Spec. Tech. Publ. No. 673. P. 87-103.

Williams, A. G. and C. G. Harfoot (1976) Factors affecting the uptake and metabolism of soluble carbohydrates by the rumen Ciliate Dasytricha ruminantium isolated from ovine rumen contents by filtration. J. Gen. Microbiol. 96:125-136.

Wu, W., M. K. Jian, J. H. Thiele and J. G. Zeikus (1995) Effect of storage on performance of methanogenic granules, Wat. Res. 29:1445-1452.

Yong S, T. and M. R. Okos (1987) Kinetic study and mathematical modeling of methanogenesis of acetate using pure cultures of methanogens, Biotechnol. Bioeng. 30:661-667.

Zehnder, J.T., C. Grotenhuis and L. W. Hulshoff Pol (ed), Granular anaerobic sludge; microbiology and Technology. Prodoc, Wagenegen, the Netherlands.

Zehnder, A. J. B., K. Ingvorsen and T. Marti (1981) Microbiology of methane bacteria. In Hughes, D. E., D. A. Stanford, B. I. Wheatley, W. Baader, G. Lettinga, E. J. Nyns, W. Versraete, and R. L. Wentworth (ed). Anaerobic digestion 1981. Elsevier Biolmedical Press, Amsterdam. P45-68.

Zeikus, J. G. (1977) The biology of methanogenic bacteria, Bacteriol. Rev. 41: 514-541.

Zeikus, J. G., Microbial population in digesters, in Anaerobic Digestion, Stafford D. A., B. I. Wheatley and D. E. Hughes ed, Applied Science Publishers LTD, Essex, England, 1979.

Zelles, L (1992) Signature fatty acids in phospholipids and lipopolysaccharides as indicators of microbial biomass and community structure in agricultural soils. Soil. Biol. Biochm. 24:317-323.

Zhang, T. C. and T. Noike (1994) Influence of retention time on reactor performance and bacterial trophic populations in anaerobic digestion processes, Wat. Res. 28:27-36.

Zinder, S. H. (1990) Conversion of acetate acid to methane by thermophiles, FEMS Microbiology Reviews 75:125-138.

Zoetemeyer, R. J., J. C. ven den Heuvel and A. Cohen (1982a) pH Influence on acidogenic dissimilation of glucose in anaerobic digester. Wat. Res. 16:303-311.

Zoetemeyer, R. J., A. J. C. M. Matthusen, A. Cohen and C. Boelhouwer (1982b) Production inhibition in the acid forming stage of the anaerobic digestion process. Wat. Res. 16:633-639.

Zhou J.-Z., Fries, M. R., Chee-Sanford, J. and J. M. Tiegje (1995) Phylogenetic analysis of a new group of denitrifiers capable of anaerobic growth on toluene: description of *Azoarcus toluyticus* sp. nov., Int. J. Syst. Bacteriol. 45:500-506.